DAH-YINN LEE
MAY 1972

Final Report HR-124
ISU – ERI – AMES – 72125

DEVELOPMENT OF A DURABILITY TEST FOR ASPHALTS

HR-124

ERI Project 717S and 828S

ENGINEERING RESEARCH INSTITUTE
IOWA STATE UNIVERSITY
AMES, IOWA 50010 USA

ENGINEERING
RESEARCH

ENGINEERING
RESEARCH

ENGINEERING
RESEARCH

ENGINEERING
RESEARCH

ENGINEERING
RESEARCH

FINAL REPORT

DEVELOPMENT OF A DURABILITY TEST FOR ASPHALTS

Dah-yinn Lee
Associate Professor of Civil Engineering

Iowa Highway Research Board Project HR-124
conducted by the
Engineering Research Institute, Iowa State University
for the
Iowa State Highway Commission

Project 717S and 828S

ENGINEERING RESEARCH INSTITUTE
IOWA STATE UNIVERSITY AMES

CONTENTS

Page

Page

I. INTRODUCTION 1

II. REVIEW OF ASPHALT DURABILITY AND DURABILITY TESTS 3

Asphalt Durability 3

Durability Tests 8

Durability Specifications 12

III. MATERIALS 15

IV. EXPERIMENTAL 23

Procedures 23

Physical Tests 23

Chemical Tests 30

V. IOWA DURABILITY TESTS 34

Development and Rationale 35

Iowa Durability Test Procedure 37

Repeatability 38

Changes in Rheological Properties 39

Ageing and Dynamic Modules 133

Ageing and Change in Thermal Properties 133

Ageing and Chemical Changes in Asphalts 141

Thin Film Plate Ageing Tests 159

VI. FIELD AGEING 167

Density-Voids Change of the Pavements 167

Behavior of Asphalts in the Pavements 172

Weathering of Asphalts as Characterized by Infrared Multiple Internal Reflection Technique Theory 176

Sample Preparation 177

Results and Discussions 179

Conclusions 188

VII. CORRELATIONS 195

VIII. APPLICATION AND ENGINEERING IMPLICATIONS OF RESULTS 215

1. Limiting Values of Selected Properties 216

2. Predicted Time to Harden to Certain Critical Values of Critical Properties 217

3. Penetration Ratio vs Time Curves 220

4. Ageing Index vs Time Curve 220

5. Chemical Parameters 220

IX. CONCLUSIONS AND RECOMMENDATIONS 225

ACKNOWLEDGMENTS 227

REFERENCES 228

APPENDIX A A-1

APPENDIX B B-1

HR-124 Testing Program B-1

APPENDIX C C-1

Field Sample Treatment Procedures C-1

APPENDIX D D-1

Iowa Durability Tests Procedure (TFOT — Pressure-Oxidation) D-1

APPENDIX E E-1

Procedure of Brittle Point Tests E-1

Sample Preparation E-2

Cooling E-2

Procedure E-3

Accuracy E-4

FIGURES

		Page
Fig. 1.	HR-124 pavement project locations.	17
Fig. 2.	General view of pressure oxidation vessel.	24
Fig. 3.	Typical rheological diagram from viscosity test.	26
Fig. 4.	General setup of Fraass brittle point test.	29
Fig. 5.	Close-up view of Fraass brittle point test.	29
Fig. 6.	Flow chart of Rostler-Steinberg analytical method.	31
Fig. 7a.	Penetration vs time of ageing, A.C. No. 1.	43
Fig. 7b.	Penetration vs time of ageing, A.C. No. 2.	43
Fig. 7c.	Penetration vs time of ageing, A.C. No. 3.	44
Fig. 7d.	Penetration vs time of ageing, A.C. No. 4.	44
Fig. 7e.	Penetration vs time of ageing, A.C. No. 5.	45
Fig. 7f.	Penetration vs time of ageing, A.C. No. 6.	45
Fig. 7g.	Penetration vs time of ageing, A.C. No. 7.	46
Fig. 7h.	Penetration vs time of ageing, A.C. No. 8.	46
Fig. 7i.	Penetration vs time of ageing, A.C. No. 9.	47
Fig. 8a.	Viscosity at 77 ^{o}F vs time of ageing, A.C. No. 1.	50
Fig. 8b.	Viscosity at 77 ^{o}F vs time of ageing, A.C. No. 2.	51
Fig. 8c.	Viscosity at 77 ^{o}F vs time of ageing, A.C. No. 3.	52
Fig. 8d.	Viscosity at 77 ^{o}F vs time of ageing, A.C. No. 4.	53
Fig. 8e.	Viscosity at 77 ^{o}F vs time of ageing, A.C. No. 5.	54
Fig. 8f.	Viscosity at 77 ^{o}F vs time of ageing, A.C. No. 6.	55
Fig. 8g.	Viscosity at 77 ^{o}F vs time of ageing, A.C. No. 7.	56
Fig. 8h.	Viscosity at 77 ^{o}F vs time of ageing, A.C. No. 8.	57
Fig. 8i.	Viscosity at 77 ^{o}F vs time of ageing, A.C. No. 9.	58

Page

Fig. 9a. Viscosity at 140 °F vs time of ageing, A.C. No. 1. 61

Fig. 9b. Viscosity at 140 °F vs time of ageing, A.C. No. 2. 62

Fig. 9c. Viscosity at 140 °F vs time of ageing, A.C. No. 3. 63

Fig. 9d. Viscosity at 140 °F vs time of ageing, A.C. No. 4. 64

Fig. 9e. Viscosity at 140 °F vs time of ageing, A.C. No. 5. 65

Fig. 9f. Viscosity at 140 °F vs time of ageing, A.C. No. 6. 66

Fig. 9g. Viscosity at 140 °F vs time of ageing, A.C. No. 7. 67

Fig. 9h. Viscosity at 140 °F vs time of ageing, A.C. No. 8. 68

Fig. 9i. Viscosity at 140 °F vs time of ageing, A. . No. 9. 69

Fig. 10a. Softening point vs time of ageing, A.C. No. 1. 75

Fig. 10b. Softening point vs time of ageing, A.C. No. 2. 75

Fig. 10c. Softening point vs time of ageing, A.C. No. 3. 76

Fig. 10d. Softening point vs time of ageing, A.C. No. 4. 76

Fig. 10e. Softening point vs time of ageing, A.C. No. 5. 77

Fig. 10f. Softening point vs time of ageing, A.C. No. 6. 77

Fig. 10g. Softening point vs time of ageing, A.C. No. 7. 78

Fig. 10h. Softening point vs time of ageing, A.C. No. 8. 78

Fig. 10i. Softening point vs time of ageing, A.C. No. 9. 79

Fig. 11a. Microductility at 77 °F vs time of ageing, A.C. No. 1. 82

Fig. 11b. Microductility at 77 °F vs time of ageing, A.C. No. 2. 82

Fig. 11c. Microductility at 77 °F vs time of ageing, A.C. No. 3. 82

Fig. 11d. Microductility at 77 °F vs time of ageing, A.C. No. 4. 83

Fig. 11e. Microductility at 77 °F vs time of ageing, A.C. No. 5. 83

Fig. 11f. Microductility at 77 °F vs time of ageing, A.C. No. 6. 84

Fig. 11g. Microductility at 77 °F vs time of ageing, A.C. No. 7. 84

Page

Fig. 11h. Microductility at 77 ^{o}F vs time of ageing, A.C. No. 8. 85

Fig. 11i. Microductility at 77 ^{o}F vs time of ageing, A.C. No. 9. 85

Fig. 12a. ΔY vs T curves. 86

Fig. 12b. T/ΔY vs T curves. 86

Fig. 13a. T/ΔY vs T, penetration change, laboratory ageing, A.C. No. 1 through 4. 87

Fig. 13b. T/ΔY vs T, penetration change, field ageing, A.C. No. 1 through 4. 87

Fig. 14a. Shear index S and complex flow c, laboratory ageing, A.C. No. 1. 93

Fig. 14b. Shear index S and complex flow c, laboratory ageing, A.C. No. 1. 93

Fig. 15a. Penetration ratio vs time, A.C. No. 1. 100

Fig. 15b. Penetration ratio vs time, A.C. No. 2. 100

Fig. 15c. Penetration ratio vs time, A.C. No. 3. 101

Fig. 15d. Penetration ratio vs time, A.C. No. 4. 101

Fig. 15e. Penetration ratio vs time, A.C. No. 5. 102

Fig. 15f. Penetration ratio vs time, A.C. No. 6. 102

Fig. 15g. Penetration ratio vs time, A.C. No. 7. 103

Fig. 15h. Penetration ratio vs time, A.C. No. 8. 103

Fig. 15i. Penetration ratio vs time, A.C. No. 9. 103

Fig. 16a. Ageing index at 77 ^{o}F vs time, A.C. No. 1. 104

Fig. 16b. Ageing index at 77 ^{o}F vs time, A.C. No. 2. 105

Fig. 16c. Ageing index at 77 ^{o}F vs time, A.C. No. 3. 106

Fig. 16d. Ageing index at 77 ^{o}F vs time, A.C. No. 4. 107

Fig. 16e. Ageing index at 77 ^{o}F vs time, A.C. No. 5. 108

Fig. 16f. Ageing index at 77 ^{o}F vs time, A.C. No. 6. 109

Fig. 16g. Ageing index at 77 ^{o}F vs time, A.C. No. 7. 110

Page

Fig. 16h. Ageing index at 77 °F vs time, A.C. No. 8. 111

Fig. 16i. Ageing index at 77 °F vs time, A.C. No. 9. 112

Fig. 17a. Ageing index at 140 °F vs time, A.C. No. 1. 113

Fig. 17b. Ageing index at 140 °F vs time, A.C. No. 2. 114

Fig. 17c. Ageing index at 140 °F vs time, A.C. No. 3. 115

Fig. 17d. Ageing index at 140 °F vs time, A.C. No. 4. 116

Fig. 17e. Ageing index at 140 °F vs time, A.C. No. 5. 117

Fig. 17f. Ageing index at 140 °F vs time, A.C. No. 6. 118

Fig. 17g. Ageing index at 140 °F vs time, A.C. No. 7. 119

Fig. 17h. Ageing index at 140 °F vs time, A.C. No. 8. 120

Fig. 17i. Ageing index at 140 °F vs time, A.C. No. 9. 121

Fig. 18a. Fraass brittle point vs time of ageing, A.C. No. 1 and 2. 131

Fig. 18b. Fraass brittle point vs time of ageing, A.C. No. 3 and 4. 131

Fig. 18c. Fraass brittle point vs time of ageing, A.C. No. 5, 6, and 7. 132

Fig. 18d. Fraass brittle point vs time of ageing, A. C. No. 8 and 9. 132

Fig. 19a. Dynamic modulus at 21 °C, A.C. No. 2 and 3. 139

Fig. 19b. Dynamic modulus at 21 °C, A.C. No. 4 and 6. 139

Fig. 19c. Dynamic modulus at 21 °C, A.C. No. 8 and 9. 140

Fig. 20a. DSC scans of original asphalts. 142

Fig. 20b. DSC scans of field aged asphalts. 142

Fig. 20c. TMA scans of original asphalts. 143

Fig. 20d. TMA scans of field aged asphalts. 143

Fig. 21a. Asphaltene content vs time of ageing, A.C. No. 1. 147

Fig. 21b. Asphaltene content vs time of ageing, A.C. No. 2. 147

Fig. 21c. Asphaltene content vs time of ageing, A.C. No. 3. 147

Page

Fig. 21d. Asphaltene content vs time of ageing, A.C. No. 4. 148

Fig. 21e. Asphaltene content vs time of ageing, A.C. No. 5. 148

Fig. 21f. Asphaltene content vs time of ageing, A.C. No. 6. 149

Fig. 21g. Asphaltene content vs time of ageing, A.C. No. 7. 150

Fig. 21h. Asphaltene content vs time of ageing, A.C. No. 8. 150

Fig. 21i. Asphaltene content vs time of ageing, A.C. No. 9. 150

Fig. 22. Oxidation of asphalt during Iowa Durability Tests as measured by weight change. 160

Fig. 23. Marginally punched card. 163

Fig. 24. Log viscosity vs time of thin film plate ageing test. 166

Fig. 25a. Pavement voids vs time, series No. 1 through 4. 169

Fig. 25b. Pavement voids vs time, series No. 6 through 9. 169

Fig. 26a. Pavement density vs time, series No. 1 through 4. 170

Fig. 26b. Pavement density vs time, series No. 6 through 9. 170

Fig. 27. IR transmission vs reflection scans, A.C. No. 1. 178

Fig. 28a. MIR diagram. 180

Fig. 28b. Base line method. 180

Fig. 29a. IR spectra of laboratory aged asphalt, A.C. No. 1. 181

Fig. 29b. IR spectra of field aged asphalt, A.C. No. 1. 182

Fig. 29c. IR spectra of original asphalts, A.C. No. 1 to 4. 183

Fig. 29c. IR spectra of field aged asphalts, A.C. No. 1 to 4. 184

Fig. 30. Carbonyl index vs time of lab ageing. 188

Fig. 31. Carbonyl index vs asphaltene content. 189

Fig. 32. Peak ratio $\Delta A9\text{-}72\ \mu / A\Delta 6.25\ \mu$ vs lab ageing time. 190

Fig. 33a. Carbonyl index vs ageing index. 191

Fig. 33b. Carbonyl index vs ageing index. 192

Page

Fig. 34a. Change in viscosity at 77 °F. 193

Fig. 34b. Change in viscosity at 77 °F. 194

Fig. 35a. Penetration correlation curves. 197

Fig. 35b. Penetration correlation curves. 197

Fig. 35c. Penetration correlation curves. 197

Fig. 35d. Penetration correlation curves. 197

Fig. 35e. Penetration correlation curves. 198

Fig. 35f. Penetration correlation curves. 198

Fig. 35g. Penetration correlation curves. 198

Fig. 35h. Penetration correlation curves. 198

Fig. 36a. Correlation curves for viscosity at 77 °F. 199

Fig. 36b. Correlation curves for viscosity at 77 °F. 199

Fig. 36c. Correlation curves for viscosity at 77 °F. 200

Fig. 37a. Softening point correlation curves. 201

Fig. 37b. Softening point correlation curves. 202

Fig. 37c. Softening point correlation curves. 203

Fig. 38a. Correlation curves for viscosity at 140 °F. 204

Fig. 38b. Correlation curves for viscosity at 140 °F. 204

Fig. 38c. Correlation curves for viscosity at 140 °F. 205

Fig. 39a. Asphaltene content correlation curves. 206

Fig. 39b. Asphaltene content correlation curves. 207

Fig. 39c. Asphaltene content correlation curves. 208

Fig. 40. Time-equivalency correlation curves for various properties. 211

Fig. 41. Log viscosity (log penetration) vs log void content of 42-month field asphalts. 212

Fig. 42. Time-equivalency correlation curves by voids level. 214

Fig. E-1. Cooling circuit connection. E-3

TABLES

		Page
Table 1.	HR-124 pavement project locations.	16
Table 2.	Characteristics of field pavement mixtures.	19
Table 3.	Properties of asphalts studied.	21
Table 4.	Viscosity at 77 °F of TFOT residues treated in oxygen bombs at 132 psig, 150 °F, and in films of 1/8 in. for 24 hr.	39
Table 4a.	Iowa Durability Test repeatability study, behavior of asphalts.	40
Table 5.	Changes in penetration during weathering.	41
Table 6.	Changes in viscosity at 77 °F.	48
Table 7.	Changes in viscosity at 140 °F.	59
Table 8.	Complex flow and shear index.	70
Table 9.	Changes in softening point during weathering.	73
Table 10.	Changes in microductility at 77 °F, cm.	80
Table 11.	Constants for predictive equations.	88
Table 12.	Limiting values of physical properties — laboratory ageing.	90
Table 13.	Limiting values of physical properties — field ageing.	91
Table 14.	Penetration ratio.	94
Table 15.	Ageing index, viscosity at 77 °F.	96
Table 16.	Ageing index, viscosity at 140 °F.	98
Table 17.	Penetration index.	123
Table 18.	Stiffness modulus.	125
Table 19.	Fraass brittle point.	128
Table 20.	Dynamic modulus.	134
Table 21.	Softening point from thermal analysis.	141

Page

Table 22. Percentage of asphaltenes. 145

Table 23. Chemical analysis. 151

Table 24. Characteristics of asphalt components. 153

Table 25. Chemical composition parameters. 155

Table 26. Durability rating of asphalts from 60 to 100 penetration grade. 157

Table 27. Percent weight gain during Iowa Durability Test. 158

Table 28. Change in oxygen content during Iowa Durability Test. 159

Table 29. Spot test. 161

Table 30. Thin film plate ageing tests. 164

Table 31. Density-voids changes of pavements. 168

Table 32. Comparison among the asphalts through changes in IR absorbance due to weathering. 185

Table 33. Changes in carbonyl index of asphalts due to weathering. 187

Table 34. Hyperbolic curve fittings for model: log $T_\ell = \frac{T_f}{a + bT_f}$, time equivalency correlation curves. 209

Table 35a. Durability rankings based on different criteria — lab ageing. 218

Table 35b. Durability rankings based on different criteria — field ageing. 219

Table 36. Correlation of pavement condition with physical properties of recovered bitumen. 222

Table 37. Summary of critical recovered asphalt properties for acceptable performance of asphaltic surfacing. 223

I. INTRODUCTION

Research Project HR-124, "Development of a Laboratory Durability Test for Asphalts," was initiated in 1966 as a long-range comprehensive program. Its ultimate objective was to develop a simple, rapid laboratory test that could be used by highway engineers to select paving asphalt according to quality, to identify inferior asphalts, and to reasonably predict the useful life of asphalts once they were incorporated in the pavements.

The original proposed study on asphalt durability involves work in the following phases:

1. Critical review of the state of the art on the durability of paving asphalts, the identification of predominant factors causing hardening during mixing, laying, and in-road service.
2. Development of an accelerated laboratory durability test to simulate changes in asphalt both during short-time production and long-term road service.
3. Correlation of hardening and other changes in asphalts during the developed laboratory durability test and changes in same asphalts in pavements.
4. Establishment of durability criteria and functional approach specifications by means of established laboratory durability tests on original asphalt.

Work in phases 1 and 2 was accomplished in the original HR-124 (1966-1967) project and was presented in Progress Report No. 1[1], a paper published in Highway Research Record 231[2], and a Special Report on the state of the art on asphalt durability[3]. The first 11 months of field correlation studies in phase 3 were conducted in HR-124 (1967-1969) and were presented in Progress Report No. 2 (October 1968). Progress Report No. 3 summarized the work accomplished during the second year of the HR-124 extension (1967-1969), i.e., the period from 1 October 1968 to 31 October 1969.

In this Final Report, attempts will be made to describe all work conducted under HR-124 up to February 29, 1972, and its implications and recommendations. The overall objectives of HR-124 (1967-1972), which this report covers, were:

- Refinement of the durability test procedure developed in HR-124 (1966-1967).
- Durability tests on asphalts used for actual paving projects in Iowa.
- Determination of changes in asphalts incorporated in the various paving. Projects from the plant and at 6-month intervals thereafter.
- Field correlations for a period up to 48 months.

II. REVIEW OF ASPHALT DURABILITY AND DURABILITY TESTS

Asphalt Durability

Current practice in the design of asphaltic paving mixtures is to try to arrive at a balanced design among a number of desirable mix properties: (a) stability, (b) durability, (c) flexibility, (d) fatigue resistance, (e) skid resistance, (f) imperviousness, and (g) fracture or tensile strength.

Studies and experiences have shown that mixtures with higher asphalt content are usually associated with a desirable durability which also gives adequate flexibility, fatigue resistance, imperviousness, and fracture strength properties. On the other hand, mixtures with lower asphalt content yield high stability and good skid resistance. As a result, asphalt paving mixture design, i.e., selection of aggregate gradation and asphalt content, is a compromise between stability and durability of the mixture.

Durability of a paving mixture is usually defined as its resistance to weathering, ageing, and traffic loading or as the ability to resist change due to these destructive or deteriorative factors.

Bituminous pavements may fail due to (a) cracking, (b) disintegration, and (c) instability, any of which may result from improper selection and use of types and amounts of asphalt. From the practical point of view, the desired durability properties of any bituminous paving binder imply that the material should resist deterioration resulting from chemical and physical changes during production, and weathering and traffic stresses and strains during service, especially changes in hardness or consistency. The increase in hardness may result in loss of ability to deform without fracture and in loss of adhesion and fatigue resistance.

The study of durability of paving asphalts is a complex problem, despite many efforts that have been spent on the subject. The major reasons are:

- Durability cannot be easily and clearly defined. The mechanisms of asphalt deterioration and the parameters to measure or indicate durability or deterioration are difficult to express in simple physical terms.
- Durability depends on the chemical makeup of asphalts, yet the chemical composition of asphalt is not well understood. The dependency of chemical makeup on the source of crude and the method of refining makes the problem even more complex.
- Durability is time dependent. The real test of durability is on the road. Road testing is not only time consuming and expensive, but many local mixture variables greatly affect durability. These factors include: type and grade of asphalt, asphalt content, type of mixture, traffic conditions, temperature, moisture, air content, film thickness, aggregate surface effects, permeability, etc.

It is generally agreed that asphalt hardening is the most important single factor that causes asphalt paving to crack and disintegrate. Therefore, the degree and rate of asphalt hardening can indicate relative durability of asphalt; many durability tests have been proposed centering around the evaluation of the resistance of asphalt to hardening.

Factors which may contribute to asphalt hardening under service conditions are[4,5]: (a) oxidation, (b) volatilization, (c) polymerization, (d) thixotropy (age hardening or hardening with time), (e) syneresis (exudation of oil), (f) separation (absorption and adsorption of asphaltic components by aggregate), (g) photo oxidation, (h) water, (i) microbiological deterioration, and (j) photochemical action.

There is considerable disagreement as to the exact mechanism and the dominant factors influencing the hardening of asphalts. However, the first four of the ten above-listed factors represent the major important factors recognized by most asphalt paving technologists both in the United States and in Europe.

In considering the various factors that may affect the durability of asphalt, it should be noted that: (a) while the quantitative measurement of the individual factors in influencing the durability of asphalt is extremely complex, if not impossible, it is to be recognized that some of these effects are more important than others in various phases of asphalt use; (b) one or more of the effects may function at the same time; and (c) all effects are influenced by time, temperature, and film thickness.

Since asphalt is used in conjunction with aggregate in paving mixtures and represents only about 5% by weight of the mixture, other variables associated with the mixture and the aggregate in the mixture should not be overlooked when evaluating the durability of the asphalt and asphalt pavement. The more important of these factors include: type and gradation of aggregate, aggregate degradation, aggregate-water adhesion (particularly in the presence of water), air voids and air voids filled with asphalt, and film thickness in the mixture. Degradation of aggregate in an asphalt paving mixture depends on the kind of aggregate, gradation, compactive effort, and particle shape, and can be evaluated by the Los Angeles Abrasion Test[6]. With respect to adhesion of asphalt to aggregate, the following general statements can be made:

- Adhesion of asphalt to aggregate, especially in the presence of water, is a surface phenomenon involving physico-chemical forces acting in the system. The problem, if one occurs, is more a result of the chemical or mineral composition of the aggregate than of the asphalt binder.
- Adhesion can be improved and stripping can be eliminated or reduced by certain fillers (such as hydrated lime and Portland cement) and other anti-stripping additives. The most effective of these show cationic surface activity.
- Most available laboratory tests to predict or evaluate aggregate-asphalt stripping or adhesion are arbitrary and have at best only qualitative value. A quantitative, objective, and definitive method is needed.

Air voids can be considered as a measure of permeability and pore surface area. Film thickness can be expressed either in terms of calculated average thickness of the asphalt film or in terms of the bitumen index which is the ratio between asphalt content and specific area of the aggregate (ft^2/lb of aggregate)[7]. Both of these variables are affected by asphalt content and aggregate gradation. Asphalt or binder content is considered the most important factor in deciding durability of a paving mixture. The effects of binder content, as reflected in terms of air voids, voids filled, and film thickness, on hardening of asphalt have been reported by many investigators[7-13]. These data emphasize the importance of obtaining low void content in the in-place asphalt concrete surfacing. The general conclusions on effects of aggregate gradation are that[7]:

- Increasing air content results in a reduction of the retained penetration as a function of aggregate gradation.
- Increasing film thickness results in an increase in the retained penetration as a function of the aggregate gradation.

Plant mixing temperature is another factor that will affect the degree of hardening that an asphalt will undergo during plant mixing. Bright and Reynolds[14] found a relatively constant hardening in asphalt with increased mixing temperatures (from 270 to 350 °F) of 2% loss in retained penetration for each rise in temperature of 10 °F. According to a more recent study of 11- to 13-year old pavements (53 projects in 19 states, including 2 in Iowa), it was concluded[11] that design of the mixture and the mixing, spreading, and compaction of the mixture at the time of construction (film thickness, air voids, and voids filled with asphalt, mixing temperature, etc.) are probably the most important factors governing the hardening of asphalt.

The consensus of opinion among asphalt paving technologists both in the USA and in Europe is that a longer life is associated with higher asphalt content and increased density, and that a sound practice in bituminous paving mixture design is to use as high a binder content as possible without losing stability. It is both significant and interesting to note that opinions differ as to the grade or hardness of binder to be used in the mixture. The American practice is to use the softest grade binder possible on the premise it would take longer for such a system to reach the critical level of hardness often indicated as a penetration of 20 or viscosity of 10^8 poises at 77 °F[15]. The United Kingdom emphasis, on the other hand, is to use the hardest possible grade of binder to get the highest possible binder content to maintain desirable level of stability.

The American practice of using the highest possible penetration grade binder was recently questioned[16] on four major considerations:

1. Using a high penetration asphalt initially does not always assure a high penetration after mixing and in service.
2. Higher asphalt consistency may be needed to obtain increased film thickness or asphalt content.
3. Based on limited fatigue test data[17-19], asphalts of low penetration may provide better fatigue resistance, especially when used in thick asphaltic surfacings.
4. Resistance to the effects of water may be increased by using lower penetration asphalts[20].

Durability Tests

Durability of asphalts has been studied by many investigators for many years to find:

- Mechanisms or causes of asphalt deterioration.
- Methods for controlling or preventing undue hardening of asphalts or improving the durability of asphalts.

- Tests to predict the behavior and durability of an asphalt during mixing, laying, and service.

Studies in the first group can be considered as basic research. Studies directed to the second and third objects can be classified as applicational research. Obviously, they are interrelated: without clear understanding of the chemical makeup of the asphalt and of the mechanism of asphalt failure by disintegration and cracking, it is difficult to devise durability improvements and to choose the properties of the asphalt for investigation in durability tests and as indices for durability. On the other hand, a reliable durability test is needed when evaluating the effectiveness of methods for durability improvement in the second category.

The investigation undertaken under HR-124 was directed toward obtaining information in the third category with the belief that: (a) there is a wide range of differences in durability among paving asphalts; (b) current specifications do not discriminate nondurable asphalts; (c) simple methods can be developed to evaluate the relative durability of asphalts, and (d) pavement service can be improved by more durable asphalts.

Almost all durability tests that have been proposed involve a study of two phases: (a) subjecting asphalt to certain treatments to speed up the hardening process, and (b) comparing the degree or the rate of hardening of the treated asphalt with actual hardening that occurred in asphalt during the mixing process and in the road. Hardening that occurred in the mixing process and in the road is usually determined by recovering the asphalt from the mix or pavement by the Abson method and by comparing the penetration, softening point, ductility, viscosity, and chemical compositional properties of the recovered asphalt with those of the original asphalt. Major differences among various proposed durability tests are the treatments or the manner in which the hardening of the asphalts is accelerated.

A majority of the treatments used to speed up the hardening of asphalt in a durability test include heating at elevated temperatures, either alone in various thicknesses of films, temperature, and duration[21-29], or in a mixture[30-32]. The more important ones in these groups are the Shattuck mixing test, the standard loss on heating test, and the thin film oven test (TFOT).

Many investigators believe that oxidation is a major factor causing asphalt hardening. Procedures for evaluating the susceptibility of asphalt to oxidation were developed by Thurston and Knowles[33], Anderson et al.[34], and Ebberts[35]. Van Oort[36] studied the durability of asphalts and showed by calculation that, under normal ageing conditions, the oxygen diffuses into the asphalt films to a depth of only a few microns. However, experiments by Blokker and Van Hoorn[37] showed that the penetration is much greater, on the order of 3 mm or more.

In recent years, particularly after the introduction of the microfilm viscometer, many investigators have used so-called microfilm durability techniques in which asphalt is aged in films of only 5 to 15 μ[36,38-40]. Hardening is measured by the viscosity ratio or ageing index after the film is exposed to heat and air.

Some investigators considered the abrasion resistance of a paving mixture as a good indicator for the hardening and durability of the binder. The shot-abrasion test[41,42] was developed to measure the change in resistance of a compacted sand-asphalt mix to a falling stream of steel shot after extended exposure in the infrared oven. A modified version of a shot-abrasion test has been used by the Bureau of Public Roads (now Federal Highway Administration) for many years in the study of asphalt and durability[43].

The durability of bitumen in theory and practice was reviewed by Blokker and Van Hoorn[37]. An accelerated test procedure for assessing the ageing characteristics of bitumens was investigated that involved treating bitumen in thin films (5 to 200 µ) in oxygen of 20 atm at 50 °C, (122 °F) and measuring relative viscosity. The same approach was used by Martin[44]. The British Road Research Laboratory[45] has developed a pressure-oxidation test for road tars by exposing tar films 7 mm thick to oxygen at 300 psi and 65 °F (149 °F) for 64 hr and measuring the change in either Fraass brittle point or equiviscous temperature (evt).

In 1963, Hveem et al.[46] presented results of an extensive study on the durability of asphalt by the shot-abrasion test and the microfilm-viscometer technique. Weathering was achieved by subjecting asphalt-sand mixtures to infrared radiation in a weathering machine. A correlation study showed that exposure of 1000 hr in the weathering machine was about equal to 5 yr of pavement service time for California conditions. For routine control testing purposes a new rolling thin film oven test (film thickness of 5 to 10 µ exposed in oven at 325 °F for 75 min) was developed to predict change in asphalt during mixing operation. To simulate weathering during service life, 20-µ films of residue from the rolling thin film oven test are weathered at 210 °F for a period of 24 hr and viscosity is determined by microviscometer. These conditions produced hardening equivalent to 1000 hr in the weathering machine at 140 °F or 5 yr of service life.

Practical and reliable information can be obtained from a laboratory durability test only when the behavior of the asphalt in the durability test can be correlated with pavement durability in the field. Correlations on the TFOT are well established[8,9,47]. Correlations between field hardening of asphalt and laboratory data were studied by Simpson et al.[52], Traxler[53], Gallaway[54], and Heithaus and Johnson[39] on microfilm durability tests. Halstead and Zenewitz[55] studied the relation between the TFOT and the microfilm durability test. Their results showed greater hardening for the microfilm test for asphalts with ageing indices greater than two.

In spite of the great amount of time and effort that have been put into the study of the durability and durability testing of asphalt, the paving industry is still in need of a logically conceived, well-designed, universally accepted, and yet relatively simple and rapid laboratory durability test for paving asphalt, which will enable the design engineer to select or specify an asphalt based on quality and to make a proper estimate of the service life of a selected asphalt.

Durability Specifications

For many years the asphalt specifications had little to do with quality and performance of asphalt, much less durability requirement.

The only test that existed that had something to do with durability was the loss on heating (LOH) test.

As a result of work by the Bureau of Public Roads, the TFO test has replaced the LOH test in the specifications of the majority of agencies in the USA. While the value of the TFO test in predicting long-term service durability of asphalt in pavements is inconclusive, the ability of the test to duplicate the hardening in asphalt during hot mixing and to qualitatively indicate the ability of an asphalt to retain its original consistency and ductility has made the TFO test one of a few tests that exists in present day asphalt specifications that may be considered a quality or durability test.

Specifications based on viscosity (at 140 °F) of TFO test residue have also been suggested, in one of the following forms:

- Viscosity ratio at 140 °F after and before TFOT[56,57].
- Maximum viscosity at 140 °F after TFOT[57].
- Range in viscosity at 140 °F after TFOT[57,58].

Correlation between the California RTFO test and Thin Film Oven (TFO) test was found good[52,59,60]. As a result of the study on test roads and California weathering conditions the durability test requirements in terms of RTFO test and viscosity and ductility at 77 °F on residue after thin film durability test are included in California's newly proposed functional specifications for paving asphalts. The maximum viscosity at 77 °F and at a shear rate of 0.05 sec^{-1} was set at 25 megapoises and the minimum microductility (0.5 cm/min) was set at 10 mm[59].

Microfilm durability techniques were used by Traxler[40,53] to study the hardening of asphalts used by the Texas Highway Department.

Time of ageing was 2 hr and the temperature used was 225 ^{o}F. However, a film of 15 μ was used in ageing instead of the 5 μ films proposed by ASTM. This was done because the thicker film more nearly approximated the geometry of the films present in most bituminous pavements. As a result of this study and Texas field experiences, the Texas Highway Department has included an ageing-index (on 15-μ films) requirement of less than 4 to 6 in its asphalt cement specifications.

III. MATERIALS

A total of eight asphalt paving projects, selected by the Iowa State Highway Commission engineers, were included in this study. Asphalt cements, plant mixes, and core (or slabs) samples were obtained from four paving projects during the late 1967 construction season; materials from four more paving projects were obtained during the early 1968 construction season. The locations of the eight pavement projects are shown in Table 1 and Fig. 1. In addition to asphalts received from the Iowa State Highway Commission, an essentially asphaltene-free asphalt cement (A.C. No. 5) was obtained from the ESSO Research and Engineering Co. and is included in the study to evaluate the role of asphaltenes in the performance of a paving asphalt.

Four 1-gal asphalt cement samples were taken from each project by district personnel of the ISHC just prior to the asphalt's entry into the mixer. Forty pounds of plant mixtures were collected from trucks immediately after their leaving the mixers and are identified throughout this report as P-samples. The trucks, from which the plant mixtures were sampled, were tagged. Pavement cores (or slabs) of about 40 lb were cut from the newly finished pavements containing the mixtures from the same tagged trucks. Half of the cores (or slabs) were taken from the wheel track and are identified as f-o-A and half of the cores (or slabs) were taken from between the wheel-tracks and are identified in this report as f-o-B. The same amounts of field core samples were taken from the respective pavement sections every six months from the time the pavement was laid and are identified as f-6,12,18 . . .-A or f-6,12,18 . . .-B.

Table 1. HR-124 pavement project locations.

Number	County	Location and project number	Date laid
1	Chickasaw	ON US 63 north of New Hampton FN-63-8(1)20-19	Nov 1967
2	Dickinson	On Iowa 327 from Iowa 276 east and north FN-327-1(1)-21-30	Oct 1967
3	Harrison	On US 75 out of Mo. Valley, north into Mondamin FN-75-2(3)21-43	Nov 1967
4	Story-Polk	On US 69 between Huxley and Ankeny FN-69-5(2)	Oct 1967
6	Monona	On US 75 from Harrison Co. line north into Ottawa 11 mi. FN-3(2)-21-67	April 1968
7	Bremer	On Iowa 3 FN-3-6(5)-21-09	May 1968
8	Keokuk	On Iowa 92 from Sigorney east FN-92-8(2)-21-54	May 1968
9	Jackson	On US 52 north of Maquoketa FN-52-1(3)-21-49	June 1968

Pertinent information obtained at each project site by the ISHC district personnel was summarized in a standard form by the personnel of the Research Department of the ISHC and delivered to the Bituminous Research Laboratory, Iowa State University, together with the samples. The information included Project Number, County, highway designation and location, station, asphalt and aggregate sources, date that the pavement was laid and the temperature of the asphalt, aggregate and fresh mix and designed aggregate gradation and asphalt content. A sample of such a summary sheet is given in Appendix A. The general characteristics

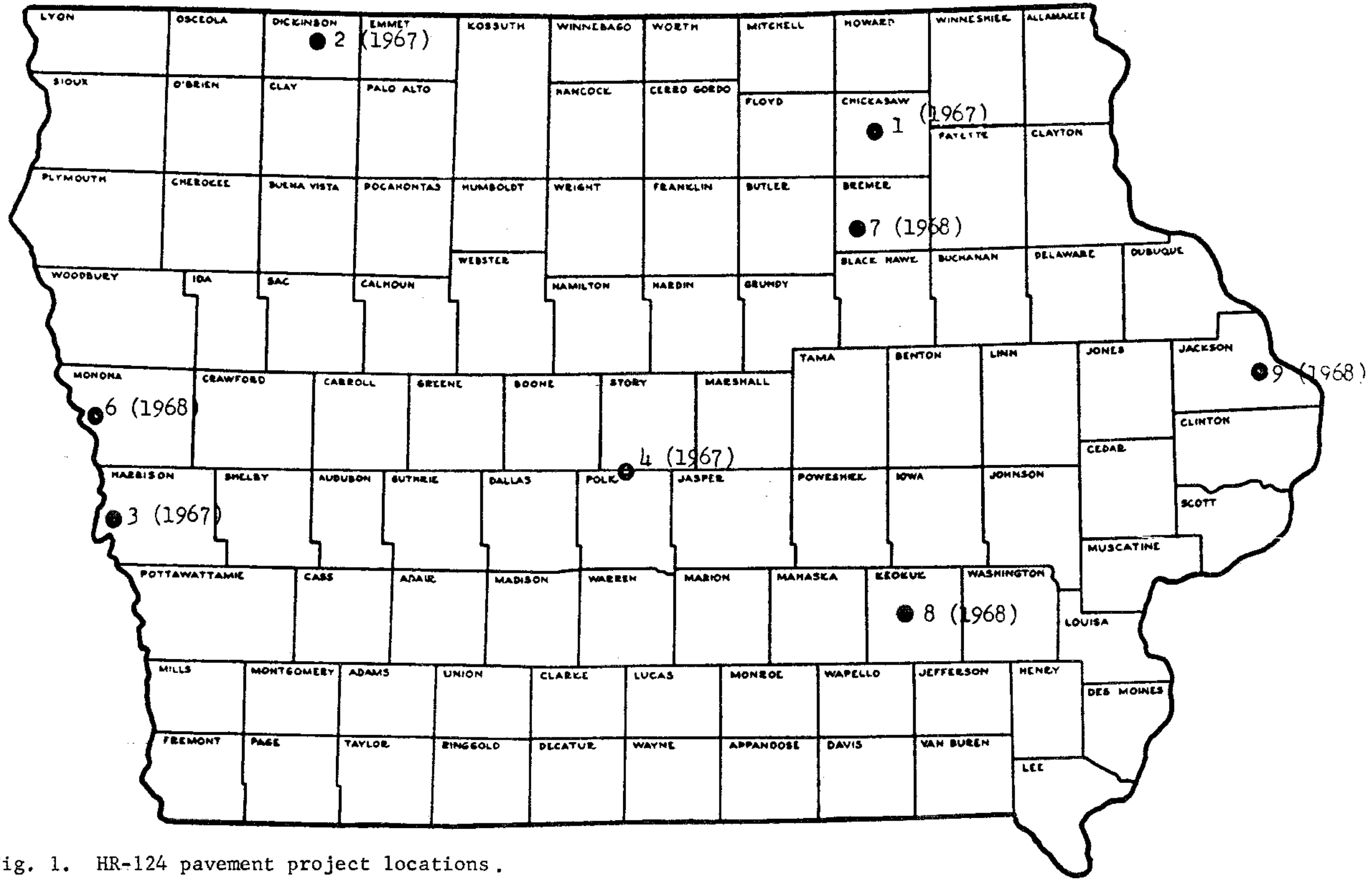

Fig. 1. HR-124 pavement project locations.

of the field pavement mixtures studied in HR-124 are tabulated in Tables 2 and 2a. Specific surface, bitumen index, and film thickness were calculated based on data supplied by the project information sheets. The original properties of the nine asphalt cements studied are given in Tables 3 and 3a.

Table 2. Characteristics of field pavement mixtures.

A.C. No.	1	2	3	4
Gradation, % passing				
3/4 in.				
1/2 in.				
3/8 in.	100	100	100	100
#4	81	89	92	78
#8	62	67	58	59
#16	44	–	–	–
#30	30	34	34	31
#50	16	21	23	18
#100	12	13	13	13
#200	9.3	9.9	9.4	9.4
Percent bitumen	7.5	6.3	6.3	7.5
Specific surface[*], ft^2/lb	40.59	45.92	44.18	41.86
Bitumen index[†], $\times 10^{-3}$	1.996	1.459	1.517	1.935
Film thickness[‡], µ	9.72	7.11	7.39	9.24
Laboratory design voids, %	6.8	6.1	6.6	9.3
Hveem side pressure[**], psi	60	46	63	48
A.C. temperature, °F	295	300	295	260
Aggregate temperature, °F	300	320	310	310
Mix temperature, °F	290	295	310	310
Initial field voids, %	8.7	9.8	11.5	12.3
ADT, 1970	2100	330	590	3000
Condition after 48 months	Transverse cracks	Excellent	Excellent	Severe trans. & long center line cracks

[*] Mix Design Methods for Asphalt Concrete, The Asphalt Institute, MS-2 (1962).

[†] Percent bitumen (aggregate basic)/specific surface.

[‡] Bitumen index × 4.870.

[**] At 400 psi vertical load.

Table 2 Continued.

A.C. No.	6	7	8	9
Gradation, % passing				
3/4 in.	100			100
1/2 in.	94			
3/8 in.	77	100	100	78
#4	60	85	85	62
#8	43	67	63	49
#16	—	—	—	—
#30	25	35	35	23
#50	19	35	25	—
#100	9	—	13	—
#200	7.1	8.4	8.9	6.7
Percent bitumen	5.0	7.0	5.3	5.5
Specific surface[*], ft^2/lb	33.44	51.06	44.34	32.66
Bitumen index[†], $\times 10^{-3}$	1.585	1.469	1.263	1.776
Film thickness[‡], μ	7.12	7.15	6.15	8.65
Laboratory design voids, %	6.8	6.1	3.5	5.8
Hveem side pressure[**], psi	55	61	55	29
A.C. temperature, °F	267	260	275	300
Aggregate temperature, °F	340	310	375	305
Mix temperature, °F	310	305	306	298
Initial voids, %	5.5	7.1	6.7	5.1
ADT, 1970	500	2000	1500	2400
Condition after 42 months	Good	Good, some cracks	Good to Excellent	Excellent

---

[*] Mix Design Methods for Asphalt Concrete, The Asphalt Institute, MS-2 (1962).

[†] Percent bitumen (aggregate basic)/specific surface.

[‡] Bitumen index × 4.70.

[**] At 400 psi vertical load.

Table 3. Properties of asphalts studied.

A.C. No.	1	2	3	4
Penetration, 77/100/5	89	94	91	90
Specific gravity, 77/77	1.017	1.026	1.042	1.011
Viscosity at 77 °F, megapoises	1.16	1.23	1.58	1.10
140 °F, poises	1356	1086	1316	1106
Softening point, °F	119.0	116.5	115.5	114.5
Flash point, COC, °F	600	595	630	625
Fire point, COC, °F	680	690	705	705
Microductility at 77 °F cm	63	71	66	77
Thin film oven test,				
Residue penetration	53	51	57	56
Weight loss, %	0.02	0.16	+ 0.01	0.00
Spot test	Neg	Neg	Neg	Neg
Source*	(a)	(a)	(b)	(b)

*(a) Blend of asphalts from Texaco at Casper, Wy., and American Petrofina, Big Springs, Tex.

(b) American Oil, Sugar Creek, Mo.

Table 3 Continued.

A.C. No.	5	6	7	8	9
Penetration, 77/100/5	84	87	95	90	92
Specific gravity, 77/77	1.017	1.019	1.042	1.003	0.999
Viscosity at 77 °F, megapoises	1.14	1.70	1.15	1.10	1.22
140 °F, poises	1781	1455	1316	1922	2060
Softening point, °F	113.0	118.0	116.0	118.0	119.5
Flash point, COC, °F	690	615	625	655	655
Fire point, COC, °F	730	670	685	735	735
Microductility at 77 °F, cm	82	55	68	51	63
Thin film oven test,					
Residue penetration	67	55	59	60	62
Weight loss, %	+ 0.01	0.07	0.07	0.24	0.16
Spot test	Neg	Neg	Neg	Neg	Neg
Source*	(b)	(c)	(c)	(a)	(a)

*(a) American Oil, Sugar Creek, Mo.

(b) Esso Research and Engineering Co.

(c) American Petrofina, Big Springs, Tex.

IV. EXPERIMENTAL

Procedures

Experimental work was carried out as planned in the research proposal, with minor modifications, and is further detailed in Appendix B. When the experimental phase of the project terminated, samples up to 48 months were tested on six pavements, and 42-month samples were tested on two other projects. Handling and treatment of pavement samples are given in Appendix C. Pressure-oxygen treatment was conducted in pressure vessels fabricated of 1/2 in. stainless steel in the Machine Shop of the Engineering Research Institute. These vessels are capable of simultaneously treating ten standard TFO test samples to a pressure of 450 psi. The interior dimensions of the vessels are 7.5 in. in diameter and 7.5 in. high. They are equipped with a pressure gauge and a relieve valve. Five of the asphalts were treated to 1000 hr. Figure 2 shows the general view of the vessel.

Physical Tests

The physical tests selected in this study are mainly for the evaluation of changes in rheological properties of asphalt with ageing or hardening and are selected tests based on the hypothesis that asphalt durability can be related to rheological behaviors.

Tests conducted on the original, laboratory aged, and recovered field asphalts are given in Appendix B. Specific gravity, penetration at 77 ^{o}F (100 gm, 5 sec), ring and ball softening point were determined following standard ASTM procedures. Viscosity at 77 ^{o}F was determined

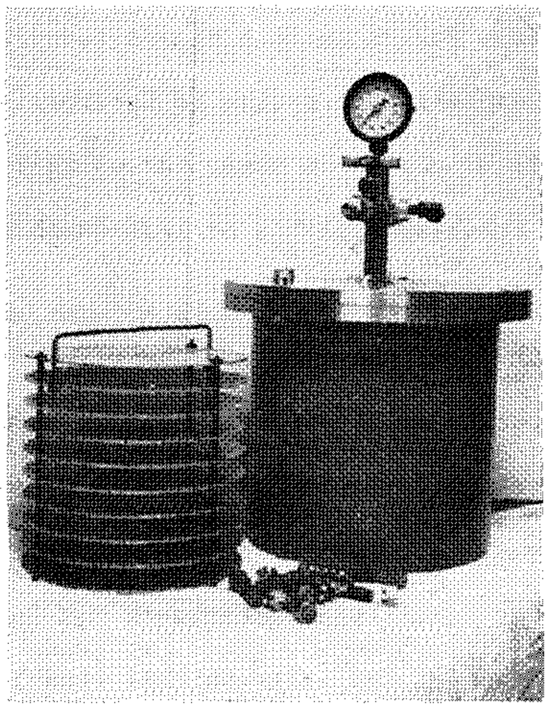

Fig. 2. General view of pressure-oxidation vessel.

by the Shell sliding-plate microviscometer using an apparatus by Hallikainen. Plots of log shearing stress vs log rate of shear and log viscosity and log rate of shear were made on all asphalts. Viscosities at a rate of shear of 5 X 10^{-2} sec^{-1}, at a constant energy input, and at a constant shearing stress of 167 gm/cm^2 were calculated. Unless otherwise stated only the viscosity at the rate of shear of 5 X 10^{-2} sec^{-1} are reported.

The slope of log rate of shear against log shearing stress linear plot is defined as the degree of complex flow, commonly designated by the letter c[61]. Determination of this constant is important, for it indicates not only the complexity or degree of deviation of the material from Newtonian behavior but its colloidal nature as well. If the slope is greater than unity ($c > 1$), the material is dilatant; if it is equal to unity ($c = 1$), the material is Newtonian; if it is less than unity ($c < 1$), the material is pseudoplastic. Experiences have shown that as asphalt ages, the degree of complex flow increases and the value of c decreases.

The shear index (S or SI) or shear susceptibility is the tangent of the angle of log shear rate vs log viscosity plot[46]. The rate of change in shear index of various asphalt during weathering was found to be related to relative durability of asphalt. According to California's Zaca-Wigmore Test Project[46], high rate of change in shear susceptibility during weathering is associated with crack-susceptible or less-durable asphalt.

Also calculated for each viscosity determination was the viscosity at constant work input[61] and the viscosity at a constant shearing stress of 167 erg/cm^2 [60]. In the constant energy input method, the viscosity value to be reported is determined by the point at which the straight line of the log shear rate vs log shear stress plot intersects the line of constant work input of a convenient level (10^4 ergs in this study). The work input is defined as the product of shear rate and shear stress. Figure 3 illustrates the determinations of c, SI, viscosity at a constant rate of shear of 5×10^{-2} sec^{-1}, and viscosity at a constant work input of 10^4 ergs.

The upper limit of the Shell sliding-plate viscometer using 20 × 30 mm polished glass plates is about 10 megapoises. For viscosities higher than 10 megapoises, such as those obtained in long period pressure-oxygen treated or artificially aged asphalts, new methods of determining viscosity at 77 °F had to be investigated. In this study two other methods of determining viscosity were used: sliding-plate with stainless steel plates and cone-plate viscometer.

Modified sliding-plate viscometers using 30 × 45 mm polished stainless steel plates are used in the early stage of the study. The new plates have the advantage of providing film areas of 6.0 cm^2 as well as 1.2 cm^2. With a film thickness of 50 to 500 μ (using spacers to form

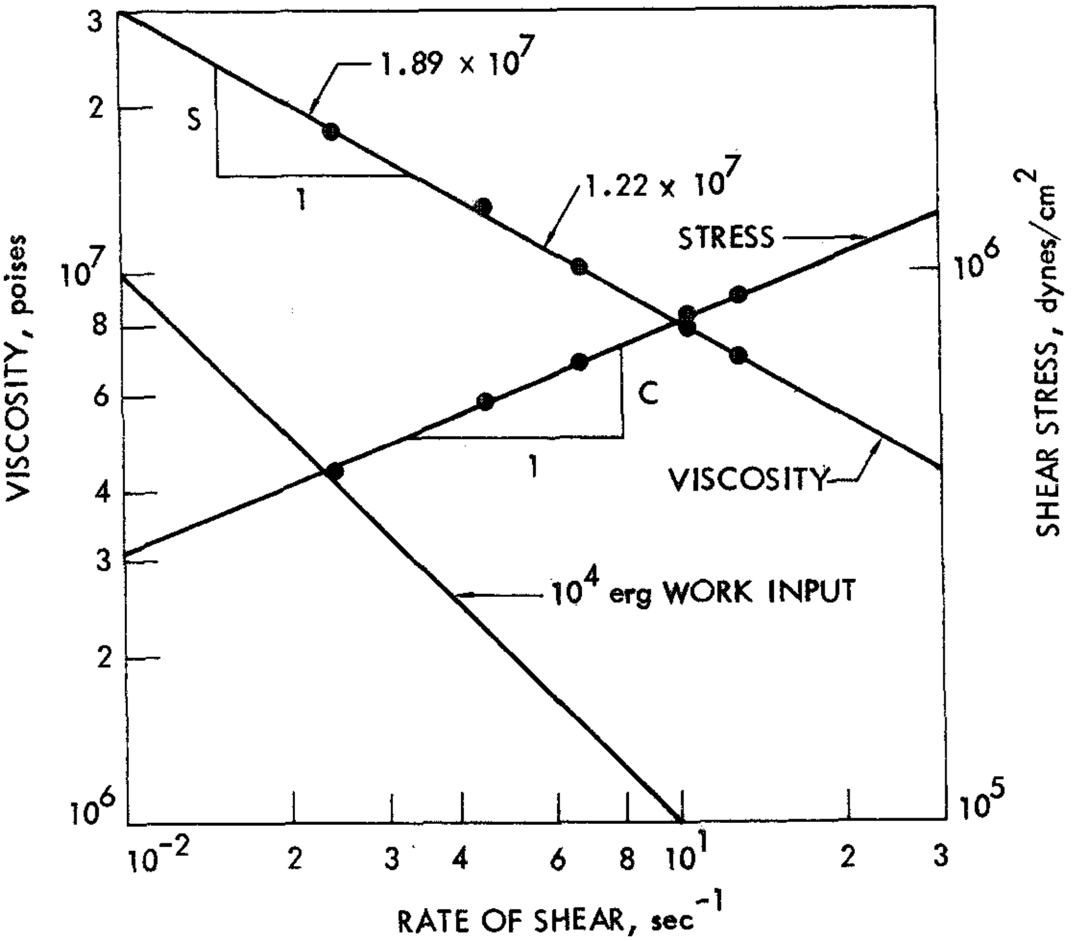

Fig. 3. Typical rheological diagram from viscosity test.

films of desired thicknesses), a working range of 1 to 10^4 megapoises can be achieved. Thus, it is possible not only to study the viscosity of aged (both natural and artificial) asphalts but also of asphalts at lower temperatures. Both the steel plates and the spacers were obtained from Hallikainen Instruments of Richmond, California. During this period, working procedures using the new plates were established and calculation charts were produced. The repeatability, about 10% of the mean, compares favorably with that obtained by using 20 × 30 mm glass plates.

The cone-plate viscometer used in this study was manufactured by Cannon Instruments Corporation, College Park, Pennsylvania, and is essentially the same as originally designed by Sisko[63].

Three basic equations were used for the calculation of viscosity, shear rate, and shear stress:

$$\text{Viscosity, poises, (p)} = K_\eta(L - 1f)(t/\theta) \quad (1a)$$

$$\text{Shear rate, sec}^{-1}\text{, }(\alpha) = K_D(\theta/t) \quad (1b)$$

$$\text{Shear stress, dynes/cm}^2\text{, }(\tau) = K_s(L - 1f) \quad (1c)$$

where t = measured time of rotation, sec

θ = measured angle of rotation, deg

L = applied load, g

$1f$ = net friction determined in calibration

K_η = viscosity constant, p-deg/g-sec

K_D = shear rate constant, deg^{-1}

K_s = shear stress constant, dynes/cm^2/g.

The three main constants are related by

$$K_D = K_s/K_\eta \ . \quad (2a)$$

The viscometer was calibrated using a standard viscosity oil obtained from the US Bureau of Standards. K_s was governed by the geometry of the instrument. In the study three cone sizes were used (with radii of 0.940, 1.880, and 3.755 cm, and respective cone angles of 0.59, 0.44, and 0.43 deg) in connection with two cords. The ranges of values of the three constants are

K_η = 13.4 to 1215

K_D = 1.692 to 2.324

K_s = 31.550 to 2061.883.

Viscosity determination involves selecting proper core size, making an asphalt film between cone and plate, applying torque loads, and observing rotation angle in some selected time interval t. Rheological diagrams can be constructed for each sample by applying various loads to the specimen and calculating corresponding shearing stress, rate of shear, and viscosity.

Viscosity at 140 °F was determined by Cannon-Manning vacuum viscometers following standard procedures.

Due to the limited quantity of recovered asphalts that would be available, all ductility tests were made at 77 °F on 1/2-in. × 1/2-in. microductility molds developed by the Phillips Petroleum Company and used in previous projects[8,64]. The use of microductility specimens also makes the differentiation among asphalts possible within the limits of the ductility machine (150 cm).

The rheological behavior of asphalts in a brittle state of subzero temperatures was studied indirectly by the Fraass brittle point test. This test has been used by Lee and Dickinson[65] in Great Britain and Jones[66,67] in Canada to evaluate low temperature behaviors of coal tars and roofing asphalts. Brittle point determinations for asphalts in this study were made on samples with a film thickness of 0.55 mm and a rate of cooling of 1 °C/min, using modified brittle point testers. The detailed procedures are given in Appendix E. Figures 4 and 5 show the general setup and the brittle point tester.

The dynamic modulus of the asphalts were determined by a Dynamic Modulus Tester PPM-5R, planar mount md model, manufactured by H. M. Morgan Company, Inc., of Cambridge, Massachusetts. The tester has been

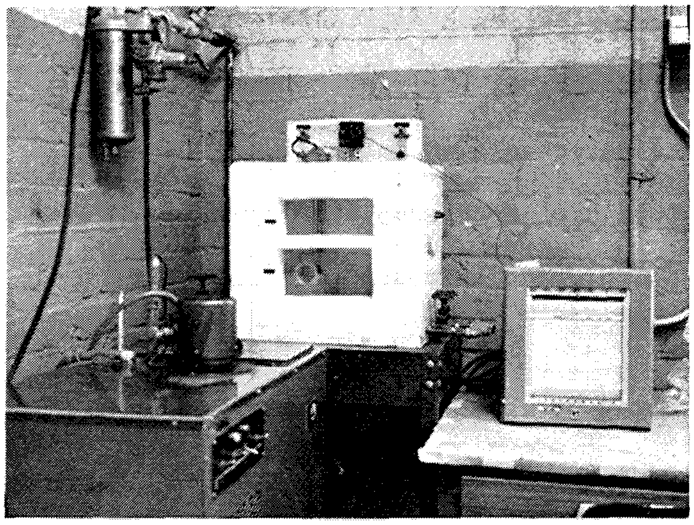

Fig. 4. General setup of Fraass brittle point test.

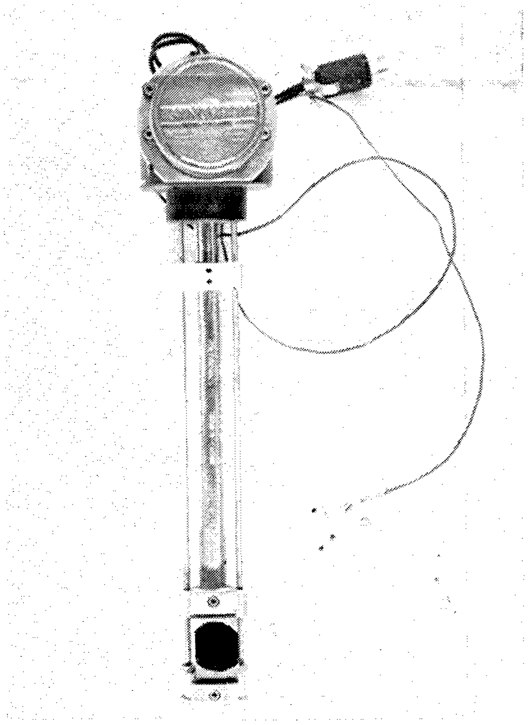

Fig. 5. Close-up view of Fraass brittle point test.

used as a recommended method by ASTM for determination of dynamic (sonic) modulus of paper and plastic sheets[68]. Sample strips of 1 in. X 4 in. were prepared by heating asphalts and pouring them on nonsound conducting silicon sponge rubber pads of 1/4 in. X 1-1/2 in. X 6 in. Sonic longitudinal velocity (c) at 21 °C and at - 10 °C were determined by measuring pulse travel times in microseconds (μsec) at several predetermined transducer separation distances of 10 to 2 cm. The sonic velocity was determined by distance vs time plot and instrument delay or zero time determined from the plot. The dynamic modulus is calculated by

$$E_s(\text{dynes/cm}^2) = \rho c^2 \times 10^{10} \text{ or} \quad (3a)$$

$$E_s(\text{psi}) = \rho c^2 \times 1.45 \times 10^5 \quad (3b)$$

where c = sonic longitudinal velocity, km/sec or mm/μsec, and
ρ = density of material, gm/cm^3.

Young's modulus E can be calculated from the sonic modulus E_s by the following equation, if Poisson's ratio ν is known:

$$E = E_s(1 - \nu^2).$$

Because the possible correlation between low temperature cracking (especially transverse) of asphalt pavements and the glass transition temperature of asphalt[70], several HR-124 asphalts were sent to duPont Instruments, Wilmington, Delaware, for thermal analysis. DSC (differential scanning calorimetry) and TMA (thermomechanical analysis) scans were made on four original asphalts (1a, 2a, 4a, and 6a), two laboratory weathered samples (1d and 1d-96), and three field aged samples (1f, 1f-24, and 1f-30) using a duPont 900 Thermal Analyzer with a DSC cell and a 941 TMA module. TMA scans were run in the expansion mode.

Chemical Tests

The chemical approach to durability studies of asphalts has been criticized as premature due to lack of definitive knowledge on chemical composition and structure of asphalt. However, this is a fundamental approach. It has been proved that chemical composition does have direct effects on rheological and durability properties of asphalt, that the relationship between asphalt durability and chemical composition could be established[12,70,71], and that the durability grouping of asphalts by chemical composition was possible[71,72].

Asphaltene content and oxygen percentage have been used as parameters for chemical changes. Asphaltene content was determined by precipitation with a Skelly F[73], and oxygen content was determined by combustion method using a Coleman Oxygen Analyzer.

Chemical analysis of asphalts 1 to 4 was also made by a method suggested by Rostler and White[70] and Halstead et al.[71] to determine the relationship between asphalt durability and $(N + A_1)/(A_2 + P)$. The procedure used in this study was essentially that described by Rostler and White. Separation of components by this method is based on the relative reactivity of various fractions with respect to acid. Figure 6 is a flow chart of the analytical procedure. Because this procedure is very time consuming (it takes 3 to 4 days for a complete analysis

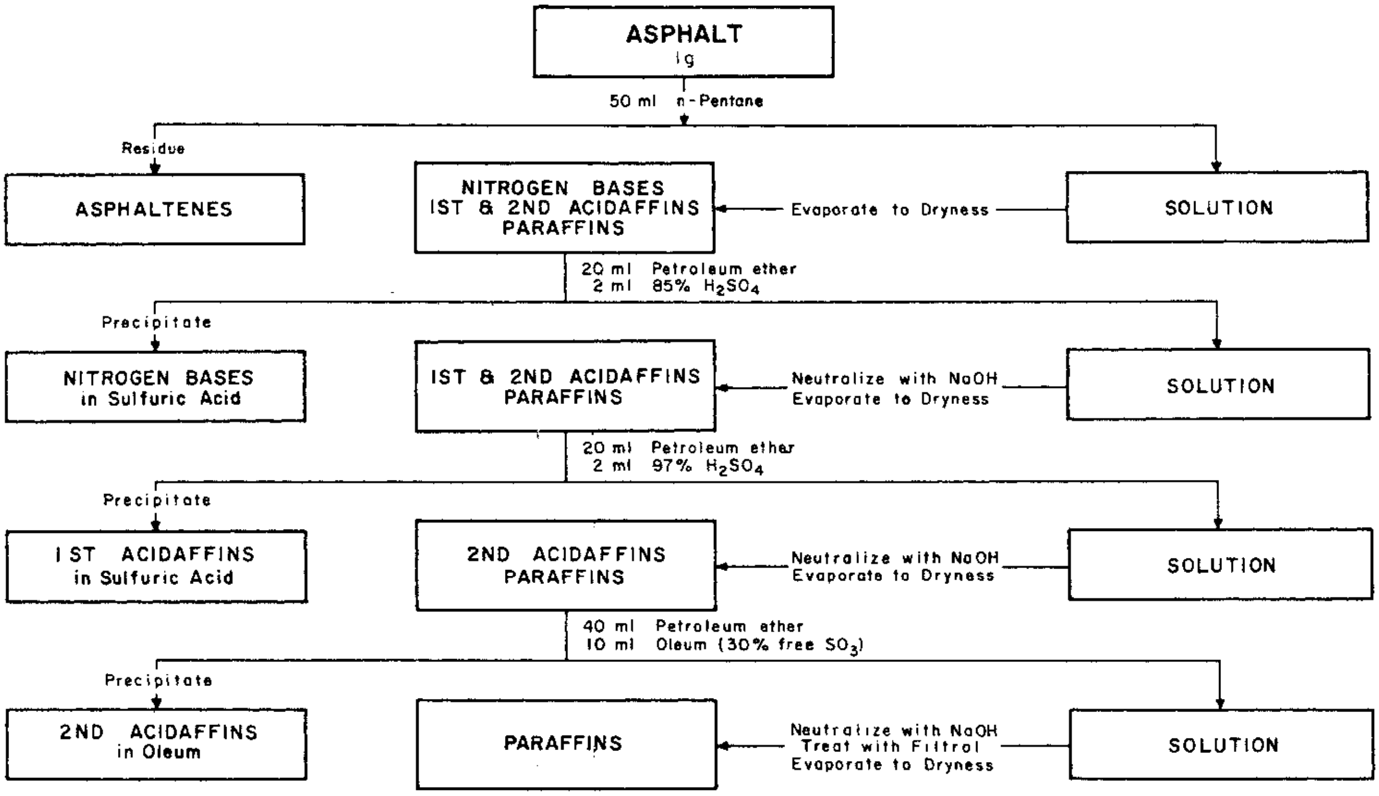

Fig. 6. Flow chart of Rostler-Steinberg analytical method.

of one sample) and is not very reproducible, a large amount of research effort in the second half (1969-71) of this project was in this phase of study.

During the second half of this investigation, analysis of asphalts by infrared spectroscopic techniques was undertaken to determine the changes in infrared spectra of asphalts during field ageing as well as laboratory ageing, and if possible to establish relationship between asphalt durability and its infrared spectrum.

Attempts to characterize asphalt by infrared spectroscopic techniques have been made by many researchers[73-81]; the most significant to date has been the finding by Greenfeld and Wright[77] that a relationship existed between durability of roofing asphalts and carbonyl index change in IR spectrum. The immediate objectives of IR examination of asphalt in this investigation were to verify the above relationship for paving asphalts, and to identify other wave lengths or peaks that may characterize durability differences among paving asphalts.

Three techniques are available for infrared spectroscopic study of asphalts:

1. Dissolving asphalt in a solvent such as carbon tetrachloride (CCl_4) and scan in a liquid cell (transmission mode).
2. Preparing asphalt films of predetermined size and thickness between sodium chloride (NaCl) crystal plates and scan in a demountable cell (transmission mode).
3. Using the multiple internal reflectance technique.

During this study all three methods were experimented with on a Beckmen IR-4 spectrophotometer. The third technique was selected for the study. It eliminates the difficulties in interpreting and inferring the results of IR spectra from asphalt in solution on the behavior of asphalt in pavement as in technique 1. It also eliminates the difficulties in preparing reproducible, uniform films of predetermined thickness (a film thickness of 50 μ was experimented) as in technique 2. In this technique sample preparation is relatively simple and comparison between different sample and different runs of the same sample is relatively easy.

V. IOWA DURABILITY TEST

The true value of any laboratory durability test should be judged from the answers to the following questions: (a) How logical or realistic is the acceleration process in the laboratory as compared with what actually occurs in the field? (b) How well can the tests or properties measured indicate the actual changes that cause deterioration of asphalt? (c) How good is the correlation between laboratory and field data?

The proposed Iowa Durability Test simulates as realistically and as completely as possible the two-stage hardening of asphalt during mixing and subsequent pavement service life. The test makes use and takes advantage of the well-established BPR thin film oven test (TFOT); it consists of first subjecting the asphalt to the TFOT and then treating the residue from the TFOT in oxygen at high pressures. The TFOT at 325 °F is used to simulate the changes that may occur in asphalt during mixing; the pressure oxidation process at 150 °F is used to simulate the changes that may occur in asphalt during pavement service life.

The effectiveness of the proposed test in accelerating the hardening and other changes of asphalt, the ability of the test in differentiating asphalts with respect to resistance to changes (both physical and chemical), and the effects of time and oxygen pressure were reported elsewhere[1-3]. In the following sections the development of the Iowa Durability Test (IDT), the established procedure, and the changes in the asphalts studied during IDT will be discussed.

Development and Rationale

In our study of the durability of asphalt and in the development of the test procedure, the following premises and concepts were formulated and followed:

1. The most important single factor that causes asphalt pavement to crack and disintegrate is the failure of the asphalt as a cementing and waterproofing agent in an asphalt mixture due to asphalt hardening. Therefore the extent and rate of asphalt hardening is considered to be indicative of the relative durability of asphalt.
2. The hardening and other pertinent changes that may occur in asphalt in an asphaltic concrete mix take place in two stages under two entirely different environments or conditions: as hardening during short periods in the mixer at higher temperatures and higher rates, and as hardening during longer periods of road service in pavement at relatively lower temperatures and lower rates. The hardening mechanisms and effects in these two stages are believed to be quite different.
3. It is believed that, among the factors causing asphalt hardening, evaporation of volatiles and high-temperature oxidation predominate during the mixing process. Oxidation at road service temperatures, especially in absence of light, seems to predominate under service conditions.
4. Any realistic durability test for asphalt should include consideration of the two stages of hardening processes of asphalt in their logical order and of their differences in mechanisms and effects.

5. In evaluating the quality or durability of asphalts, one is concerned with not only the characteristics of the original asphalt but even more importantly with the binder characteristics – viscosity, tendency to harden, susceptibility to oxidation, colloidal stability, etc. – of the asphalt in the finished pavement. This would include study of the asphalt after the first stage of hardening and would provide assurance that the properties of the binder following construction are satisfactory for future pavement performance.
6. Hardening during the mixing process may be simulated and predicted in the laboratory by the BPR thin film oven test. Additional hardening and other changes in the asphalt in service may be simulated by laboratory pressure-oxidation tests at road service temperature on residue of the TFOT.
7. A definite correlation may be established, at least on a local basis, between field hardening and performance of asphalt and laboratory-accelerated hardening during a logically conceived and realistic durability test. The asphalt hardening in the field in terms of years could be reasonably predicted in terms of hours or days.

It was with these concepts and considerations that the Iowa Durability Test was devised. The overall program included the following steps:

1. Determining the rheological and colloidal-chemical properties of the original asphalts,
2. Running the BPR thin film oven tests and determining the characteristics of asphalts on the residues,

3. Treating the TFOT residues in oxygen at 150 °F under various pressures for various lengths of time,
4. Determining asphalt characteristics on pressure-oxidized TFOT residues,
5. Establishing field service correlation, and
6. Establishing asphalt quality or usefulness criteria in terms of rheological or chemical properties or both.

Iowa Durability Test Procedure

To stimulate or reproduce the two-stage ageing and hardening of the asphalts in the field, the laboratory durability test procedure finally adopted was:

1. BPR Thin Film Oven test on the original asphalt,
2. Pressure-oxidation treatment on the residue from the TFO test in a pressure vessel for up to 1000 hr under the following conditions:

   Film thickness: 1/8 in.
   Temperature: 150 °F
   Pressure: 20 atm oxygen,
3. Evaluation of the physical and chemical changes in asphalt during the artificial ageing process in relation to the original properties of the asphalt.

The detailed procedures are given in Appendix D.

Repeatability

The repeatability and reproducibility of IDT is obviously affected by the repeatability and reproducibility of the TFOT, which were studied and reported elsewhere[61,80]. The repeatability of the pressure-oxidation test in pressure bomb during the initial phase of HR-124 was reported in Refs. 1 and 2. The repeatability was determined by making repeat treatments under identical conditions of: temperature (150 °F), pressure (132 psig), film thickness (1/8 in.), and duration (24 hr) on residues of TFO tests from two asphalts. Repeatability was measured by viscosity with a sliding-plate microviscometer at 77 °F and at a rate of shear of 5×10^{-2} sec^{-1}. The results of six treatments on each asphalt are given in Table 4.

Based on these results, it was concluded that the pressure-oxidation test is reproducible. The variability or accuracy of the proposed durability test procedure is controlled by the variability and reproducibility of the TFOT and viscosity determinations.

During the second phase of HR-124, the repeatability of the Iowa Durability Test in 7-1/2 in. pressure vessels was again tested on asphalts No. 2 and 6. The repeatability was evaluated by penetration, viscosity at 77 °F, and rate of shear of 5×10^{-2} sec^{-1}, as well as softening point. The results are shown in Table 4a.

The IDT in a 7-1/2 in. pressure vessel, run under prescribed procedure, was considered repeatable.

Table 4. Viscosity at 77 °F of TFOT residues treated in oxygen bombs at 132 psig, 150 °F and in films of 1/8 in. for 24 hr.

Bomb	A.C. A	A.C. B
A	12.8	4.95
A	13.5	4.50
A	13.5	5.00
Av bomb A	13.3	4.82
B	13.3	5.00
B	13.3	5.00
B	13.0	5.20
Av bomb B	13.2	5.07
Grand average	13.2	4.15
Standard deviation	0.283	0.233
Maximum deviation from mean, %	3.0	9.1
Average deviation from mean, %	1.8	2.9

Changes in Rheological Properties

Rheological changes in asphalts during IDT were measured by penetration, viscosity at 77 °F, at 140 °F, softening point, ductility, brittle point and sonic modulus. The results of penetration change with time are given in Table 5 and are plotted in Figs. 3 through 7i. The results of viscosity change measured at 77 °F and at 5×10^{-2} sec^{-1} with time are given in Table 6. Plots of log viscosity vs time are shown in Figs. 8a through 8i. Similar results for viscosity at 140 °F are given in Table 7 and Figs. 9a through 9i. From viscosity at 77 °F

Table 4a. Iowa Durability Test repeatability study, behavior of asphalts.

A.C.	Treatment	Time, hr	Penetration	Viscosity, megapoises	Softening point, °C
2	TFOT	0	54.0	5.4	55.0
	1	24	33.5	11.7	56.5
	2	24	34.0	11.8	57.0
6	TFOT	0	55.0	3.8	53.0
	1	48	32.0	14.4	60.5
	2	48	31.0	14.8	60.0
	1	96	27.0	20.2	62.5
	2	96	27.5	21.0	62.5

data, complex flow index c and shear susceptibility index S or SI were calculated for all nine asphalts and are given in Table 8. Viscosity at constant energy input or work η_w and at constant shearing stress η_e were also calculated for asphalts 1 to 4 and are given in Table 8. Results of softening point are given in Table 9 and are plotted in Figs. 10a through 10i. Changes in microductility at 77 °F with laboratory ageing time are given in Table 10 and Figs. 11a through 11i. Except in a few instances for ductility, all the above property changes were found to follow the hyperbolic model suggested by Brown et al.[83] This is significant because it agrees with reported actual field hardening in service[83-86]. It also suggests that (a) the IDT is realistic and (b) that the correlation between field hardening and hardening of asphalt in the IDT is possible.

Table 5. Changes in penetration during weathering.

Project number		Penetration, 77/100/5								
		1	2	3	4	5	6	7	8	9
		(A. C. Number)								
Original (a)		89	94	91	90	84	87	95	90	92
TFOT (d)		53	54	57	56	67	55	59	60	62
Lab ageing										
24 hr (d24)		30	34	36	38[‡]	49[‡]	50	44[‡]	44[‡]	37
48 hr (d48)		29	30	30	31	41	32	37[‡]	33	27
96 hr (d96)		26	25	26	25	37	27	29[‡]	30	24
240 hr (d240)		19	20	20	20	27	22	19[‡]	26	21[‡]
480 hr (d480)		13[‡]	17	16[‡]	17[‡]	20[‡]	21	16[‡]	22[‡]	23
1000 hr (d1000)		11	13[‡]	8	10	11	14	10	15	–
Field ageing										
Plant (p)		60	72	57	67	–	71	76	74	79
0 months (f0)	A[*]	57	67	57	62	–	–	79	71	64
	B[†]	57	67	57	62	–	–	–	–	–
6 months (f6)	A	61	56	48	57	–	39	41	43	51
	B	56	58	52	62	–	40	41	43	56
12 months (f12)	A	43	37	42	39	–	37	35	42	53
	B	39	38	38	35	–	39	42	45	49
18 months (f18)	A	41	38	40	34	–	34	35	35	39
	B	43	36	39	36	–	34	35	36	41
24 months (f24)	A	39	35	35	38	–	36	37	38	41
	B	36	35	34	29	–	35	36	39	39
30 months (f30)	A	35	33	32	30	–	33	35	35	40
	B	33	31	34	32	–	34	33	35	38
36 months (f36)	A	36	34	30	30	–	–	36	36	36
	B	37	32	29	30	–	–	35	35	31

Table 5. Continued.

Project number		Penetration, 77/100/5								
		1	2	3	4	5	6	7	8	9
		(A. C. Number)								
42 months (f42)	A	37	33	31	29	–	28	–	34	–
	B	39	29	32	28	–	28	–	34	–
48 months (f48)	A	28	28	27	26					
	B	31	28	27	26					

*A, in wheel tracks.

†B, between wheel tracks.

‡Interpolated value.

According to this theory, the changes in physical properties of asphalt are a hyperbolic function of time and approach a definite limit with time. Brown et al. have suggested the following equation to express the hardening of asphalts in the field:

$$\Delta Y = \frac{T}{a + bT} \tag{3}$$

or

$$\frac{T}{\Delta Y} = a + bT \tag{4}$$

where ΔY = change in penetration (or softening point or ductility) with time T or the difference between the zero-life value and the value for any subsequent year

T = time

a = constant, the intercept of the Eq. (2) line on the ordinate

b = slope of the line Eq. (4)

$1/b$ = the ultimate change (limiting value of change) of penetration at infinite time.

Note that from the limiting values of change, 1/b the limiting values of properties (Y_u) can also be calculated. Both values could be used

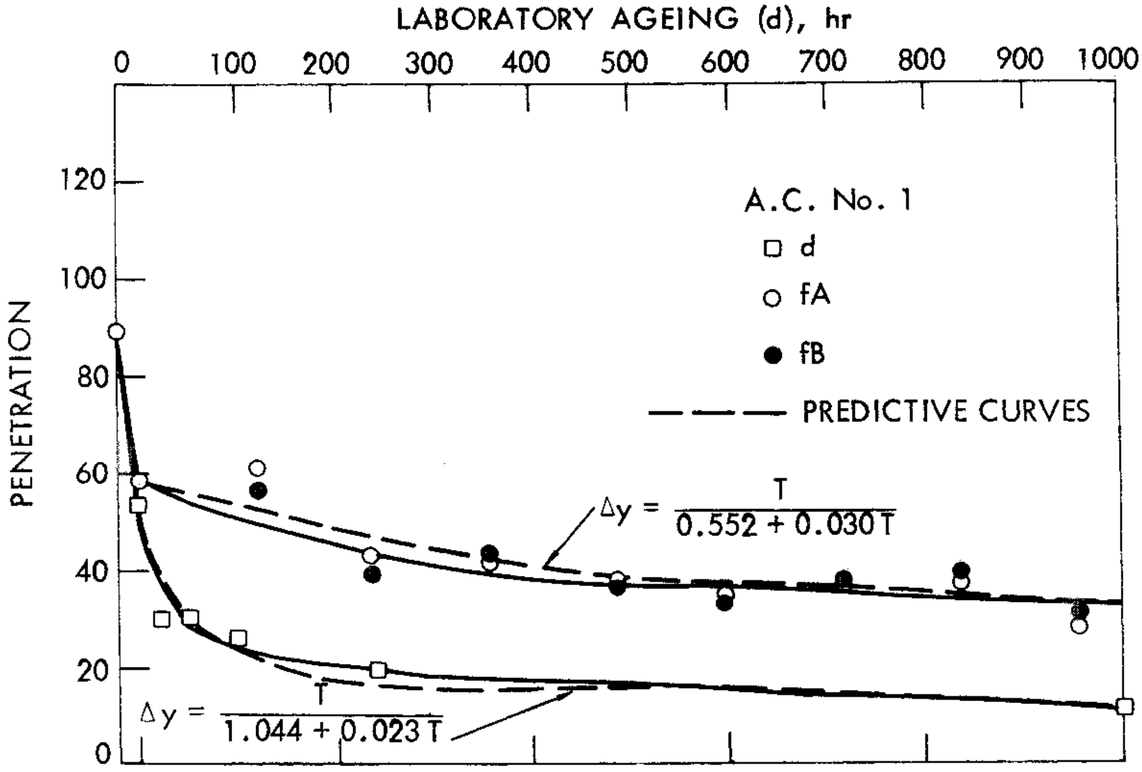

Fig. 7a. Penetration vs time of ageing, A.C. No. 1.

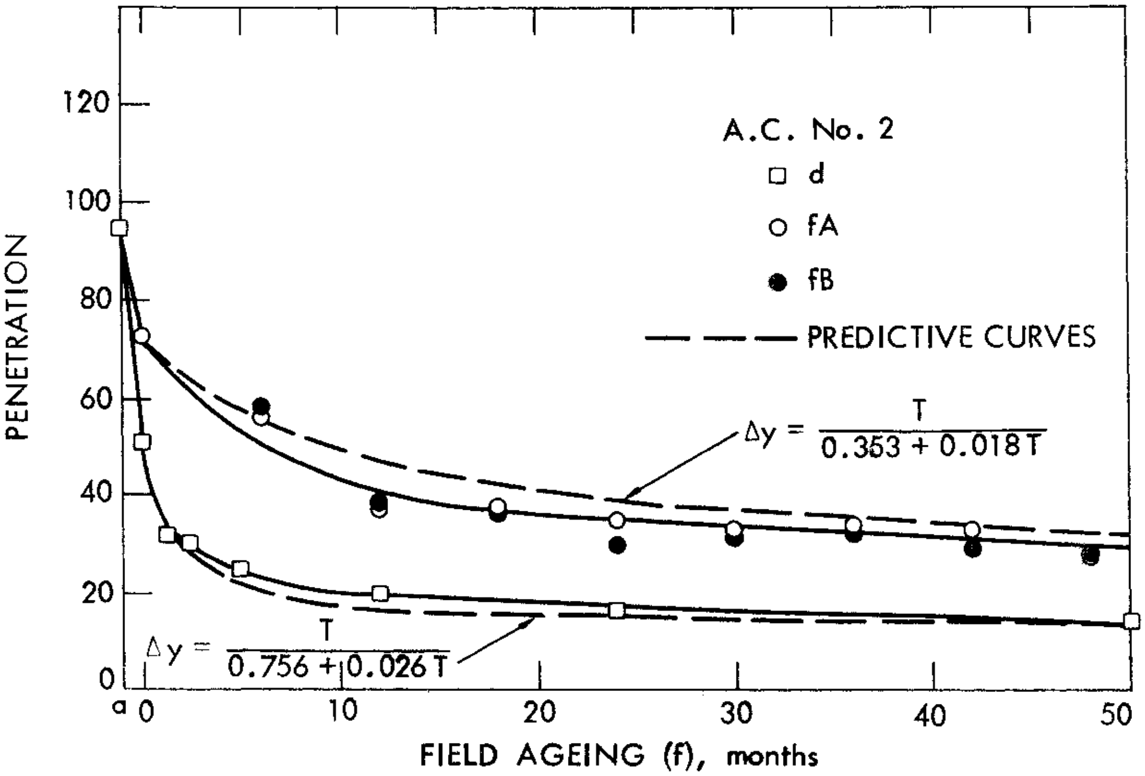

Fig. 7b. Penetration vs time of ageing, A.C. No. 2.

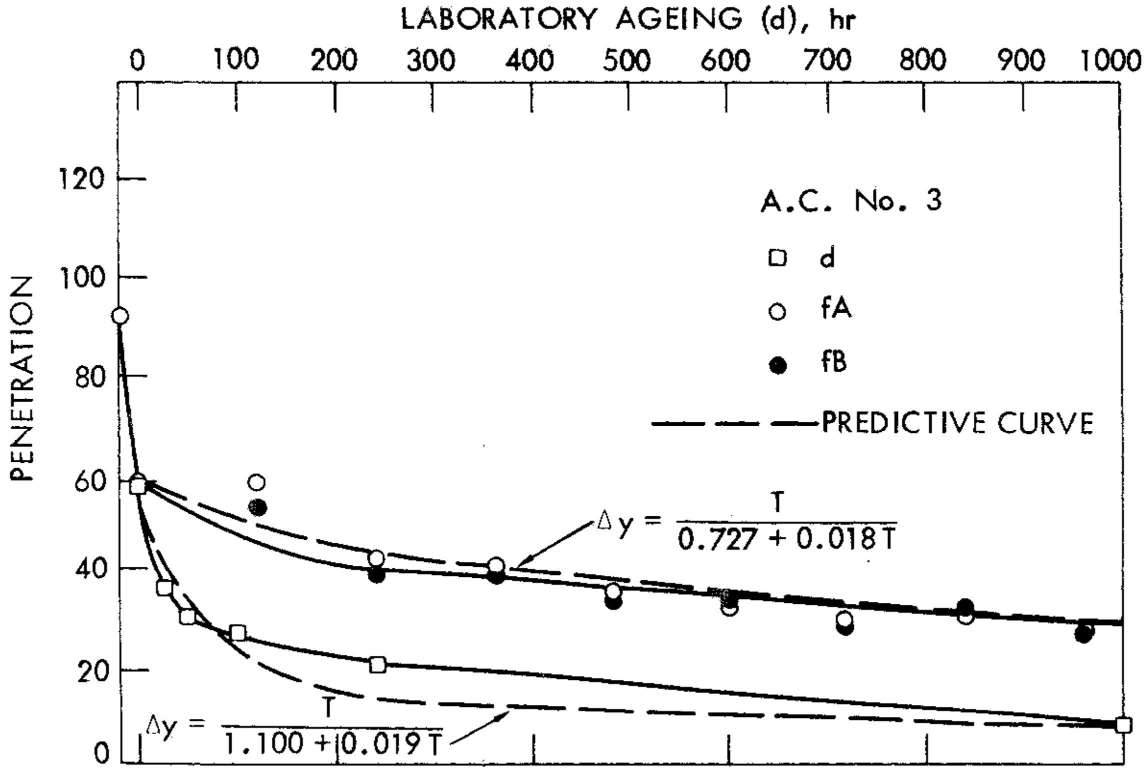

Fig. 7c. Penetration vs time of ageing, A.C. No. 3.

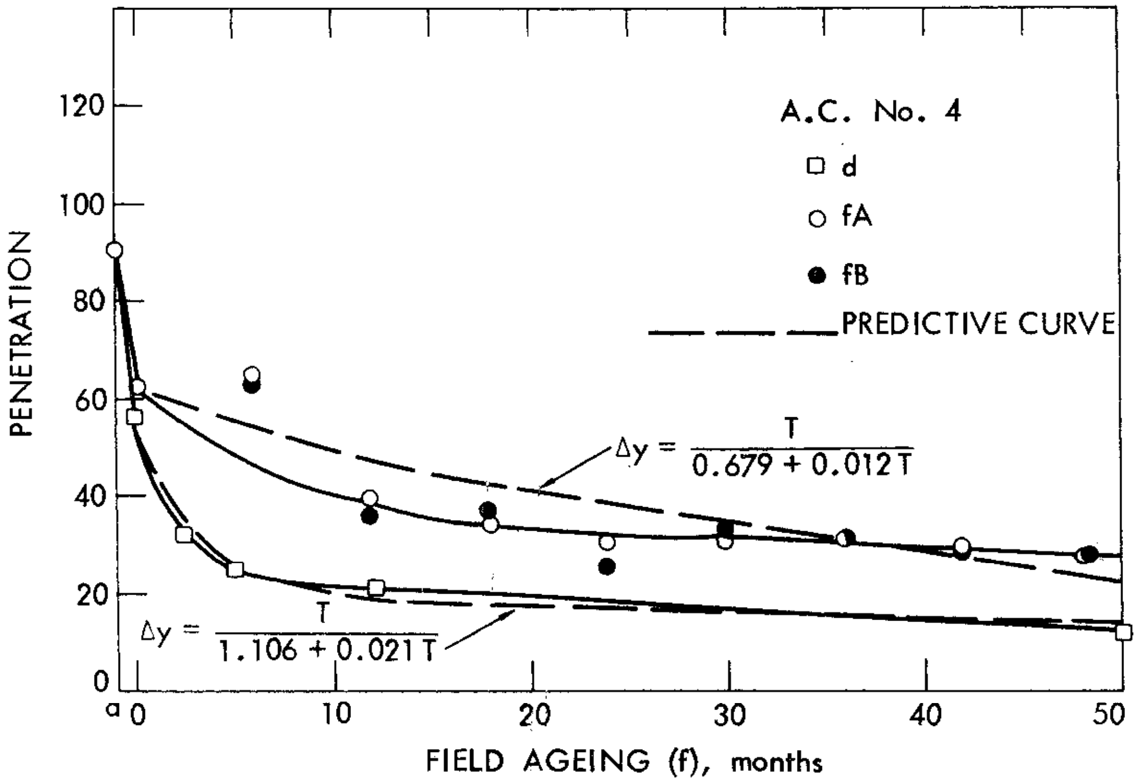

Fig. 7d. Penetration vs time of ageing, A.C. No. 4.

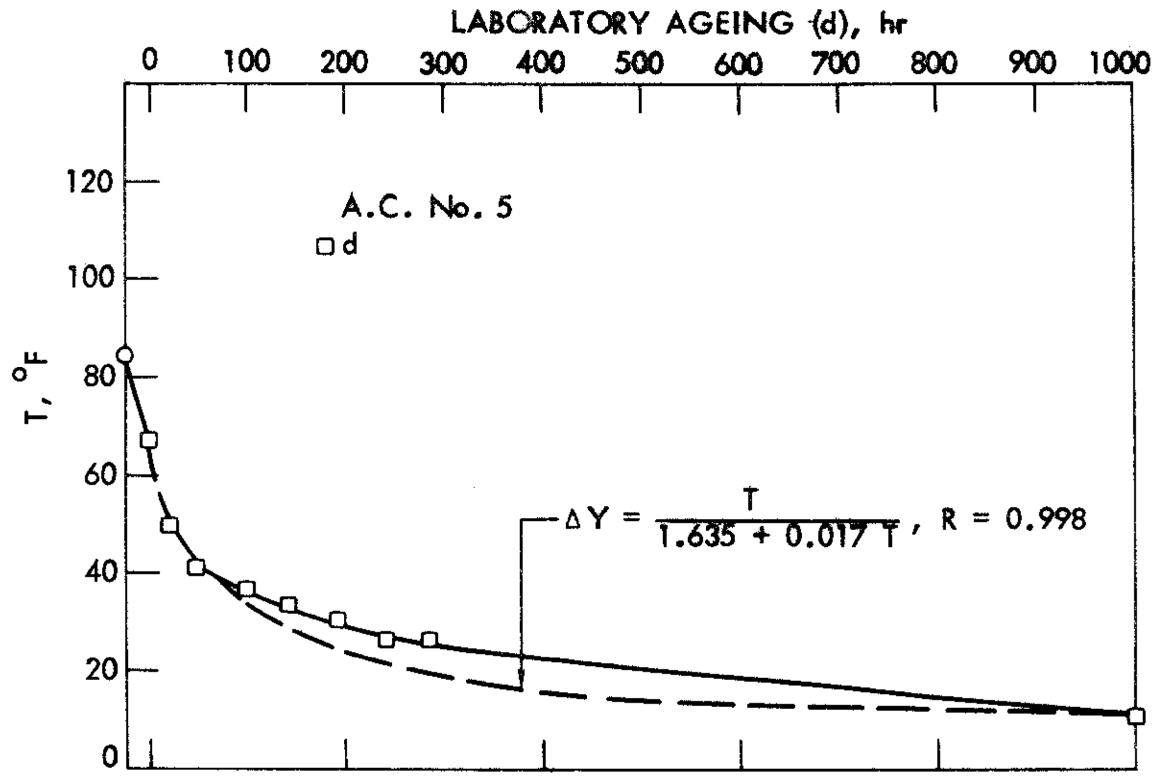

Fig. 7e. Penetration vs time of ageing, A.C. No. 5.

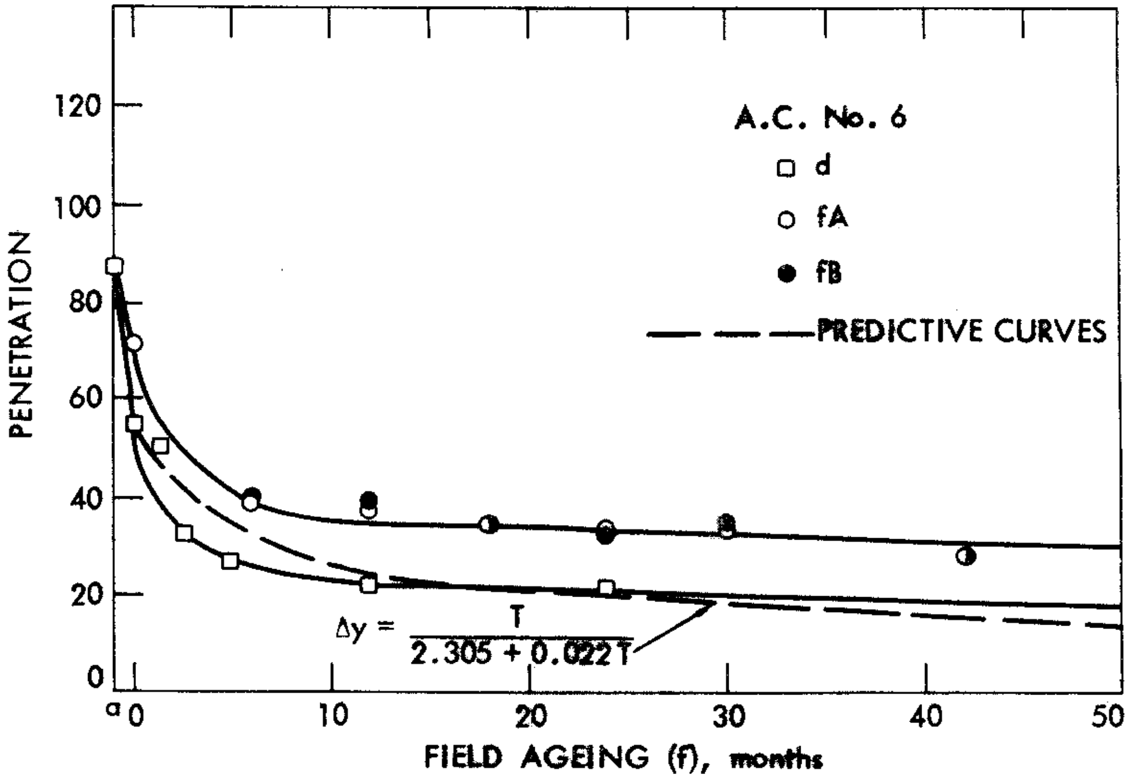

Fig. 7f. Penetration vs time of ageing, A.C. No. 6.

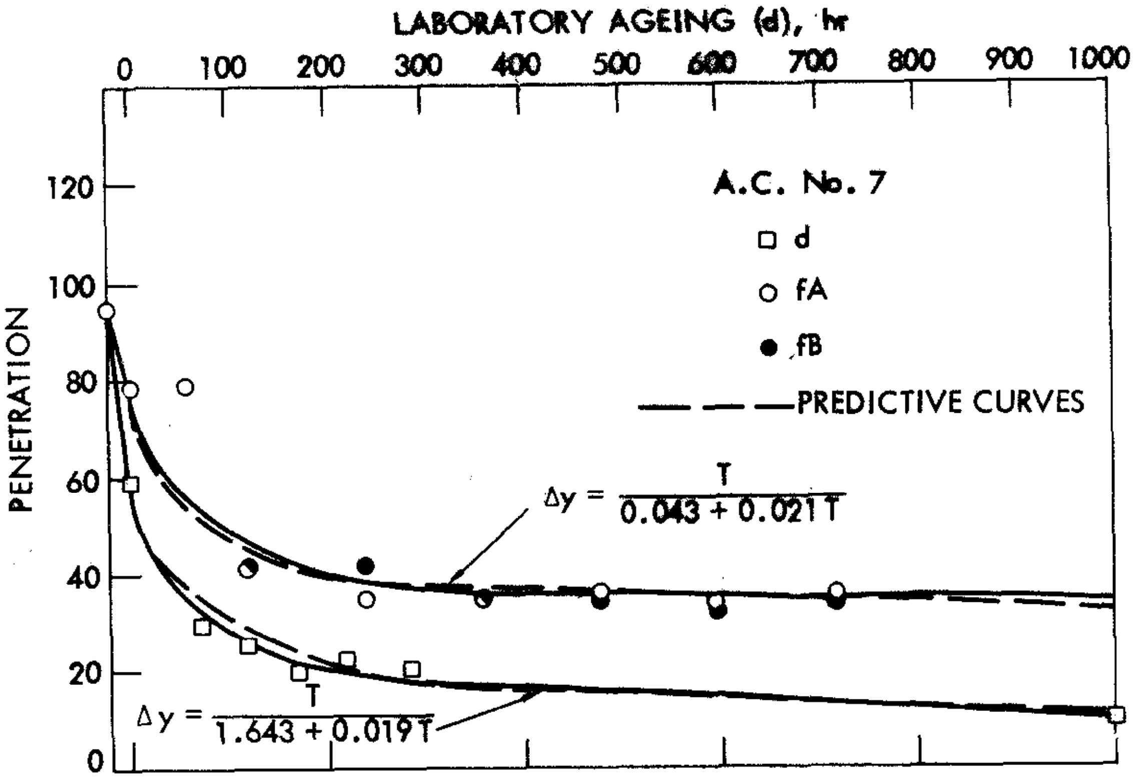

Fig. 7g. Penetration vs time of ageing, A.C. No. 7.

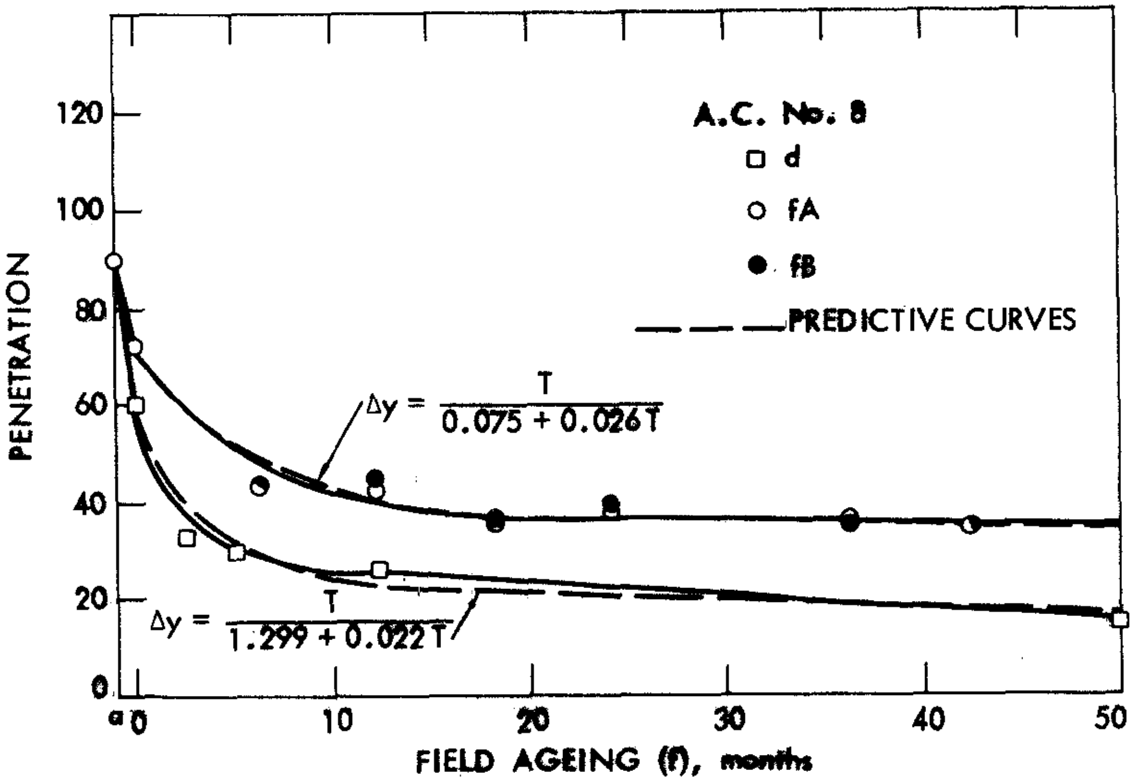

Fig. 7h. Penetration vs time of ageing, A.C. No. 8.

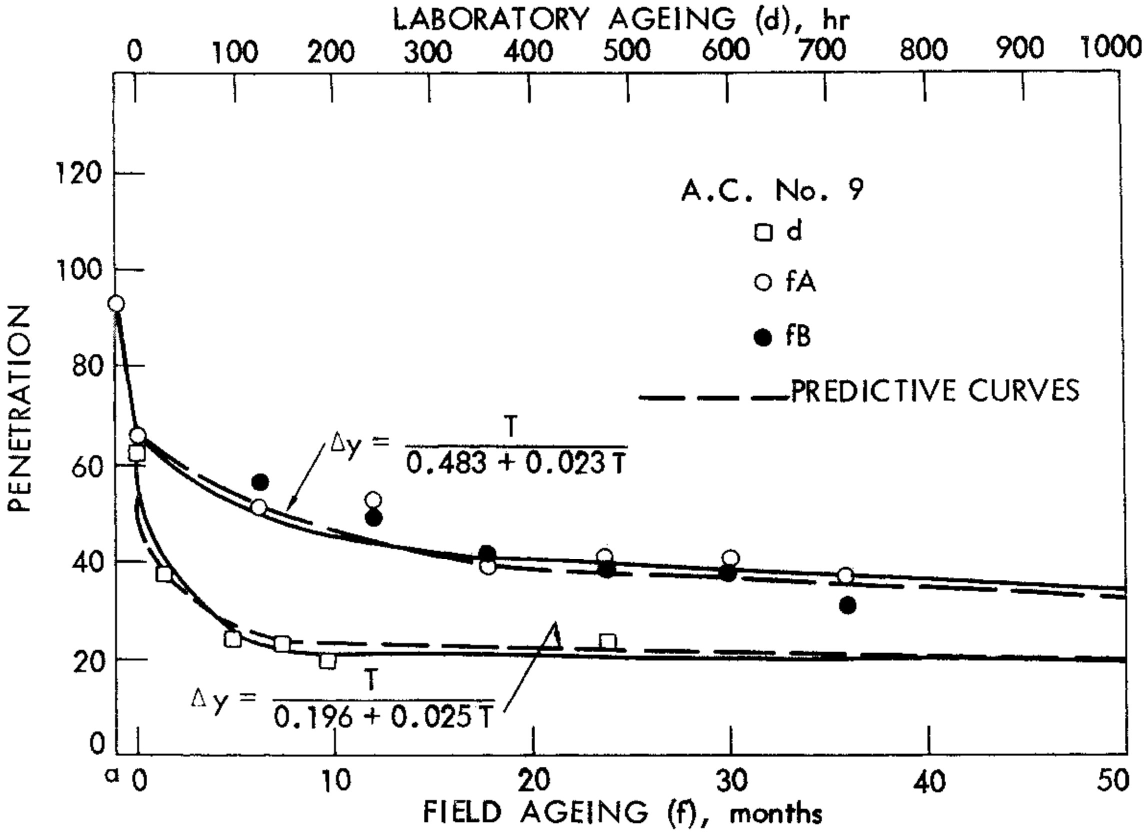

Fig. 7i. Penetration vs time of ageing, A.C. No. 9.

as numerical measures for comparison of the relative performances of asphalts. Thus an asphalt with a high value of limiting change of penetration or a low value of limiting penetration could be considered as inferior to one with a low value of limiting change of penetration or a high value of limiting penetration. The significance of constants a, b, and 1/b is illustrated in Figs. 12a and 12b by two asphalts with the same initial penetration with different rate of change with time. Figures 13a and 13b show $T/\Delta Y$ vs T for penetration change of A.C. No. 1 through 4.

Experimental data were fitted to Eq. (4) by the least-square linear regression method. The resultant equations in terms of a and b are given in Table 11. Also reported are correlation coefficients R and the ultimate change 1/b. Predicted curves were also plotted in all

Table 6. Changes in viscosity at 77 °F.

A.C. No.		Viscosity at 77 °F, megapoises								
		1	2	3	4	5	6	7	8	9
Original (a)		1.16	1.23	1.58	1.10	1.14	1.70	1.15	1.10	1.22
TFOT (d)		4.22	5.35	3.70	3.09	1.68	3.80	3.90	4.15	2.86
Lab ageing										
24 hr (d24)		18.4	11.7	9.50	9.0‡	3.50‡	–	7.00‡	8.30‡	10.30
48 hr (d48)		20.5	19.3	14.2	15.7	5.60	14.60	12.50‡	12.60	12.50
96 hr (d96)		23.9	24.6	19.2	22.6	7.40	21.00	22.00‡	14.80	15.00
240 hr (d240)		44.0	36.2	47.0	36.9	13.50	33.00	51.00‡	38.00	27.50‡
480 hr (d480)		64.5‡	38.5	76.0‡	52.0‡	14.70‡	37.00	78.50	53.50‡	45.00‡
1000 hr (d1000)		89.0	–	118.0	64.0	17.30	72.00	99.20	64.00	69.00‡
Field ageing										
Plant (p)		4.30	4.70	3.40	3.09	–	2.81	2.07	3.42	2.29
0 months (f0)	A*	4.87	4.60	3.39	3.01	–	–	2.25	2.14	2.61
	B†	4.87	4.60	3.39	3.01	–	–	–	–	–
6 months (f6)	A	4.30	5.98	3.40	3.56	–	8.58	8.30	6.40	4.90
	B	5.70	5.35	3.78	3.50	–	8.70	8.74	6.40	3.90
12 months (f12)	A	9.80	8.90	9.66	11.2	–	10.60	9.80	14.50	11.50
	B	9.54	9.20	–	12.2	–	11.90	9.80	12.50	8.90

Table 6. Continued.

A.C. No.		Viscosity at 77 °F, megapoises 1	2	3	4	5	6	7	8	9
18 months (f18)	A	12.7	8.33	12.4	13.9	—	12.10	12.80	11.50	10.50
	B	11.5	10.28	12.0	15.5	—	13.80	12.00	10.90	10.50
24 months (f24)	A	12.2	—	12.6	21.0	—	12.70	14.50	9.80	12.00
	B	15.0	15.0	11.9	18.6	—	7.80	12.20	8.90	8.40
30 months (f30)	A	14.5	18.5	17.0	20.5	—	13.50	12.00	13.50	9.68
	B	18.5	19.2	13.2	21.6	—	17.50	12.00	14.00	9.10
36 months (f36)	A	12.3	13.8	21.0	16.2	—	—	13.80	—	11.50
	B	12.5	16.0	19.6	17.7	—	—	—	—	—
42 months (f42)	A	13.4	17.8	18.8	16.2	—	17.50	—	12.50	—
	B	9.5	16.5	14.0	22.2	—	—	—	—	—
48 months (f48)	A	19.2	19.6	20.7	21.8					
	B	16.4	20.9	16.1	22.0					

[*] A, in wheel tracks.

[+] B, between wheel tracks.

[‡] Interpolated value.

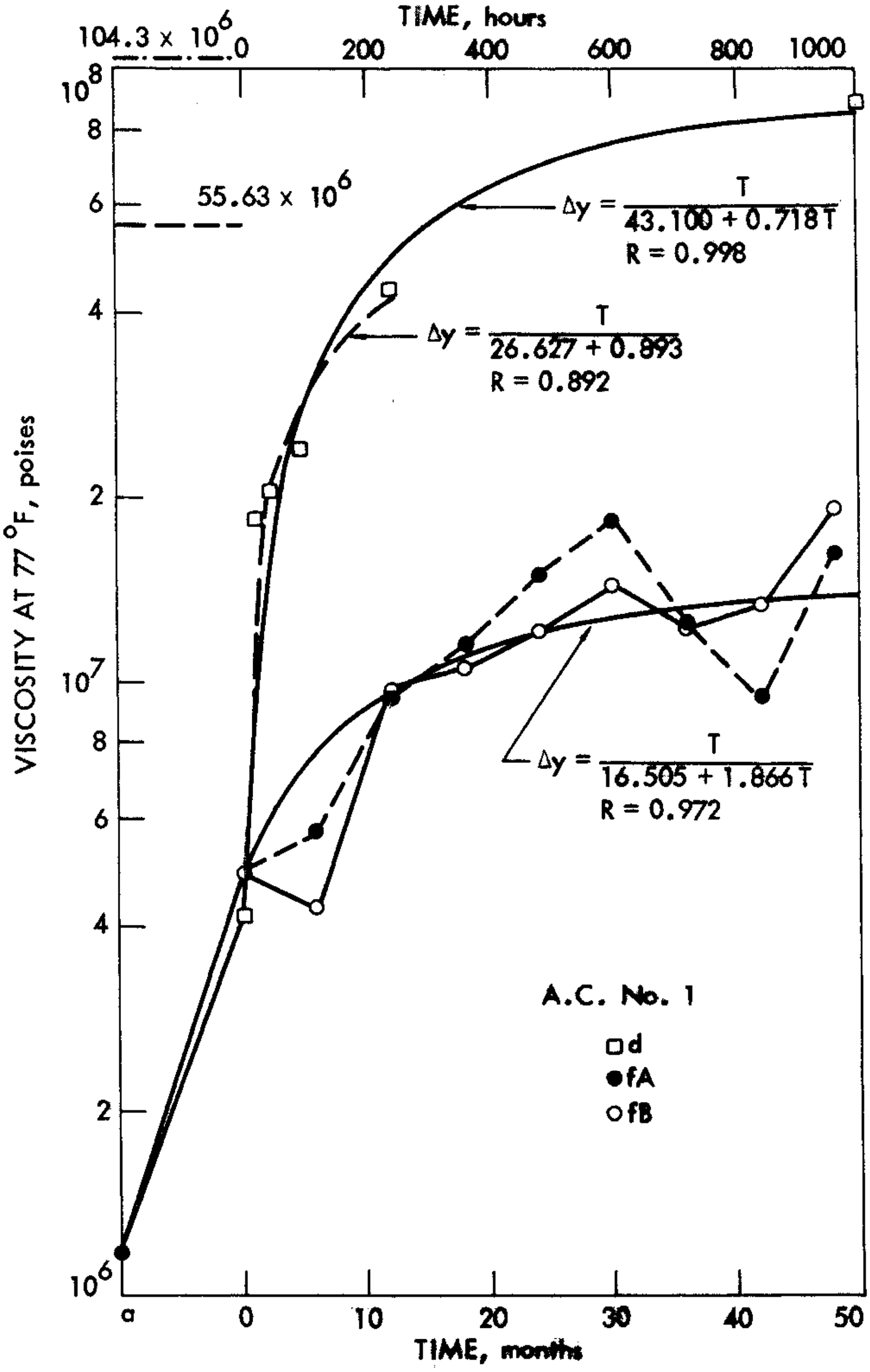

Fig. 8a. Viscosity at 77 °F vs time of ageing, A.C. No. 1.

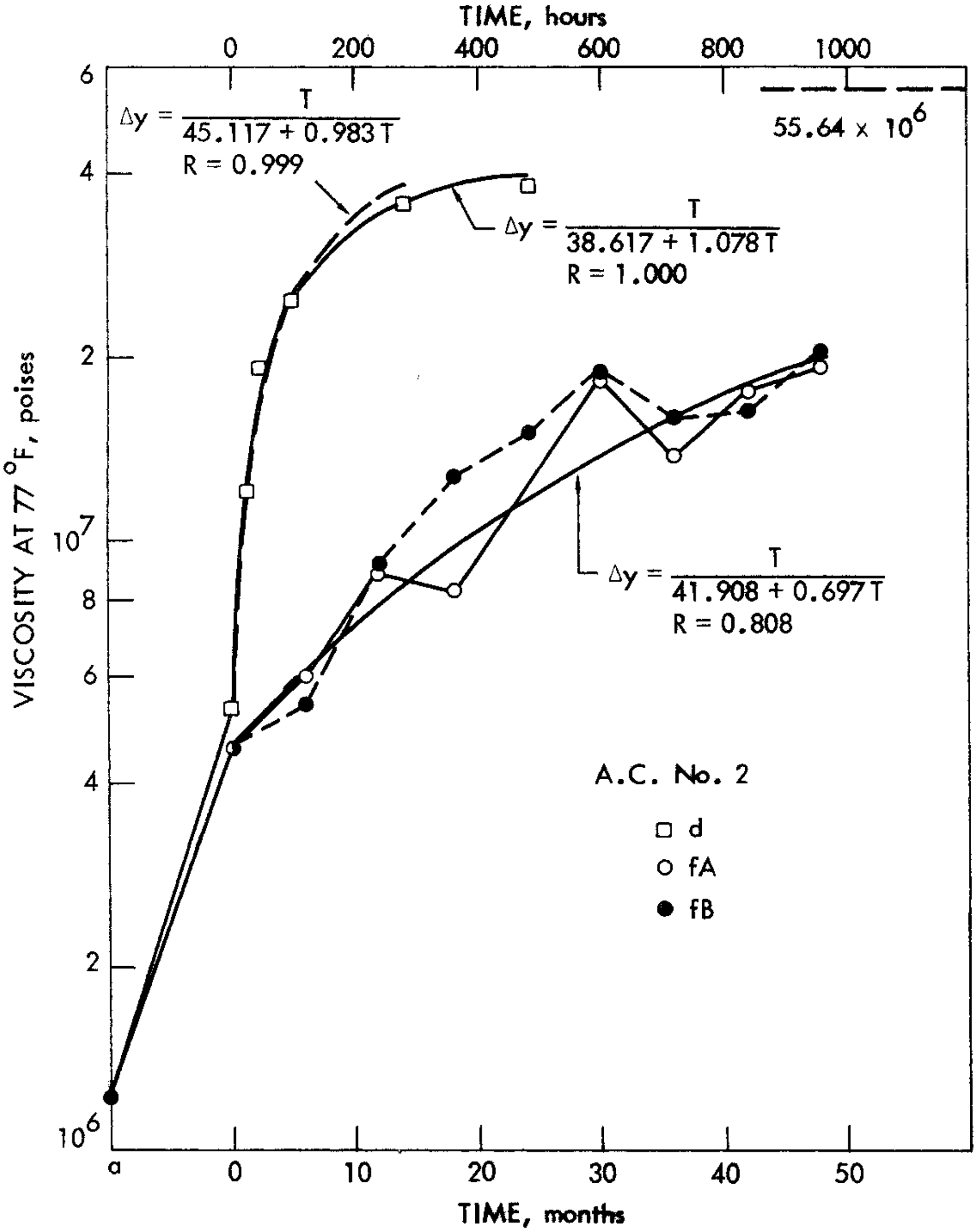

Fig. 8b. Viscosity at 77 °F vs time of ageing, A.C. No. 2.

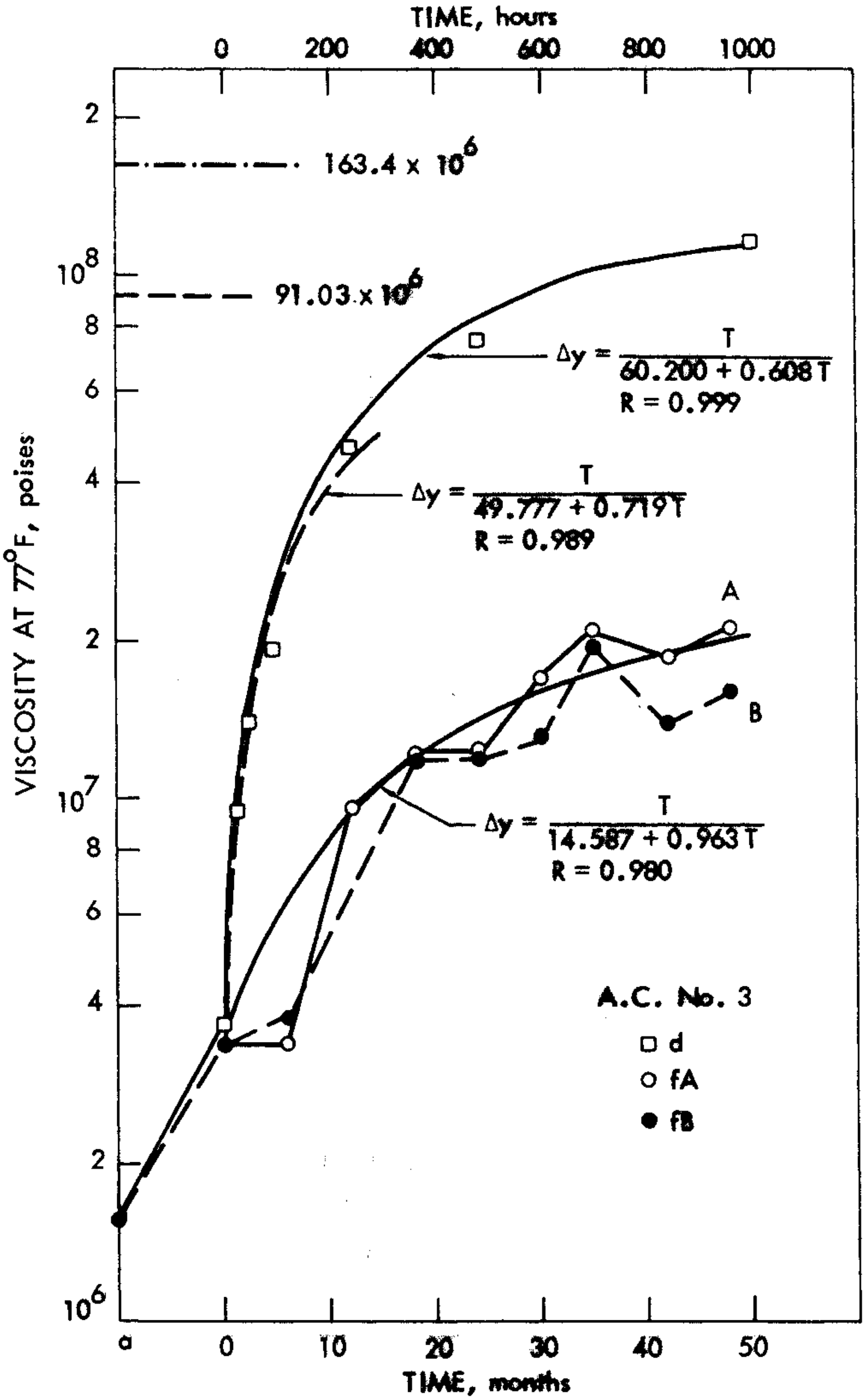

Fig. 8c. Viscosity at 77 °F vs time of ageing, A.C. No. 3.

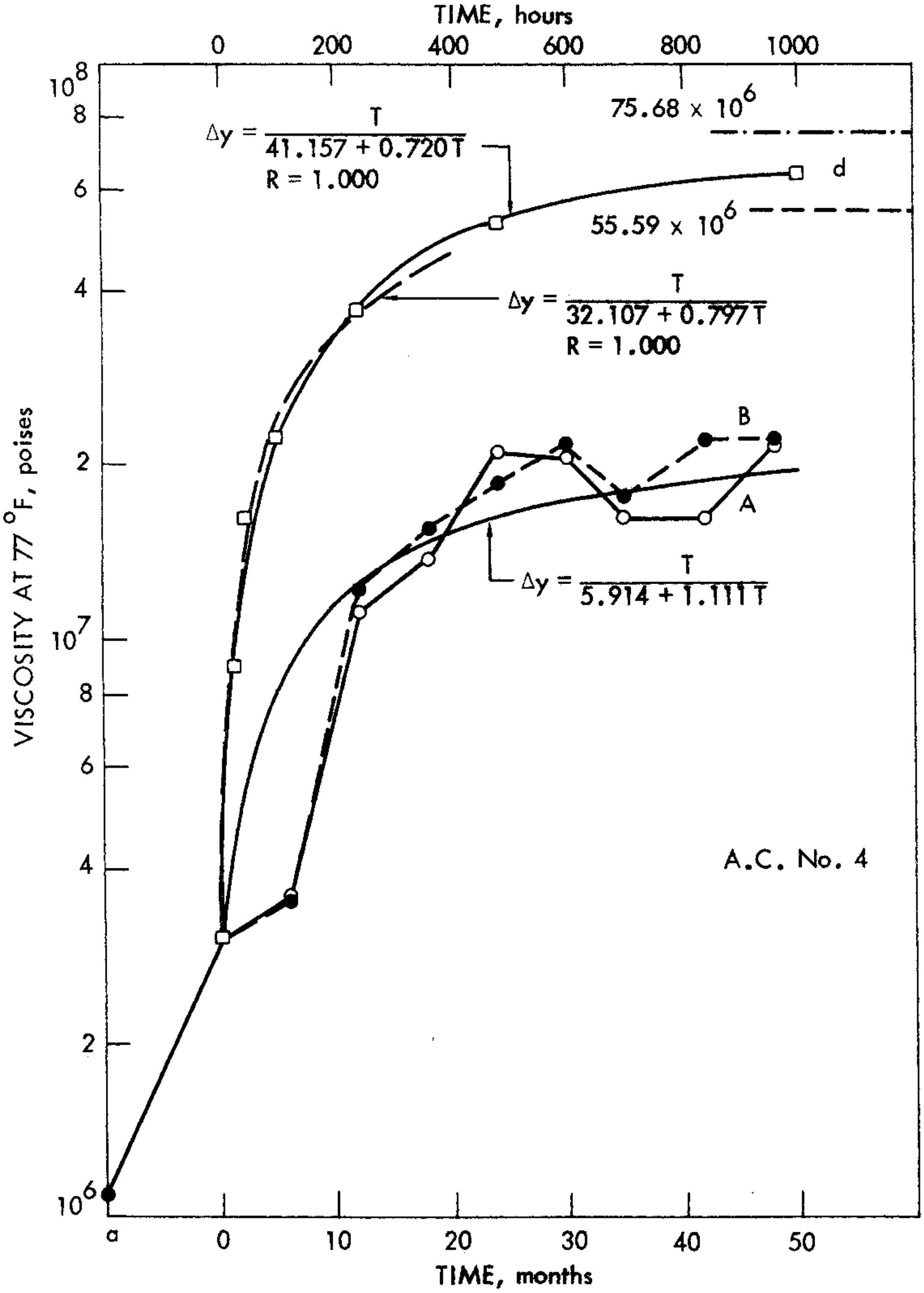

Fig. 8d. Viscosity at 77 °F vs time of ageing, A.C. No. 4.

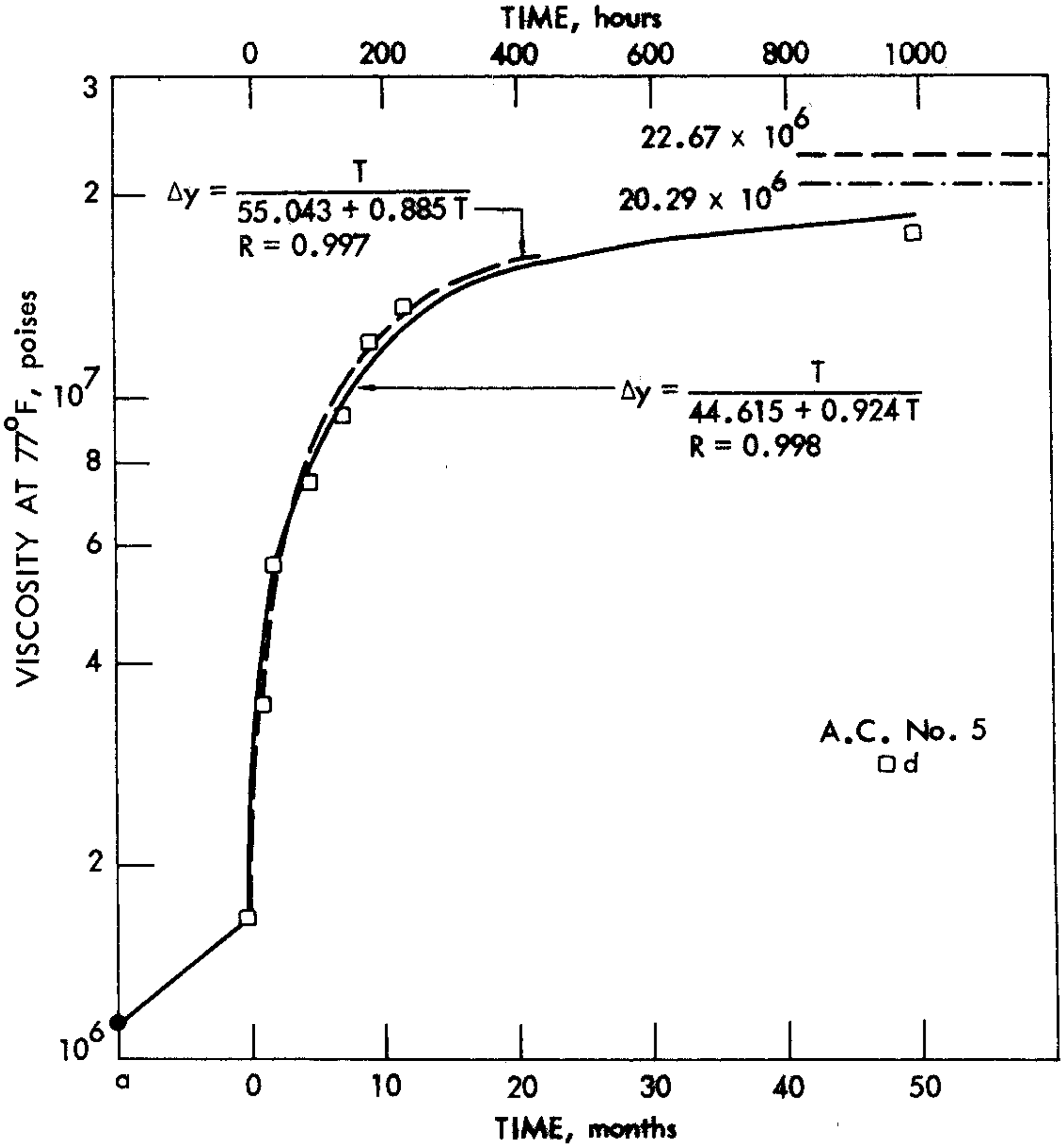

Fig. 8e. Viscosity at 77 °F vs time of ageing, A.C. No. 5.

pertinent curves in dashed lines and with equations given. Almost without exception, the fittings, as indicated by R values, were excellent. It can thus be concluded that the changes of rheological properties as measured by penetration, viscosity, softening point, and ductility is a hyperbolic function of time during IDT, i.e., the penetration and ductility decrease, and the viscosity and softening point increase with time approaching definite limiting values.

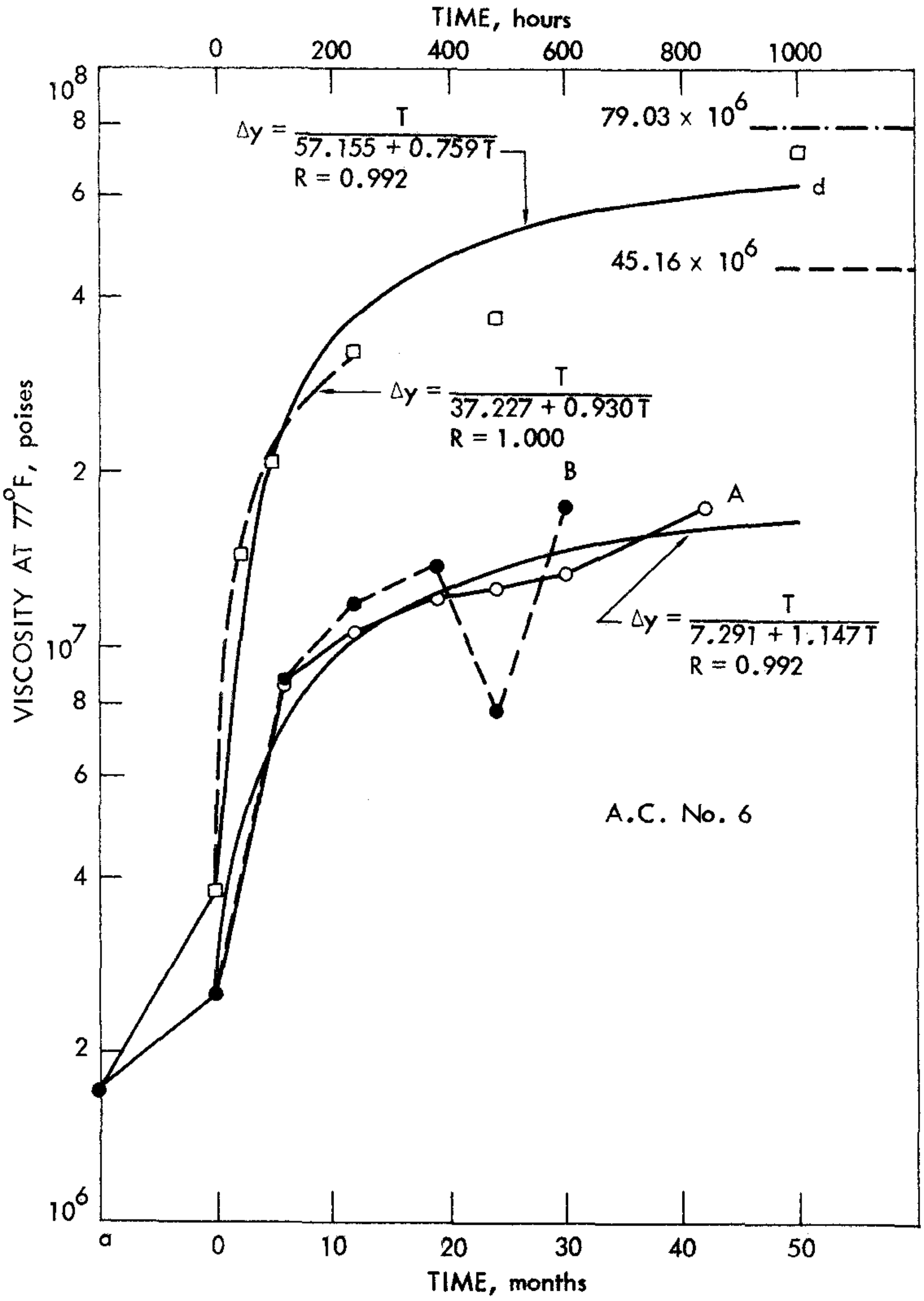

Fig. 8f. Viscosity at 77 °F vs time of ageing, A.C. No. 6.

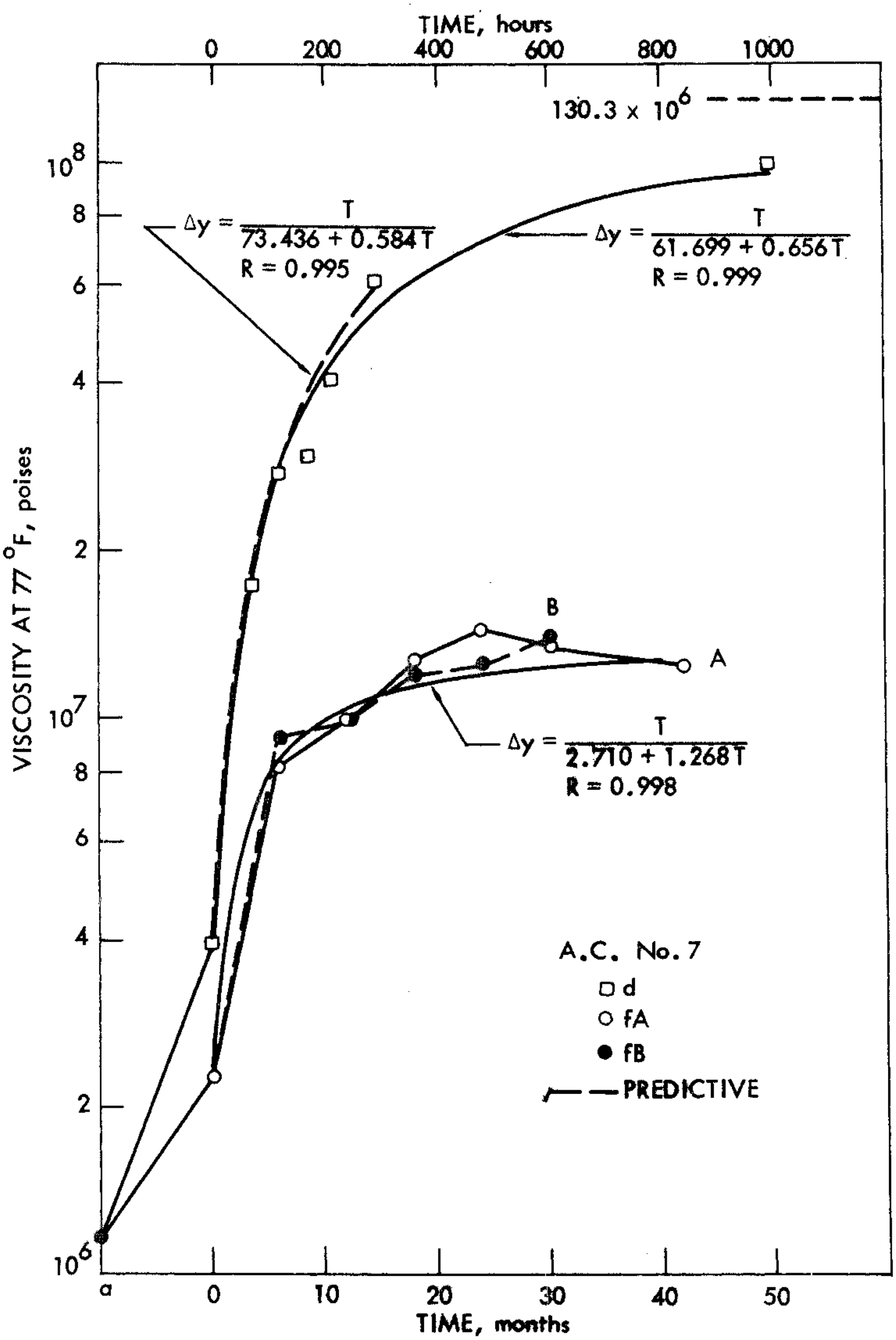

Fig. 8g. Viscosity at 77 °F vs time of ageing, A.C. No. 7.

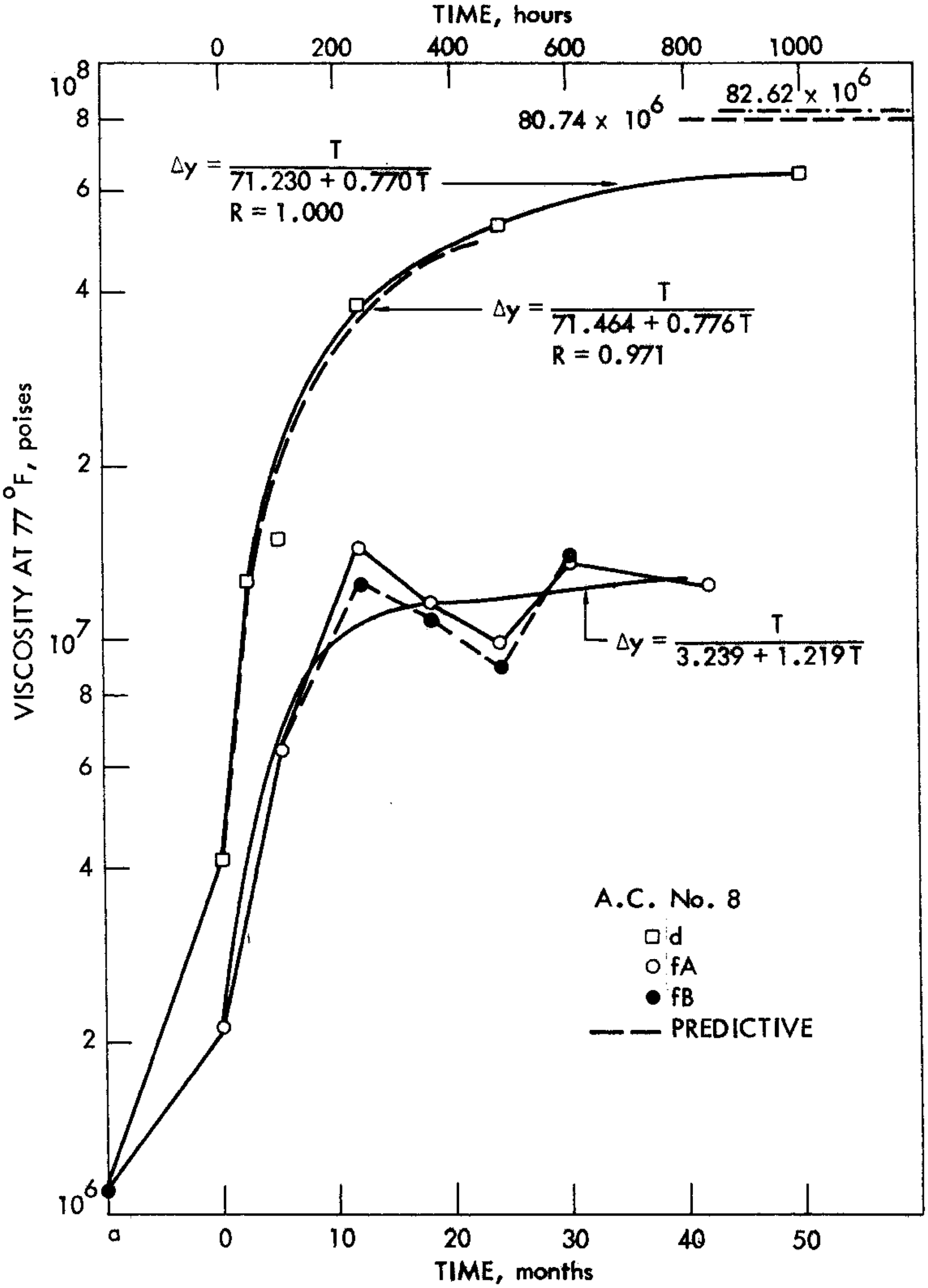

Fig. 8h. Viscosity at 77 °F vs time of ageing, A.C. No. 8.

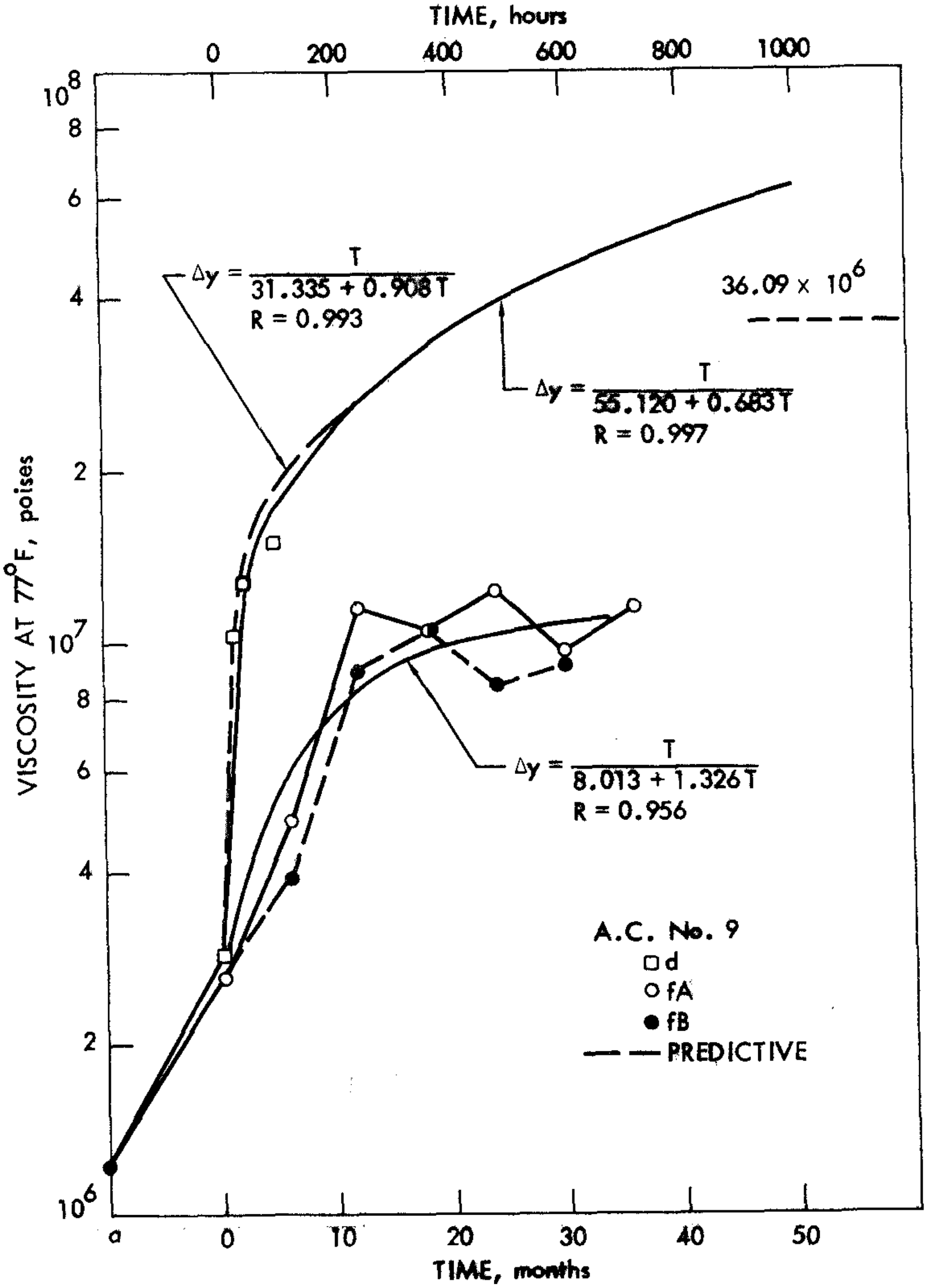

Fig. 8i. Viscosity at 77 °F vs time of ageing, A.C. No. 9.

Table 7. Changes in viscosity at 140 °F.

A.C. No.		Viscosity at 140 °F, poises								
		1	2	3	4	5	6	7	8	9
Original (a)		1,356	1,086	1,316	1,106	1,781	1,350	1,316	1,922	2,837
TFOT (d)		2,368	3,448	4,041	3,556	2,341	3,556	3,538	4,376	4,412
Lab ageing										
24 hr (d24)		12,094	10,849	5,812	–	–	–	7,400[‡]	10,500[‡]	12,558
48 hr (d48)		15,248	17,022	7,979	11,830	4,891	12,457	9,000[‡]	20,199	13,826
96 hr (d96)		23,276	34,249	12,772	13,930	4,459	19,550	12,800[‡]	24,472	23,497
240 hr (d240)		81,254	89,639	28,062	23,479	7,727	33,431	26,900[‡]	44,731	–
480 hr (d480)		–	–	–	–	16,500[‡]	52,000[‡]	53,500[‡]	66,000	–
1000 hr (d1000)		200,000	–	130,000	71,560	37,000	80,000	130,000	120,000	–
Field ageing										
Plant (p)		2,182	2,045	1,913	2,136	–	2,096	2,070	2,634	3,428
0 months (f0)	A[*]	2,294	2,931	2,122	1,781	–	–	2,130	2,456	4,001
	B[†]	2,294	2,931	2,122	1,781	–	–	–	–	–
6 months (f6)	A	2,716	3,735	2,820	2,582	–	7,546	5,506	7,762	4,824
	B	3,555	3,412	3,038	2,525	–	6,227	5,737	9,292	5,852
12 months (f12)	A	5,814	8,165	4,634	5,984	–	5,167	4,634	9,717	4,593
	B	6,722	8,098	5,829	5,964	–	8,181	4,597	9,005	5,358

Table 7. Continued.

A.C. No.		Viscosity at 140 °F, poises								
		1	2	3	4	5	6	7	8	9
18 months (f18)	A	4,733	6,964	5,331	5,077	—	9,436	6,753	13,468	6,663
	B	3,717	7,806	4,799	6,178	—	—	—	—	8,109
24 months (f24)	A	5,158	9,742	6,437	7,672	—	7,797	5,950	9,676	8,653
	B	6,675	10,204	6,217	8,526	—	—	—	—	—
30 months (f30)	A	6,710	9,341	6,229	7,960	—	9,250	6,644	13,092	9,392
	B	8,506	9,588	5,593	8,605	—	8,567	—	—	—
36 months (f36)	A	5,747	9,991	7,218	7,777	—	—	7,270	10,532	13,940
	B	7,031	12,792	8,130	7,484	—	—	—	—	—
42 months (f42)	A	6,448	12,173	6,951	7,598	—	12,384	—	12,925	—
	B	4,954	10,054	9,969	—	—	—	—	—	—
48 months (f48)	A	11,044	13,773	8,305	8,490					
	B	9,473	14,082	7,549	8,647					

[*] A, in wheel tracks.

[†] B, between wheel tracks.

[‡] Interpolated value.

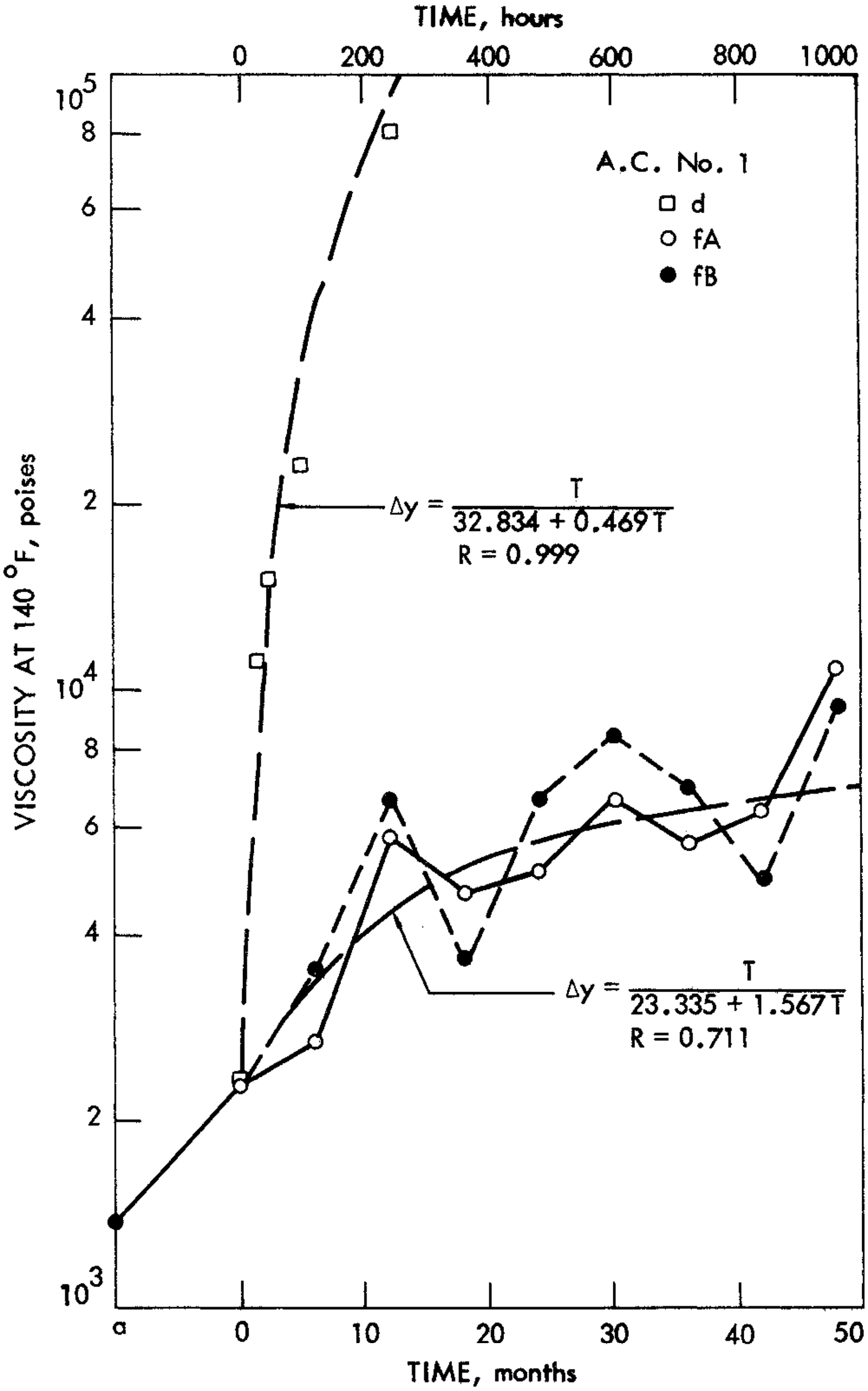

Fig. 9a. Viscosity at 140 °F vs time of ageing, A.C. No. 1.

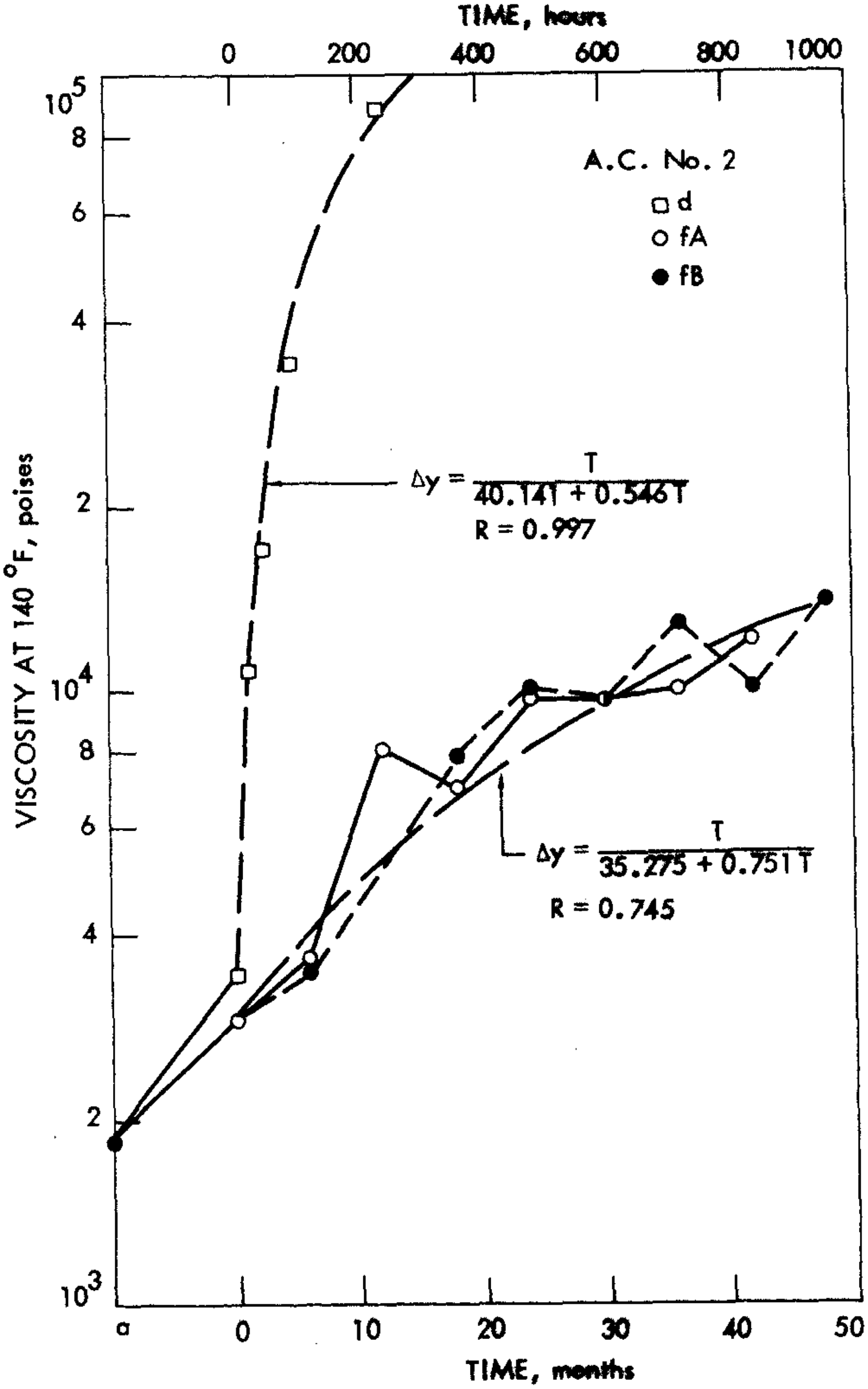

Fig. 9b. Viscosity at 140 °F vs time of ageing, A.C. No. 2.

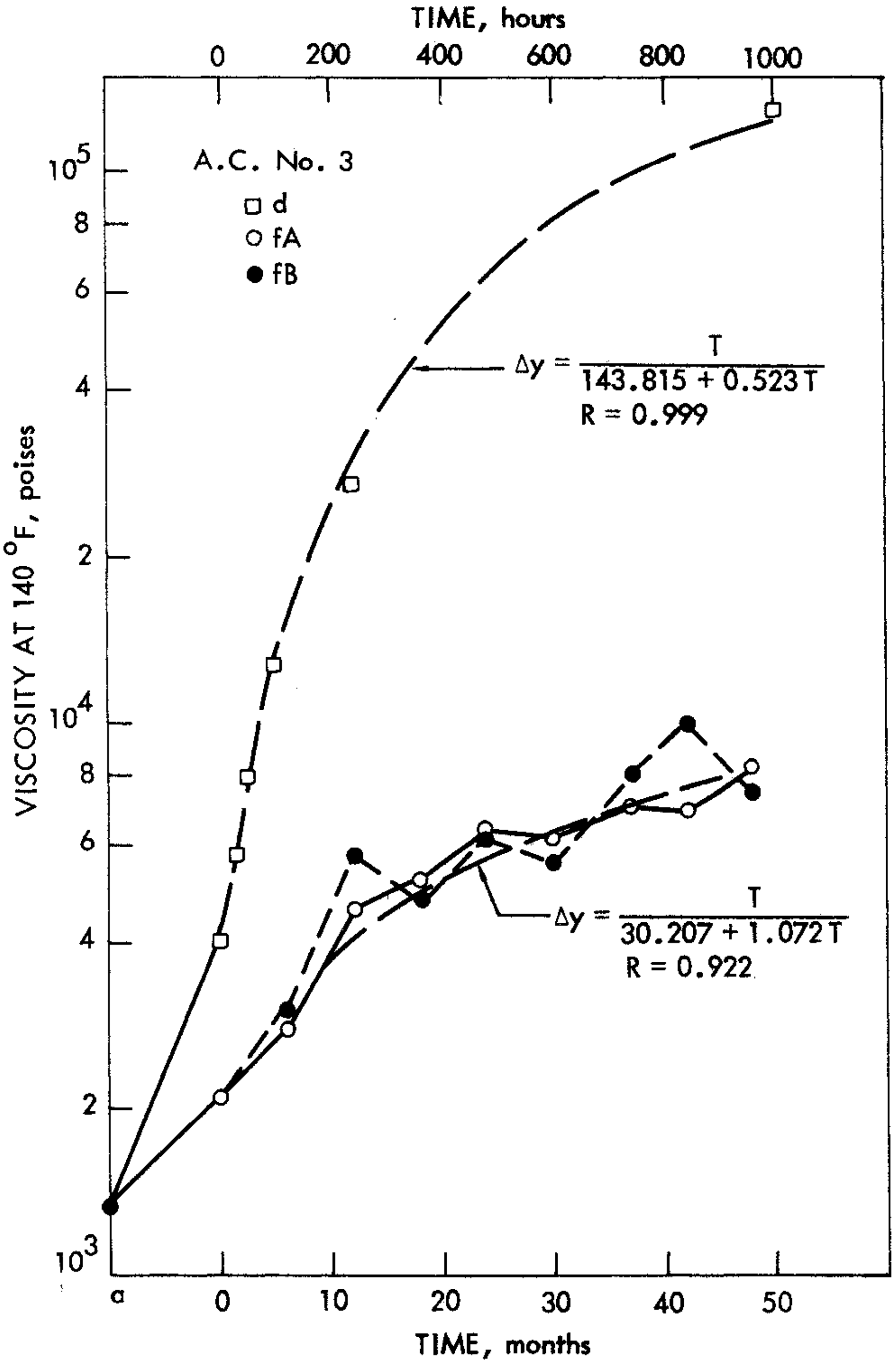

Fig. 9c. Viscosity at 140 °F vs time of ageing, A.C. No. 3.

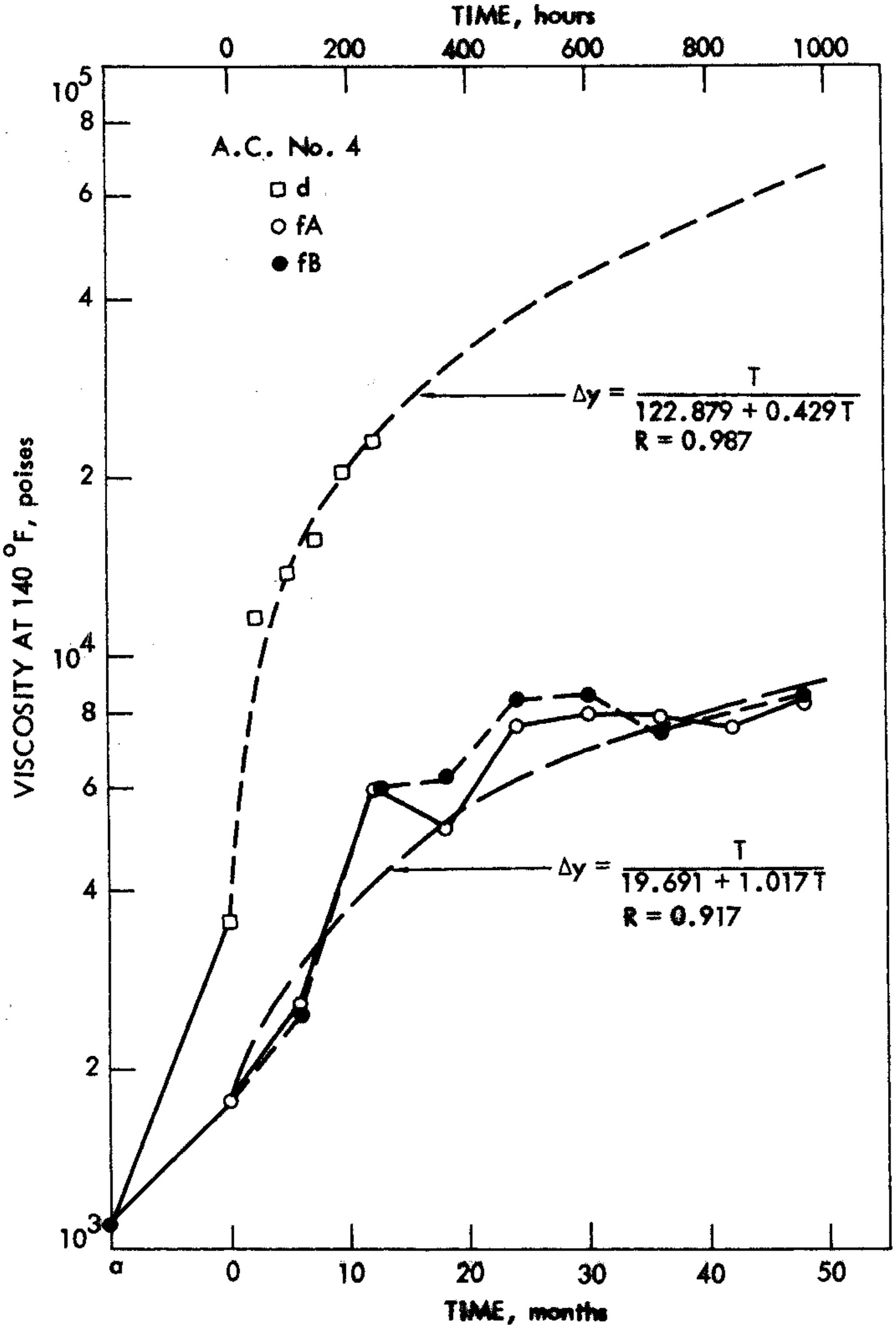

Fig. 9d. Viscosity at 140 °F vs time of ageing, A.C. No. 4.

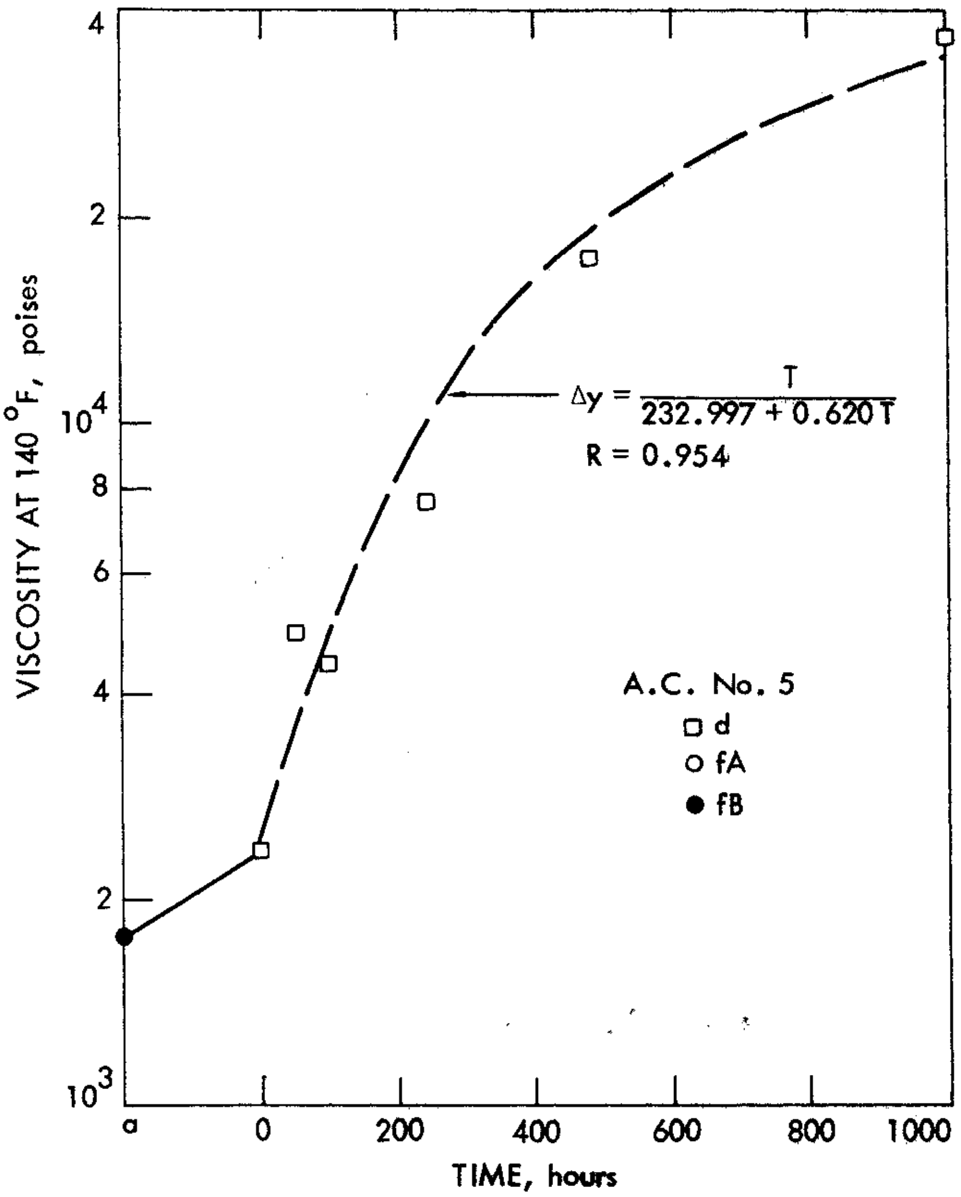

Fig. 9e. Viscosity at 140 $^{\circ}$F vs time of ageing, A.C. No. 5.

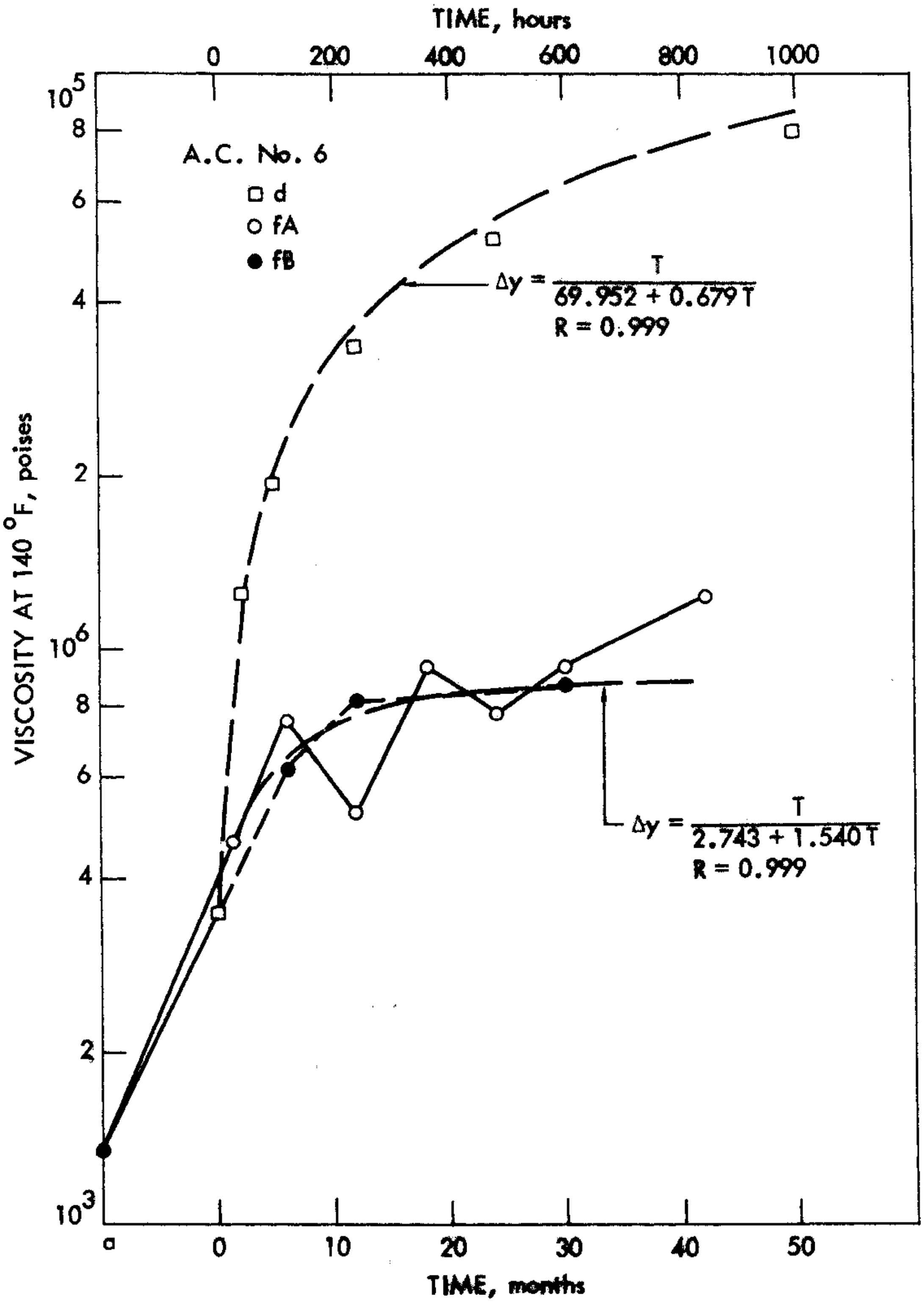

Fig. 9f. Viscosity at 140 °F vs time of ageing, A.C. No. 6.

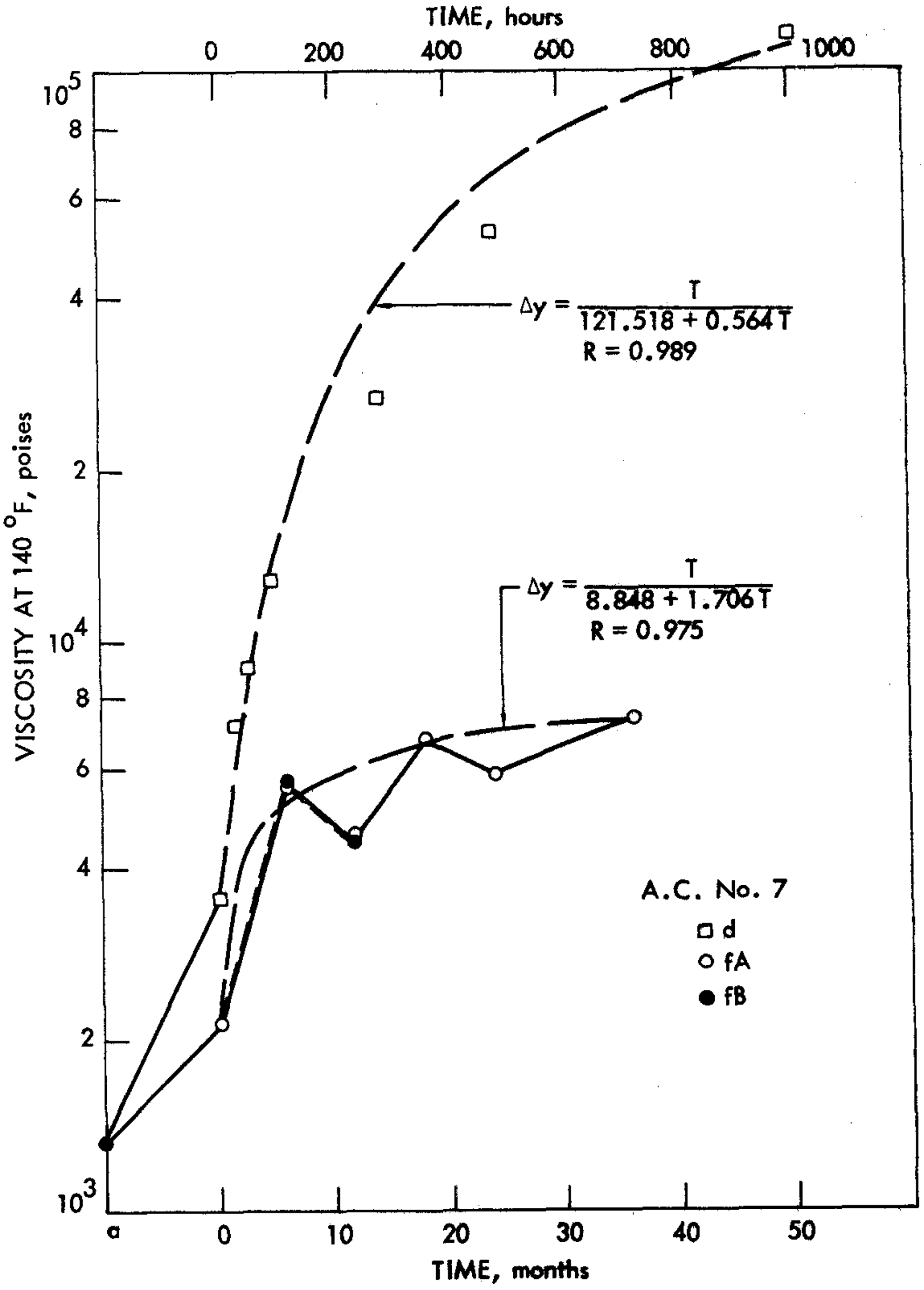

Fig. 9g. Viscosity at 140 °F vs time of ageing, A.C. No. 7.

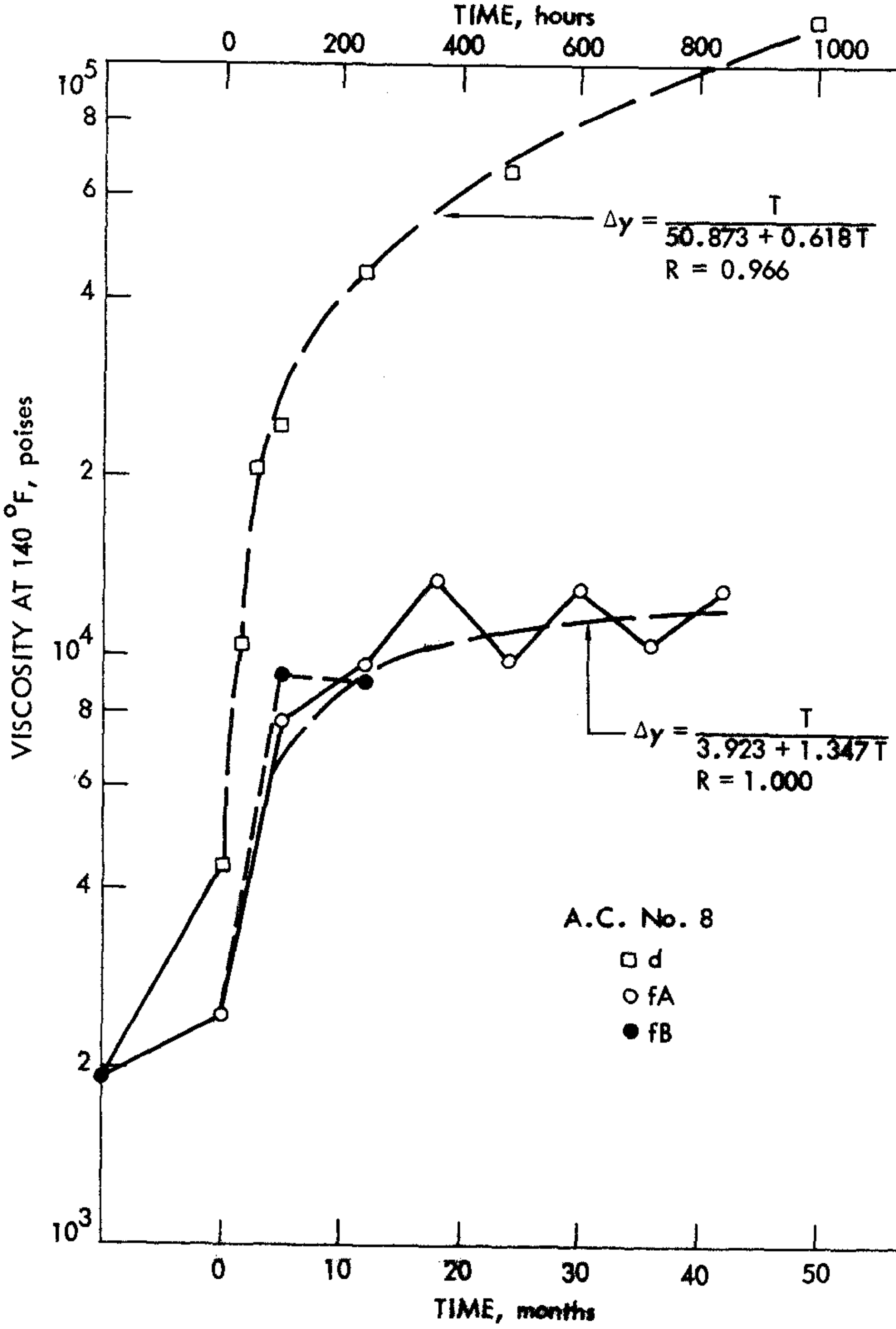

Fig. 9h. Viscosity at 140 °F vs time of ageing, A.C. No. 8.

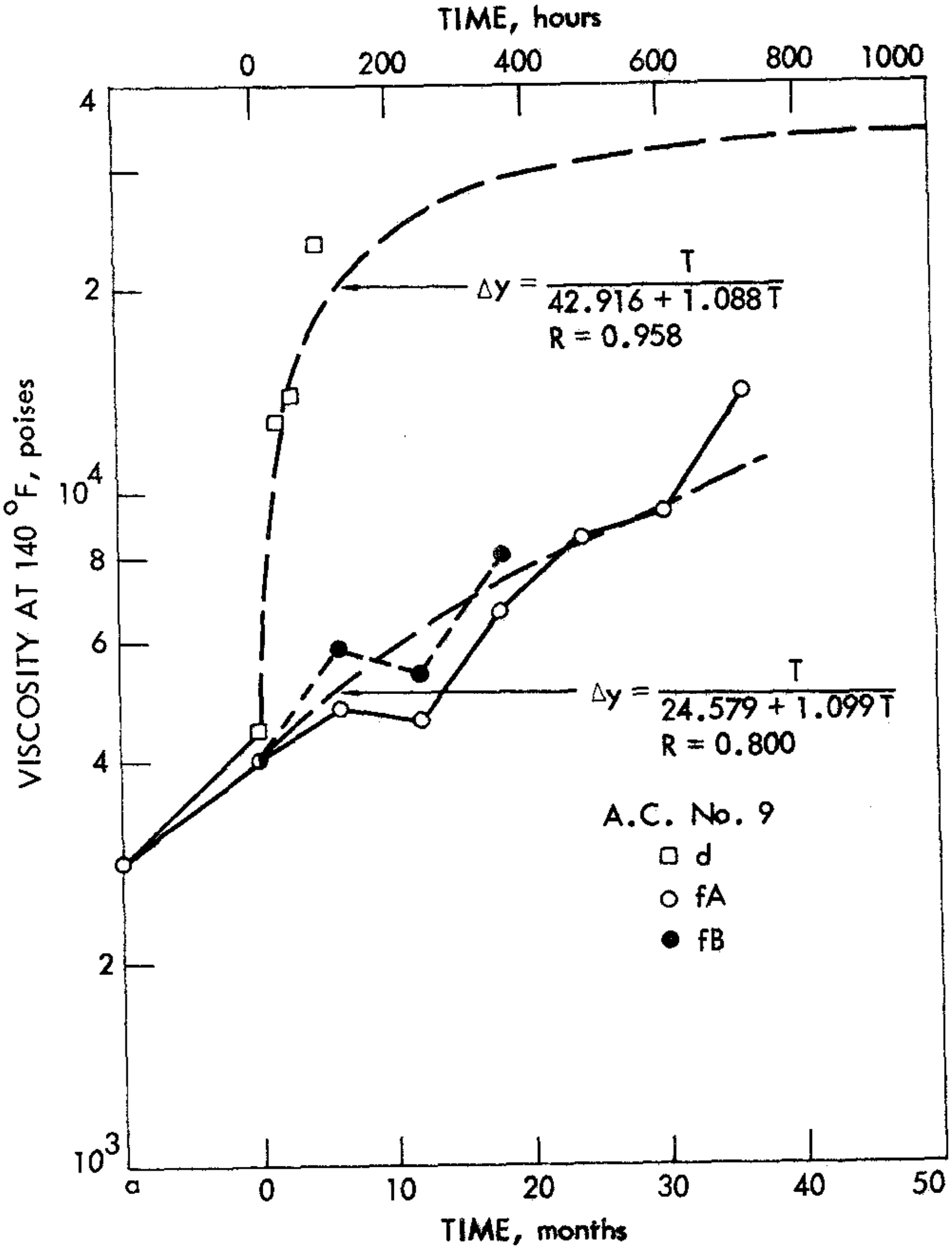

Fig. 9i. Viscosity at 140 °F vs time of ageing, A.C. No. 9.

Table 8. Complex flow and shear index.

		A.C. No. 1				A.C. No. 2				A.C. No. 3				A.C. No. 4	
		C	SI	η/w, megapoises	η/ℓ, megapoises	C	SI	η/w, megapoises	η/ℓ, megapoises	C	SI	η/w, megapoises	η/ℓ, megapoises	C	SI
Original (a)		0.975	0.000	1.16	1.16	1.006	0.031	1.16	1.19	1.000	0.000	–	–	0.989	0.000
TFOT (d)		0.919	0.087	4.20	4.10	0.794	0.224	5.50	6.05	0.847	0.143	3.67	3.76	0.991	0.060
Lab ageing															
24 hr (d24)		1.018	0.010	18.20	17.80	0.713	0.286	13.80	19.00	–	–	–	–	0.966	0.061
48 hr (d48)		0.590	0.413	29.80	60.00	0.645	0.342	26.70	51.50	0.829	0.167	15.9	19.0	1.352	0.240
96 hr (d96)		0.480	0.660	33.90	55.50	0.604	0.365	23.80	22.0	0.509	0.488	–	–	1.202	0.203
240 hr (d240)		0.308	0.760	190.00	–	–	–	–	–	0.351	0.543	–	–	0.932	0.509
480 hr (d480)		–	–	–	–	0.349	0.596	–	–	–	–	–	–	–	–
1000 hr (d1000)		–	–	–	–	–	–	–	–	–	–	–	–	0.869	0.705
Field ageing															
Plant (p)		0.968	0.050	4.30	4.35	0.950	0.021	8.20	8.30	0.966	0.029	3.40	3.40	0.967	0.000
0 months (f0)		0.967	0.236	5.00	5.55	1.126	0.088	4.60	4.49	0.932	0.020	–	–	0.971	0.000
6 months (f6)	A*	0.831	0.183	4.35	4.57	0.730	0.354	6.40	7.72	0.830	0.136	3.36	3.40	1.000	0.083
	B†	0.815	0.200	5.90	6.50	0.890	0.136	5.49	5.80	0.935	0.035	3.78	3.79	0.973	0.000
12 months (f12)	A	0.875	0.029	10.50	11.00	0.713	0.285	10.20	13.40	0.940	0.074	9.35	9.70	0.981	0.078
	B	0.842	0.317	15.10	30.80	0.715	0.273	10.50	13.70	–	–	–	–	0.870	0.147
18 months (f18)	A	0.856	0.178	18.50	73.50	0.695	0.283	10.20	15.20	0.692	0.490	17.00	30.40	0.839	0.146
	B	0.824	0.240	15.80	59.00	0.705	0.272	11.40	14.80	0.550	0.450	17.20	37.00	0.985	0.255
24 months (f24)	A	0.750	0.248	15.00	19.30	–	–	–	–	0.613	0.409	16.70	30.50	0.911	0.134
	B	0.658	0.412	21.20	40.50	0.707	0.327	22.20	49.00	0.896	0.087	–	–	0.775	0.200
30 months (f30)	A	0.654	0.398	20.00	36.80	0.635	0.309	24.60	42.50	0.864	0.151	19.00	22.50	0.778	0.236
	B	0.578	0.423	28.00	65.80	0.491	0.415	28.70	78.40	0.797	0.225	15.50	19.80	0.615	0.423
36 months (f36)	A	0.596	0.400	15.60	26.90	0.607	0.336	17.70	32.90	0.665	0.341	29.10	52.80	0.790	0.214
	B	0.695	0.340	15.50	23.80	0.560	0.417	22.80	50.00	0.872	0.139	22.00	26.00	0.735	0.198
42 months (f42)	A	0.685	0.381	16.30	22.60	0.675	0.346	24.10	43.00	–	–	–	–	0.992	0.156
	B	0.686	0.301	10.70	13.60	0.756	0.262	20.20	29.00	0.821	0.180	15.80	19.30	0.786	0.235
48 months (f48)	A	0.780	0.343	24.00	35.50	0.725	0.314	26.00	41.80	0.863	0.125	23.10	27.40	0.766	0.211
	B	0.801	0.222	19.50	26.00	0.645	0.359	26.90	41.50	0.867	0.000	16.10	16.10	0.973	0.133

*A, in wheel tracks.

†B, between wheel tracks.

η/w = viscosity at constant work of 10^4 ergs.

η/ℓ = viscosity at constant stress of 1.63×10^5 dynes/cm^2.

Table 8. Continued.

	A.C. No. 5		A.C. No. 6		A.C. No. 7		A.C. No. 8		A.C. No. 9	
	C	SI	C	SI	C	SI	C	SI	C	SI
Original (a)	1.000	0.017	1.056	0.117	0.983	0.013	0.933	0.067	0.949	0.052
TFOT (d)	0.949	0.017	–	–	0.932	0.070	0.833	0.133	1.000	0.185
Lab ageing										
24 hr (d24)	–	–	0.839	0.140	–	–	–	–	0.767	0.222
48 hr (d48)	0.983	0.052	0.667	0.333	–	–	0.600	0.333	0.824	0.222
72 hr (d72)	–	–	–	–	0.806	0.182	–	–	–	–
96 hr (d96)	1.000	0.012	0.700	0.300	–	–	0.633	0.300	0.753	0.158
120 hr (d120)	–	–	–	–	0.740	0.354	–	–	–	–
144 hr (d144)	0.740	–	0.625	0.369	–	–	0.674	0.359	0.649	0.354
168 hr (d168)	–	–	–	–	0.839	0.276	–	–	–	–
192 hr (d192)	0.932	0.052	0.577	0.374	–	–	0.740	0.287	0.649	0.354
216 hr (d216)	–	–	–	–	0.839	0.440	–	–	–	–
240 hr (d240)	0.976	0.033	0.667	0.400	–	–	0.767	0.467	–	–
288 hr (d288)	–	–	–	–	0.732	0.494	–	–	–	–
480 hr (d480)	–	–	0.541	0.400	–	–	–	–	0.558	0.400
1000 hr (d1000)	–	–	0.374	0.535	–	–	–	–	–	–

Table 8. Continued.

		A.C. No. 5		A.C. No. 6		A.C. No. 7		A.C. No. 8		A.C. No. 9	
		C	SI	C	SI	C	SI	C	SI	C	SI
Field ageing											
Plant (p)		—	—	1.000	0.050	1.035	0.000	0.933	0.000	0.949	0.052
0 months (f0)		—	—	—	—	0.939	0.000	1.000	0.067	0.630	0.353
6 months (f6)	A[*]	—	—	0.600	0.367	0.927	0.057	1.072	0.054	0.869	0.176
	B[†]	—	—	0.781	0.196	0.983	0.140	0.800	0.233	0.854	0.249
12 months (f12)	A	—	—	0.600	0.357	0.966	0.035	0.869	0.036	0.824	0.123
	B	—	—	0.767	0.133	0.965	0.035	0.935	0.176	0.869	0.176
18 months (f18)	A	—	—	0.300	0.421	0.840	0.133	0.500	0.367	0.761	0.219
	B	—	—	0.500	0.433	0.741	0.235	0.733	0.167	0.608	0.400
24 months (f24)	A	—	—	0.800	0.268	0.900	0.144	0.700	0.367	0.758	0.375
	B	—	—	0.351	0.732	0.930	0.269	0.700	0.400	0.621	0.278
30 months (f30)	A	—	—	0.528	0.313	—	—	0.638	0.367	0.667	0.351
	B	—	—	0.684	0.271	0.833	0.200	0.677	0.217	0.672	0.316
36 months (f36)	A	—	—	—	—	0.803	0.192	—	—	0.672	0.353
	B	—	—	—	—	—	—	—	—	—	—
42 months (f42)	A	—	—	0.700	0.314	—	—	0.833	0.317	—	—
	B	—	—	—	—	—	—	—	—	—	—

[*] A, in wheel tracks.

[†] B, between wheel tracks.

Table 9. Changes in softening point during weathering.

A.C. No.		Softening point, R and B, °F								
		1	2	3	4	5	6	7	8	9
Original (a)		119.0	116.5	115.5	114.5	113.0	118.0	116.0	118.0	119.5
TFOT (d)		127.5	131.0	123.0	126.0	119.0	127.0	123.0	129.0	119.5
Lab ageing										
24 hr (d24)		141.0	134.0	131.0	133.5‡	121.5‡	–	125.5‡	136.0‡	132.5
48 hr (d48)		140.5	143.0	138.0	138.0	126.5	140.0	128.5‡	142.5	136.0
96 hr (d96)		143.5	149.0	140.5	141.0	126.0	143.0	134.0‡	144.5	145.5
240 hr (d240)		159.0	152.5	145.0	148.5	134.0	152.0	146.6‡	150.0	151.5‡
480 hr (d480)		168.0‡	167.0	154.5‡	154.5‡	143.8‡	163.7‡	160.5‡	164.0‡	–
1000 hr (d1000)		175.0	170.0‡	171.0	173.5	154.0	174.0	171.0	173.0	–
Field ageing										
Plant (p)		130.5	129.0	127.5	122.5	–	118.0	120.0	124.0	116.0
0 months (f0)	A*	127.5	125.0	125.0	119.0	–	–	118.0	132.0	124.0
	B†	127.5	123.0	125.0	119.0	–	–	–	–	–
6 months (f6)	A	124.0	128.0	122.5	120.5	–	133.5	132.0	136.0	132.0
	B	125.0	120.5	125.5	120.5	–	133.0	130.0	136.0	126.0
12 months (f12)	A	129.0	135.0	130.0	130.0	–	134.0	129.5	134.0	138.0
	B	129.5	137.5	131.0	131.0	–	138.5	130.0	126.0	132.0

Table 9. Continued.

A.C. No.		Softening point, R and B, °F								
		1	2	3	4	5	6	7	8	9
18 months (f18)	A	130.0	137.0	—	134.0	—	135.0	132.8	136.4	132.0
	B	132.0	136.0	128.0	134.0	—	140.0	132.8	136.0	130.0
24 months (f24)	A	129.5	134.5	136.5	136.5	—	129.0	138.0	138.0	136.0
	B	136.0	138.0	136.5	136.5	—	—	—	—	—
30 months (f30)	A	137.0	140.0	136.5	135.5	—	140.0	137.0	141.0	136.0
	B	138.0	137.0	—	136.0	—	—	—	—	—
36 months (f36)	A	138.0	143.5	138.0	134.5	—	—	137.0	—	139.0
	B	140.0	142.0	138.0	136.5	—	—	—	—	—
42 months (f42)	A	133.0	138.0	140.0	134.5	—	142.0	—	144.0	—
	B	129.0	138.2	141.0	134.6	—	—	—	—	—
48 months (f48)	A	134.5	136.5	136.5	136.5	—	—	—	—	—
	B	137.3	136.4	134.6	136.4	—	—	—	—	—

[*] A, in wheel tracks.

[†] B, between wheel tracks.

[‡] Interpolated value.

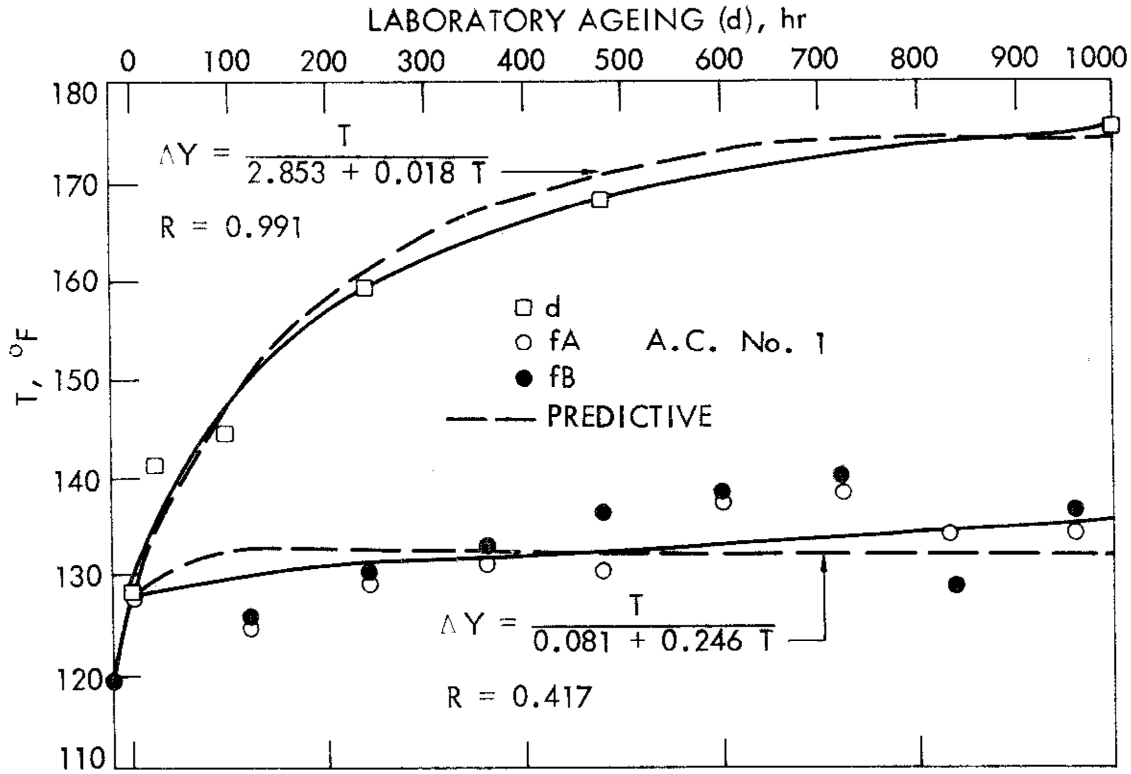

Fig. 10a. Softening point vs time of ageing, A.C. No. 1.

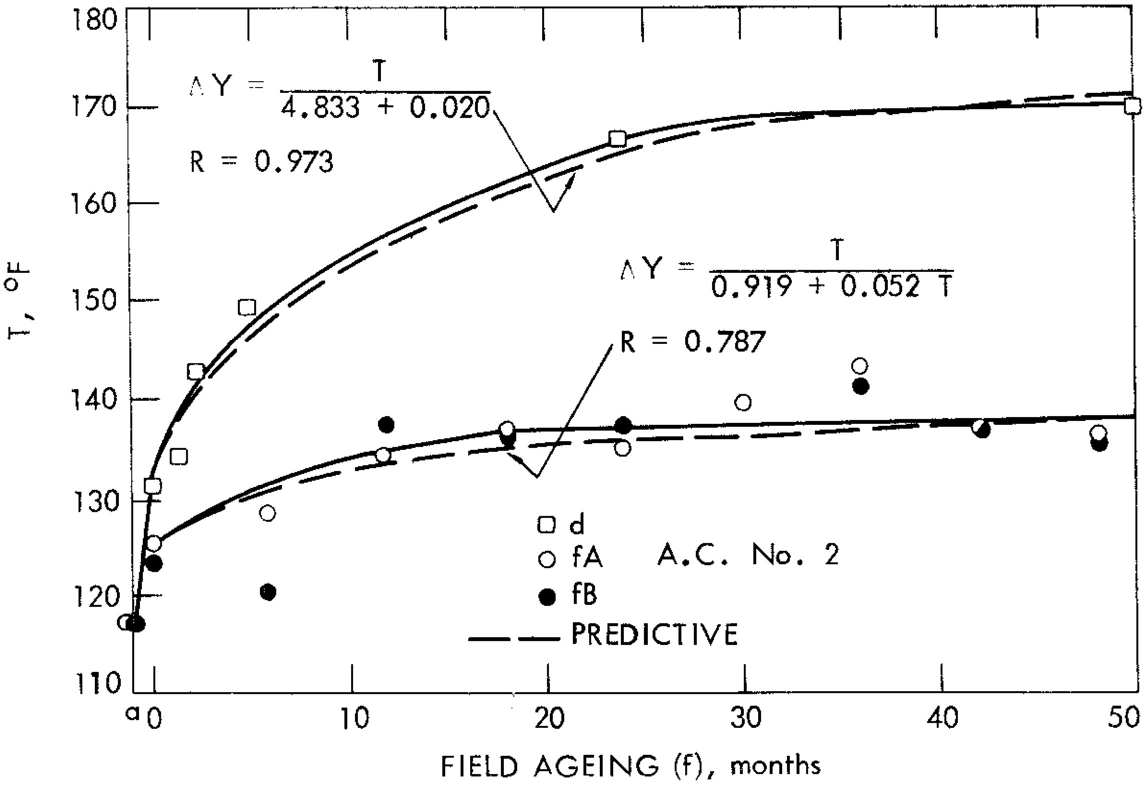

Fig. 10b. Softening point vs time of ageing, A.C. No. 2.

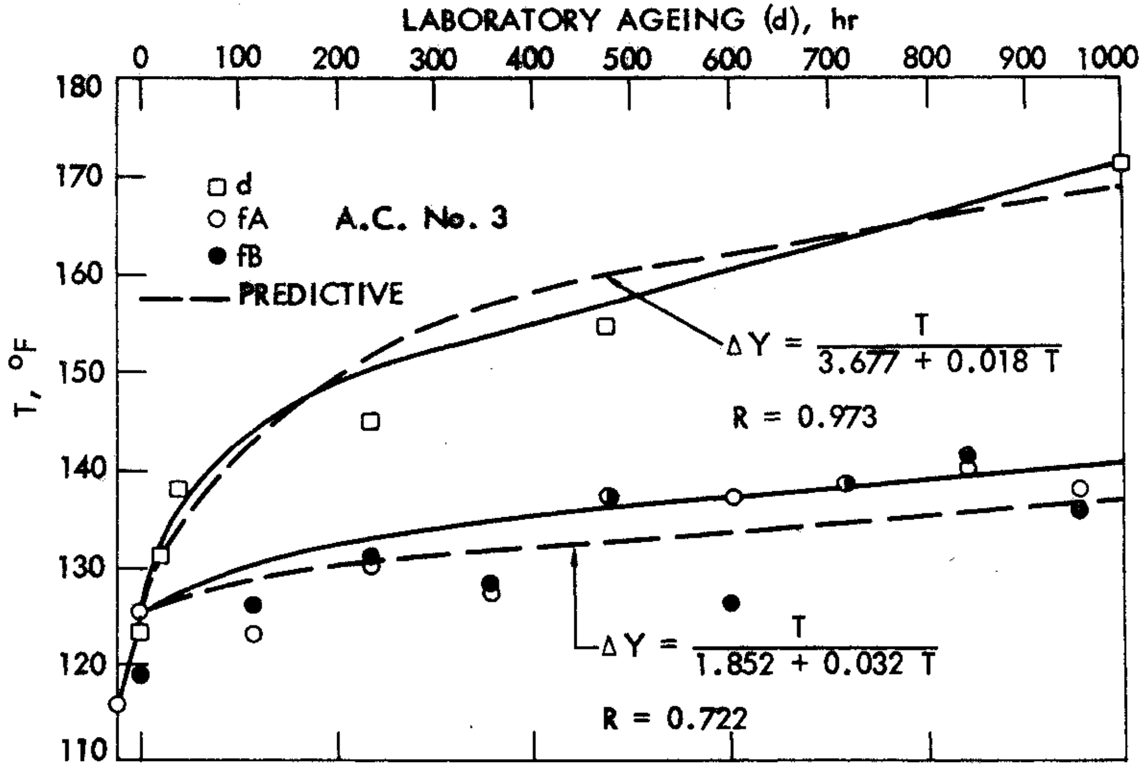

Fig. 10c. Softening point vs time of ageing, A.C. No. 3.

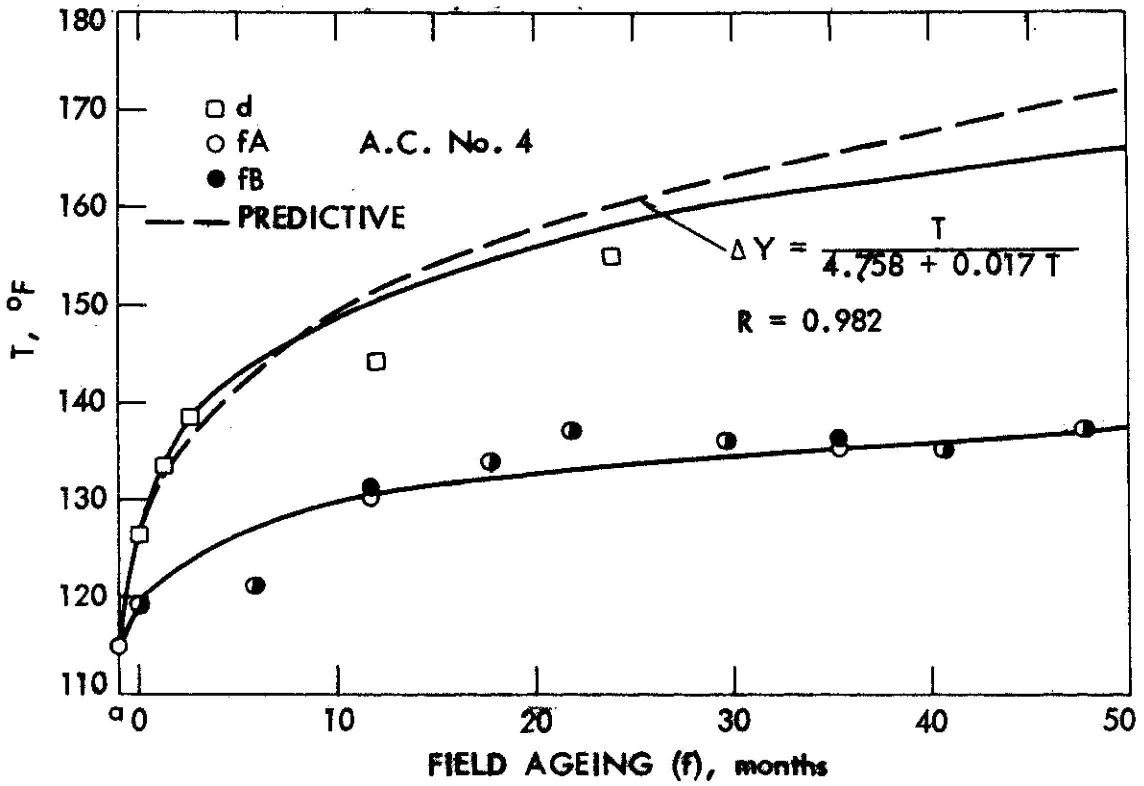

Fig. 10d. Softening point vs time of ageing, A.C. No. 4.

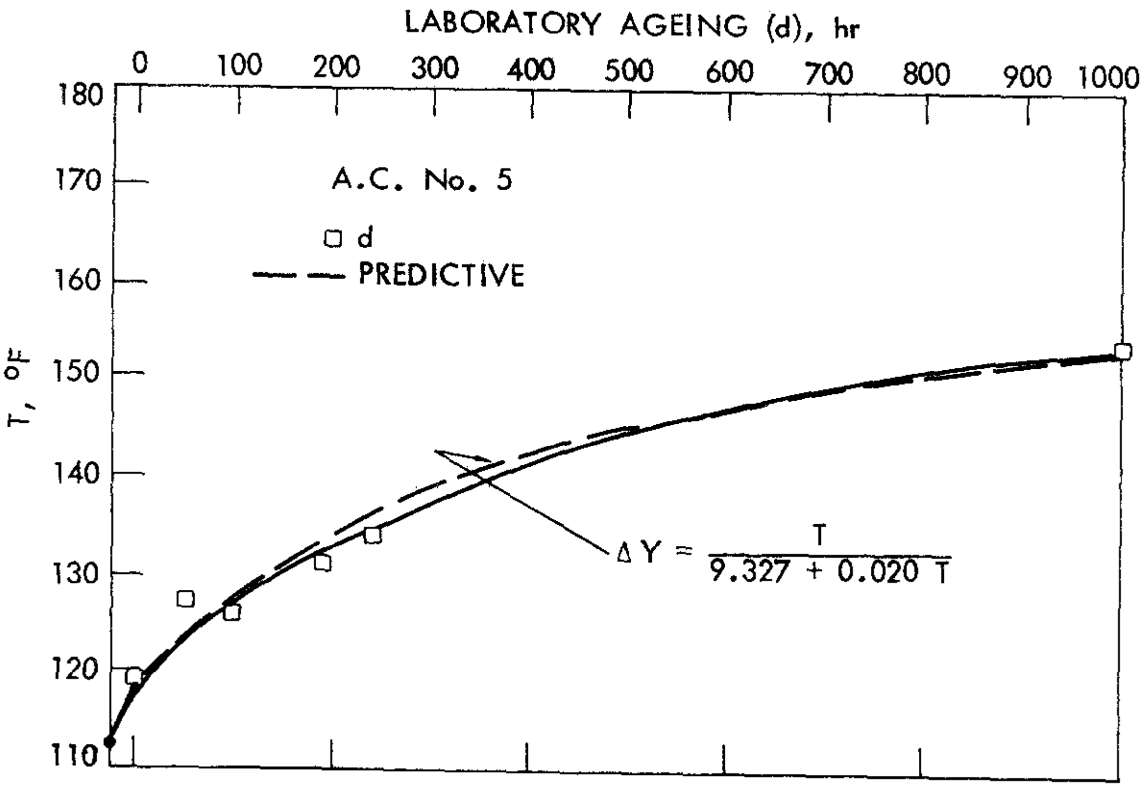

Fig. 10e. Softening point vs time of ageing, A.C. No. 5.

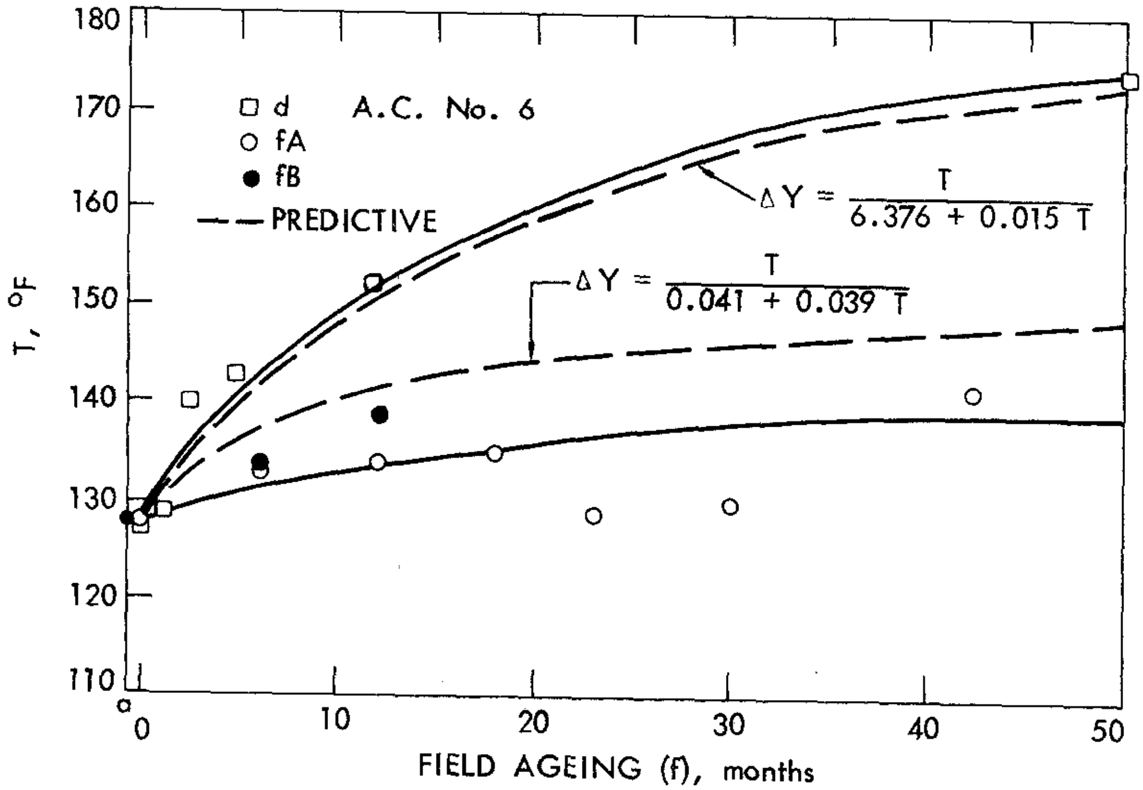

Fig. 10f. Softening point vs time of ageing, A.C. No. 6.

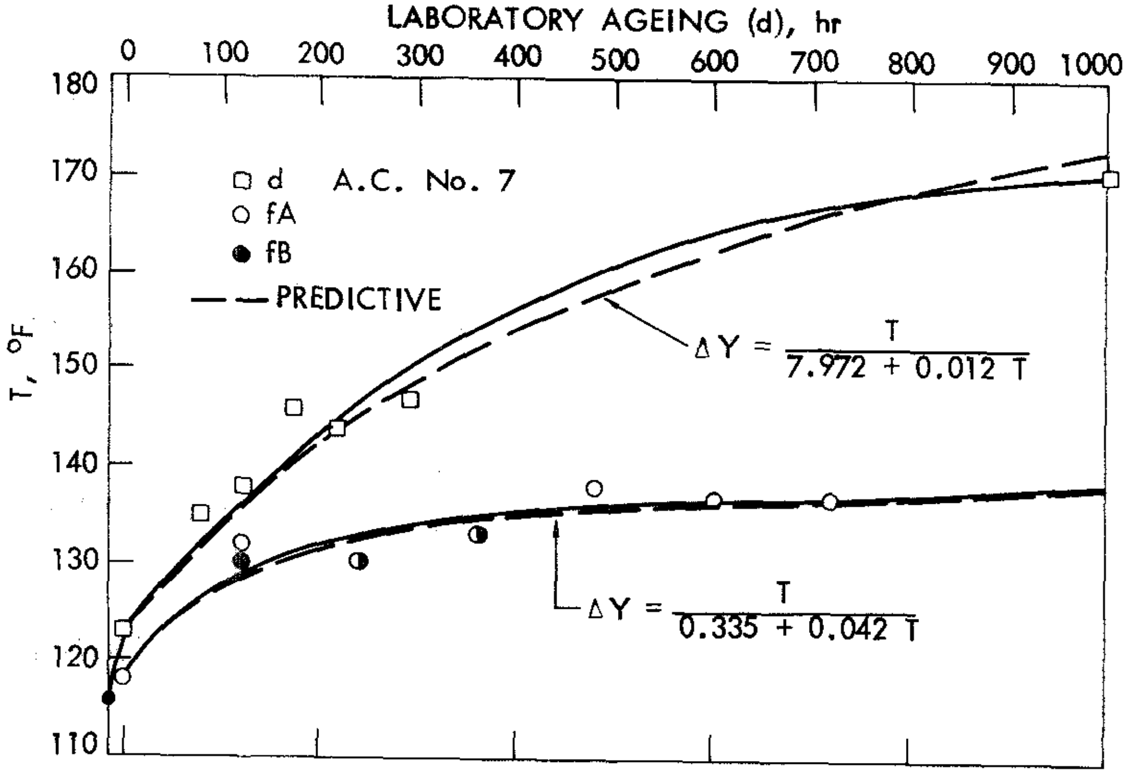

Fig. 10g. Softening point vs time of ageing, A.C. No. 7.

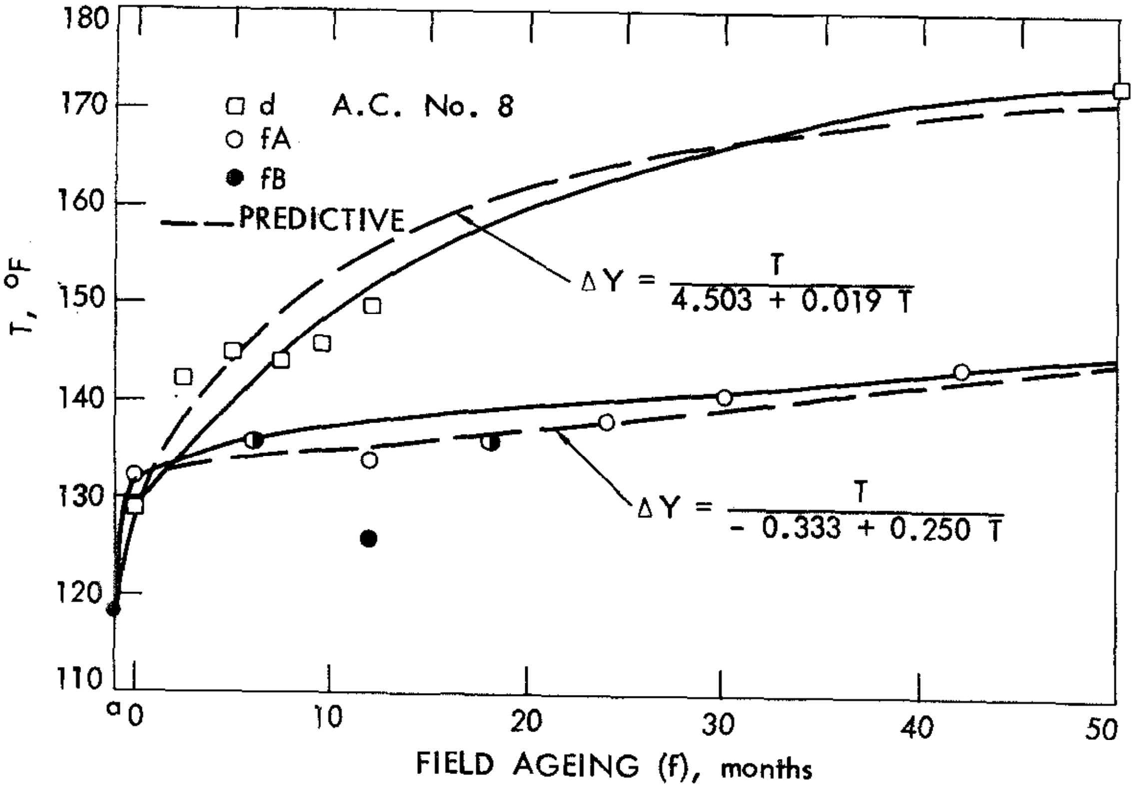

Fig. 10h. Softening point vs time of ageing, A.C. No. 8.

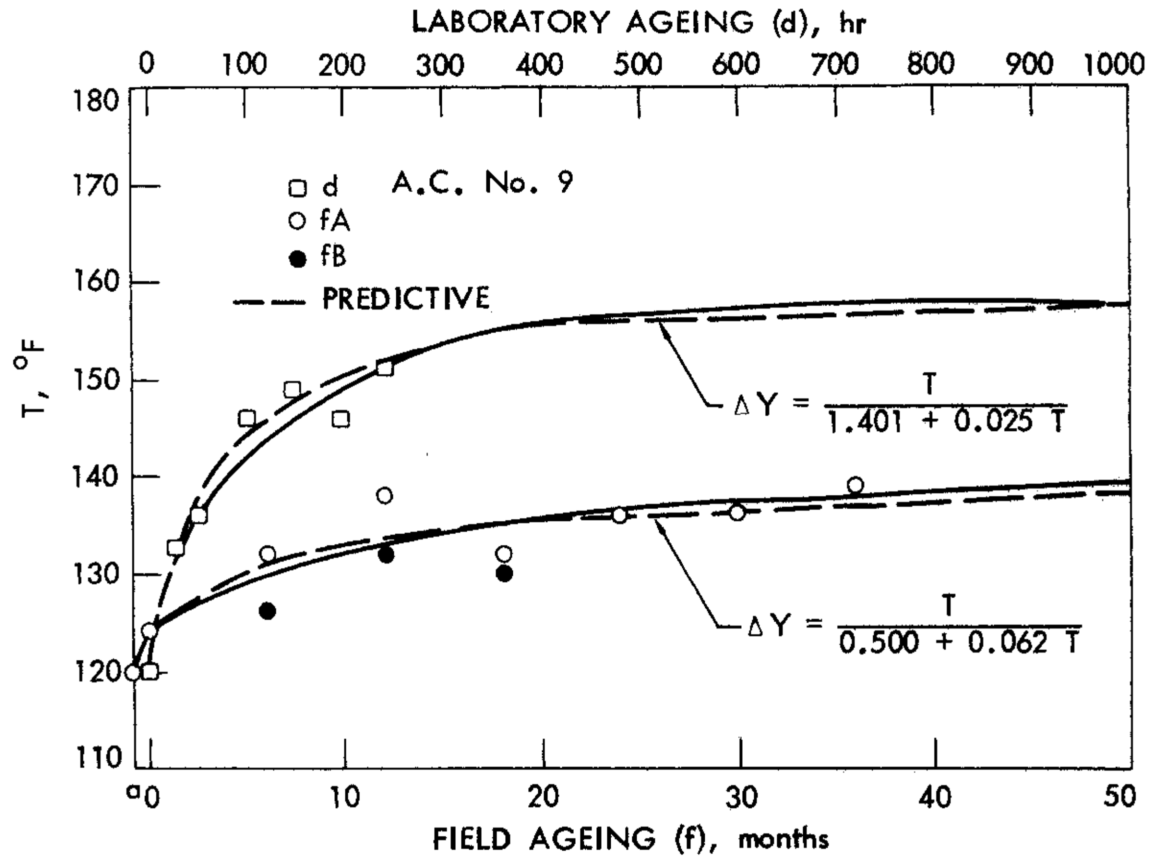

Fig. 10i. Softening point vs time of ageing, A.C. No. 9.

For log viscosity at 77 °F vs laboratory ageing time plots (Figs. 8a through 8i), two least square fitting curves were indicated, those only with data up to 240 hr were used (dashed lines) and those fitted with data up to 1000 hr laboratory ageing (solid lines). Limiting viscosities (viscosity at infinite time) for the nine asphalts studied were calculated by applying the following equation:

$$Y_u = Y_o + \frac{1}{b} \qquad (5)$$

where Y_u = ultimate or limiting value

Y_o = initial value (d - o)

$1/b$ = ultimate change.

Table 10. Changes in microductility at 77 °F, cm.

A.C. No.		1	2	3	4	5	6	7	8	9
Original (a)		63	71	72	67	81.4	53.0	68.4	51.0	63.0
TFOT (d)		46	36	82	89	91.0	57.0	84.0	60.0	55.0
Lab ageing										
24 hr (d24)		9.2	5.4	59	82	101.0[‡]	16.0[‡]	70.0[‡]	20.0[‡]	11.0
48 hr (d48)		5.0	3.0	50	41	102.6	5.1	56.0[‡]	7.0	5.5
96 hr (d96)		2.6	2.0	20	23	122.0	3.0	29.0[‡]	4.0	6.7
240 hr (d240)		2.0	1.5	5.2	4.7	115.0	0.5	8.0[‡]	2.0	–
480 hr (d480)		–	–	–	3.8	79.0[‡]	1.0[‡]	4.0[‡]	1.5[‡]	–
1000 hr (d1000)		0.5	–	0.4	1.8	- 0.3	1.1	1.3	1.0	–
Field ageing										
Plant (p)		48	62	87	93	–	75.0	68.0	67.0	65.0
0 months (f0)	A[*]	69	72	78	81	–	–	60.0	67.0	79.0
	B[†]	69	72	78	102	–	–	–	–	68.0
6 months (f6)	A	87	62	102	102	–	23.0	73.0	15.0	37.0
	B	87	63	95	101	–	23.0	64.5	14.6	28.0
12 months (f12)	A	63	27	44	58	–	24.4	76.0	25.0	57.0
	B	70	–	82	56	–	31.0	101.0	24.0	47.0

Table 10. Continued.

A.C. No.		1	2	3	4	5	6	7	8	9
18 months (f18)	A	70	33	88	84	—	—	55.5	8.5	16.5
	B	76	35	79	85	—	—	80.5	11.0	16.5
24 months (f24)	A	65	14	21	69	—	23.0	57.8	—	—
	B	16	9.0	43	55	—	—	—	—	—
30 months (f30)	A	16	7.7	84	65	—	7.2	—	5.9	—
	B	17	8.0	69	74	—	—	—	—	—
36 months (f36)	A	15	8.3	35	26	—	—	50.7	—	—
	B	17	6.3	35	37	—	—	—	—	—
42 months (f42)	A	16.5	10.0	43	37	—	4.7	—	5.0	—
	B	14.0	4.0	34	12	—	—	—	—	—
48 months (f48)	A	4.8	3.8	28	28					
	B	6.0	—	29	15					

---

[*] A, in wheel tracks.

[†] B, between wheel tracks.

[‡] Interpolated value.

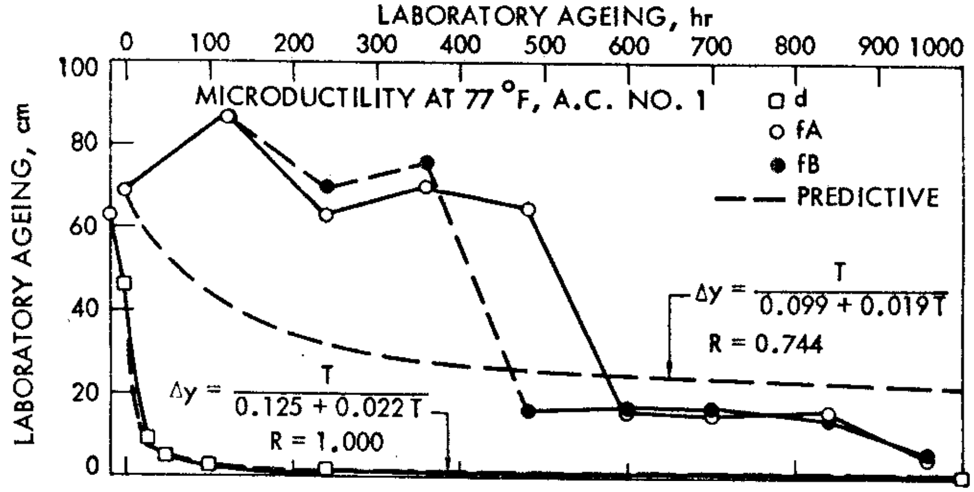

Fig. 11a. Microductility at 77 °F vs time of ageing, A.C. No. 1.

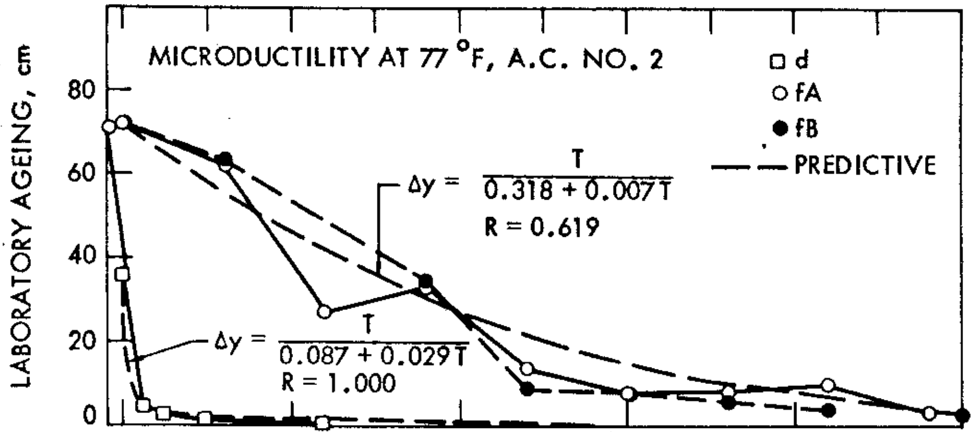

Fig. 11b. Microductility at 77 °F vs time of ageing, A.C. No. 2.

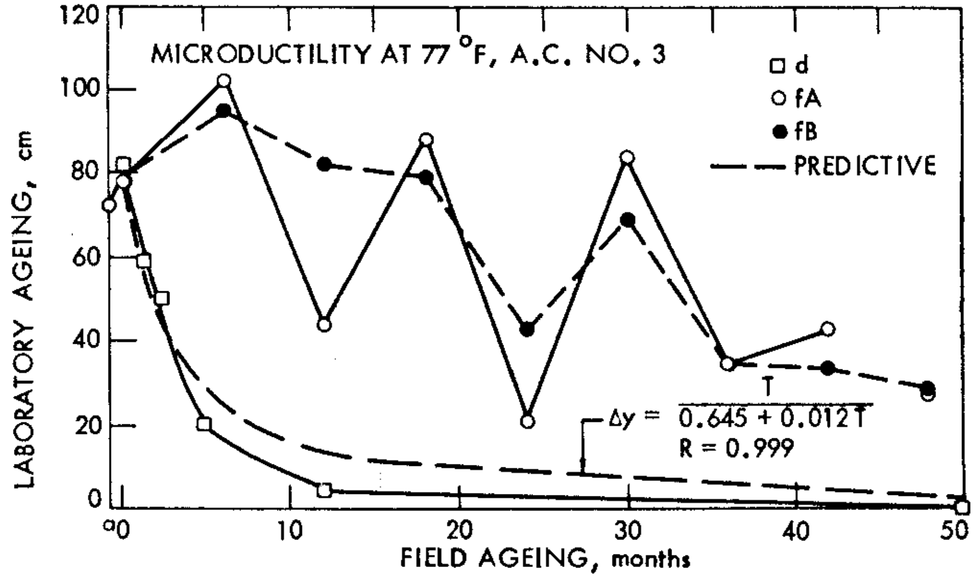

Fig. 11c. Microductility at 77 °F vs time of ageing, A.C. No. 3.

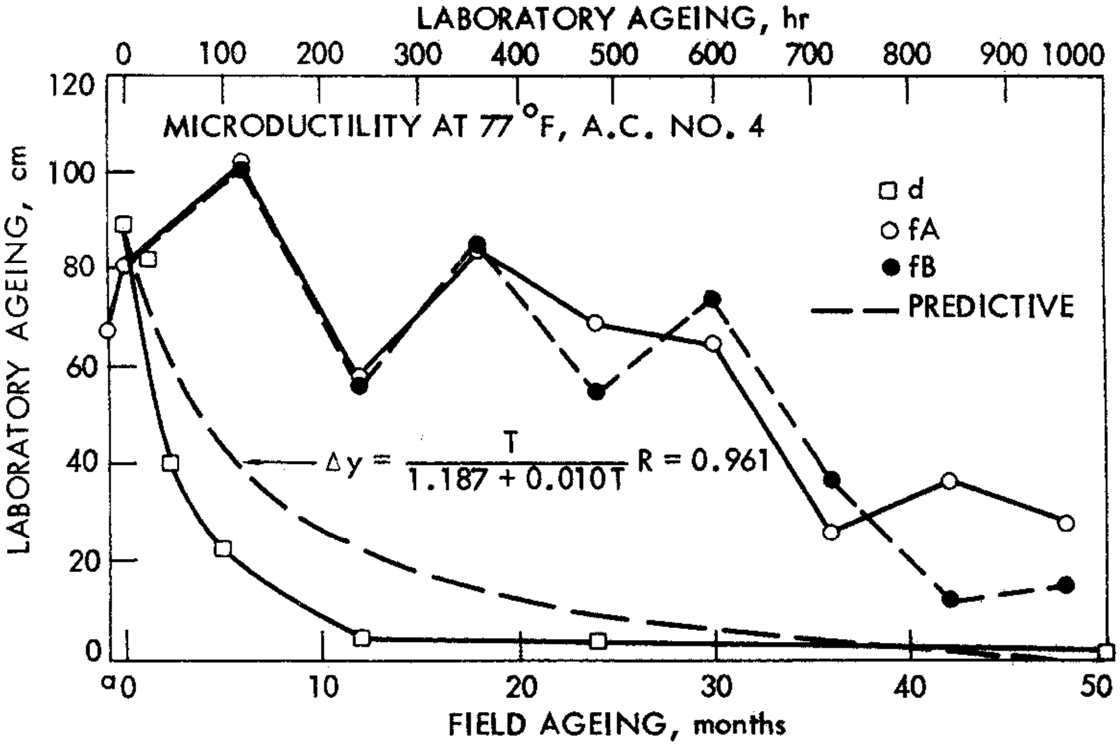

Fig. 11d. Microductility at 77 °F vs time of ageing, A.C. No. 4.

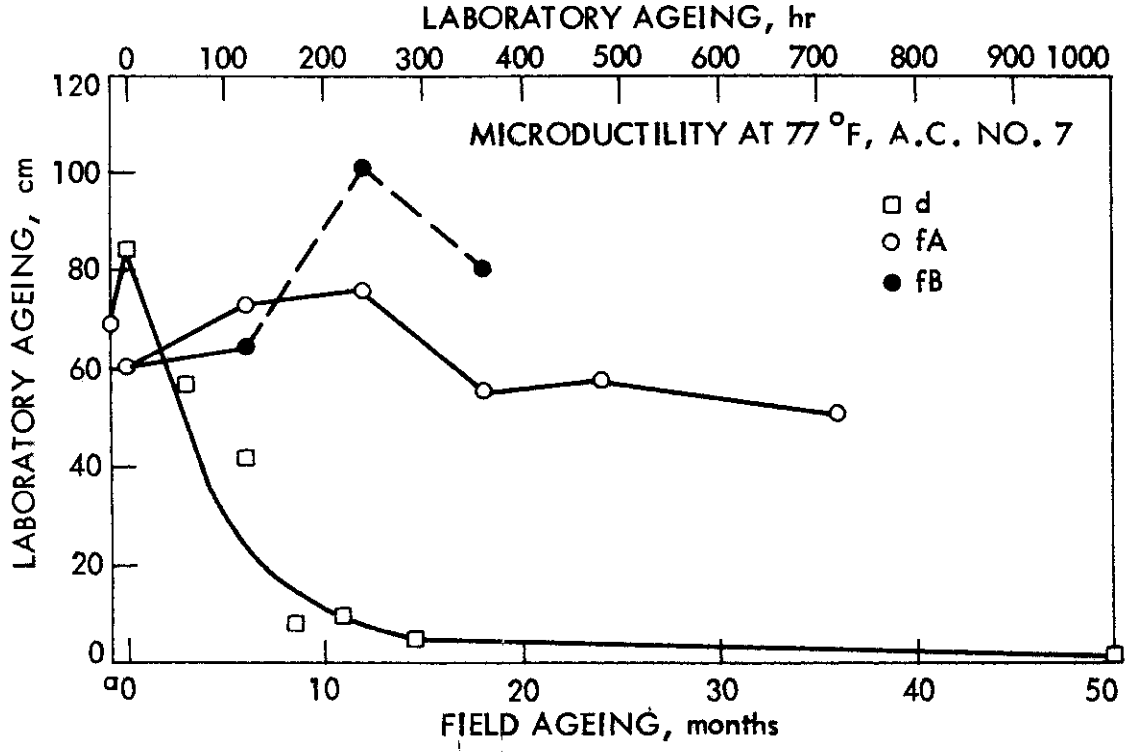

Fig. 11e. Microductility at 77 °F vs time of ageing, A.C. No. 5.

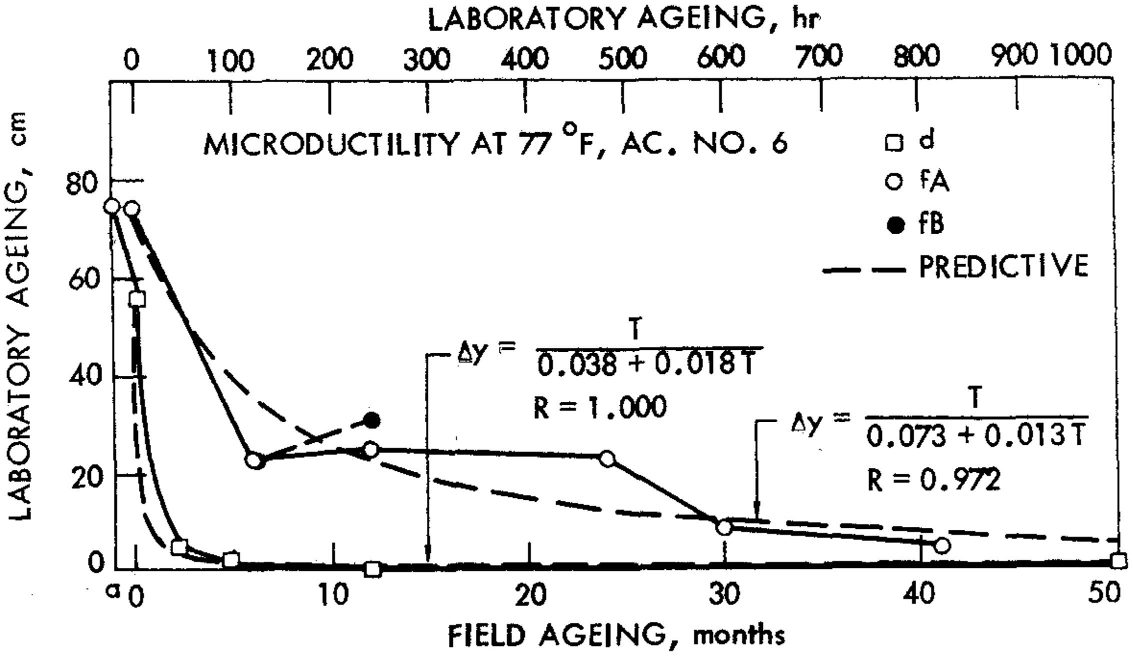

Fig. 11f. Microductility at 77 °F vs time of ageing, A.C. No. 6.

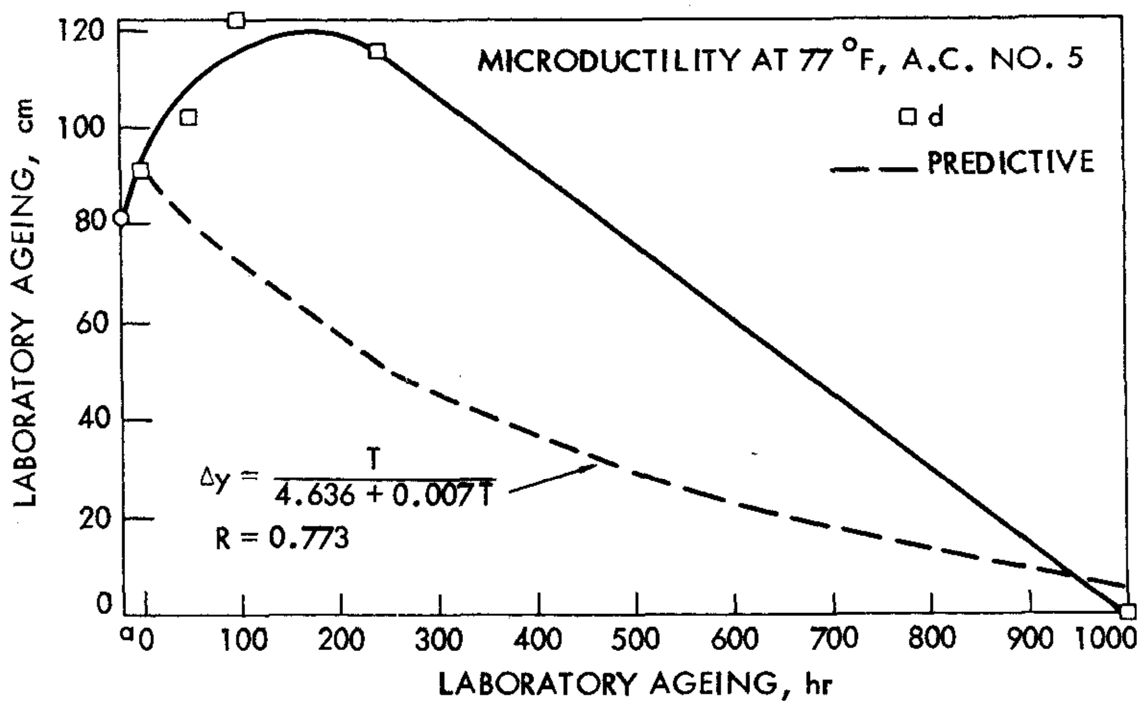

Fig. 11g. Microductility at 77 °F vs time of ageing, A.C. No. 7.

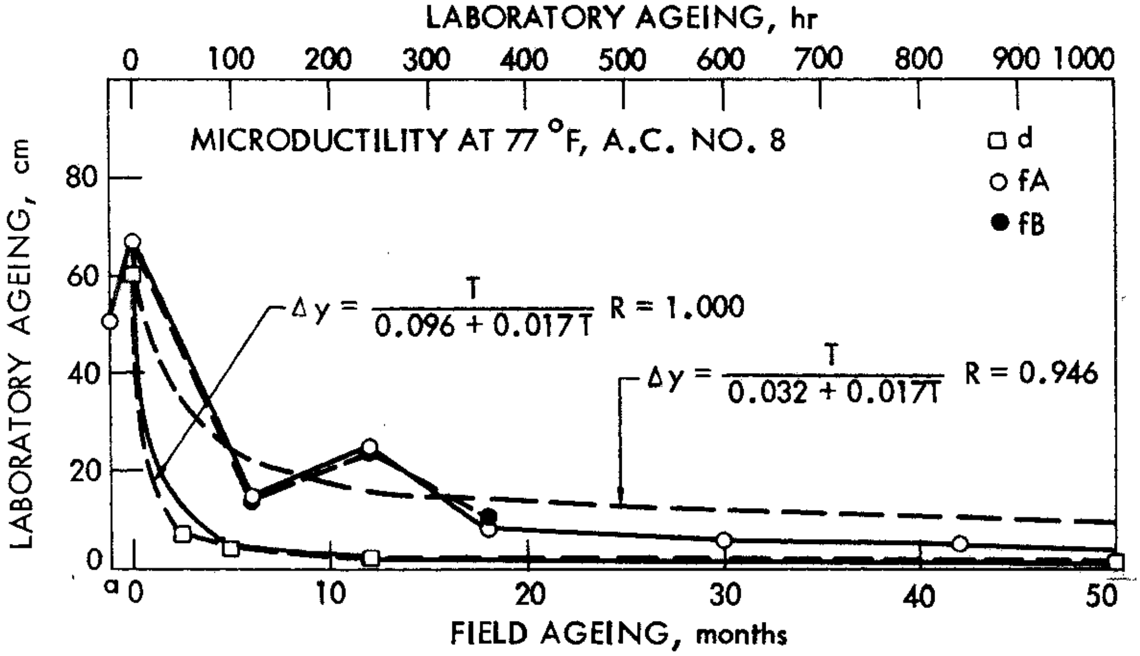

Fig. 11h. Microductility at 77 °F vs time of ageing, A.C. No. 8.

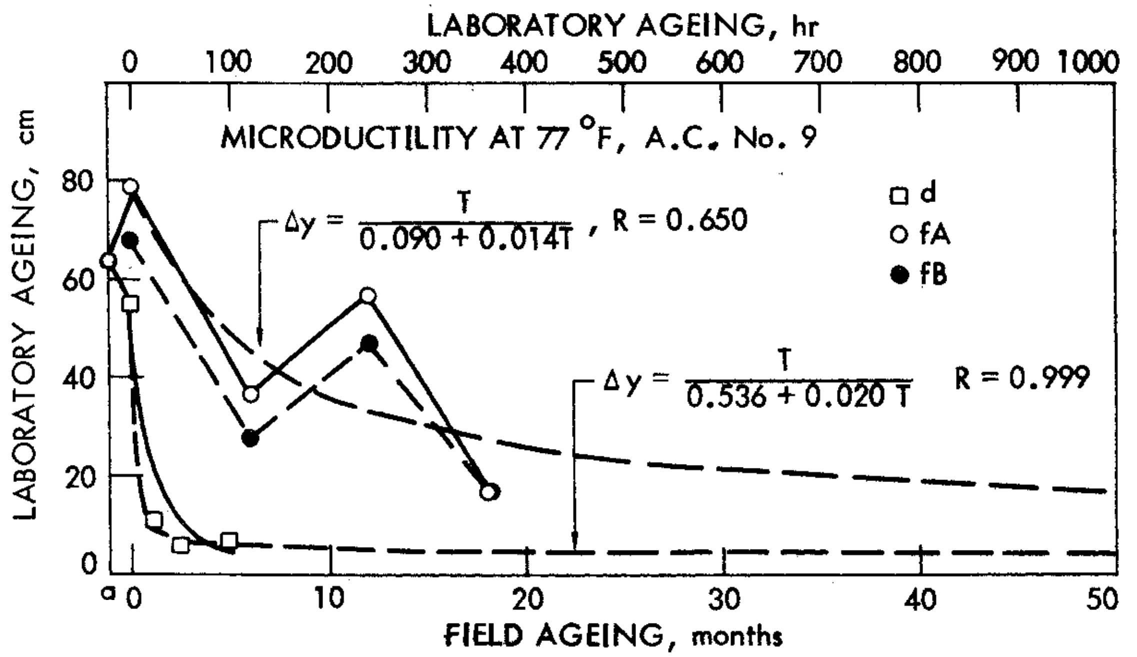

Fig. 11i. Microductility at 77 °F vs time of ageing, A.C. No. 9.

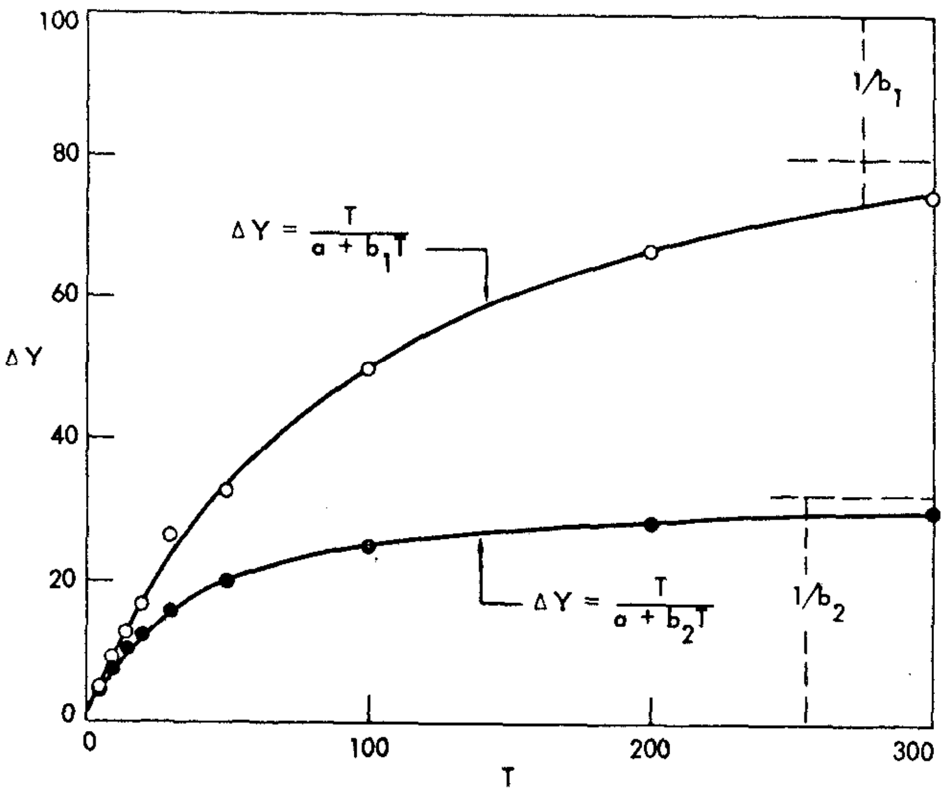

Fig. 12a. ΔY vs T curves.

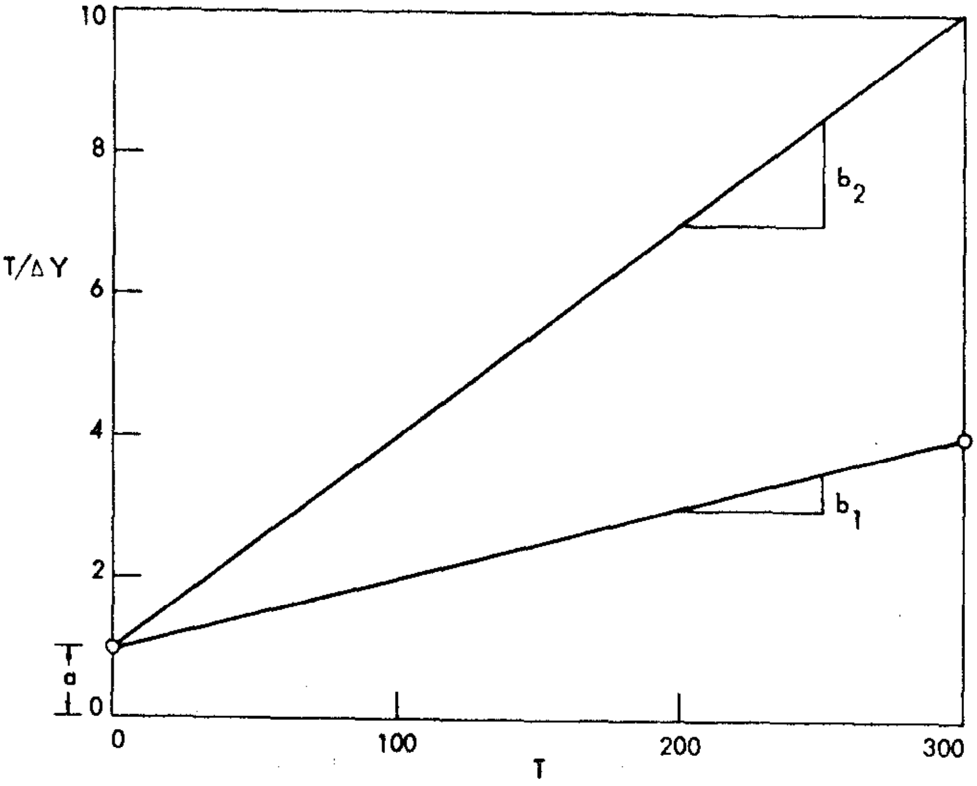

Fig. 12b. T/ΔY vs T curves.

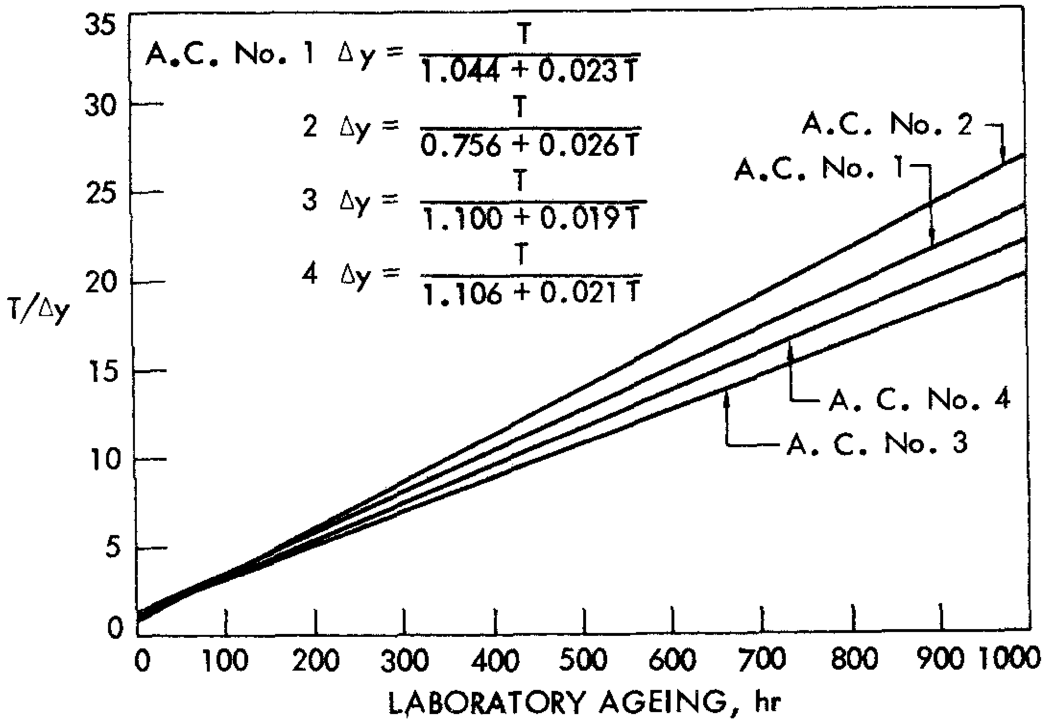

Fig. 13a. T/ΔY vs T, penetration change, laboratory ageing, A.C. No. 1 through 4.

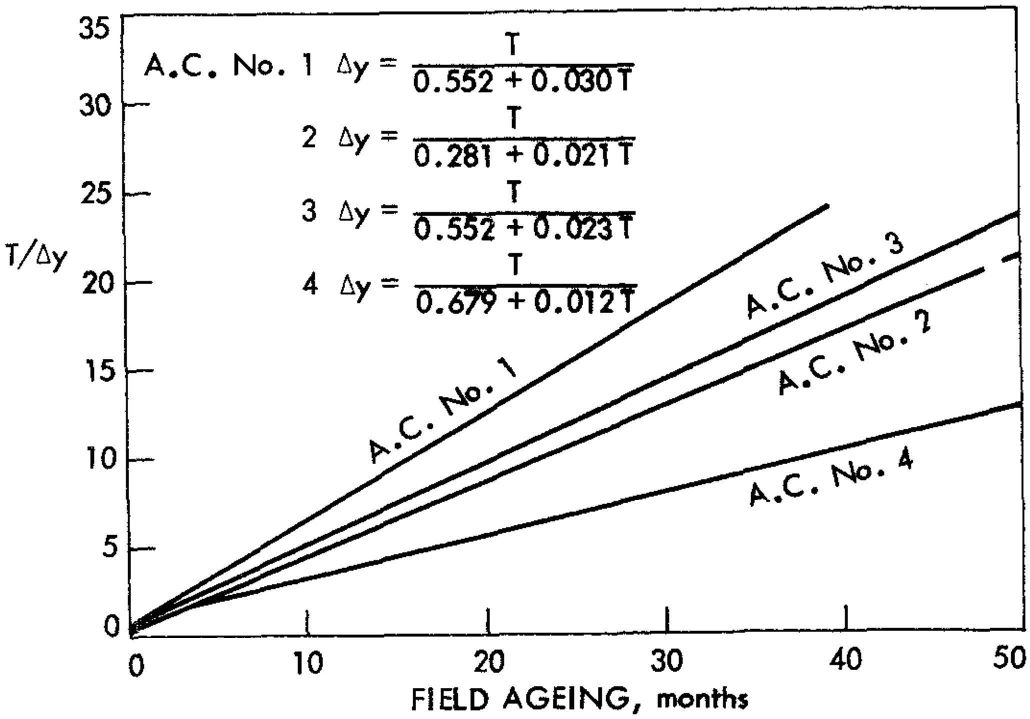

Fig. 13b. T/ΔY vs T, penetration change, field ageing, A.C. No. 1 through 4.

Table 11. Constants for predictive equations.

	Property	A.C. No. 1				A.C. No. 2				A.C. No. 3			
		a	R	b	1/b	a	R	b	1/b	a	R	b	1/b
d	Penetration	1.044	0.999	0.023	43.478	0.756	1.000	0.026	38.462	1.100	0.998	0.019	52.632
fA[*]		0.552	0.925	0.030	33.333	0.281	0.963	0.021	47.619	0.552	0.984	0.023	43.478
fB[+]		0.241	0.956	0.024[‡]	41.667	0.353	0.924	0.018	55.556	0.727	0.793	0.018	55.556
d	Viscosity at 77 °F	43.100	0.998	0.718	1.393	45.117	0.999	0.983	1.017	60.200	0.999	0.608	1.645
fA		10.505	0.972	1.866	0.536	41.908	0.808	0.697	1.435	14.587	0.980	0.963	1.038
fB		16.745	0.831	1.620	0.617	27.828	0.916	0.988	1.012	13.229	0.962	1.197	0.836
d	Viscosity at 140 °F	32.834	0.999[‡]	0.469	0.018	40.141	0.997	0.546	1.832	143.815	0.999	0.523	1.912
fA		51.534	0.477	0.663	1.508	35.275	0.745	0.751	1.332	30.207	0.922	1.072	0.933
fB		23.335	0.711	1.567	0.638	49.482	0.236	0.335	2.985	25.868	0.866	1.128	0.887
d	Softening point	2.853	0.991	0.180	55.556	4.833	0.973	0.020	50.000	3.617	0.973	0.018	55.556
fA		5.498	0.123	0.028	35.714	0.919	0.787	0.052	19.231	1.048	0.772	0.026[‡]	38.462
fB		0.081	0.417	0.246	4.065	0.436	0.919	0.066	15.152	0.695	0.844	0.039[‡]	25.641
d	Microductility	0.125	1.000	0.022	45.455	0.087	1.000	0.029	34.483	0.645	0.999	0.012	83.333
fA		0.099	0.744	0.019	52.632	0.318	0.619	0.007	142.860	0.816	0.201	0.021	47.619
fB		0.030	0.694	0.023	43.478	0.399	0.269	0.003	333.330	0.570	0.102	0.001[‡]	1.000
d	Asphaltenes	11.348	0.996	0.108	9.259	13.842	0.967	0.102	9.804	21.855	0.926	0.049	20.408
fA		2.108	0.825	0.082[‡]	12.195	4.741	0.502	0.080[‡]	12.500	1.226	0.972	0.284	3.521
fB		2.446	0.499	0.034[‡]	29.412	4.078	0.768	0.076[‡]	13.158	2.341	0.587	0.224	4.464

	Property	A.C. No. 4				A.C. No. 5				A.C. No. 6			
		a	R	b	1/b	a	R	b	1/b	a	R	b	1/b
d	Penetration	1.106	0.999	0.021	47.619	1.635	0.997	0.017	58.824	2.305	0.989	0.022	45.455
fA		0.679	0.604	0.012	83.333					0.089	0.990	0.022	45.455
fB		0.024	0.969	0.029	34.483					0.099	0.990	0.022	45.455
d	Viscosity at 77 °F	41.157	1.000	0.720	1.389	44.615	0.998	0.924	1.082	57.155	0.992	0.759	1.318
fA		5.914	0.970	1.111	0.900					7.291	0.992	1.147	0.872
fB		6.094	0.987	1.035	0.966					4.041	0.824	1.435	0.697
d	Viscosity at 140 °F	122.879	0.987	0.429	2.331	232.997	0.954	0.620	1.613	69.952	0.999	0.679	1.473
fA		19.691	0.917	1.017	0.983					9.676	0.952	1.125	0.889
fB		19.681	0.862	0.947	1.056					2.743	0.999	1.540	0.649
d	Softening point	4.748	0.982	0.017	58.824	9.327	0.958	0.020	50.000	6.376	0.881	0.015	66.667
fA		1.990	0.092	0.006	166.667					0.401	0.759	0.039	25.641
fB		2.011	0.101	0.007	142.857					0.183	0.999	0.035	28.571
d	Microductility	1.187	0.961	0.010	100.00	4.636	0.773	0.007	142.857	0.038	1.000	0.018	55.556
fA		- 0.432	0.972	0.052	19.231					0.073	0.972	0.013	76.923
fB		- 1.036	0.802	0.114	8.772					- 0.433	1.000	0.026	38.462
d	Asphaltenes	20.137	0.901	0.057	17.544	44.065	0.389	0.024	41.667	11.796	0.995	0.980	10.204
fA		7.538	0.078	0.013	76.923					2.756	0.438	0.037[‡]	27.027
fB		2.038	0.822	0.221	4.525					1.184	0.964	0.068[‡]	14.706

---

[*] A, in wheel tracks.

[+] B, between wheel tracks.

[‡] Adjusted Y_o.

Table 11. Continued.

	Property	A.C. No. 7				A.C. No. 8				A.C. No. 9			
		a	R	b	1/b	a	R	b	1/b	a	R	b	1/b
d	Penetration	1.643	0.999	0.019	52.632	1.299	0.997	0.022	45.455	0.196	0.999	0.025	40.000
fA[*]		0.010	0.999	0.023	43.478	0.075	0.996	0.026	38.462	0.483	0.817	0.023	43.478
fB[+]		0.043	0.996	0.021	47.619	0.107	0.992	0.025	40.000	0.629	0.629	0.014	71.429
d	Viscosity at 77 °F	61.699	0.999	0.656	1.524	71.230	1.000	0.770	1.299	55.120	0.997	0.683	1.464
fA		3.417	0.993	1.185	0.844	3.239	0.986	1.219	0.820	8.013	0.956	1.326	0.754
fB		2.710	0.998	1.268	0.789	4.420	0.950	1.191	0.840	17.879	0.792	1.110	0.901
d	Viscosity at 140 °F	121.518	0.989	0.564[‡]	1.773	50.873	0.996	0.618[‡]	1.618	42.916	0.958	1.088[‡]	0.919
fA		8.848	0.975	1.706	0.586	3.923	1.000	1.347	0.742	24.579	0.800	1.099	0.910
fB		25.547	1.000	6.582	0.152	- 0.501	1.000	1.814	0.551	- 4.227	1.000	3.568	0.280
d	Softening point	7.972	0.981	0.012	83.333	4.503	0.978	0.019	52.632	1.401	0.996	0.025	40.000
fA		0.335	0.957	0.042	23.810	3.625	0.046	0.005	200.000	0.500	0.880	0.062	16.129
fB		0.189	0.975	0.060	16.667	- 0.333	0.933	0.250	4.000	–	–	–	–
d	Microductility	1.034	0.987	0.011	90.909	0.096	1.000	0.017	58.824	0.036	0.999	0.020	50.000
fA		- 1.936	0.851	0.295	3.390	0.043	0.913	0.016	62.500	0.180	0.356	0.012	83.333
fB		1.642	1.000	0.012	83.333	0.032	0.946	0.017	58.824	0.090	0.650	0.014	71.429
d	Asphaltenes	32.374	0.946	0.060	16.667	12.885	0.983	0.080	12.500	5.565	0.994	0.108	9.259
fA		2.350	0.712	0.147	6.803	0.466	0.888	0.122	8.197	3.266	0.723	0.027	37.037
fB		1.643	0.941	0.259	3.861	- 0.128	0.994	0.159	6.289	2.003	0.810	0.065	15.385

[*] A, in wheel tracks.

[+] B, between wheel tracks.

[‡] Adjusted Y_o.

They were indicated by horizontal broken lines. Limiting values for penetration, viscosity at 77 °F and softening point for laboratory aged samples were calculated and are given in Table 12. Limiting values for field pavement asphalts are given in Table 13.

It can be noted that the equations for the prediction curves for 240-hr fittings are different from 1000-hr fittings. Therefore, except for A.C. No. 5 and 8, the limiting values for viscosity at 77 °F are also different. However, the critical first 200-hr portion of the curves are in general agreement.

The limiting values have been suggested by Brown et al.[82] as an index in comparing performance or potential behavior of asphalts. However, as pointed out by the author[2], when it is used as the only index

Table 12. Limiting values of physical properties — laboratory ageing.

A.C. No.	Property	Original (a)	TFOT (d)	Ultimate change 1/b	Limiting value Y_u
1	Penetration	89	53	42.48	9.52
2		94	54	38.46	15.54
3		91	57	52.63	4.37
4		90	56	47.62	8.38
5		84	67	58.82	8.18
6		87	65	45.46	19.54
7		95	59	52.68	6.37
8		90	60	45.46	14.54
9		92	62	40.00	22.00
1	Viscosity at 77 °F, $\times 10^6$ poises	1.16	4.22	1.393 (1.120)*	104.3 (55.63)*
2		1.23	5.35	1.017	55.64
3		1.58	3.76	1.645 (1.391)*	163.4 (91.03)*
4		1.10	3.09	1.389 (1.255)*	75.68 (55.59)*
5		1.14	1.68	1.082 (1.130)*	20.29 (22.67)*
6		1.70	3.80	1.318 (1.075)*	79.03 (45.16)*
7		1.15	3.90	1.524	130.3
8		1.10	4.15	1.299 (1.289)*	82.62 (80.74)*
9		1.22	2.86	1.464 (1.101)*	83.26 (36.09)*
1	Softening point, °F	119.0	127.5	55.56	183.06
2		116.5	131.0	50.00	181.00
3		115.5	123.0	55.56	178.56
4		114.5	126.0	58.82	184.82
5		113.0	119.0	50.00	169.00
6		124.0	127.0	66.67	193.67
7		116.0	123.0	83.33	206.33
8		118.0	129.0	52.63	181.63
9		119.5	119.5	40.00	159.50

*If only data up to 240 hr are used in regression analysis.

Table 13. Limiting values of physical properties — field ageing.

A.C. No.	Property	Original (a)	Field (f - o)	Ultimate change 1/b	Limiting value Y_u
1	Penetration	89	57	33.33	23.67
2		94	67	47.62	19.38
3		91	57	43.48	13.52
4		90	62	34.48	27.52
6		87	71	45.46	25.54
7		95	79	43.48	35.52
8		90	71	38.46	32.54
9		92	64	43.48	20.52
1	Viscosity at 77 °F, × 10^6 poises	1.16	4.37	0.536	16.73
2		1.23	4.60	1.435	125.5
3		1.58	3.39	1.038	37.00
4		1.10	3.01	0.900	23.91
6		1.70	2.81	0.872	20.92
7		1.15	2.25	0.844	15.71
8		1.10	2.14	0.820	22.59
9		1.22	2.61	0.754	14.81
1	Softening point, °F	119.0	127.5	35.71	163.21
2		116.5	125.0	19.23	144.23
3		115.5	125.0	38.46	163.46
4		114.5	119.0	166.67	285.67
6		124.0	118.0	25.64	143.64
7		116.0	118.0	23.81	141.81
8		118.0	132.0	200.00	332.0
9		119.5	124.0	16.13	140.13

in asphalt durability or quality evaluation, it can be misleading. The reason is that in reality asphalt will not last forever or to infinite time. More likely than not the asphalt will reach a critical value of penetration or viscosity or ductility or other controlling property and fail before it reaches the limiting value or infinite time. Therefore, it is this critical value or values of the controlling property or properties, and the time the asphalt in question takes to reach this value that is of the utmost practical concern. It is entirely possible that an asphalt A that showed a higher limiting penetration than an asphalt B could reach a critical penetration quicker in service life and fail earlier than B, and would properly be considered a poorer asphalt.

For this reason, it was suggested that[2], instead of or in addition to limiting values of penetration or viscosity, the time an asphalt would take to reach a critical penetration — e.g., 20 — or viscosity — say, 20 megapoises at 77 °F — be calculated from the hyperbolic Eq. (4) and be used as an index to indicate the relative durability of asphalt. The use of these concepts as applied to quality control and durability prediction for asphalt will be discussed in Chapter VIII.

From viscosity data it is shown that ageing in IDT resulted in a decrease in the degree of complex flow c and an increase in shear susceptibility S (Table 8 and Figs. 14a and 14b). Here, again, the behavior of asphalts in IDT appeared to be in agreement with other reported field findings[46,84].

Asphalt hardening can also be expressed in terms of penetration ratio (penetration, original/penetration, aged) (Table 14) or viscosity ratio (viscosity, aged/viscosity, original). The viscosity ratio at 77 °F is often called the ageing index. Results of viscosity ratio for asphalts in IDT were calculated and are given in Table 15 for viscosity at 77 °F and in Table 16 for viscosity at 140 °F. Linear relationships were found between log penetration ratio and log time (Figs. 15a through 15i) and between log viscosity ratio and log time during IDT ageing (Figs. 16a through 16i, and 17a through 17i). From these plots relative durability or hardening susceptibility of asphalts

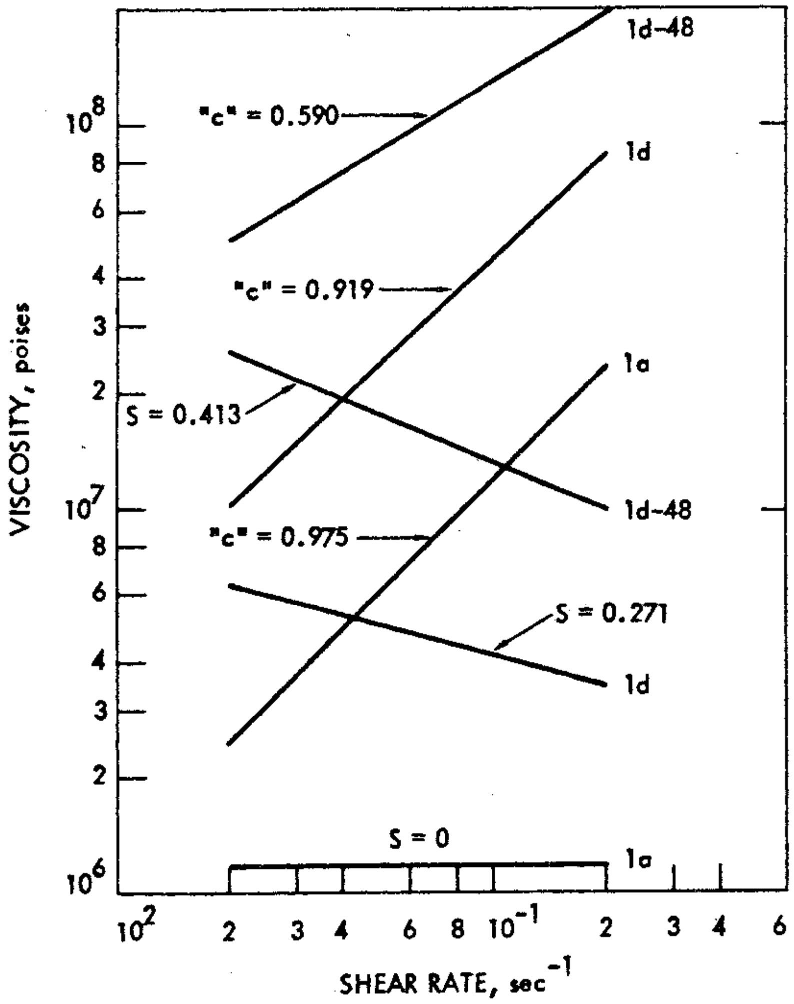

Fig. 14a. Shear index S and complex flow c, laboratory ageing, A.C. No. 1.

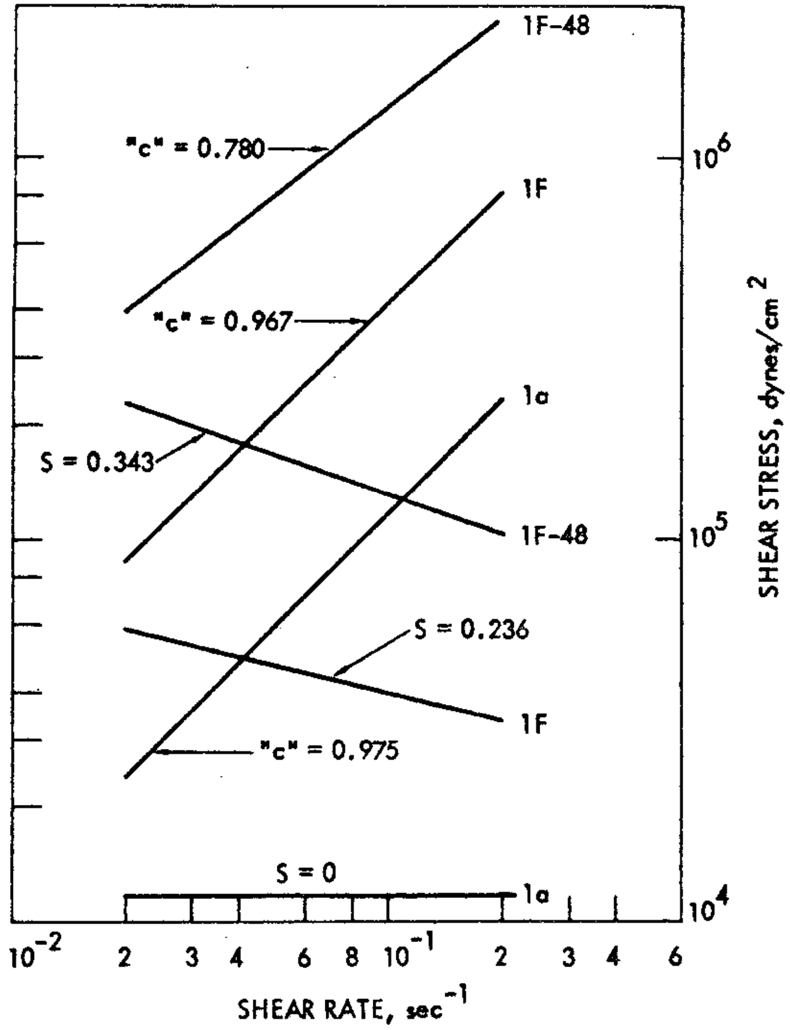

Fig. 14b. Shear index S and complex flow c, laboratory ageing, A.C. No. 1.

Table 14. Penetration ratio.

A.C. No.		1	2	3	4	5	6	7	8	9
Original (a)		1.00	1.00	1.00	1.00	1.00	1.00	1.00	1.00	1.00
TFOT (d)		1.68	1.74	1.60	1.61	1.25	1.58	1.61	1.50	1.48
Lab ageing										
24 hr (d24)		2.97	2.76	2.53	2.37	1.71[‡]	1.74	2.16[‡]	2.05[‡]	2.49
48 hr (d48)		3.07	3.13	3.03	2.90	2.05	2.72	2.57[‡]	2.73	3.41
96 hr (d96)		3.42	3.76	3.50	3.60	2.27	3.22	3.28[‡]	3.00	3.83
240 hr (d240)		4.68	4.70	4.55	4.50	3.11	3.95	5.00[‡]	3.46	4.38
480 hr (d480)		–	5.53	–	–	4.20[‡]	4.14	5.94[‡]	4.09[‡]	4.00
1000 hr (d1000)		8.09	–	11.38	9.00	7.64	6.21	9.50	6.00	–
Field ageing										
Plant (p)		1.48	1.31	1.60	1.34	–	1.23	1.25	1.22	1.16
0 months (f0)	A[*]	1.56	1.40	1.60	1.45	–	–	1.20	1.27	1.44
	B[†]	1.56	1.40	1.60	1.45	–	–	–	–	–
6 months (f6)	A	1.85	1.68	1.90	1.34	–	2.23	2.32	2.09	1.80
	B	1.59	1.62	1.75	1.45	–	2.18	2.32	2.09	1.64
12 months (f12)	A	2.07	2.54	2.17	2.31	–	2.35	2.71	2.14	1.74
	B	2.28	2.47	2.39	2.57	–	2.23	2.26	2.00	1.88

Table 14. Continued.

A.C. No.		1	2	3	4	5	6	7	8	9
18 months (f18)	A	2.17	2.47	2.28	2.65	–	2.56	2.71	2.57	2.36
	B	2.07	2.61	2.33	2.50	–	2.56	2.71	2.50	2.24
24 months (f24)	A	2.28	2.69	2.60	2.37	–	2.42	2.57	2.37	2.24
	B	2.47	2.69	2.68	3.10	–	2.49	2.64	2.31	2.36
30 months (f30)	A	2.54	2.85	2.84	3.00	–	2.64	2.71	2.57	2.30
	B	2.70	3.03	2.68	2.81	–	2.56	2.88	2.57	2.42
36 months (f36)	A	2.47	2.76	3.03	3.00	–	–	2.64	2.50	2.56
	B	2.41	2.94	3.14	3.00	–	–	2.71	2.57	2.97
42 months (f42)	A	2.41	2.85	2.94	3.10	–	3.11	–	2.65	–
	B	2.28	3.24	2.84	3.21	–	3.11	–	2.65	–
48 months (f48)	A	3.18	3.36	3.37	3.46					
	B	2.87	3.36	3.37	3.46					

[*] A, in wheel tracks.

[†] B, between wheel tracks.

[‡] Interpolated value.

Table 15. Ageing index, viscosity at 77 ^{o}F.

A.C. No.		1	2	3	4	5	6	7	8	9
Original (a)		1.00	1.00	1.00	1.00	1.00	1.00	1.00	1.00	1.00
TFOT (d)		3.64	4.35	2.34	2.81	1.47	2.24	3.39	3.77	2.34
Lab ageing										
24 hr (d24)		15.86	9.51	6.01	8.18[‡]	3.07[‡]	–	6.09[‡]	7.55[‡]	8.44
48 hr (d48)		17.67	15.69	8.99	14.27	4.91	8.59	10.87[‡]	11.45	10.25
96 hr (d96)		20.60	20.00	12.15	20.55	6.49	12.35	19.13[‡]	13.45	12.30
240 hr (d240)		37.93	29.43	29.75	33.55	11.84	19.41	44.35[‡]	34.55	22.54[‡]
480 hr (d480)		–	31.30	48.10[‡]	47.27[‡]	12.90[‡]	21.76	68.26[‡]	48.64[‡]	36.89[‡]
1000 hr (d1000)		76.72	–	74.68	58.18	15.18	42.35	86.26	58.18	56.56[‡]
Field ageing										
Plant (p)		3.71	3.82	2.15	2.81	–	1.65	1.80	3.11	1.88
0 months (f0)	A[*]	4.20	3.74	2.15	2.74	–	–	1.96	1.95	2.14
	B[†]	4.20	3.74	2.15	2.74	–	–	–	–	–
6 months (f6)	A	3.71	4.86	2.15	3.24	–	5.05	7.22	5.82	4.02
	B	4.91	4.35	2.39	3.18	–	5.12	7.60	5.82	3.20
12 months (f12)	A	8.45	7.24	6.52	10.18	–	6.24	8.52	13.18	9.43
	B	8.22	7.48	6.20	11.09	–	7.00	8.52	11.36	7.30

Table 15. Continued.

A.C. No.		1	2	3	4	5	6	7	8	9
18 months (f18)	A	9.14	7.48	7.09	12.91	–	7.12	11.13	10.45	8.61
	B	9.91	8.36	6.65	14.09	–	8.12	10.43	9.91	8.61
24 months (f24)	A	10.52	–	7.97	19.09	–	7.47	12.61	8.91	9.84
	B	12.93	12.20	7.53	16.91	–	4.59	10.61	8.09	6.89
30 months (f30)	A	12.50	15.04	10.76	18.64	–	7.94	10.43	12.27	7.93
	B	15.95	15.61	8.35	19.64	–	10.29	10.43	12.73	7.46
36 months (f36)	A	10.60	11.22	13.29	14.73	–	–	12.00	–	9.43
	B	10.78	13.01	12.41	16.09	–	–	–	–	–
42 months (f42)	A	11.55	14.47	11.90	14.73	–	10.29	–	11.36	–
	B	8.19	13.41	8.86	20.18	–	–	–	–	–
48 months (f48)	A	16.55	15.93	13.10	19.82					
	B	14.14	16.99	10.19	20.00					

[*] A, in wheel tracks.

[†] B, between wheel tracks.

[‡] Interpolated value.

Table 16. Ageing index, viscosity at 140 ^{o}F.

A.C. No.		1	2	3	4	5	6	7	8	9
Original (a)		1.00	1.00	1.00	1.00	1.00	1.00	1.00	1.00	1.00
TFOT (d)		1.75	3.17	3.07	3.22	1.31	2.63	2.69	2.28	1.56
Lab ageing										
24 hr (d24)		8.92	9.99	4.42	–	–	3.04	5.93	5.46	4.43
48 hr (d48)		11.24	15.67	6.06	10.70	2.75	9.23	7.45	10.51	4.87
96 hr (d96)		17.17	31.54	9.71	12.59	2.50	14.48	9.73	12.73	8.28
240 hr (d240)		59.92	82.54	21.32	21.23	4.34	9.95	18.92	23.27	–
480 hr (d480)		–	–	–	–	–	–	–	–	–
1000 hr (d1000)		147.49	–	98.78	232.16	20.77	59.26	98.77	62.42	–
Field ageing										
Plant (p)		1.61	1.88	1.45	1.93	–	1.55	1.57	1.37	1.21
0 months (f0)	A*	1.69	2.70	1.61	1.61	–	–	1.62	1.28	1.41
	B†	1.69	2.70	1.61	1.61	–	–	–	–	–
6 months (f6)	A	2.00	3.44	2.14	2.33	–	5.59	4.18	4.04	1.70
	B	2.62	3.14	2.31	2.28	–	4.61	4.36	4.83	2.06
12 months (f12)	A	4.29	7.52	3.52	5.41	–	3.83	3.52	5.05	1.62
	B	4.96	7.46	4.43	5.39	–	6.06	3.49	4.68	1.89

Table 16. Continued.

A.C. No.		1	2	3	4	5	6	7	8	9
18 months (f18)	A	3.49	6.41	4.05	4.59	—	6.99	5.13	7.01	2.35
	B	2.74	7.19	3.65	5.59	—	—	—	—	2.96
24 months (f24)	A	3.80	8.97	4.89	6.94	—	5.78	4.52	5.03	3.05
	B	4.92	9.40	4.72	7.71	—	—	—	—	—
30 months (f30)	A	4.95	8.60	4.73	7.20	—	6.85	5.05	6.81	3.31
	B	6.27	8.83	4.25	7.78	—	6.35	—	—	—
36 months (f36)	A	4.24	9.20	5.48	7.03	—	—	5.52	5.48	4.91
	B	5.19	11.78	6.18	6.77	—	—	—	—	—
42 months (f42)	A	4.76	11.21	5.28	6.87	—	9.17	—	6.72	—
	B	3.65	9.26	7.58	—	—	—	—	—	—
48 months (f48)	A	8.14	12.68	6.31	7.68					
	B	6.99	12.97	5.74	7.82					

*A, in wheel tracks.

†B, between wheel tracks.

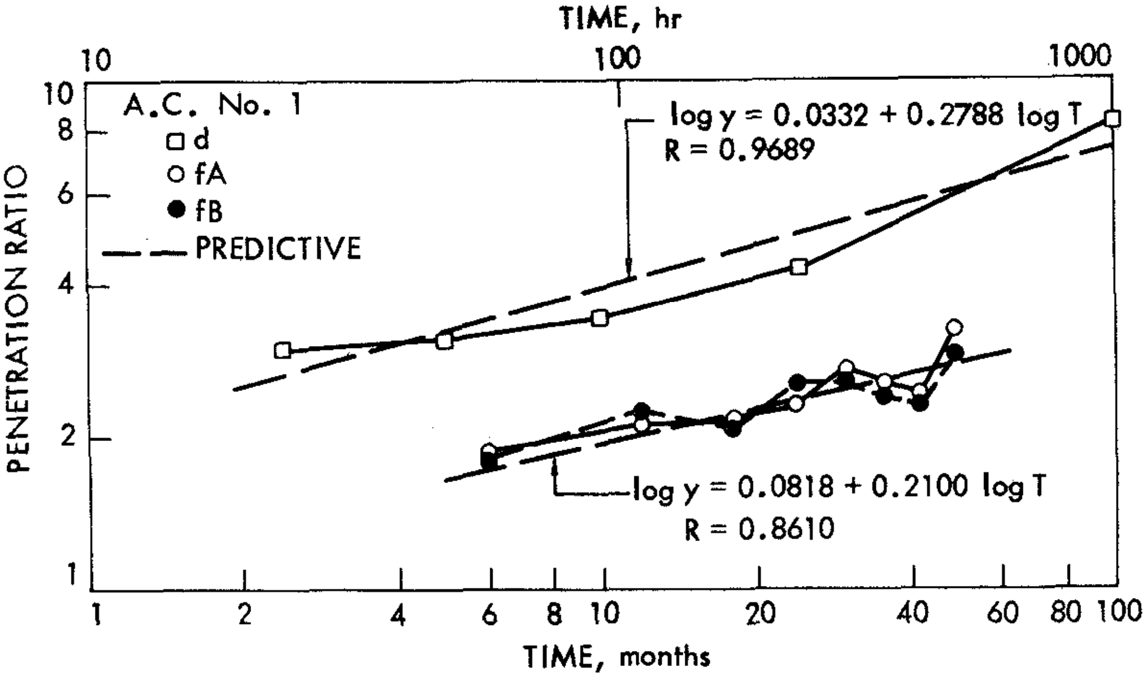

Fig. 15a. Penetration ratio vs time, A.C. No. 1.

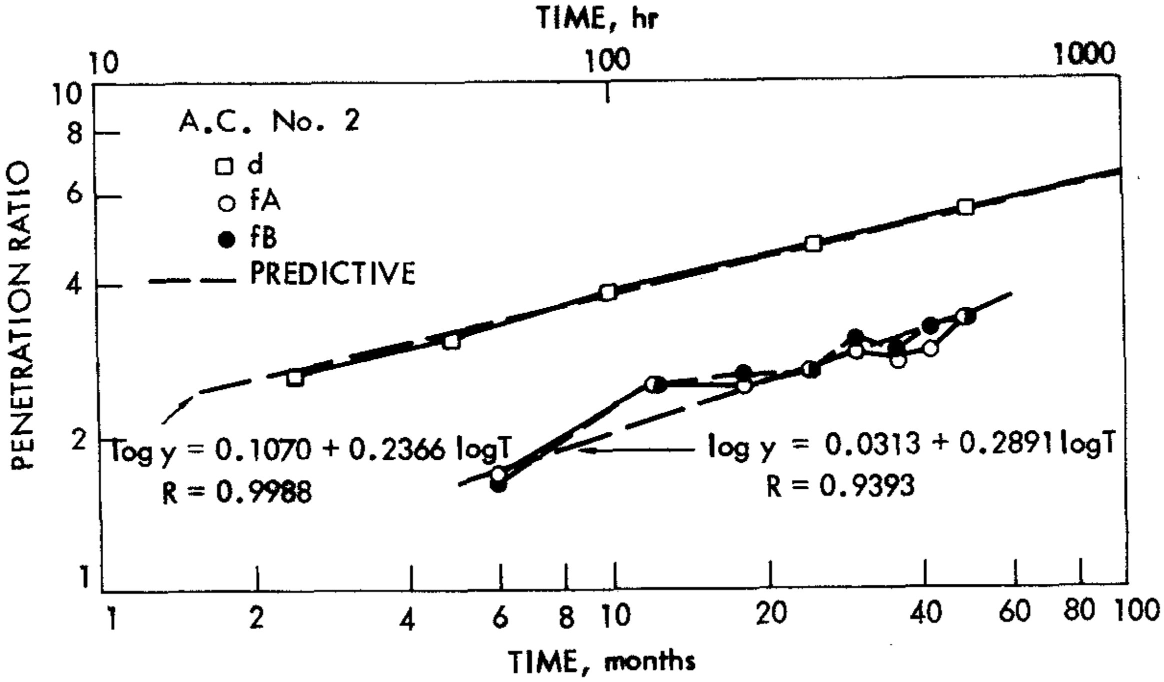

Fig. 15b. Penetration ratio vs time, A.C. No. 2.

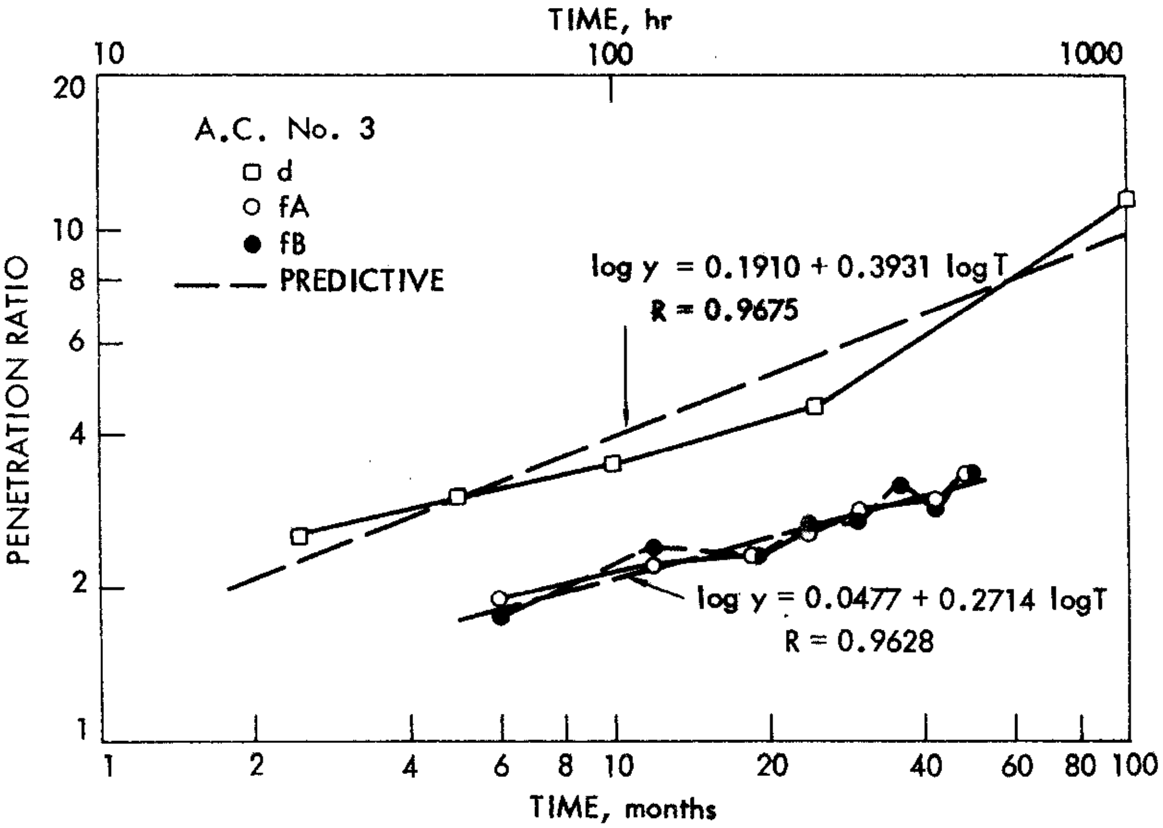

Fig. 15c. Penetration ratio vs time, A.C. No. 3.

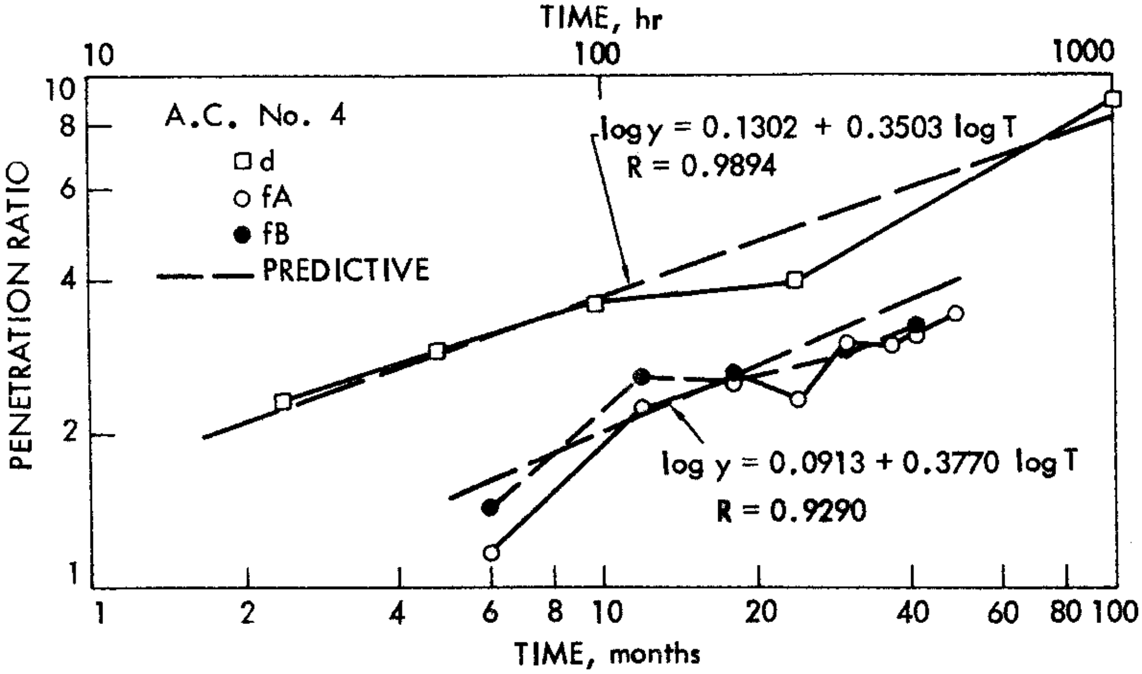

Fig. 15d. Penetration ratio vs time, A.C. No. 4.

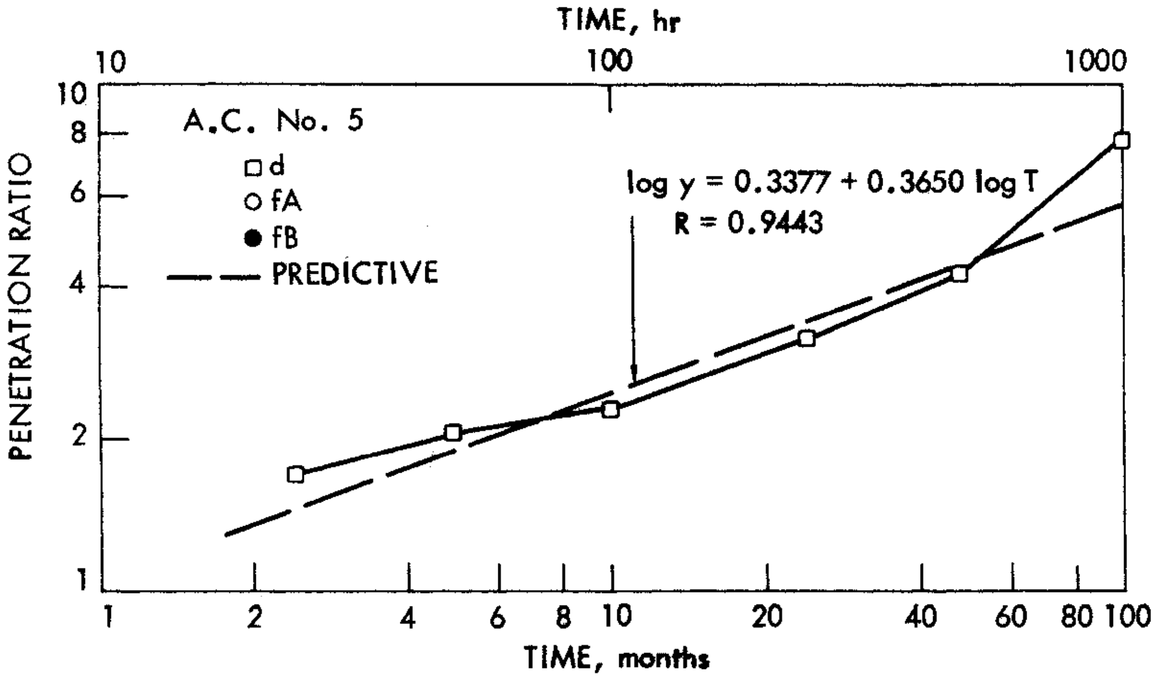

Fig. 15e. Penetration ratio vs time, A.C. No. 5.

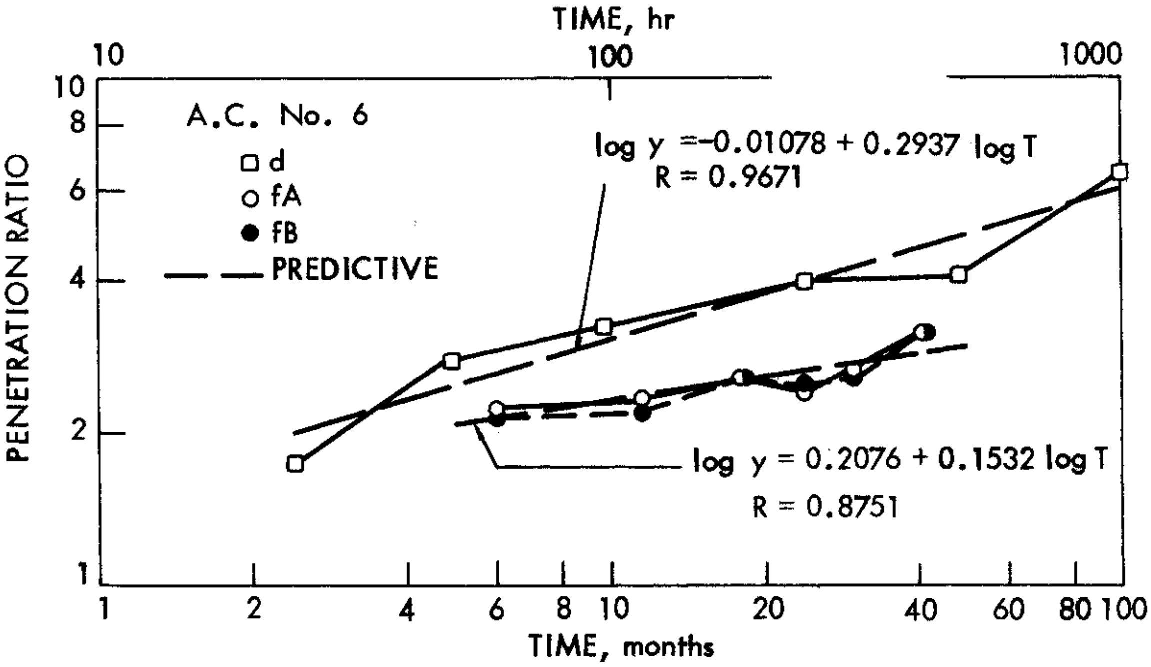

Fig. 15f. Penetration ratio vs time, A.C. No. 6.

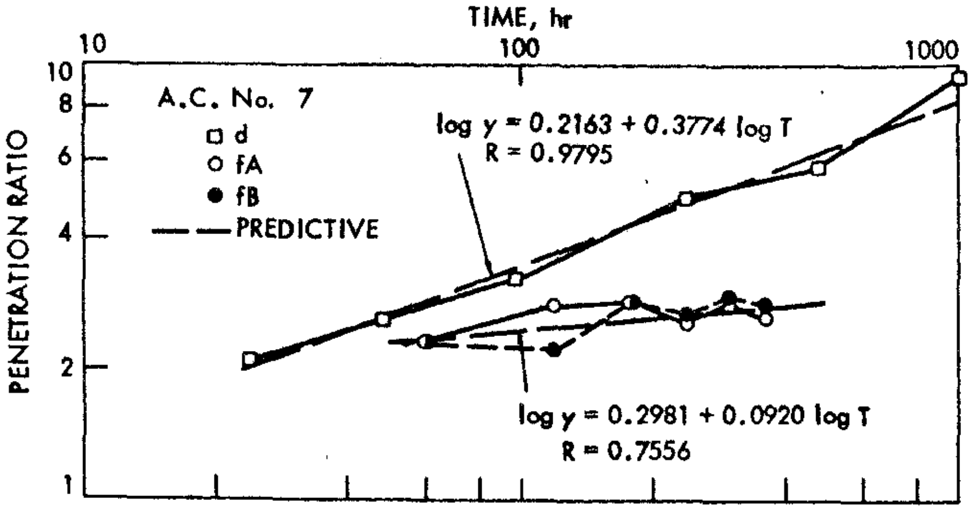

Fig. 15g. Penetration ratio vs time, A.C. No. 7.

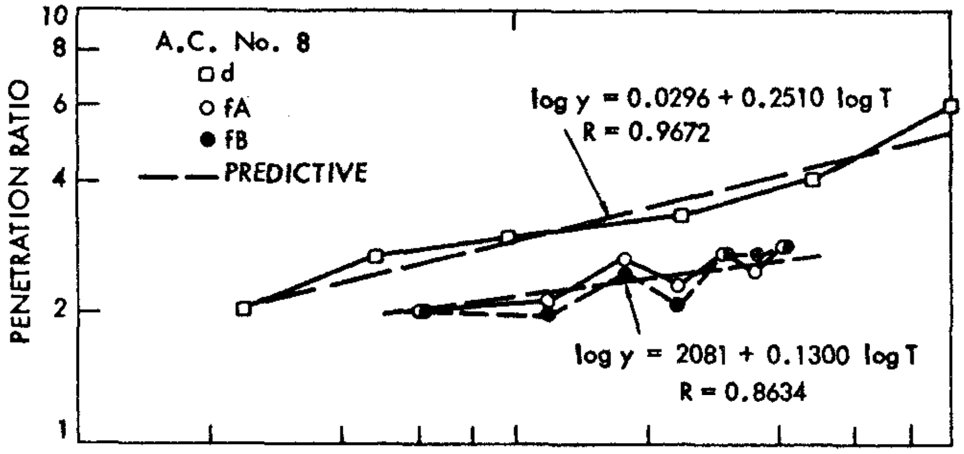

Fig. 15h. Penetration ratio vs time, A.C. No. 8.

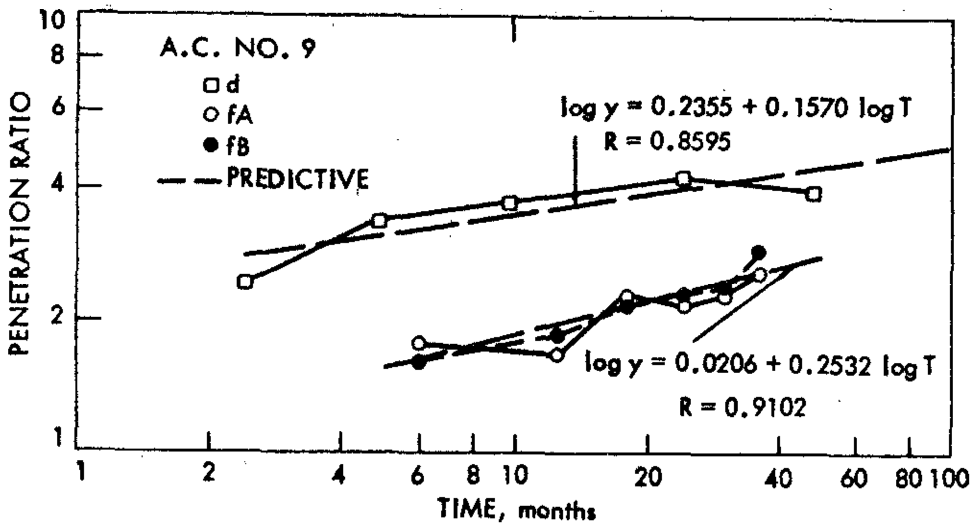

Fig. 15i. Penetration ratio vs time, A.C. No. 9.

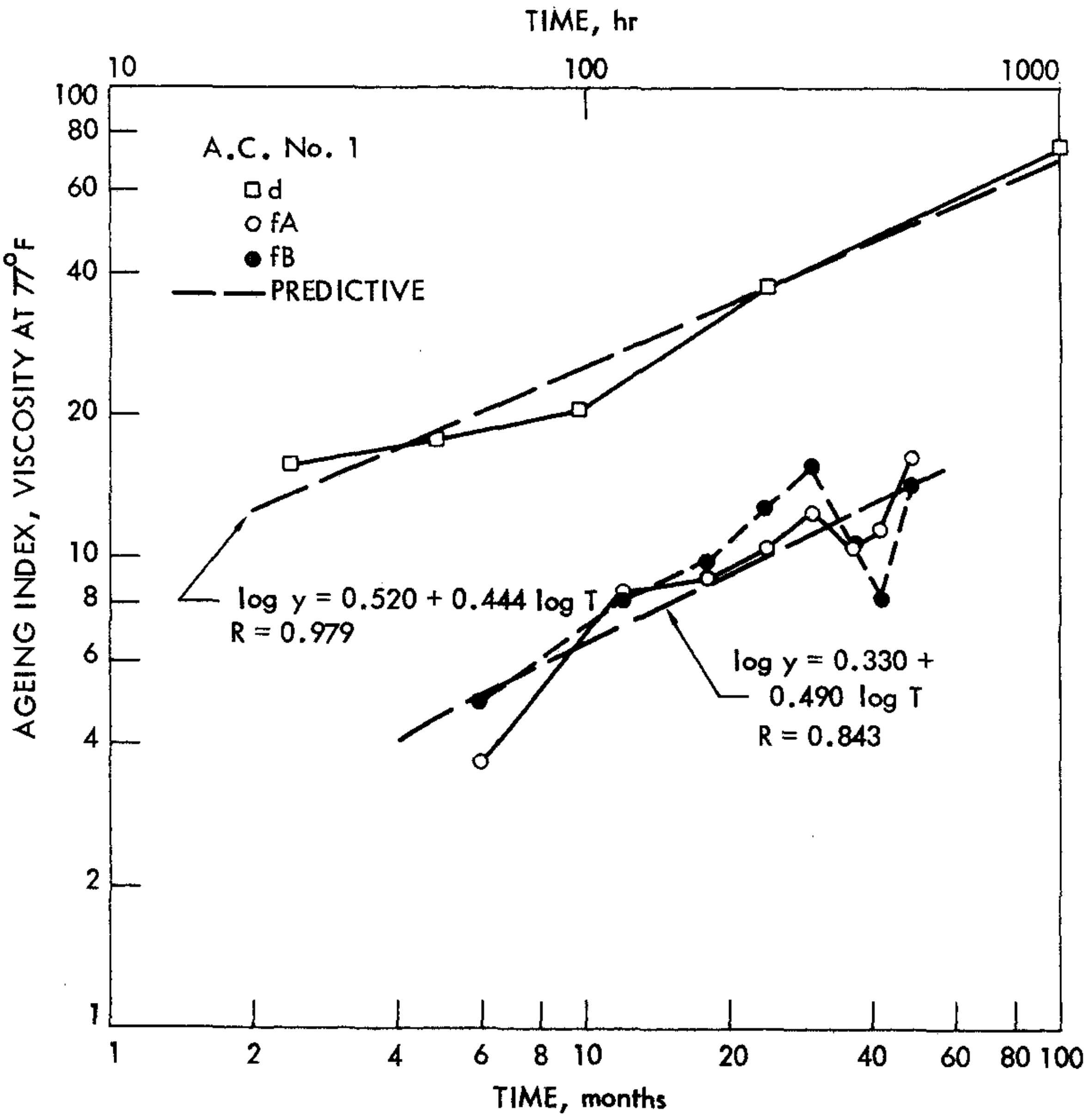

Fig. 16a. Ageing index at 77 °F vs time, A.C. No. 1.

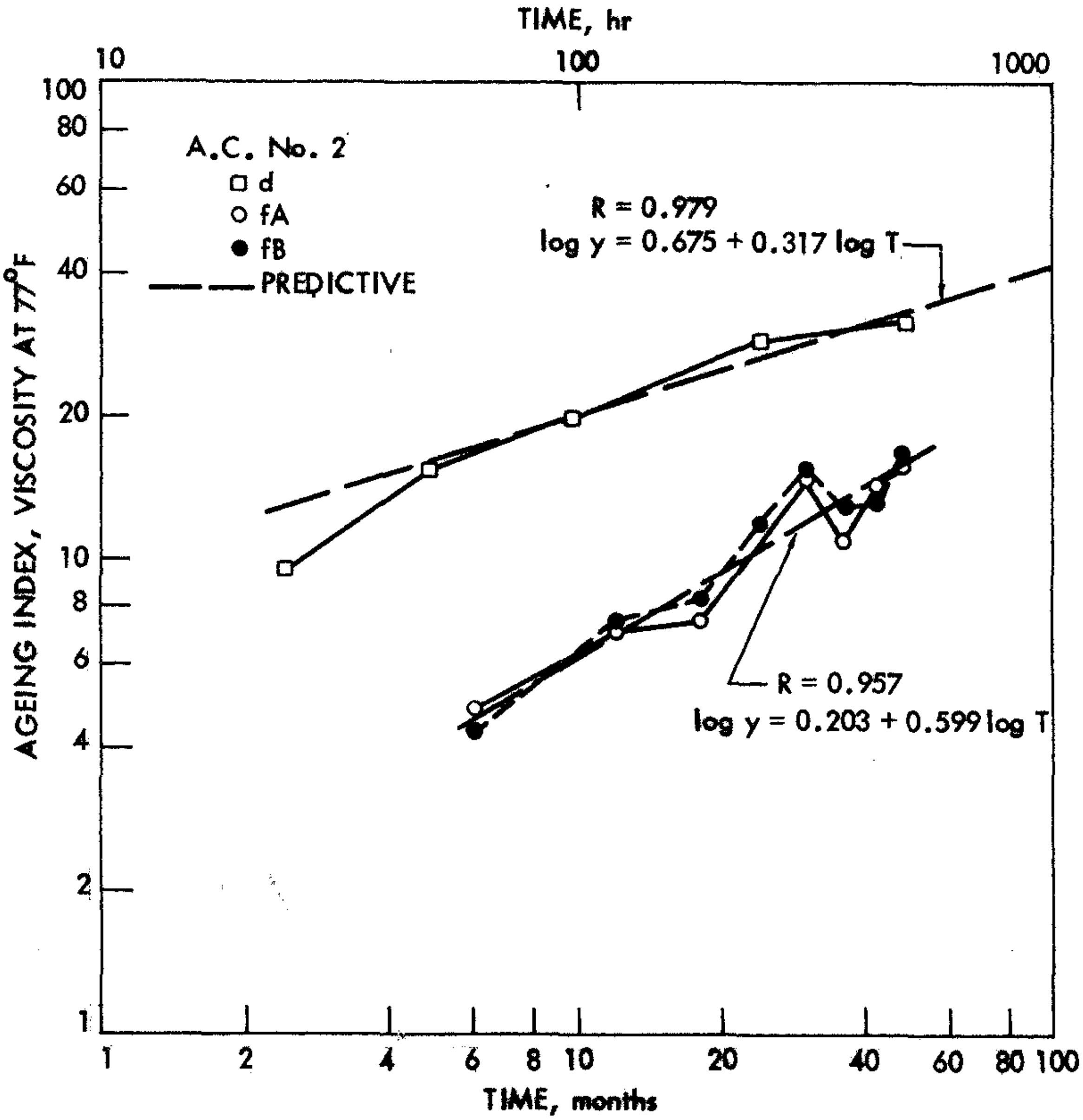

Fig. 16b. Ageing index at 77 °F vs time, A.C. No. 2.

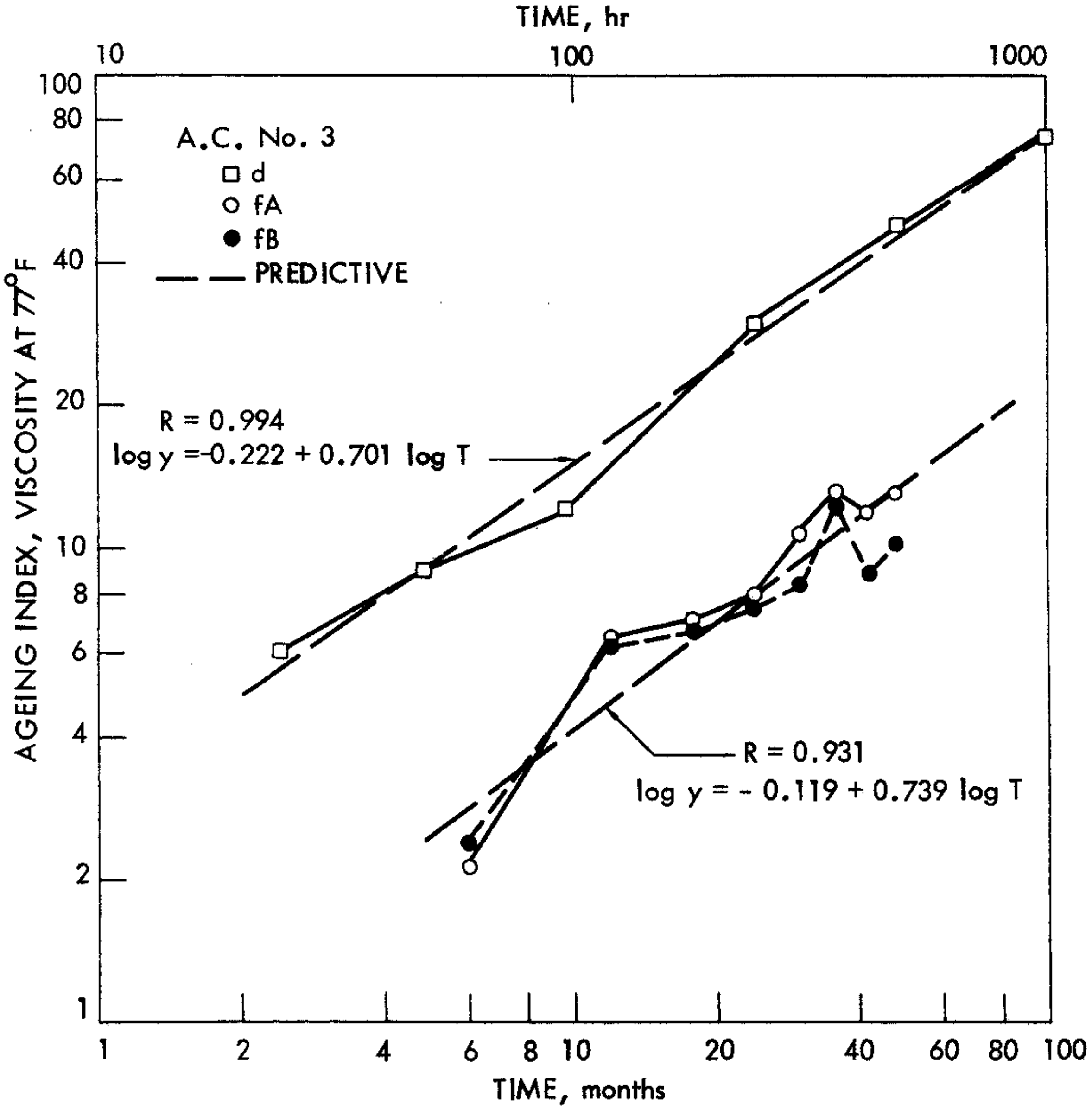

Fig. 16c. Ageing index at 77 °F vs time, A.C. No. 3.

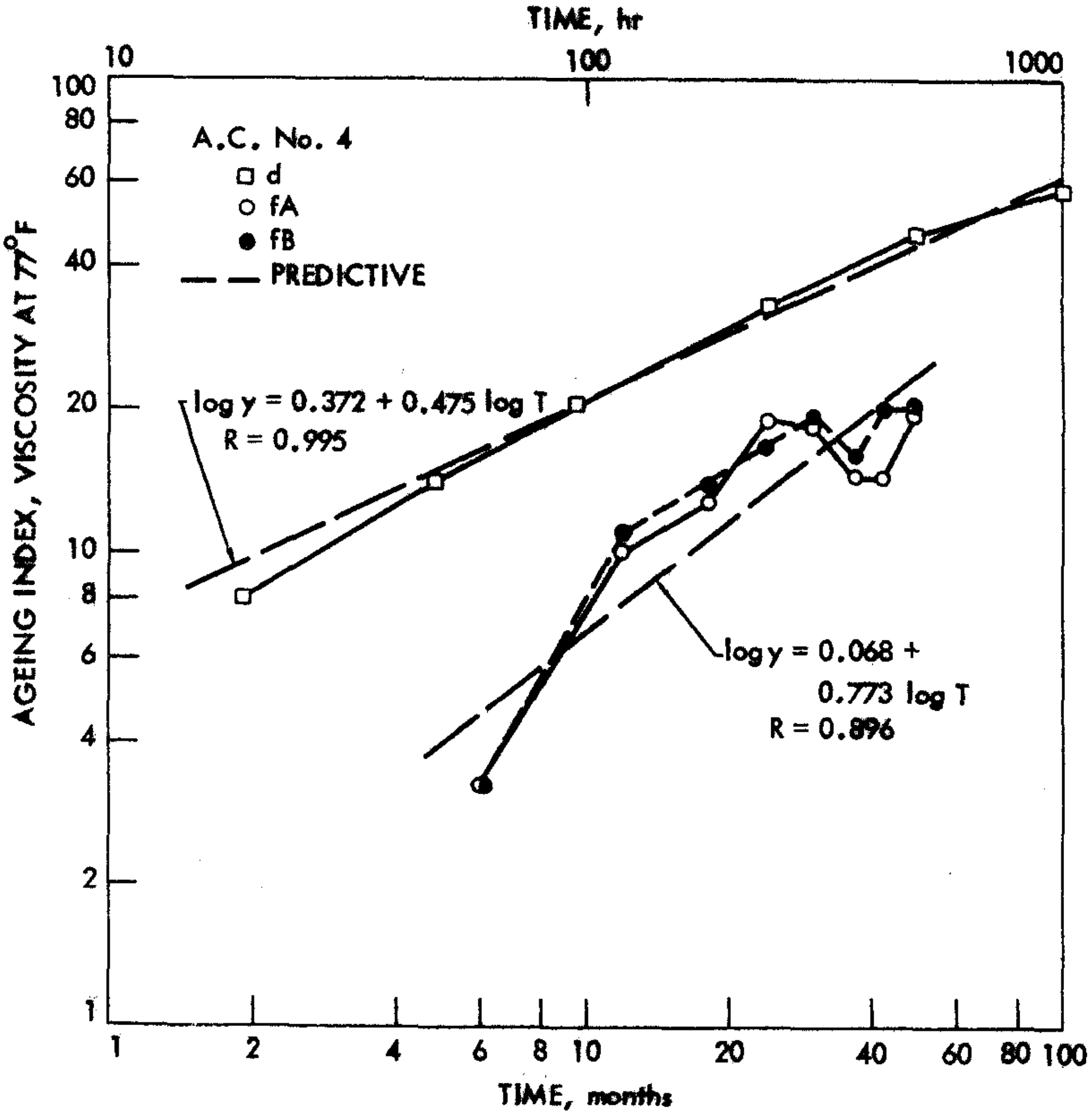

Fig. 16d. Ageing index at 77 °F vs time, A.C. No. 4.

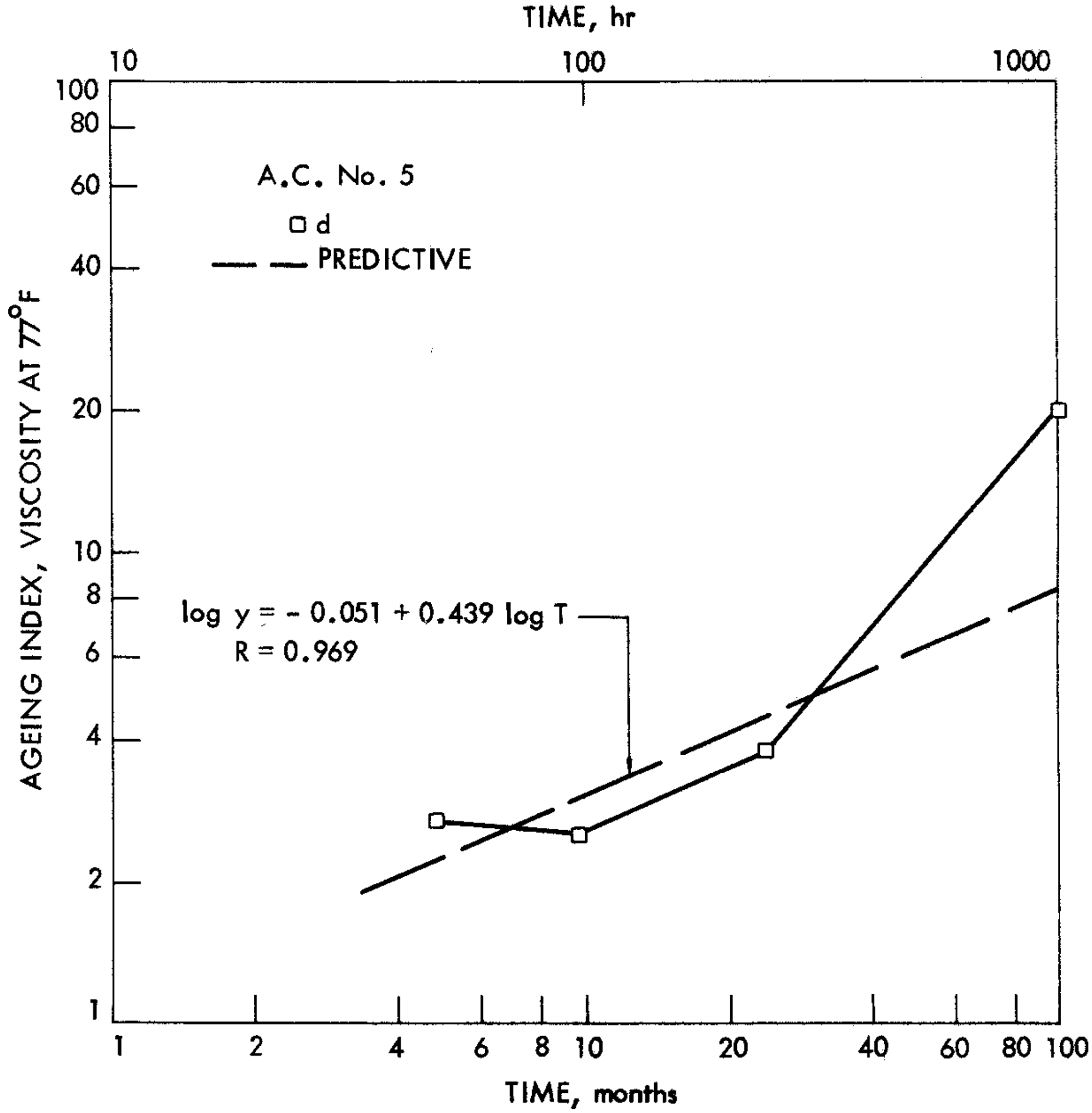

Fig. 16e. Ageing index at 77 °F vs time, A.C. No. 5.

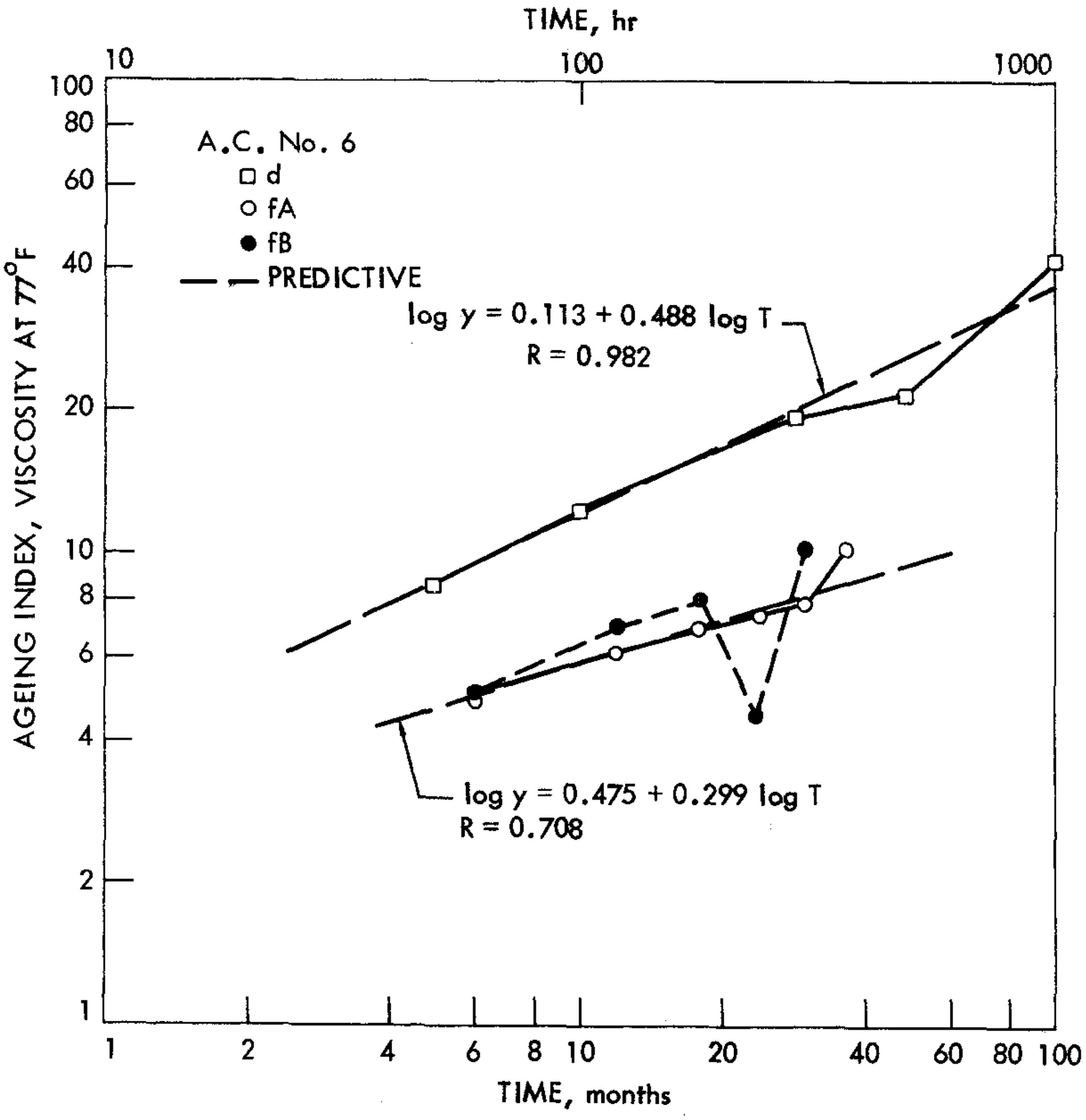

Fig. 16f. Ageing index at 77 °F vs time, A.C. No. 6.

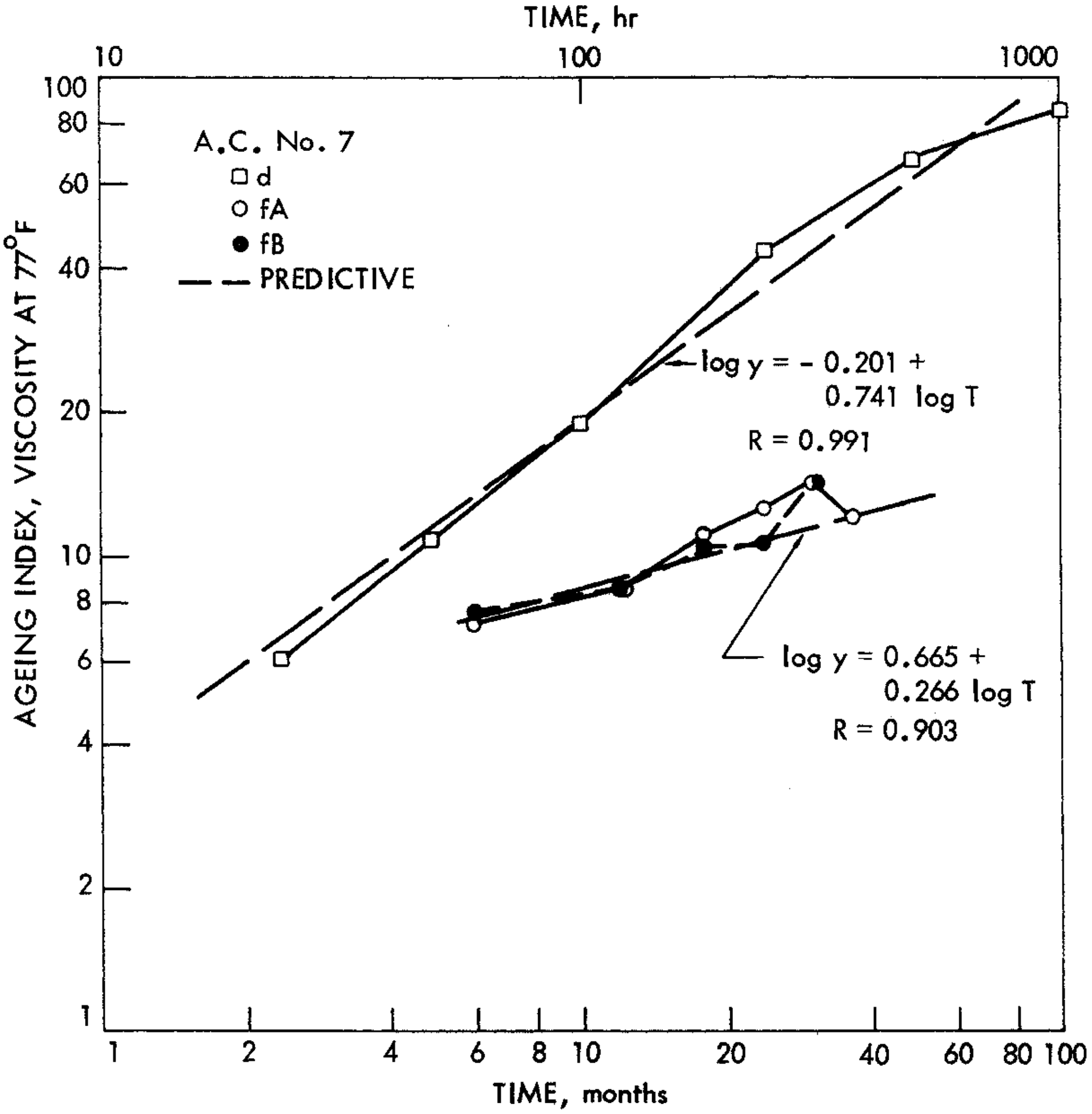

Fig. 16g. Ageing index at 77 °F vs time, A.C. No. 7.

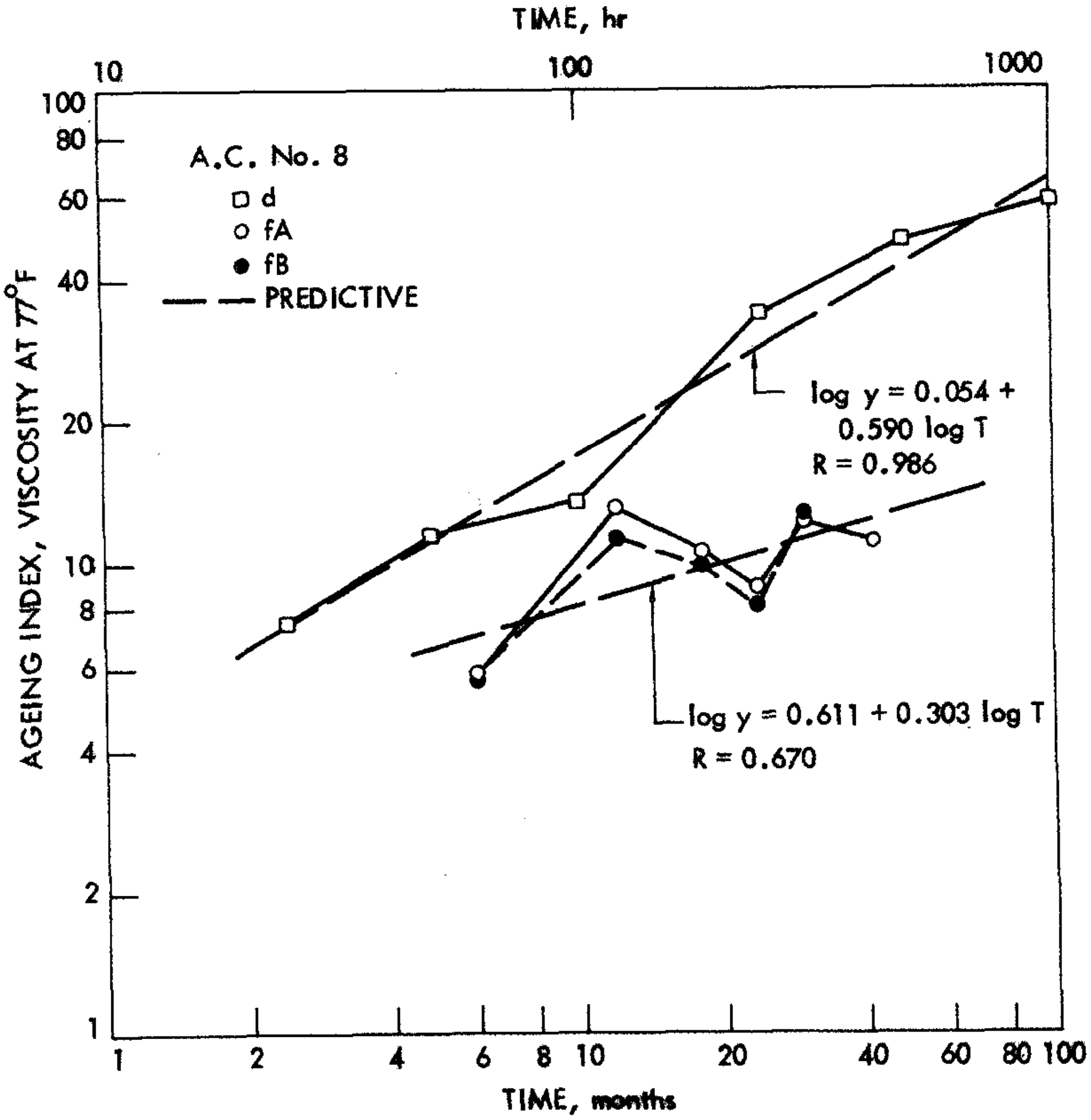

Fig. 16h. Ageing index at 77 °F vs time, A.C. No. 8.

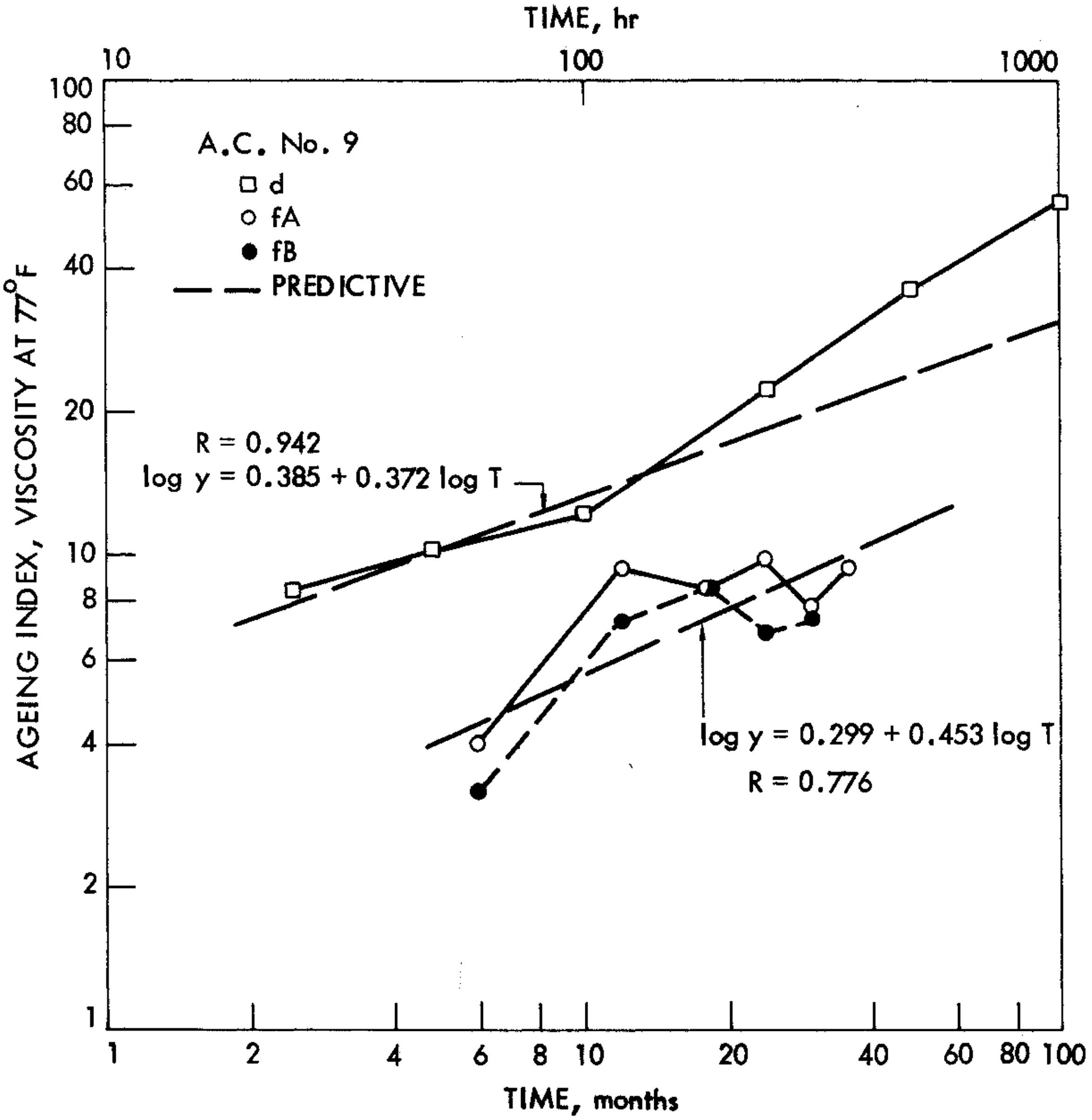

Fig. 16i. Ageing index at 77 °F vs time, A.C. No. 9.

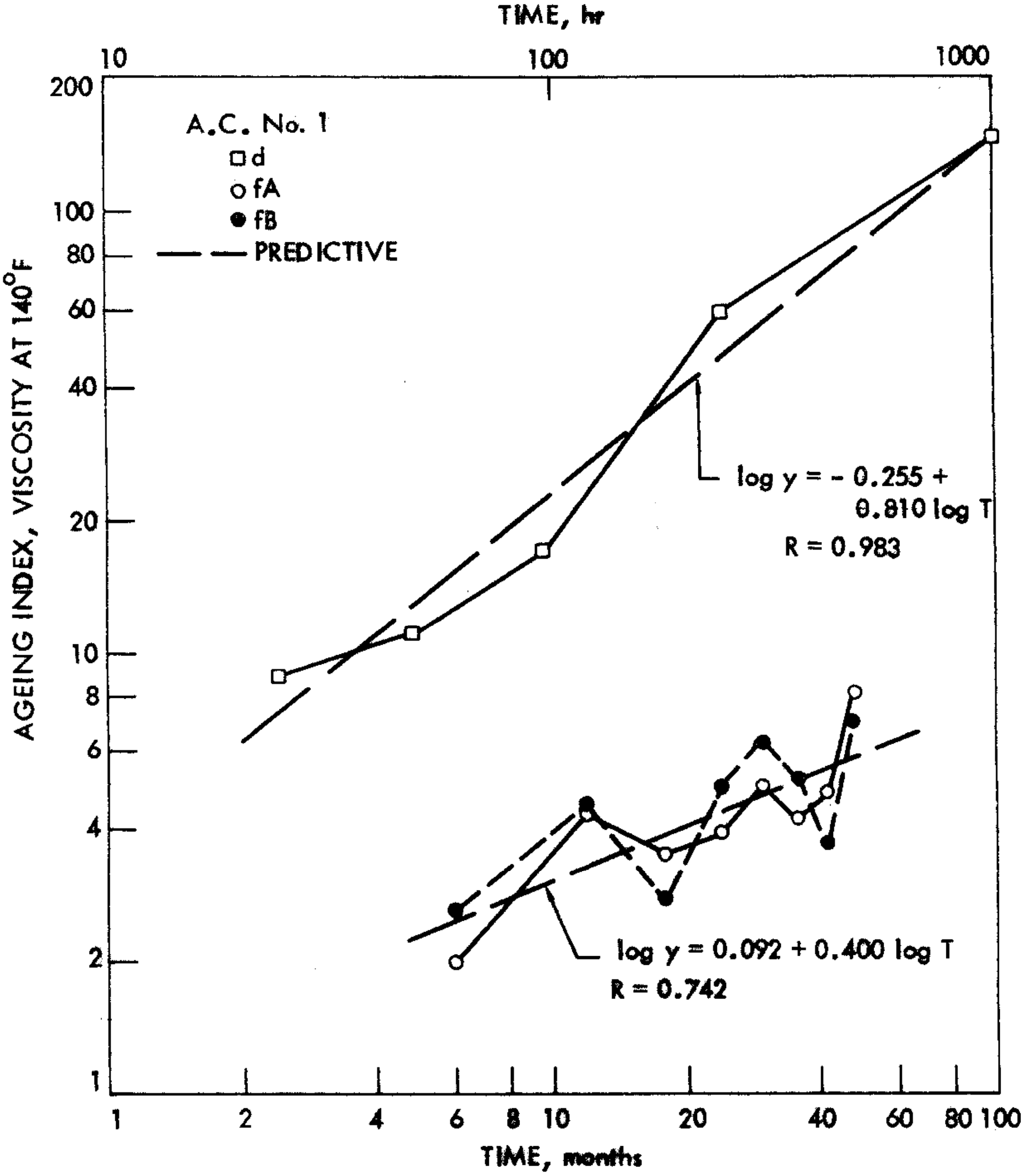

Fig. 17a. Ageing index at 140 °F vs time, A.C. No. 1.

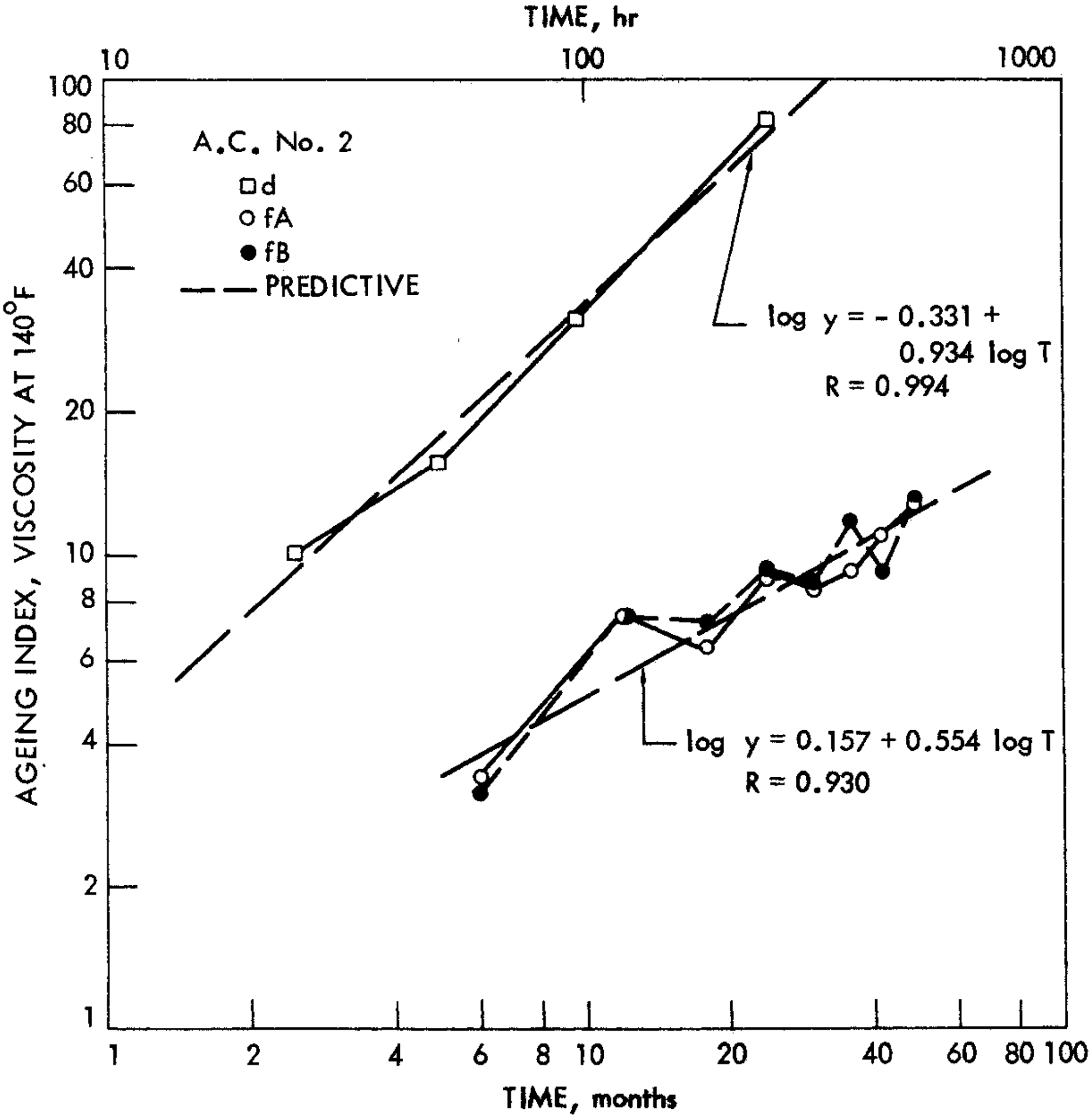

Fig. 17b. Ageing index at 140 °F vs time, A.C. No. 2.

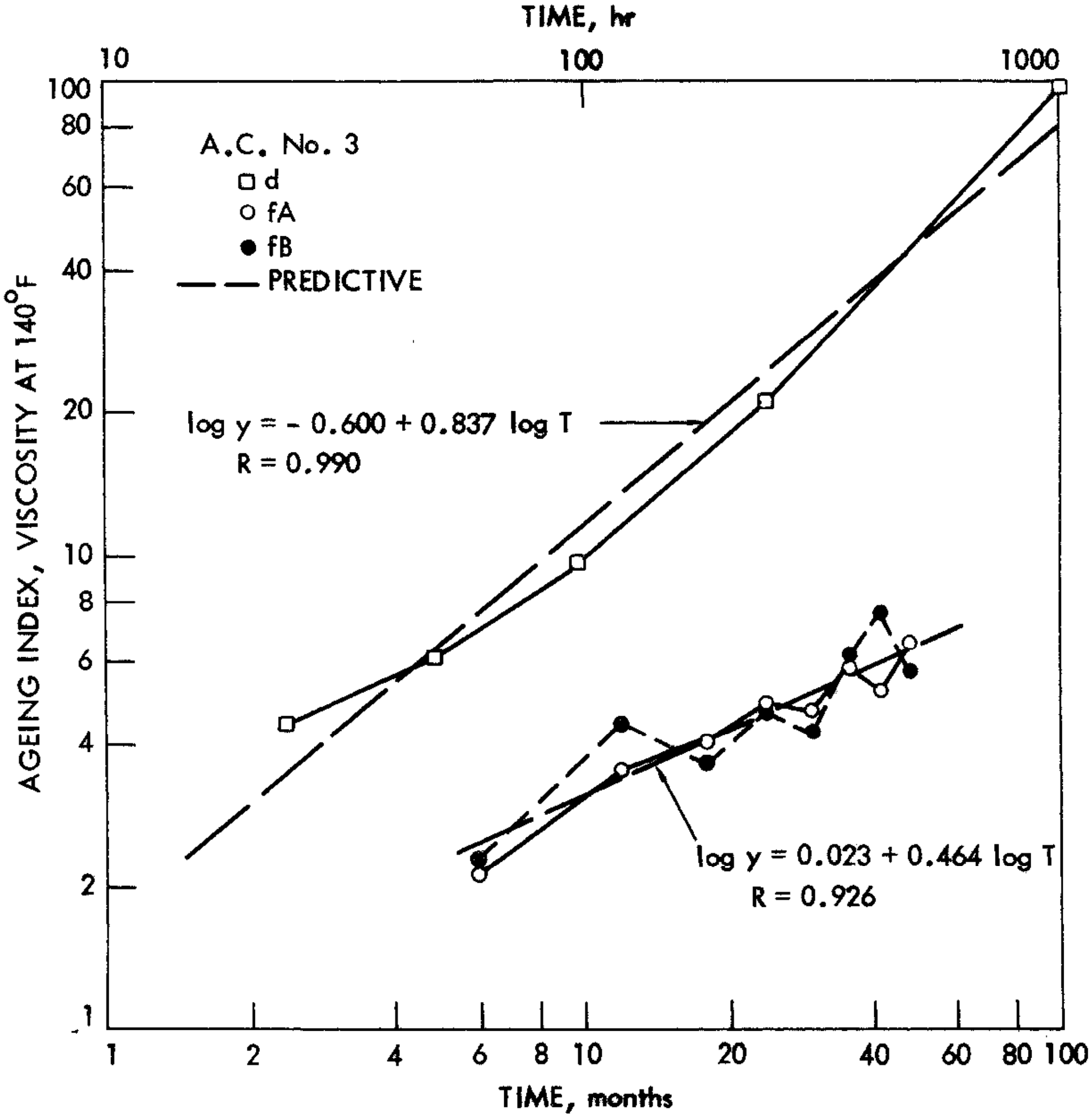

Fig. 17c. Ageing index at 140 °F vs time, A.C. No. 3.

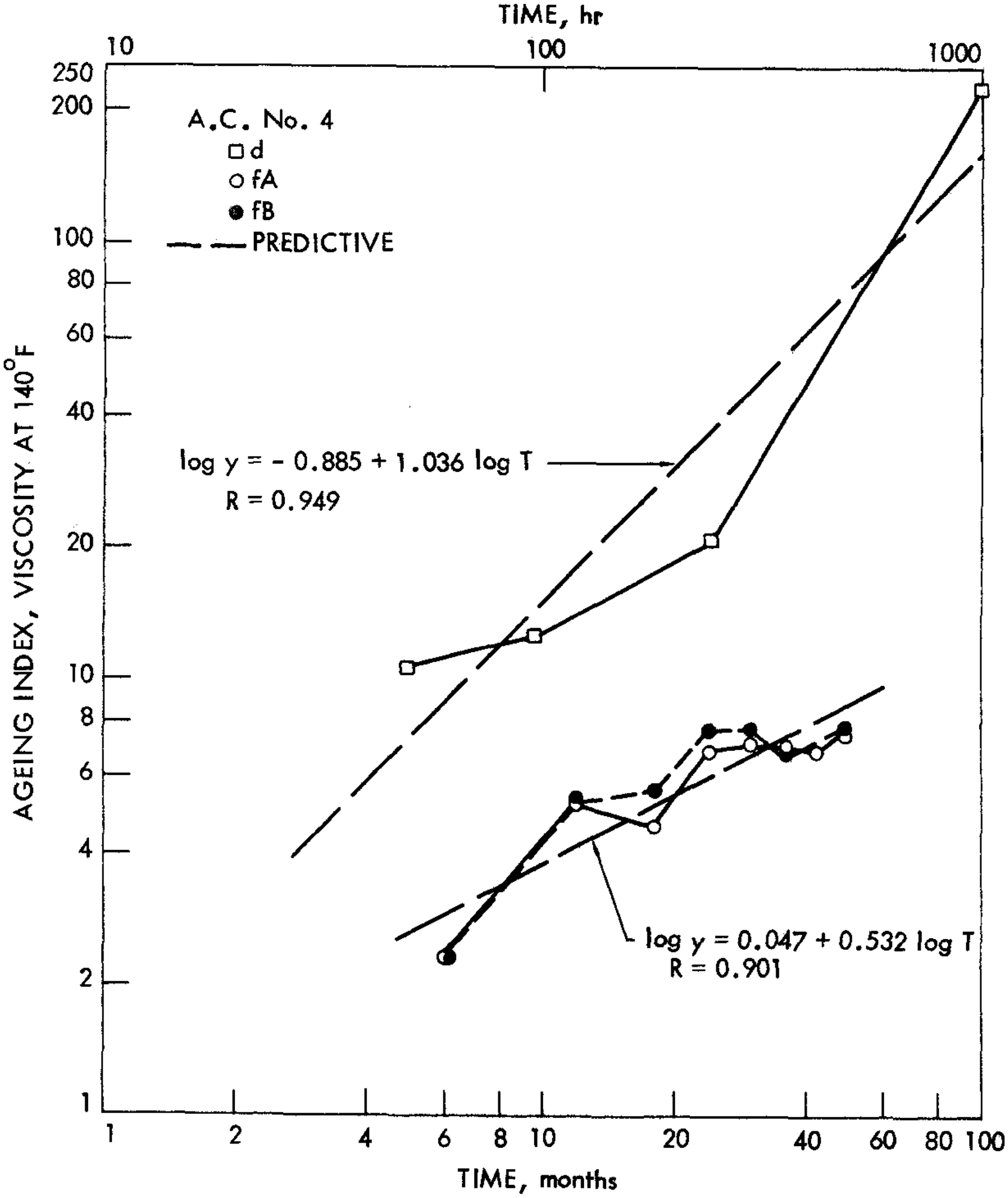

Fig. 17d. Ageing index at 140 °F vs time, A.C. No. 4.

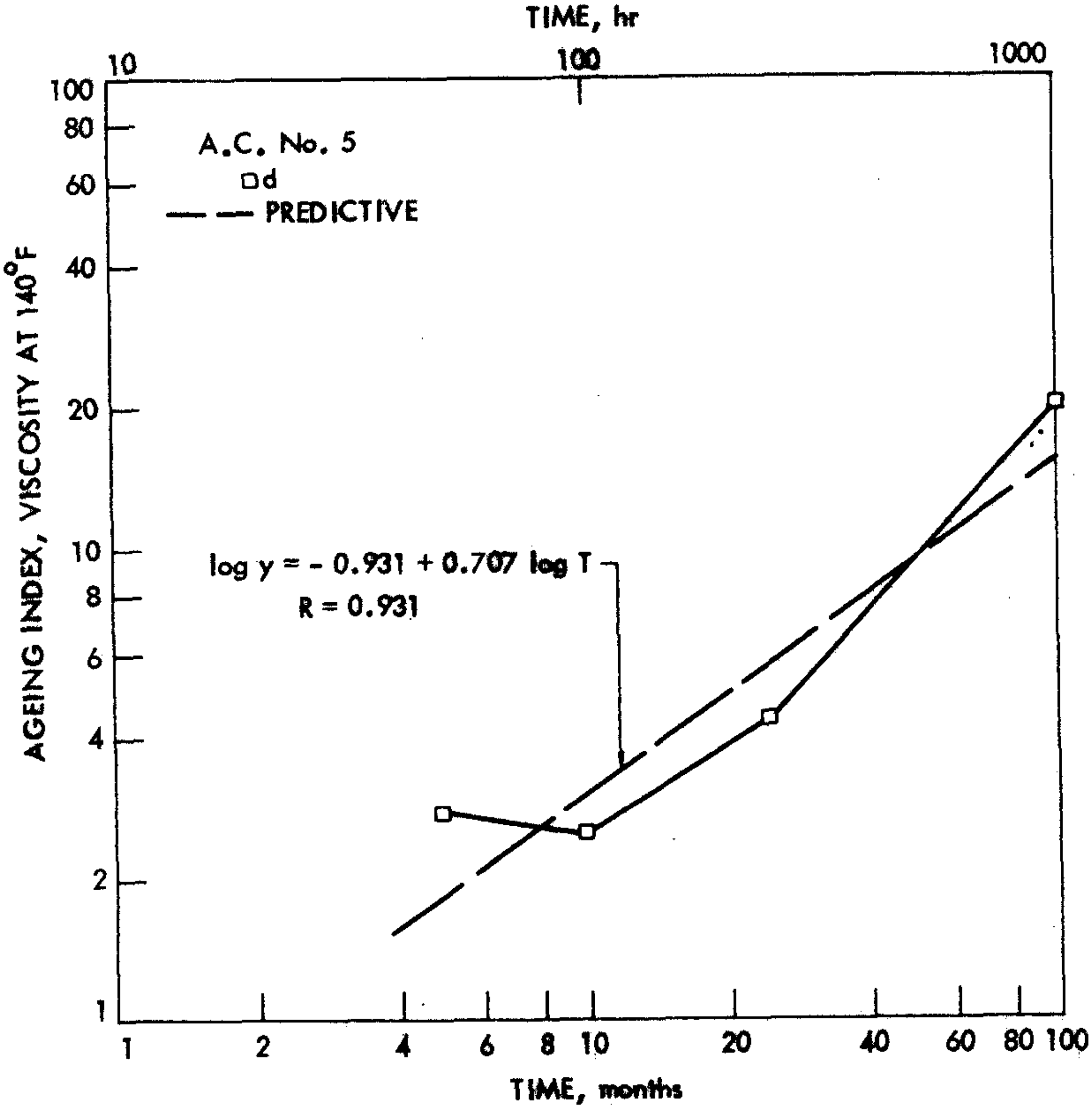

Fig. 17e. Ageing index at 140 °F vs time, A.C. No. 5.

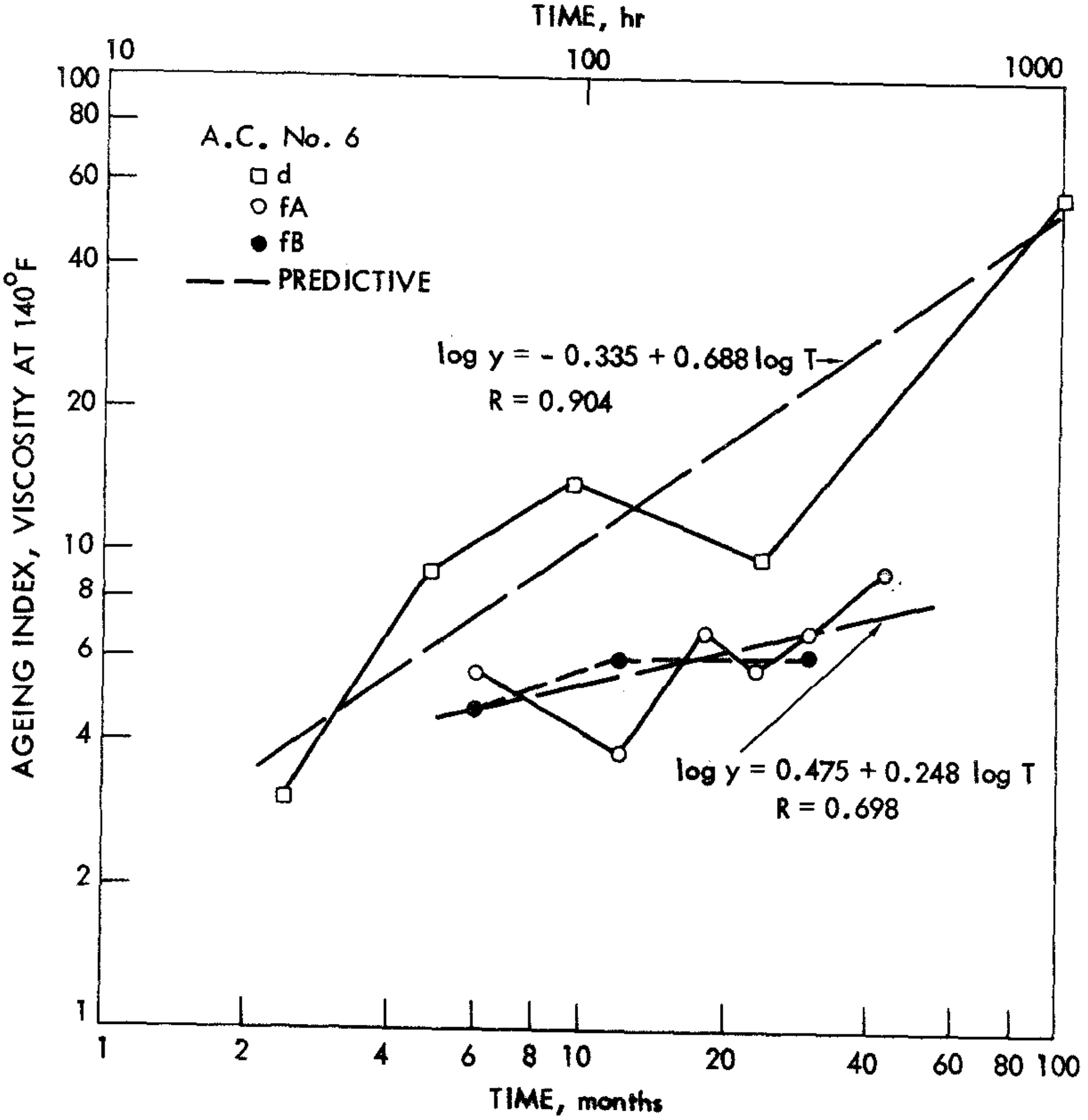

Fig. 17f. Ageing index at 140 °F vs time, A.C. No. 6.

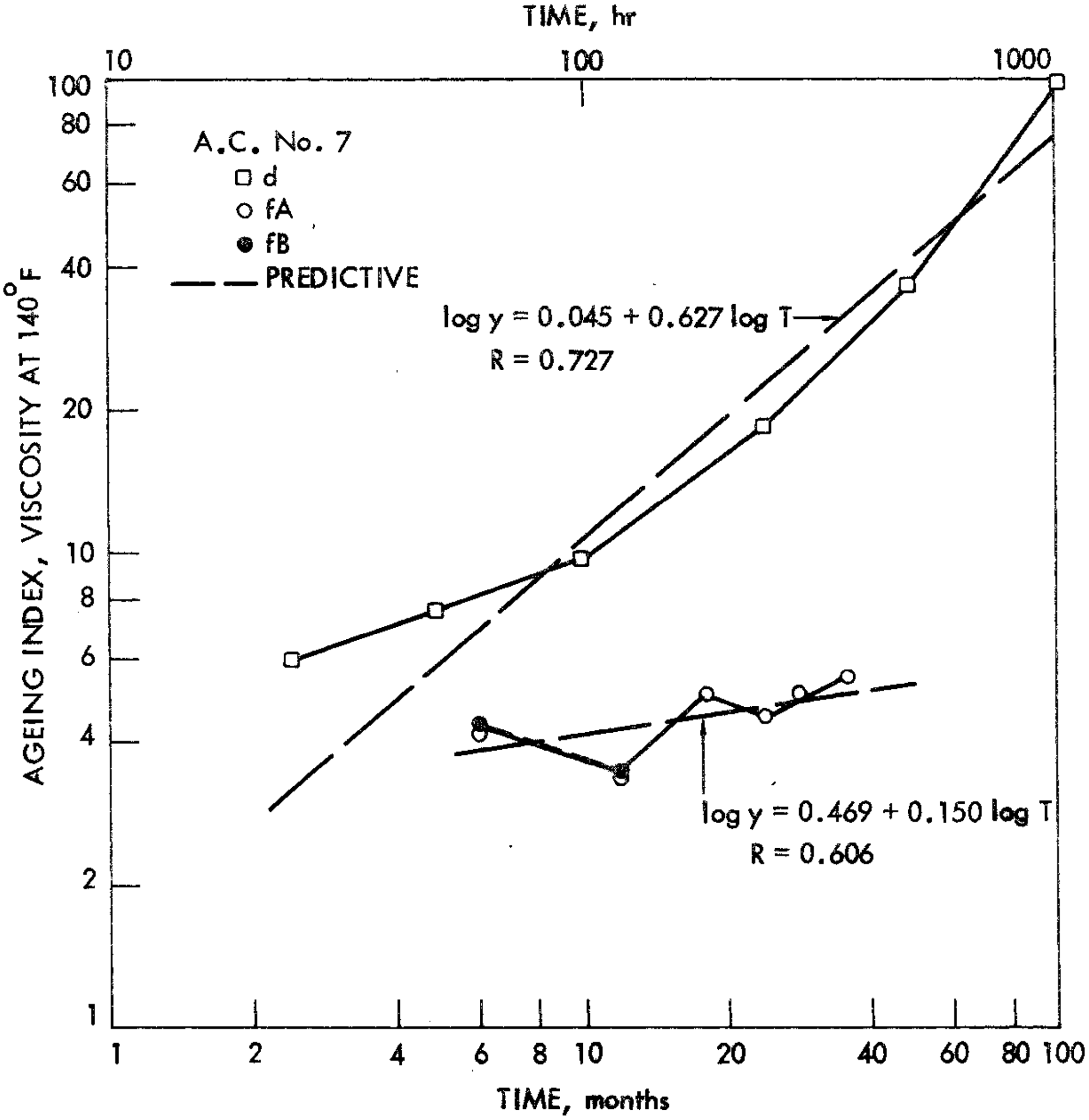

Fig 17g. Ageing index at 140 °F vs time, A.C. No. 7.

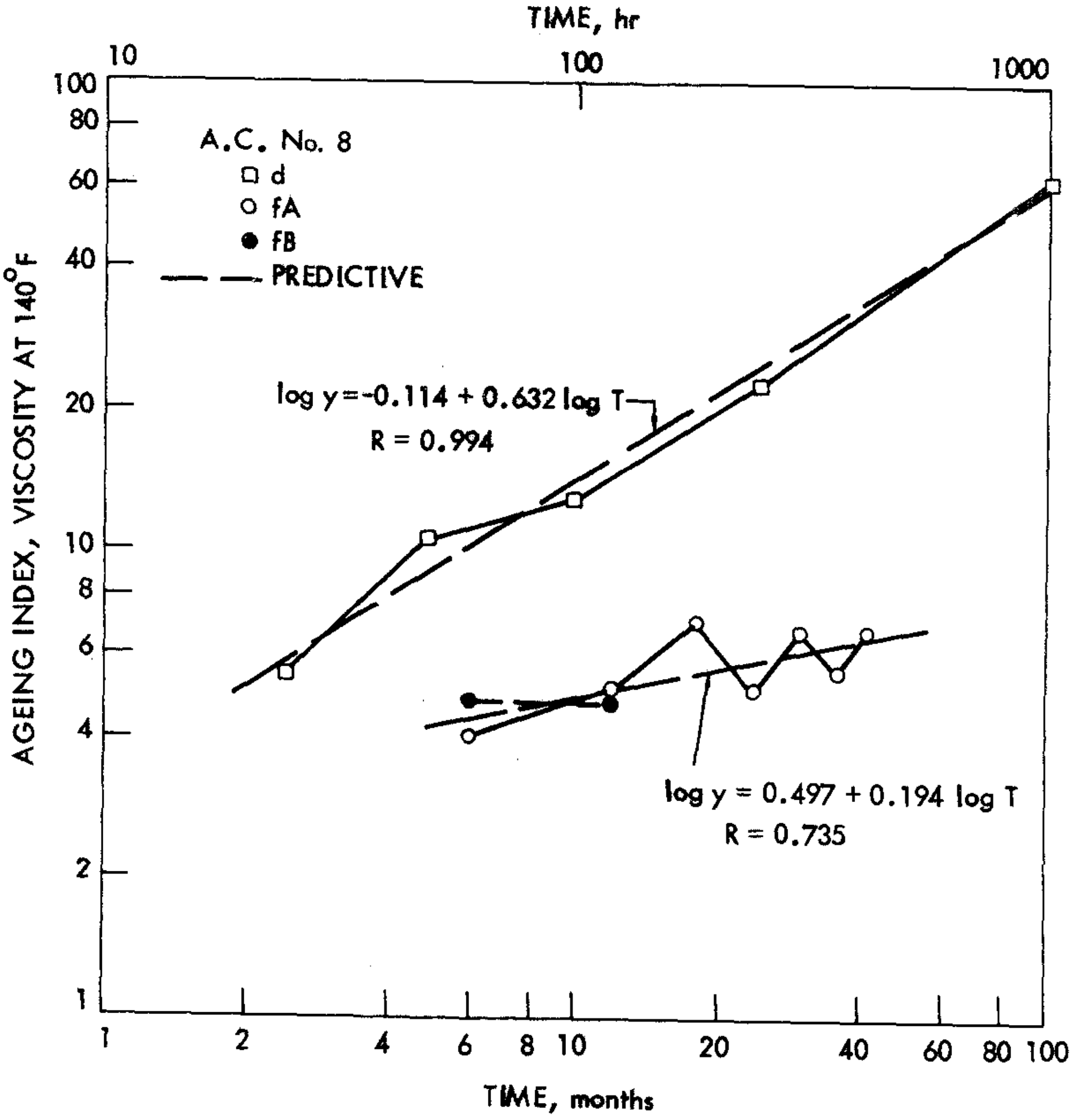

Fig. 17h. Ageing index at 140 °F vs time, A.C. No. 8.

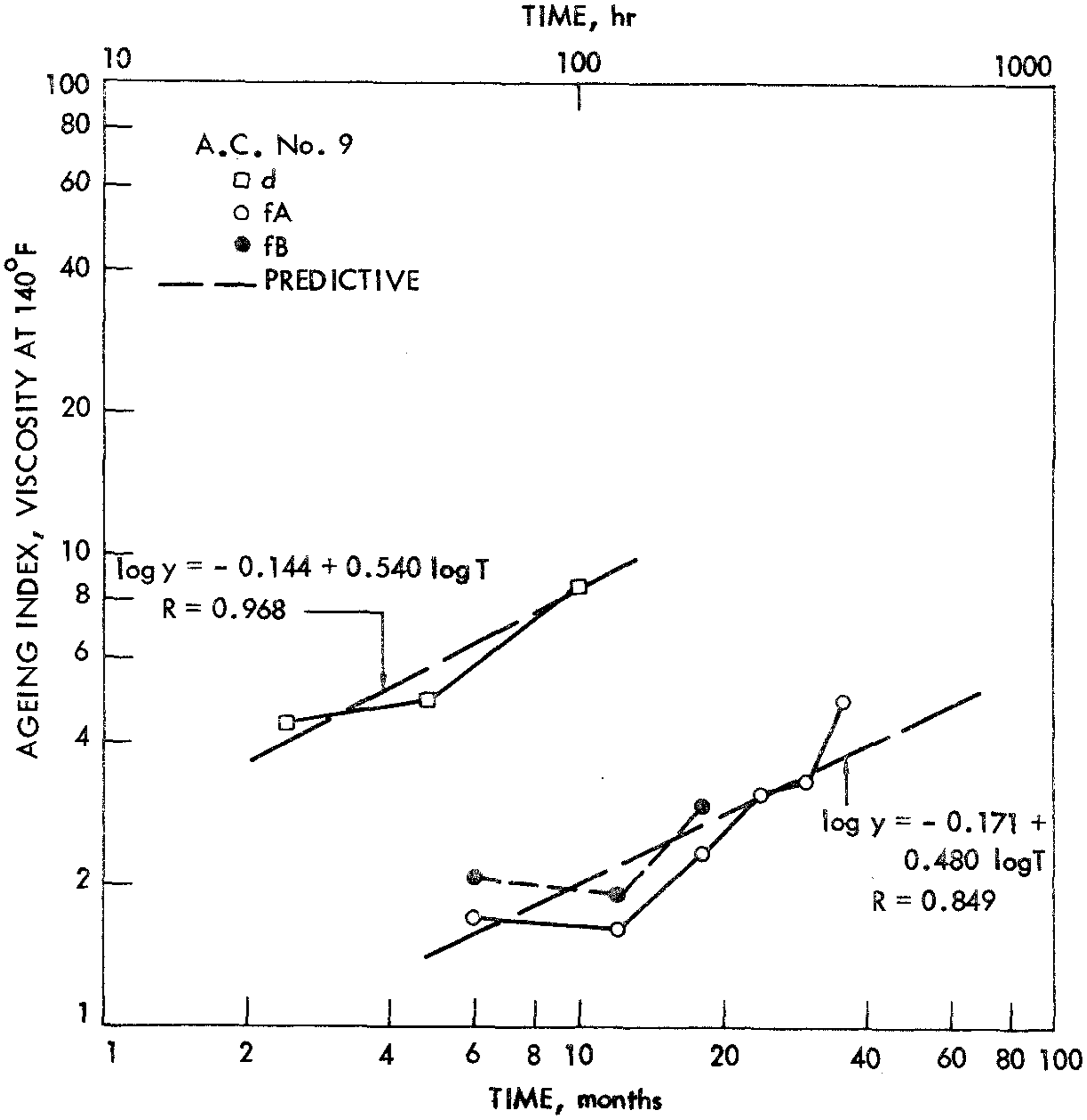

Fig. 17i. Ageing index at 140 °F vs time, A.C. No. 9.

of different original penetration or viscosity can be compared. Application of these concepts in specifications and quality control will be discussed in Chapter VIII.

From penetration and R and R softening point data, and from nomographs by Henkelom[87], the penetration index (PI) and the stiffness modulus of both laboratory and field aged asphalts were determined. In determining stiffness a temperature of 0 ^{o}F and a time of loading of 0.01 sec were assumed. Results of PI are given in Table 17. Calculated stiffness is given in Table 18.

According to Pfeiffer and Van Doormaal[88], who first introduced the penetration index, it can give a measure of both temperature susceptibility and, more importantly, the rheological type in terms of the deviation of a material from Newtonian behavior. By this system asphalts normally used for paving purposes have a PI of between + 1 and - 1. Asphalts with a PI below - 2 are substantially Newtonian, are more temperature susceptible, and are usually characterized by brittleness at low temperatures. Asphalts with an index above + 2 are less temperature susceptible and less brittle and show large deviation from Newtonian behavior. However, data obtained in this study showed no significant consistency to justify any conclusion.

Stiffness modulus is a parameter developed by Van der Poel[89] and used by many as a convenient concept to describe the viscoelastic response of asphalt under wide ranges of stress, strain (rate of shear or time of loading), and temperature conditions. It can be related to viscosity (at low rate of shear or long loading time) and elastic modulus (at short loading time or high rate of shear) and

Table 17. Penetration index.

A.C. No.		1	2	3	4	5	6	7	8	9
Original (a)		0.0	- 0.4	- 0.8	- 0.6	- 1.2	0.1	- 0.1	0.1	0.5
TFOT (d)		- 0.2	0.1	- 0.8	- 0.3	- 0.8	- 0.1	- 0.3	0.3	- 0.7
Lab ageing										
24 hr (d24)		0.0	- 0.5	- 0.6	- 0.3	- 1.1	—	- 0.8	1.2	- 0.2
48 hr (d48)		- 0.1	0.3	- 0.2	0.0	- 0.9	0.0	- 0.7	0.4	- 0.5
96 hr (d96)		0.0	0.4	- 0.3	- 0.2	- 1.1	1.0	- 0.6	0.4	0.2
240 hr (d240)		0.7	0.3	- 0.2	0.0	- 0.8	0.6	0.0	0.8	0.3
480 hr (d480)		0.8	1.2	0.2	0.3	- 0.5	1.4	1.3	1.6	—
1000 hr (d1000)		1.1	0.9	0.2	0.8	- 2.0	1.5	0.6	1.6	—
Field ageing										
Plant (p)		0.4	0.8	0.0	- 0.4	—	- 0.6	- 0.1	0.2	- 0.7
0 months (f0)		0.0	0.0	- 0.2	- 0.8	—	—	- 0.2	1.2	- 0.2
6 months (f6)	A*	- 0.4	0.4	- 1.2	- 0.9	—	- 0.2	- 0.1	0.4	0.4
	B†	- 0.4	- 0.9	- 0.6	- 0.4	—	- 0.2	- 0.5	0.4	- 0.4
12 months (f12)	A	- 0.6	- 0.2	- 0.6	- 0.6	—	0.0	- 0.8	0.0	1.1
	B	- 0.4	0.0	- 0.6	- 0.7	—	0.3	- 0.5	- 0.7	0.3

Table 17. Continued.

A.C. No.		1	2	3	4	5	6	7	8	9
18 months (f18)	A	- 0.6	0.0	- 1.0	- 1.3	—	- 0.2	0.0	0.0	- 0.1
	B	- 0.3	0.0	- 0.8	- 1.2	—	0.2	0.0	0.1	- 0.6
24 months (f24)	A	- 0.7	- 0.4	0.0	0.0	—	- 0.7	0.2	0.5	0.3
	B	- 0.3	0.0	0.0	- 0.3	—	—	—	—	—
30 months (f30)	A	- 0.2	0.1	- 0.2	- 0.6	—	0.2	0.0	0.8	0.2
	B	- 0.1	0.0	- 1.4	- 0.4	—	—	—	—	—
36 months (f36)	A	0.0	0.5	- 0.2	- 0.6	—	—	0.1	—	0.2
	B	0.4	0.3	- 0.2	- 0.4	—	—	—	—	—
42 months (f42)	A	- 0.5	0.0	0.0	- 0.6	—	0.2	—	0.6	—
	B	- 0.7	- 0.2	0.1	- 0.7	—	—	—	—	—
48 months (f48)	A	- 0.8	- 0.4	- 0.6	- 0.8					
	B	- 0.4	- 0.4	- 0.8	- 0.8					

*A, in wheel tracks.

†B, between wheel tracks.

Table 18. Stiffness modulus.

A.C. No.		psi × 10^5								
		1	2	3	4	5	6	7	8	9
Original (a)		1.088	0.305	1.595	1.450	2.030	1.015	0.725	0.870	0.725
TFOT (d)		1.740	1.595	2.683	1.740	2.175	1.595	1.595	1.088	1.740
Lab ageing										
24 hr (d24)		2.320	2.465	2.610	2.030	2.465	–	2.465	1.653	2.030
48 hr (d48)		3.263	2.610	2.828	2.175	2.610	2.175	2.320	1.885	2.755
96 hr (d96)		2.320	3.045	2.610	2.320	2.755	2.015	2.755	1.740	2.320
240 hr (d240)		2.610	3.190	2.755	2.755	2.900	2.030	2.610	1.595	2.320
480 hr (d480)		2.755	3.335	2.828	3.190	2.900	1.740	2.740	1.595	–
1000 hr (d1000)		2.900	3.408	2.900	3.045	4.060	2.175	3.190	2.030	–
Field ageing										
Plant (p)		1.160	0.725	1.450	1.595	–	1.740	1.305	1.160	2.030
0 months (f0)		1.450	1.450	1.450	2.030	–	–	1.378	1.653	2.030
6 months (f6)	A*	1.813	2.465	2.610	2.610	–	2.175	2.030	1.450	1.305
	B†	1.813	2.320	2.030	1.740	–	2.175	2.175	1.450	1.740
12 months (f12)	A	2.320	2.030	2.465	2.465	–	1.740	2.465	1.885	0.725
	B	2.175	2.103	2.465	2.610	–	2.030	2.175	2.610	1.450

Table 18. Continued.

A.C. No.		psi × 10^5								
		1	2	3	4	5	6	7	8	9
18 months (f18)	A	1.595	3.045	2.755	3.335	–	2.320	1.740	1.740	1.885
	B	1.450	2.900	2.755	3.408	–	1.740	1.740	1.740	2.465
24 months (f24)	A	2.683	1.595	1.885	1.740	–	2.175	1.595	1.450	1.595
	B	2.610	1.740	1.885	2.175	–	–	–	–	–
30 months (f30)	A	2.175	2.610	2.900	2.900	–	2.030	2.030	1.015	1.595
	B	2.320	3.480	1.885	2.683	–	–	–	–	–
36 months (f36)	A	2.030	2.683	2.538	2.755	–	–	1.885	–	1.740
	B	1.595	2.610	2.538	2.610	–	–	–	–	–
42 months (f42)	A	2.465	2.175	2.465	2.871	–	2.320	–	1.595	–
	B	2.871	2.175	2.610	2.900	–	–	–	–	–
48 months (f48)	A	2.900	3.335	2.828	2.900					
	B	2.755	3.480	2.900	2.900					

[*] A, in wheel tracks.

[†] B, between wheel tracks.

can provide a simplified measure for asphalt characterization for structural design and evaluation purposes and for low temperature behavior.

The data in Table 18 clearly showed the increase in stiffness with ageing and the parallel between laboratory ageing and field service ageing. Correlations were not made due to data scatter. Since stiffness can be easily determined for selected temperatures and loading times by using simple penetration and softening point test results and since it has been related to low temperature pavement cracking[90], the use of this parameter in future asphalt specifications should be investigated.

Ageing and Increase in Brittleness of Asphalts

The increase in the hardness of an asphalt is generally considered its most important physical change, from a practical viewpoint. Asphalt hardening for asphalts studied in this project, both laboratory aged and field samples, was determined directly by penetration, softening point, ductility, and viscosity at 140 ^{o}F and at 77 ^{o}F, and indirectly by such parameters as complex flow change, penetration index, shear susceptibility, ageing index, etc. However, viscosity of aged asphalt in a brittle state of subzero temperatures could not be determined, due to instrumentation limitations.

This problem was solved by the modified Fraass brittle point test. The results of brittle point changes in IDT are given in Table 19.

Studies[91] have shown that the brittle point temperature is an equiviscous temperature corresponding to a viscosity of 4×10^9 poises. Thus the tests in fact give the temperature at which the asphalt has a

Table 19. Fraass brittle point.

A.C. No.		Brittle point, °C 1	2	3	4	5	6	7	8	9
Original (a)		- 20.5	- 21.0	- 16.5	- 17.5	- 15.3	- 21.0	- 20.0	- 20.0	- 20.0
TFOT (d)		- 17.0	- 18.0	- 14.0	- 17.0	- 13.0	- 20.0	- 21.5	- 19.0	- 19.0
Lab ageing										
24 hr (d24)		- 16.5	- 17.0	- 13.0	—	—	- 15.5	- 16.5‡	—	- 18.0
48 hr (d48)		- 16.0	- 14.0	- 12.0	- 13.0	- 14.0	- 18.0	- 15.5‡	- 16.5	- 17.5
96 hr (d96)		- 15.0	- 12.5	- 12.0	- 12.0	- 13.7	- 15.5	- 14.0‡	- 15.0	- 15.5
240 hr (d240)		- 14.5	- 11.0	- 12.0	- 13.5	- 13.0	- 12.5	- 12.5‡	- 13.0‡	- 14.5‡
480 hr (d480)		—	- 10.5	—	—	- 12.0	- 12.0	- 12.0‡	- 12.5‡	- 14.5
1000 hr (d1000)		- 2.0	—	- 3.0	- 18.0	- 13.0	- 18.0	- 11.5	- 18.0	—
Field ageing										
Plant (p)		- 19.0	- 18.0	- 15.0	- 17.0	—	- 20.0	- 18.5	- 18.0	- 18.5
0 months (f0)	A*	- 20.0	- 18.0	- 16.5	- 15.0	—	—	- 18.0	- 19.5	- 19.0
	B†	—	—	—	—	—	—	—	—	—
6 months (f6)	A	- 19.0	- 19.5	- 14.0	- 16.0	—	- 15.0	- 14.5	- 18.0	- 16.0
	B	- 18.5	- 18.0	- 17.0	- 16.5	—	- 14.0	- 15.7	- 17.0	- 17.0
12 months (f12)	A	- 17.5	- 17.0	- 18.0	- 15.0	—	- 18.0	- 16.0	- 17.5	- 17.5
	B	- 16.5	- 16.5	- 15.0	- 15.0	—	- 18.0	- 16.0	- 17.5	- 17.5

Table 19. Continued.

A.C. No.		Brittle point, °C								
		1	2	3	4	5	6	7	8	9
18 months (f18)	A	- 21.0	- 18.5	- 20.0	- 14.5	—	- 17.0	- 14.5	- 18.0	- 18.5
	B	- 20.0	- 20.5	- 16.0	- 14.5	—	- 16.0	- 16.0	- 18.0	- 19.0
24 months (f24)	A	- 21.0	—	- 14.5	- 14.0	—	- 15.5	- 15.5	- 16.5	- 17.0
	B	- 19.0	- 18.5	- 14.5	- 13.5	—	—	—	—	—
30 months (f30)	A	- 15.5	- 15.5	- 14.0	- 13.5	—	- 15.5	- 15.0	- 16.0	- 16.5
	B	—	—	—	—	—	—	—	—	—
36 months (f36)	A	- 15.5	- 15.0	- 13.0	- 12.0	—	- 15.5	- 15.0	- 16.0	- 16.5
	B	—	—	—	—	—	—	—	—	—
42 months (f42)	A	- 15.0	- 15.5	- 13.0	- 13.0					
	B	—	—	—	—					
48 months (f48)	A	- 13.0	- 14.0	- 12.5	- 12.0					
	B	—	—	—	—					

---

[*] A, in wheel tracks.

[†] B, between wheel tracks.

[‡] Interpolated value.

viscosity of 4×10^9 poises, and as hardness or brittleness increases there is a corresponding increase in brittle point.

Brittle point determinations for asphalt studied in HR-124 were made on samples with a film thickness of 0.55 mm and a rate of cooling of 1 °C/min. Figures 18a through 18d show the rate at which the brittle point temperature changes with the length of exposure of the asphalts in the accelerated durability test as well as in the field. A progressive increase in the brittle temperatures is observed for all but three asphalts. A slow rate of change of brittleness would indicate a durable material capable of withstanding severe exposure conditions.

Asphalts No. 4, 6, and 8 have initial increases in brittleness followed by progressive decreases as ageing progresses beyond 200 hr. According to Jones[66] this is characteristic of very durable asphalts. Whether this is the case for these asphalts in HR-124, only extended field correlation can answer. Based on most durability criteria (Table 27, Chapter VIII), this is true for A.C. No. 6 and 8, but not for A.C. No. 4. Also significant is the very slight change in brittle point for asphalt No. 5, which is a special, nearly asphaltene-free asphalt.

Since viscosity increased with time but brittle points did not all increase with time, the suggested relationship between brittle point temperature and viscosity may not hold for all asphalts.

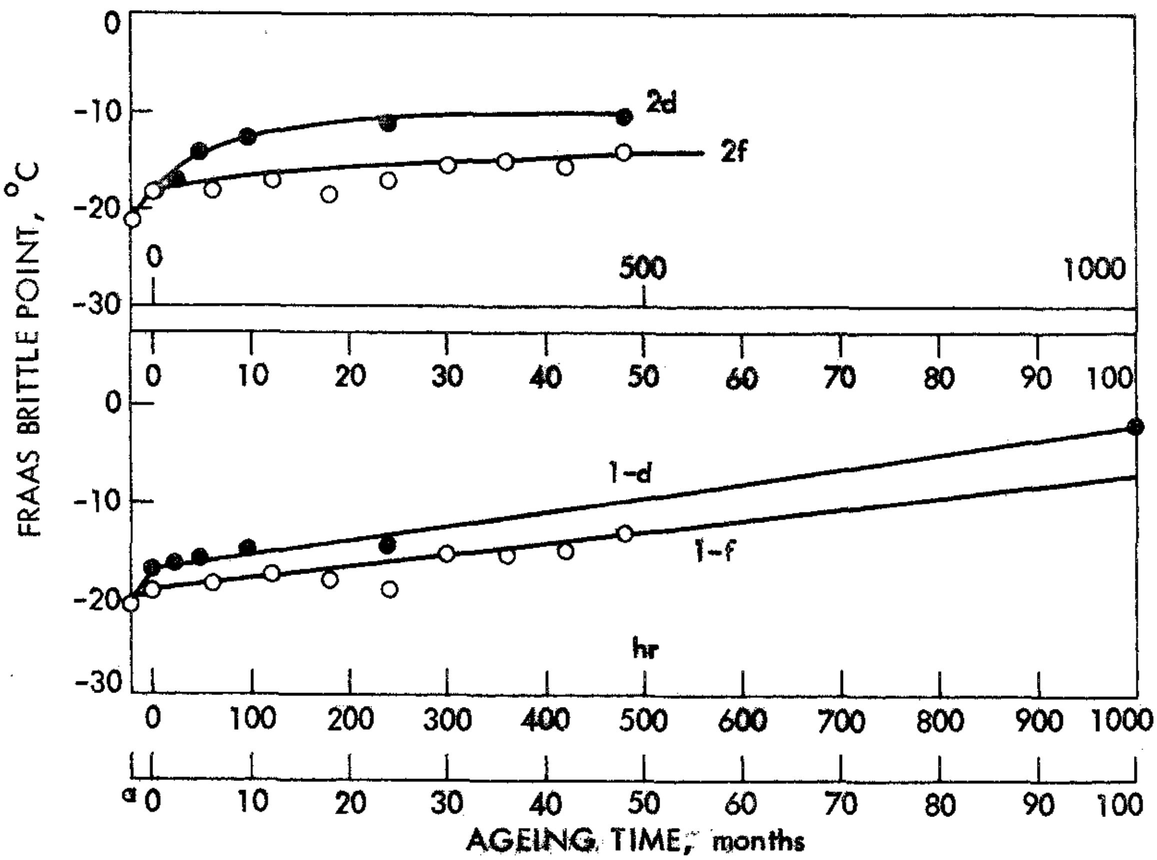

Fig. 18a. Fraass brittle point vs time of ageing, A.C. No. 1 and 2.

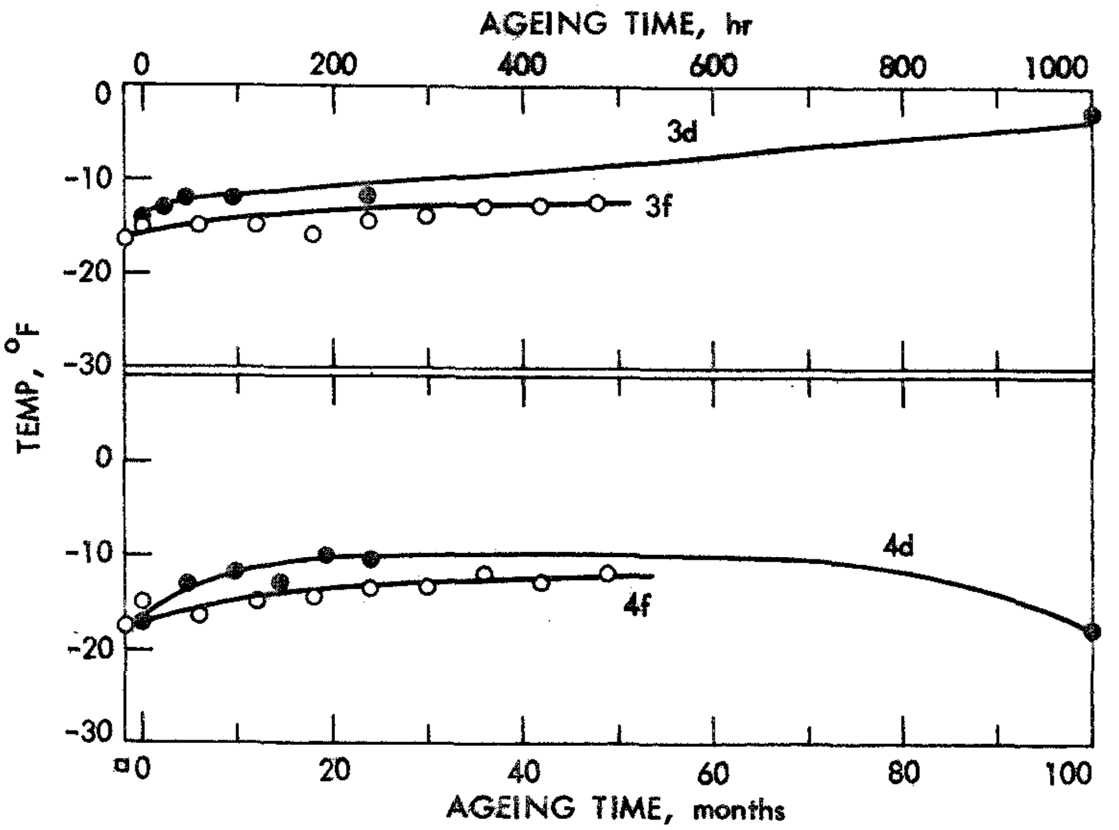

Fig. 18b. Fraass brittle point vs time of ageing, A.C. No. 3 and 4.

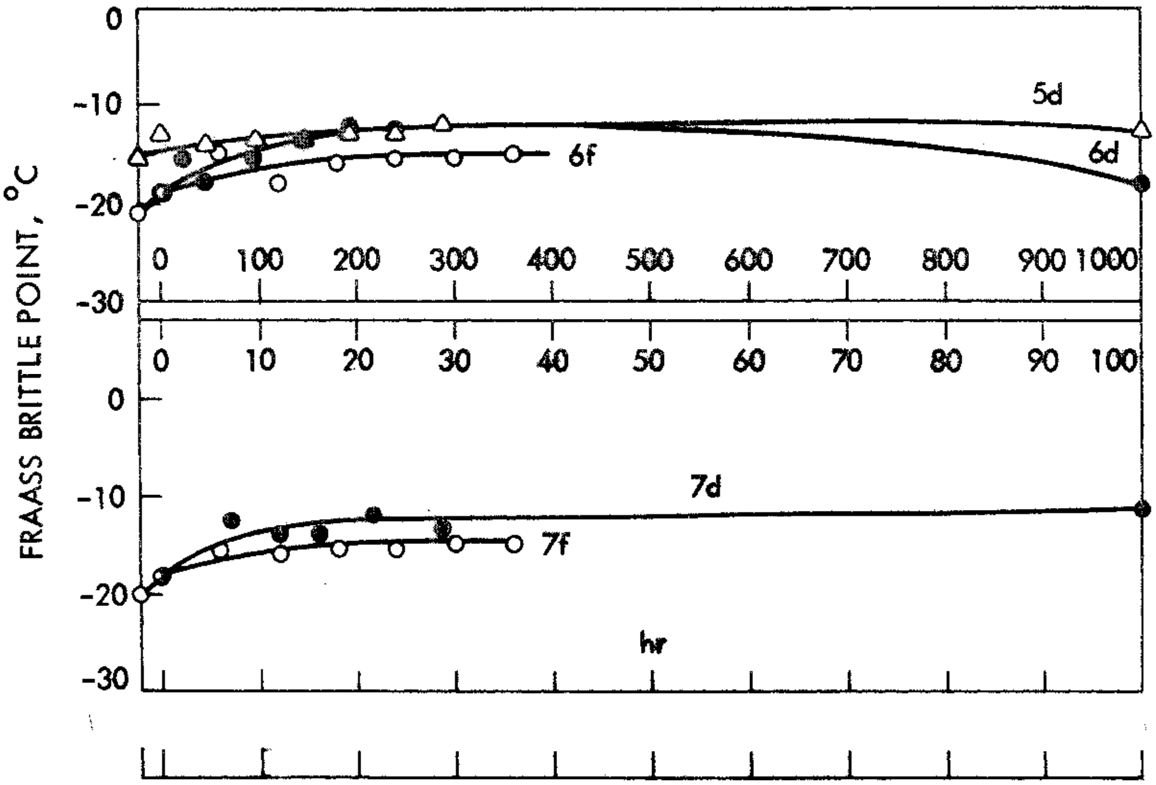

Fig. 18c. Fraass brittle point vs time of ageing, A.C. No. 5, 6, and 7.

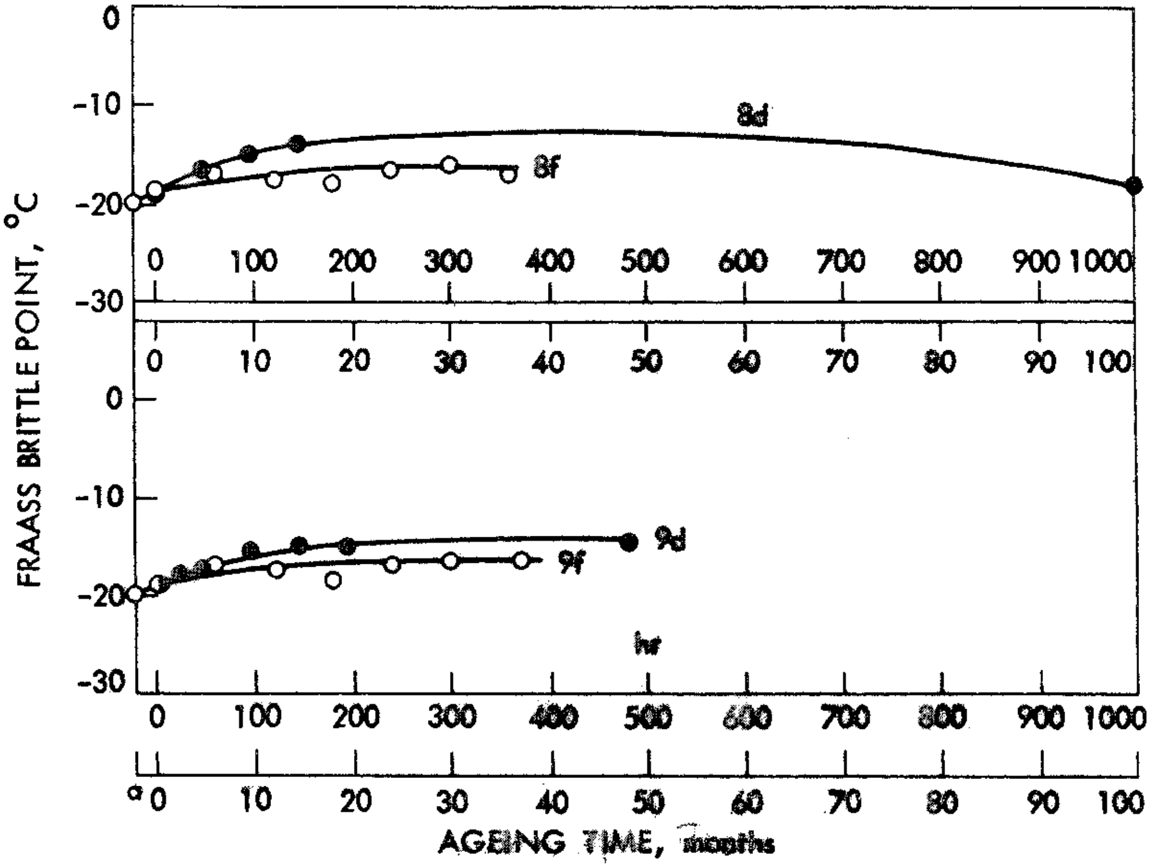

Fig. 18d. Fraass brittle point vs time of ageing, A.C. No. 8 and 9.

Ageing and Dynamic Modulus

The dynamic modulus of elasticity was determined, with a dynamic modulus tester PPM-5R with planar mount option, by measurement of the sonic velocity of a longitudinal mechanical pulse in asphalt films. The dynamic moduli of both laboratory and field aged samples were determined at both 21 and - 10 °C. The results, reported both in terms of sonic velocity C and sonic modulus E_s, are given in Table 20. Although the sonic modulus tester has been used for some years in research and development on paper, film, leather, membranes, fabric, plastics, etc., this was the first time it was used on asphalts. Preliminary studies were made on effects of temperature, film thickness and strip size, transducer orientation and type of backings. Possibly because of the effects of viscosity and thus the differences in transducer penetration in the asphalt being tested, the data on dynamic modulus were very inconsistent. The dynamic modulus changes with time of ageing were shown in Figs. 19a, 19b, and 19c. The general increase in E_s with ageing time can be observed. Because the non-destructive nature of this test, the wide temperature range it can be used (- 50 °C to 200 °C) and its simplicity in testing, it is potentially an ideal instrument in studying ageing, fatigue and modulus properties of asphalts.

Ageing and Change in Thermal Properties

Asphalts No. 1, 2, 4, and 6 were studied by thermal analysis to detect differences in thermal responses and in the effects of laboratory

Table 20. Dynamic modulus.

	A.C. No. 1				A.C. No. 2			
	21 °C[‡]		- 10 °C[‡]		21 °C		- 10 °C	
	C^2[*]	E[†]	C^2	E	C^2	E	C^2	E
Original (a)	0.4217	61,146.5	2.0409	295,930.5	0.2862	41,499.0	2.4414	354,003
TFOT (d)	0.4444	64,438.0	3.0779	446,295.5	0.3721	53,954	2.3670	343,215
Lab ageing								
24 hr (d24)	–	–	–	–	0.3544	51,388	2.4414	354,003
48 hr (d48)	–	–	–	–	0.3923	56,883	2.3670	343,215
96 hr (d96)	0.5932	86,014.0	2.5195	365,327.0	0.3956	57,362	2.4414	354,003
240 hr (d240)	0.4931	71,499.5	2.4414	354,003.0	0.3908	56,666	2.5195	365,328
480 hr (d480)	–	–	–	–	0.6829	99,021	–	–
1000 hr (d1000)	–	–	–	–	0.6829	99,021	–	–
Field ageing								
Plant (p)	–	–	–	–	0.3481	50,475	2.7779	402,796
0 months (f0)	0.3790	54,955.0	2.5195	365,327.5	0.4163	60,363	2.5195	365,328
6 months (f6)	0.3969	57,550	2.6014	377,203.0	0.3498	50,721	2.2958	332,891
12 months (f12)	0.3745	54,310	2.8727	416,541.5	0.3906	56,637	2.6014	337,203
18 months (f18)	0.3908	56,666.0	2.2958	332,891.0	0.4409	63,931	2.4414	354,003
24 months (f24)	0.4110	59,595.0	2.3670	343,215.0	0.4247	61,582	2.5195	365,328
30 months (f30)	0.4206	60,987.0	2.6873	389,658.5	0.3564	51,678	3.0779	446,296
36 months (f36)	0.4096	59,392	2.9725	431,012.0	0.3542	51,368	2.6014	377,203
42 months (f42)	0.4330	62,785.0	2.4414	354,003.0	0.3652	52,954	1.9290	279,705
48 months (f48)	0.4273	61,958.5	–	–	0.3652	52,954	2.6014	377,203

Table 20. Continued.

	A.C. No. 3				A.C. No. 4			
	21 °C‡		- 10 °C‡		21 °C		- 10 °C	
	C^{2*}	$E^{\dagger}$	C^2	E	C^2	E	C^2	E
Original (a)	0.3721	53,955	2.2958	332,891	0.3420	49,590	2.6873	389,659
TFOT (d)	–	–	–	–	0.5329	77,270	2.4414	354,003
Lab ageing								
24 hr (d24)	0.5104	74,008	2.3308	337,966	–	–	–	–
48 hr (d48)	0.4959	71,906	2.4414	354,003	0.6202	89,929	–	–
96 hr (d96)	0.5699	82,635.5	2.2276	323,002	0.6719	97,426	2.7321	396,155
240 hr (d240)	0.6202	89,929	2.3670	343,215	0.6829	99,021	2.4414	354,003
480 hr (d480)	–	–	–	–	–	–	–	–
1000 hr (d1000)	0.6829	99,021	2.8729	416,542	0.7022	101,819	2.6014	377,203
Field ageing								
Plant (p)	0.4826	69,977	2.4414	354,003	0.4160	60,324	2.9725	431,013
0 months (f0)	0.3387	49,115	2.6873	389,659	0.3844	55,738	2.1627	313,592
6 months (f6)	0.4163	60,364	2.3670	343,215	0.4597	66,657	2.4414	354,003
12 months (f12)	0.4504	65,308	2.3670	343,215	0.5570	80,765	2.5195	365,328
18 months (f18)	0.4512	65,424	2.3308	337,966	0.6062	87,899	2.9725	431,013
24 months (f24)	0.4725	68,513	2.2958	332,891	0.5655	81,998	2.9220	423,690
30 months (f30)	0.4476	64,902	2.4414	354,003	0.5784	83,868	2.7321	396,155
36 months (f36)	0.5041	73,095	2.4800	359,600	0.6011	87,160	2.6873	389,659
42 months (f42)	0.4225	61,263	2.9220	423,960	0.6104	88,508	2.5195	365,328
48 months (f48)	0.4858	70,441	2.4037	348,537	0.5874	85,173	2.3670	343,215

Table 20. Continued.

	A.C. No. 5				A.C. No. 6			
	21 °C*		- 10 °C*		21 °C		- 10 °C	
	C^{2*}	E†	C^2	E	C^2	E	C^2	E
Original (a)	0.6831	99,050	2.6873	389,659	0.4331	62,800	2.5195	365,328
TFOT (d)	0.6805	98,673	2.5195	365,328	0.4962	71,949	3.1887	462,362
Lab ageing								
24 hr (d24)	–	–	–	–	0.4915	71,268	–	–
48 hr (d48)	0.6892	99,934	2.9725	431,013	0.5529	80,171	2.6014	377,203
96 hr (d96)	0.6400	92,800	2.2614	327,903	0.4959	71,906	2.9725	431,013
144 hr (d144)	0.6719	97,425	2.6439	383,366	0.5105	74,023	3.1325	454,213
192 hr (d192)	0.7245	105,053	2.6873	389,659	0.5828	884,506	3.1325	454,213
240 hr (d240)	0.8521	123,555	2.6439	383,366	–	–	–	–
288 hr (d288)	0.6400	92,800	2.2958	332,891	–	–	–	–
480 hr (d480)	–	–	–	–	0.4996	72,442	2.6014	377,203
1000 hr (d1000)	0.8495	123,178	2.4800	359,600	0.4994	72,413	2.7321	396,155
Field ageing								
Plant (p)	–	–	–	–	0.4659	67,556	2.2958	332,981
0 months (f0)	–	–	–	–	–	–	–	–
6 months (f6)	–	–	–	–	0.4628	67,106	2.7321	396,155
12 months (f12)	–	–	–	–	0.4724	68,498	2.8727	416,542
18 months (f18)	–	–	–	–	0.4692	68,038	2.9725	431,013
24 months (f24)	–	–	–	–	0.4893	70,949	2.6439	383,366
30 months (f30)	–	–	–	–	0.4659	67,556	2.7321	396,155
36 months (f36)	–	–	–	–	–	–	–	–
42 months (f42)	–	–	–	–	0.5067	73,472	2.8248	409,596
48 months (f48)	–	–	–	–	–	–	–	–

Table 20. Continued.

	A.C. No. 7				A.C. No. 8			
	21 °C‡		- 10 °C‡		21 °C		- 10 °C	
	C^{2*}	$E^{\dagger}$	C^2	E	C^2	E	C^2	E
Original (a)	0.4111	59,610	2.9725	431,013	0.3506	50,837	2.6014	377,203
TFOT (d)	0.4858	70,441	2.5600	371,200	0.3980	57,710	2.5195	365,328
Lab ageing								
24 hr (d24)	–	–	–	–	–	–	–	–
48 hr (d48)	–	–	–	–	0.4245	61,553	2.6873	389,659
72 hr (d72)	0.5872	85,144	3.0779	446,296	0.4386	63,597	2.4414	345,003
144 hr (d144)	–	–	–	–	0.4628	67,106	2.8248	409.596
192 hr (d192)	–	–	–	–	0.4416	64,032	2.6439	383,366
240 hr (d240)	–	–	–	–	0.4474	64,873	2.8248	409,596
288 hr (d288)	0.5448	78,996	2.6014	377,203	–	–	–	–
480 hr (d480)	–	–	–	–	–	–	–	–
1000 hr (d1000)	0.6202	89,929	2.6014	377,203	0.4948	71,716	2.6873	389,659
Field ageing								
Plant (p)	0.3721	53,955	3.0245	438,553	0.3956	57,362	3.0245	438,553
0 months (f0)	0.3956	57,362	2.6439	383,366	0.4275	61,988	2,6439	383,366
6 months (f6)	0.5329	77,271	3.0245	438,553	0.4536	65,772	2.9725	431,013
12 months (f12)	0.5489	79,591	2.8248	409,596	0.4302	62,379	2.6873	389,659
18 months (f18)	0.4225	61,263	2.9220	423,690	0.4567	66,222	2.7321	396,155
24 months (f24)	0.4489	65,091	–	–	0.4477	64,917	2.8727	416,542
30 months (f30)	0.5329	77,271	2.5195	365,327	0.4445	64,453	2.4800	359,600
36 months (f36)	0.5252	76,154	3.2465	470,743	0.4386	63,597	2.6014	377,203
42 months (f42)	–	–	–	–	0.4356	63,162	2.3308	337,966
48 months (f48)	–	–	–	–	–	–	–	–

Table 20. Continued.

	A.C. No. 9			
	21 °C‡		- 10 °C‡	
	C^{2*}	$E^{\dagger}$	C^2	E
Original (a)	0.3564	51,678	2.4800	359,600
TFOT (d)	0.3956	57,362	2.3670	343,215
Lab ageing				
24 hr (d24)	0.4131	59,900	2.4414	354,003
48 hr (d48)	0.4140	60,030	2.7321	396,155
96 hr (d96)	0.4277	62,017	2.5600	371,200
144 hr (d144)	0.4421	64,105	2.4037	348,537
192 hr (d192)	0.4545	65,903	2.4414	354,003
480 hr (d480)	0.4496	64,801	2.5600	371,200
1000 hr (d1000)	—	—	—	—
Field ageing				
Plant (p)	0.3600	52,200	2.6873	389,659
0 months (f0)	0.3630	52,635	2.4037	348,537
6 months (f6)	0.3906	56,637	2.7779	402,796
12 months (f12)	0.3600	52,200	2.9220	423,690
18 months (f18)	0.4341	62,945	2.5195	365,328
24 months (f24)	0.4178	60,581	2.4414	354,003
30 months (f30)	0.4110	59,595	2.4415	354,003
36 months (f36)	0.4275	61,988	2.8727	416,542
42 months (f42)	—	—	—	—
48 months (f48)	—	—	—	—

---

[*] C = sonic longitudinal velocity in km/sec.

[†] $E(psi) = \rho c^2 \times 1.45 \times 10^5$, where ρ = density in g/cm^3 = 1.000.

[‡] Average of two specimens at 21 °C; results of single determination at - 10 °C.

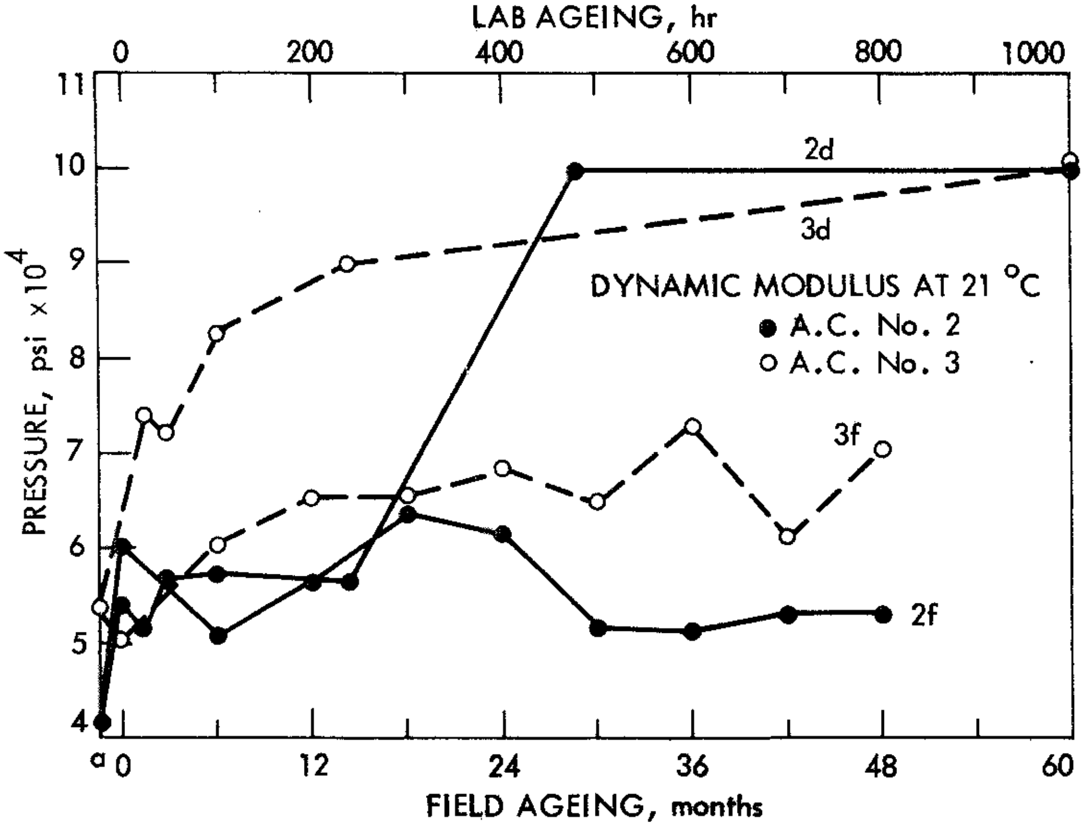

Fig. 19a. Dynamic modulus at 21 °C, A.C. No. 2 and 3.

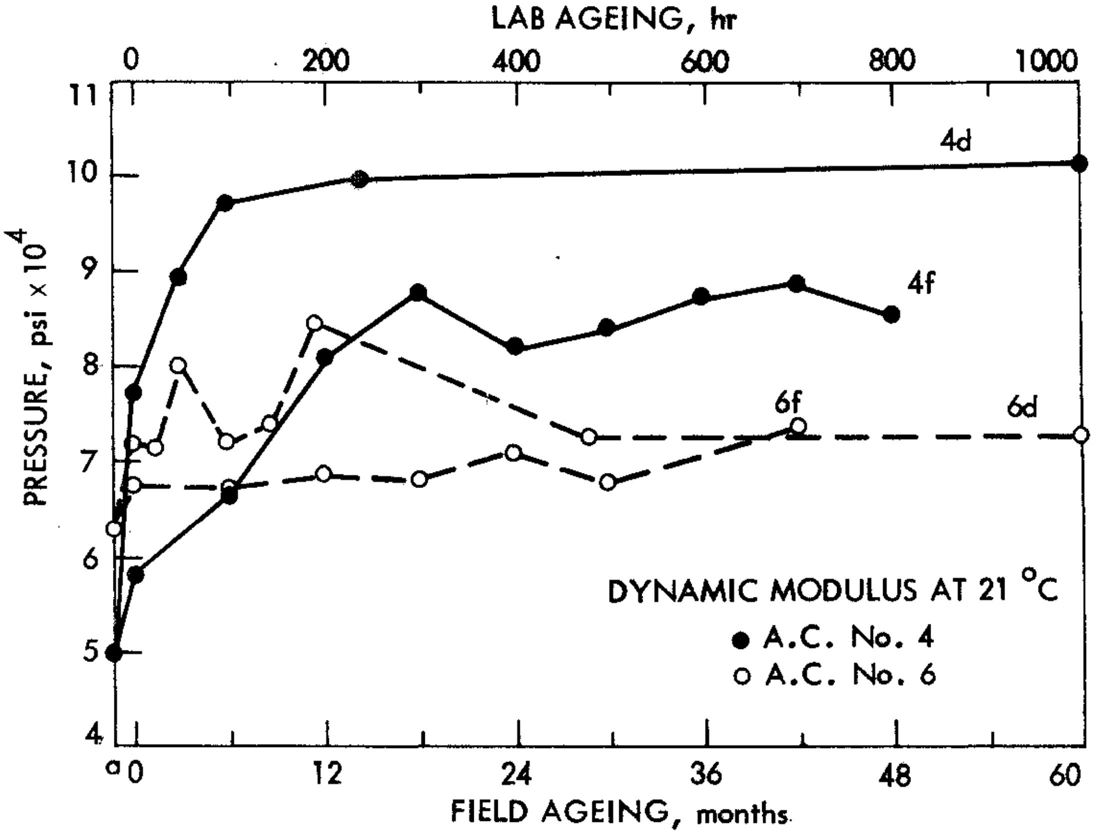

Fig. 19b. Dynamic modulus at 21 °C, A.C. No. 4 and 6.

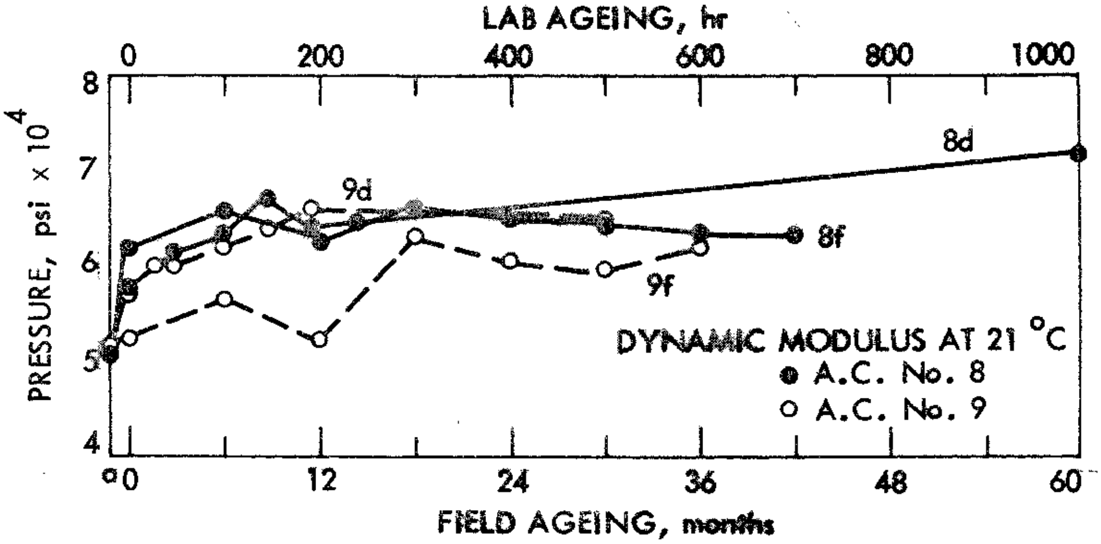

Fig. 19c. Dynamic modulus at 21 °C, A.C. No. 8 and 9.

and field weathering. Thermal analysis is generally defined as the study of the response of some material property as a function of temperature. In differential scanning calorimetry (DSC) the heat change of a sample is continuously measured over a desired temperature range. The thermomechanical analysis (TMA) measures changes in vertical dimension of a sample either in expansion or in penetration as the temperature is changed. It was thought that DSC or TMA analysis would indicate valuable information on asphalt during ageing because of their possible relationship with glass transition temperature, softening point, and asphalt pavement cracking[92-95].

The samples were sent to DuPont for analysis in two groups: 1f-24, 1f-30, 2a, 4a, and 6a were the first batch and 1a, 1d, 1d-96, and 1f were the second. Because of the differences in probes used (a penetration probe was used in the first group, an expansion probe in the second), the softening points from the second group were generally higher than those from the first group (Table 21). Examining data within groups, it seemed to be significant that: (a) there were obvious differences in thermal responses among asphalts of the same penetration grade, and (b) there was a definite increase in softening points either in DSC or TMC with weathering. Figures 20a and 20b show DSC scans of original and field aged samples and Fig. 20c and 20d show TMA scans of the same asphalts in the first group.

Table 21. Softening point from thermal analysis.

Sample	TMA, °C	DSC, °C
1a	26.5	32.0
1d	33.5	32.0
1d-96	44.0	33.0
1f	45.0	34.0
1f-24	11.0	10.0
1f-30	14.5	12.5
2a	11.5	9.0
4a	20.0	16.0
6a	13.5	14.0

Ageing and Chemical Changes in Asphalts

The chemical approach to the durability study of asphalts has been criticized as premature, due to the lack of definitive knowledge of the chemical composition and structure of asphalt. However, this is a fundamental approach. It has been proved that chemical composition does have direct effects on the rheological and durability properties of asphalt, that the relationship between asphalt durability and chemical composition can be established[70] and that the durability grouping of asphalts by chemical composition was possible[71,72].

When asphalt cement ages and hardens, the degree and rate of rheological change is due to changes in chemical composition. In

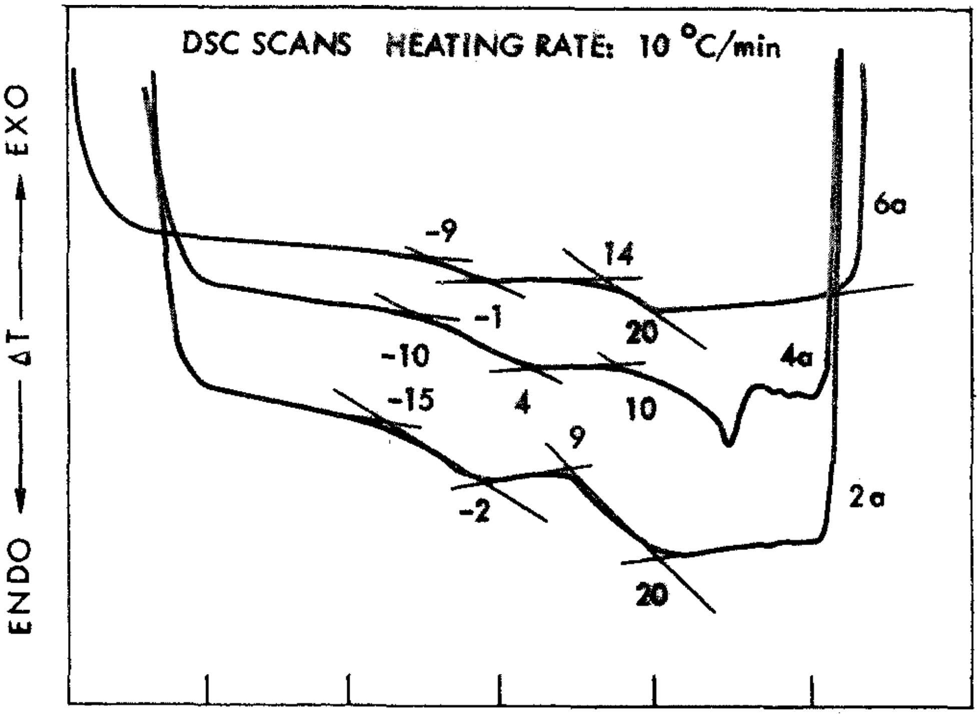

Fig. 20a. DSC scans of original asphalts.

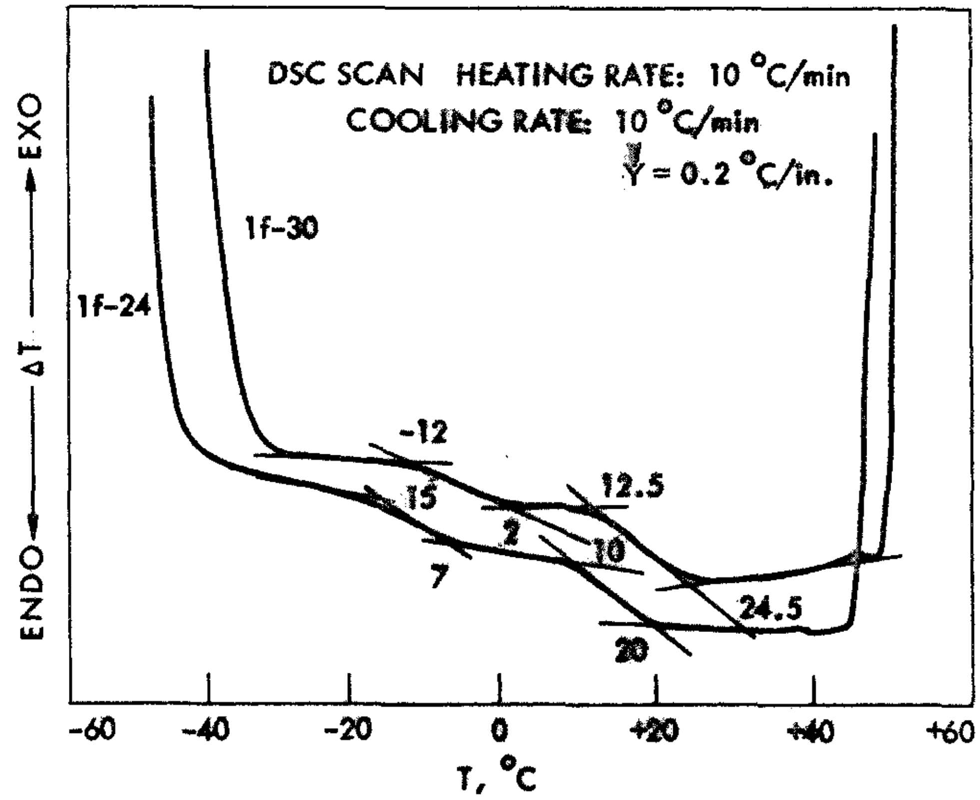

Fig. 20b. DSC scans of field aged asphalts.

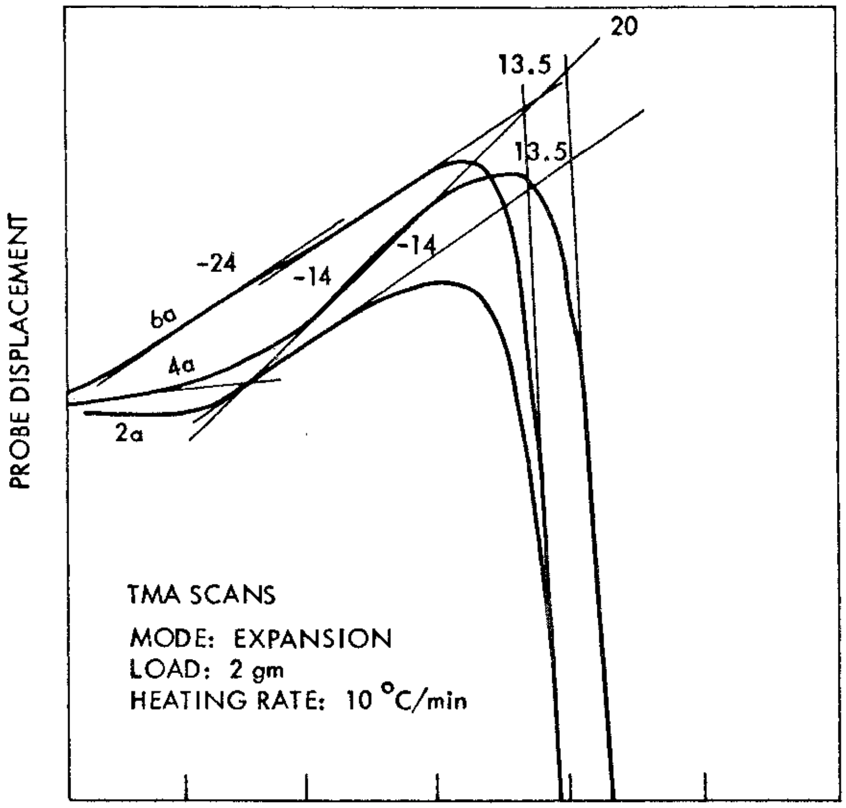

Fig. 20c. TMA scans of original asphalts.

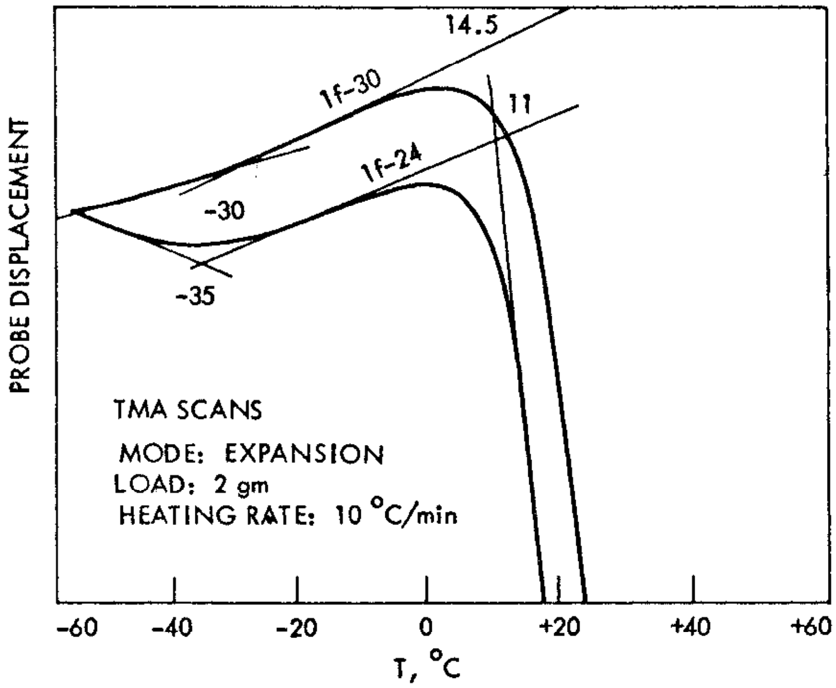

Fig. 20d. TMA scans of field aged asphalts.

order to study the rate and degree of hardening or ageing, it is desirable to establish measurable indicator(s) of chemical change.

In this investigation, chemical changes in asphalt during ageing were measured by: (a) determining the asphaltene content, (b) determining chemical composition by the Rostler-White method, (c) determining oxygen content, (d) spot testing, and (e) using IR spectroscopy.

The formation of asphaltenes that results from weathering (oxidation and/or polymerization), has long been observed. The increase in viscosity (hardening of asphalt) and the change in colloidal structure (from sol or sol-gel to gel-type materials) or the increase in complex flow that accompanies the increase in asphaltene content have been postulated by many researchers as the cause for asphalt failure by cracking. Thus the change in asphaltene content was used in this study as an important parameter in asphalt durability evaluation. By some investigators[64,96], the change in asphaltene content was considered the ONLY reliable indicator of chemical change in asphalt cements.

The percentage of asphaltenes as given by the Skelly F precipitation method for all asphalts studied are given in Table 22. Changes in asphaltene content with time of ageing in IDT are given in Figs. 21a through 21i. Three important observations can be made:

1. Ageing is accompanied by increase in asphaltene content.
2. Change in asphaltene content is a hyperbolic function of time. Except for A.C. No. 5, which is an unusual asphaltene-free asphalt, regression coefficients for the plot of $T/\Delta Y$ vs T were all above 0.90, and were all significant at the 95% level (Table 11).

Table 22. Percentage of asphaltenes.

A.C. No.		1	2	3	4	5	6	7	8	9
Original (a)		17.72	17.85	15.69	14.52	4.55	15.64	17.80	11.30	11.11
TFOT (d)		20.60	21.23	19.37	18.33	5.70	19.20	20.20	14.35	14.18
Lab ageing										
24 hr (d24)		23.34	23.50	21.06	–	6.70‡	–	22.00‡	16.00‡	18.55
48 hr (d48)		23.50	23.85	21.67	22.14	8.07	22.30	22.80‡	19.20	19.70
96 hr (d96)		24.05	24.85	22.69	23.11	7.93	22.88	24.20‡	19.15	19.12
240 hr (d240)		27.14	26.54	24.57	26.52	10.96	27.13	26.20‡	21.06	20.50‡
480 hr (d480)		27.60‡	29.37	27.50‡	29.80‡	14.40‡	27.35	27.50‡	22.40‡	22.60
1000 hr (d1000)		28.99	–	34.17	31.10	22.02	28.22	31.10	25.70	–
Field ageing										
Plant (p)		20.26	20.04	19.04	18.83	–	19.48	20.70	13.95	11.96
0 months (f0)	A*	19.96	20.75	18.22	19.10	–	–	19.30	12.35	12.82
	B†	–	–	–	19.88	–	–	–	–	–
6 months (f6)	A	20.11	20.87	19.84	18.38	–	20.39	20.44	17.85	14.48
	B	21.31	20.11	25.97	22.56	–	21.56	20.74	–	15.51
12 months (f12)	A	20.31	21.86	21.29	21.24	–	20.71	23.07	17.95	16.39
	B	21.26	21.45	–	21.81	–	19.93	–	18.85	16.68

Table 22. Continued.

A.C. No.		1	2	3	4	5	6	7	8	9
18 months (f18)	A	23.21	20.69	21.40	21.45	—	23.83	24.59	19.49	18.04
	B	21.68	23.12	20.00	22.20	—	24.95	23.14	19.73	18.80
24 months (f24)	A	21.16	—	22.02	21.27	—	28.56	23.49	19.73	18.50
	B	23.03	23.95	20.99	24.52	—	28.30	—	18.74	—
30 months (f30)	A	24.02	22.78	20.99	23.66	—	24.16	24.82	20.73	19.69
	B	24.71	22.85	20.65	23.94	—	—	—	—	—
36 months (f36)	A	25.08	23.96	21.49	23.83	—	—	23.04	17.88	21.84
	B	25.58	24.30	23.98	23.05	—	—	22.40	—	—
42 months (f42)	A	24.03	24.91	24.36	23.51	—	28.00	—	21.38	—
	B	—	—	—	—	—	—	—	—	—
48 months (f48)	A	25.38	24.91	24.15	25.16					
	B	33.23	25.20	24.99	24.97					

---

[*] A, in wheel tracks.

[†] B, between wheel tracks.

[‡] Interpolated value.

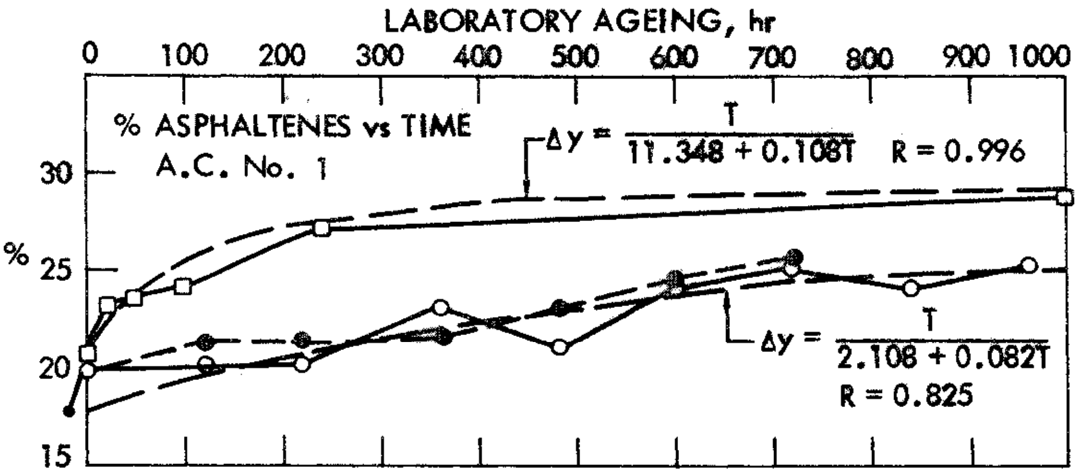

Fig. 21a. Asphaltene content vs time of ageing, A.C. No. 1.

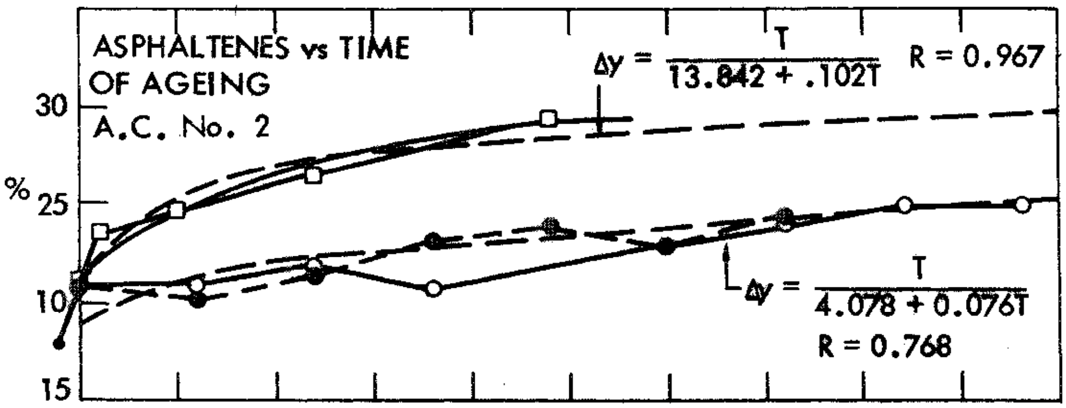

Fig. 21b. Asphaltene content vs time of ageing, A.C. No. 2.

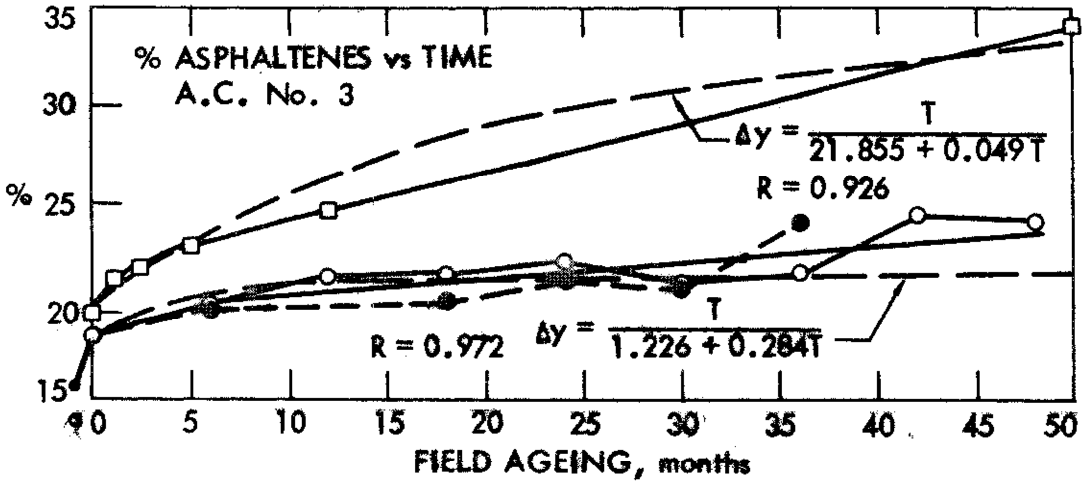

Fig. 21c. Asphaltene content vs time of ageing, A.C. No. 3.

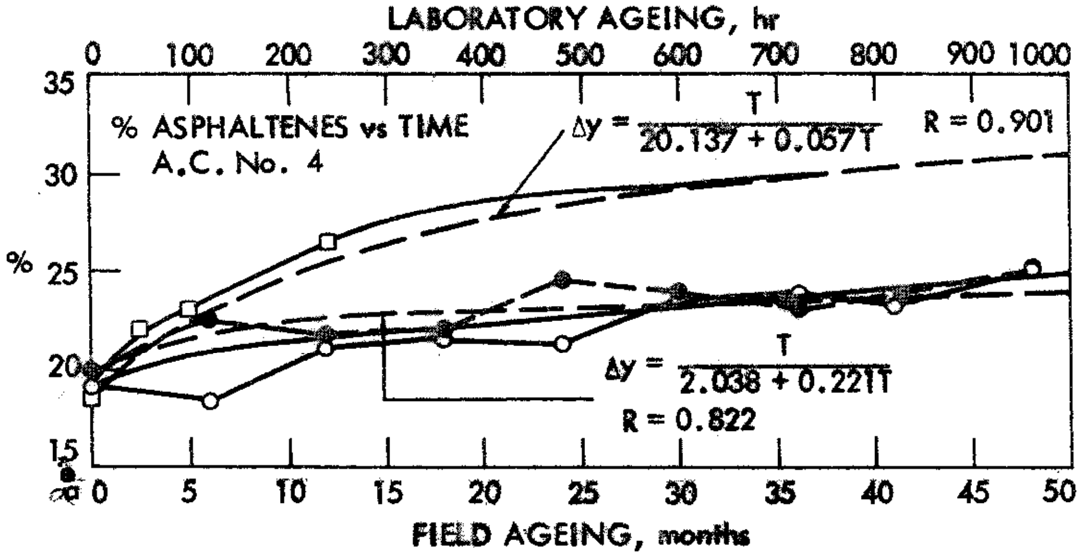

Fig. 21d. Asphaltene content vs time of ageing, A.C. No. 4.

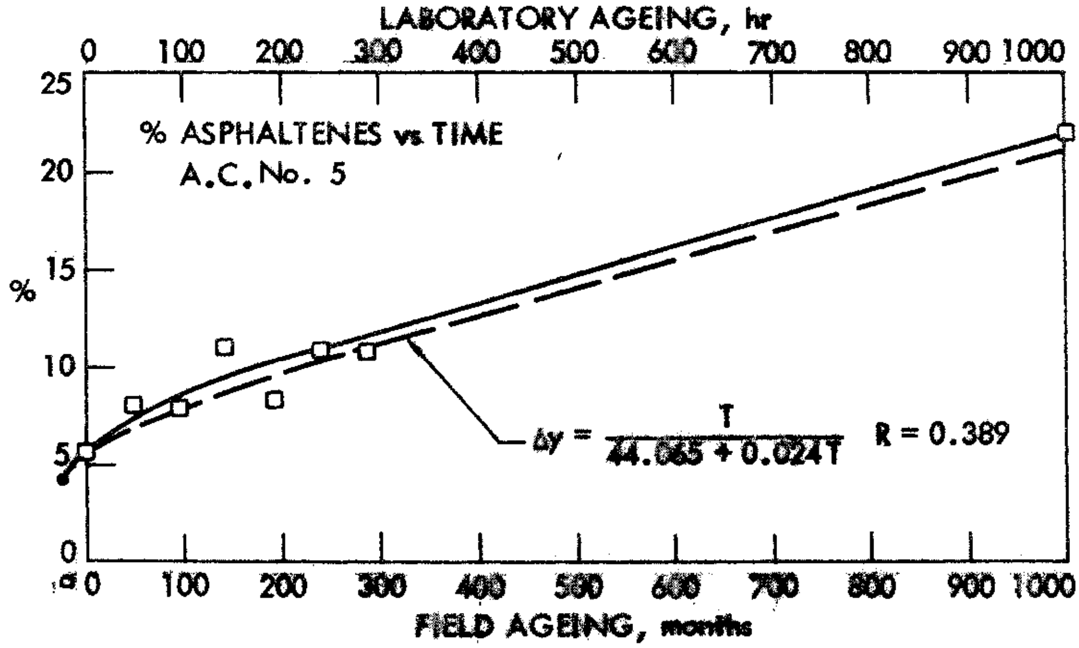

Fig. 21e. Asphaltene content vs time of ageing, A.C. No. 5.

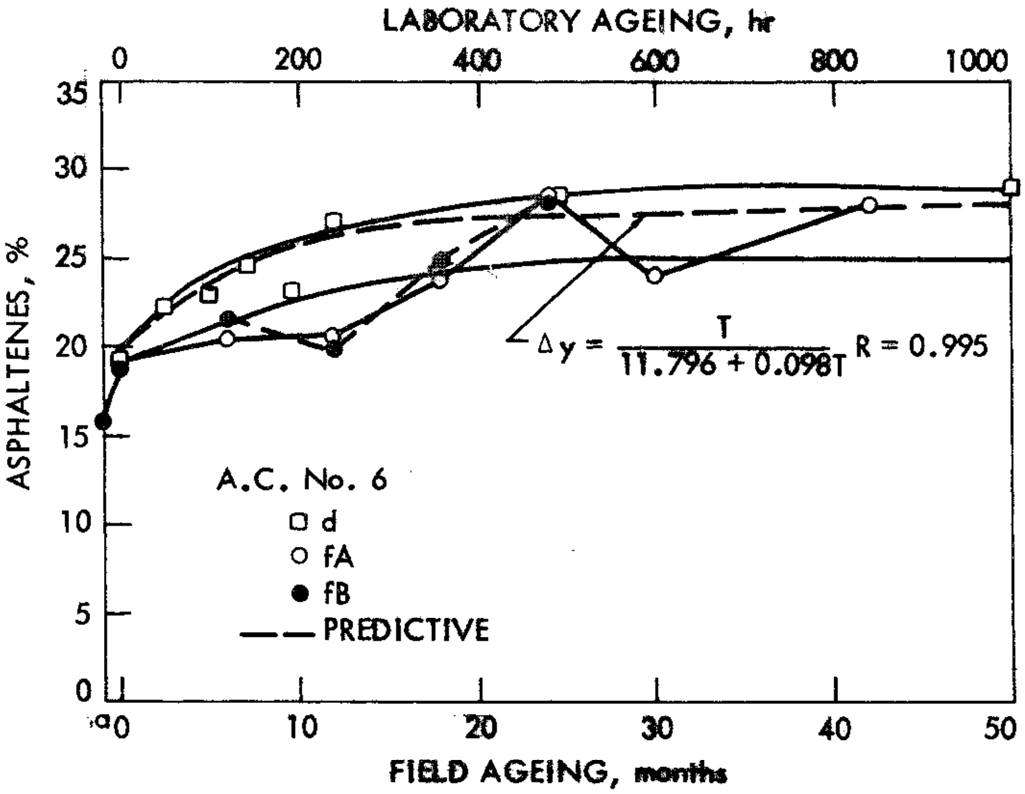

Fig. 21f. Asphaltene content vs time of ageing, A.C. No. 6.

3. Rates of asphaltene content formation are different for different asphalts (a varied from 5.6 to 32.4, b varied from 0.05 to 0.99). The ultimate change in asphaltene content varied from 9 to 20%.

Chemical compositions of asphalts No. 1 through 4 by the Rostler-White method are given in Table 23. This method defines asphalt as consisting of five, well-defined reactions, each with groups of components of like chemical reactivity (see Table 24). The chemical reactivity of the pentane soluble (maltene) fractions in decreasing order are: N, A_1, A_2, and P. This method of analysis was found to be time consuming and not as repeatable as other reports have suggested (each figure in Table 23 represents an average of at least four

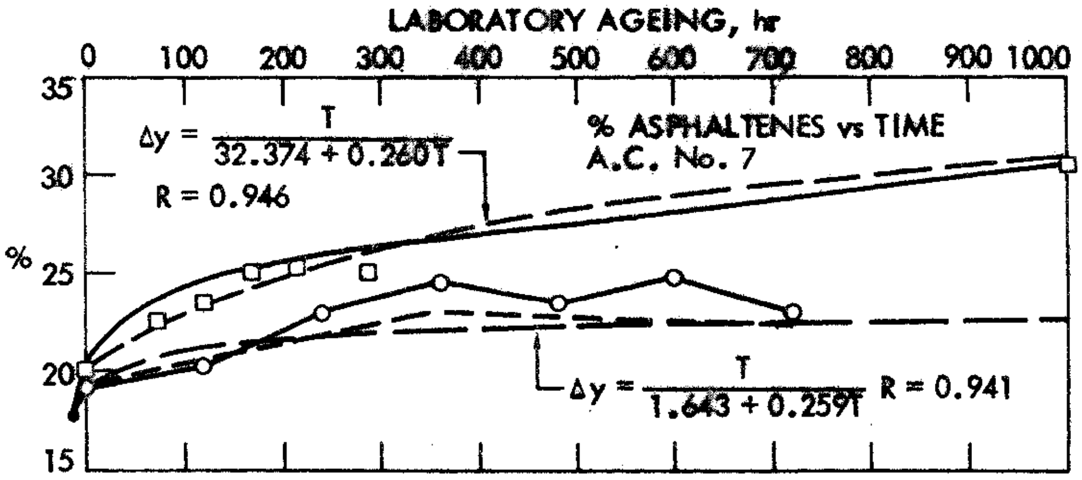

Fig. 21g. Asphaltene content vs time of ageing, A.C. No. 7.

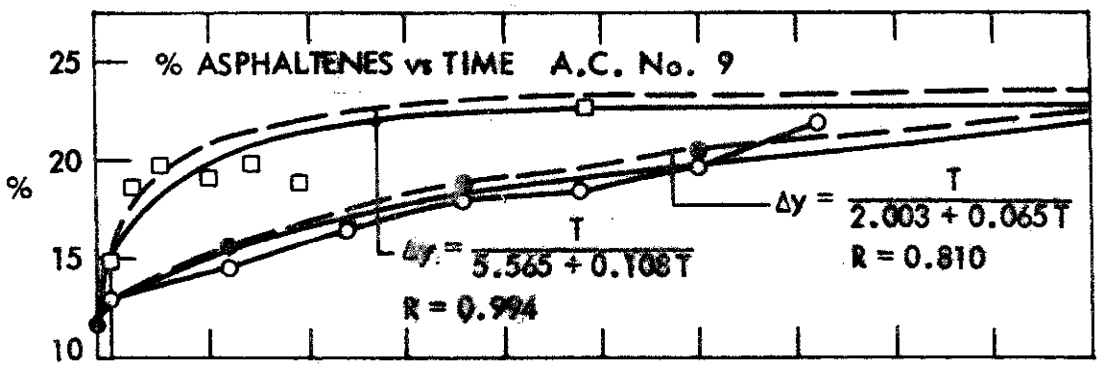

Fig. 21h. Asphaltene content vs time of ageing, A.C. No. 8.

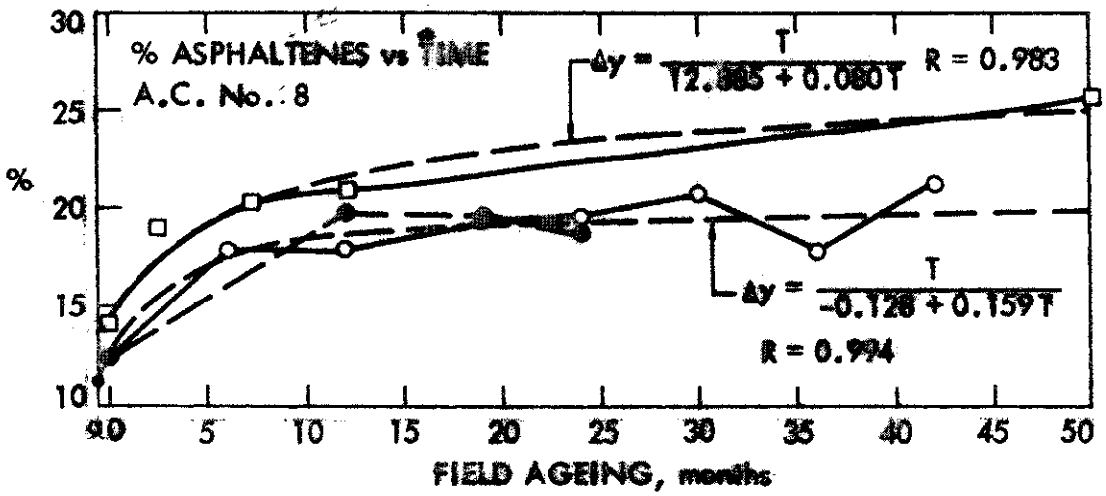

Fig. 21i. Asphaltent content vs time of ageing, A.C. No. 9.

Table 23. Chemical analysis.

		A.C. No. 1						A.C. No. 2					
		% A	% N	% A_1	% A_2	% P	Total %	% A	% N	% A_1	% A_2	% P	Total %
Original (a)		21.09	22.74	19.83	19.23	17.12	100.00	21.60	21.76	18.12	24.12	14.41	100.01
TFOT (d)		21.60	19.58	15.71	25.49	17.60	99.98	20.78	25.33	13.35	25.93	14.36	99.75
Lab ageing													
24 hr (d24)		26.80	19.07	16.22	26.75	11.17	100.01	26.90	19.57	14.34	26.11	13.08	100.00
48 hr (d48)		28.05	23.50	10.01	24.47	13.37	99.40	–	–	–	–	–	–
96 hr (d96)		28.92	24.31	11.60	22.97	12.28	100.08	30.03	19.44	13.41	24.80	12.38	100.06
240 hr (d240)		–	–	–	–	–	–	–	–	–	–	–	–
480 hr (d480)		–	–	–	–	–	–	32.27	15.94	15.77	22.59	13.05	99.62
1000 hr (d1000)		36.43	13.72	11.74	22.91	14.96	99.76	–	–	–	–	–	–
Field ageing													
Plant (p)		22.85	24.66	13.72	24.99	13.32	99.54	24.77	21.75	16.29	24.09	13.11	100.01
0 months (f0)	A*	24.21	20.94	16.38	25.96	13.50	100.99	24.57	21.77	16.01	24.48	11.43	98.26
	B†	–	–	–	–	–	–	–	–	–	–	–	–
6 months (f6)	A	21.19	23.21	17.16	22.19	15.29	99.04	24.78	22.46	16.55	20.18	16.42	100.39
	B	–	–	–	–	–	–	–	–	–	–	–	–
12 months (f12)	A	24.63	19.82	17.03	23.59	15.28	100.45	–	–	–	–	–	–
	B	–	–	–	–	–	–	–	–	–	–	–	–
18 months (f18)	A	24.06	23.44	17.42	22.50	13.74	101.16	25.97	17.59	16.47	24.01	12.66	96.70
	B	–	–	–	–	–	–	–	–	–	–	–	–
24 months (f24)	A	23.61	21.07	14.83	24.20	16.31	100.02	–	–	–	–	–	–
	B	–	–	–	–	–	–	–	–	–	–	–	–
30 months (f30)	A	24.86	21.16	15.57	23.69	15.73	101.01	–	–	–	–	–	–
	B	–	–	–	–	–	–	–	–	–	–	–	–
36 months (f36)	A	26.90	22.18	13.51	27.53	9.52	99.64	30.19	18.72	14.24	23.26	13.59	100.00
	B	–	–	–	–	–	–	–	–	–	–	–	–
42 months (f42)	A	26.10	20.80	14.61	25.79	12.71	100.01	28.11	20.40	14.27	23.14	14.09	100.01
	B	–	–	–	–	–	–	–	–	–	–	–	–
48 months (f48)	A	30.49	20.96	15.92	23.59	8.03	98.99						
	B	–	–	–	–	–	–						

Table 23. Continued.

		A.C. No. 3						A.C. No. 4					
		% A	% N	% A_1	% A_2	% P	Total %	% A	% N	% A_1	% A_2	% P	Total %
Original (a)		19.38	25.38	19.42	24.38	11.45	100.01	19.00	26.08	14.00[‡]	23.00[‡]	8.17	100.01
TFOT (d)		21.14	25.37	17.03	22.62	12.14	98.30	23.88	25.01	14.98	23.40	9.75	97.02
Lab ageing													
24 hr (d24)		23.90	27.33	16.08	23.90	8.44	99.65	23.06	25.92	15.24	23.47	10.31	98.00
48 hr (d48)		—	—	—	—	—	—	—	—	—	—	—	—
96 hr (d96)		—	—	—	—	—	—	—	—	—	—	—	—
240 hr (d240)		28.00	26.98	11.92	23.16	9.95	100.01	30.26	26.95	10.93	22.35	9.51	100.00
480 hr (d480)		—	—	—	—	—	—	—	—	—	—	—	—
1000 hr (d1000)		37.63	23.10	10.06	19.19	10.06	100.04	—	—	—	—	—	—
Field ageing													
Plant (p)		22.31	24.59	17.31	26.11	9.53	99.85	20.82	27.40	19.87	22.53	9.82	100.01
0 months (f0)	A[*]	22.45	24.96	17.39	22.53	12.68	100.01	23.53	27.41	14.60	24.23	10.24	100.01
	B[†]	—	—	—	—	—	—	—	—	—	—	—	—
6 months (f6)	A	24.41	27.83	13.55	24.67	8.93	99.39	22.49	29.01	12.30	26.53	9.68	100.01
	B	—	—	—	—	—	—	—	—	—	—	—	—
12 months (f12)	A	—	—	—	—	—	—	—	—	—	—	—	—
	B	—	—	—	—	—	—	—	—	—	—	—	—
18 months (f18)	A	—	—	—	—	—	—	25.01	28.78	12.82	24.63	8.76[‡]	100.00[‡]
	B	—	—	—	—	—	—	—	—	—	—	—	—
24 months (f24)	A	—	—	—	—	—	—	—	—	—	—	—	—
	B	—	—	—	—	—	—	—	—	—	—	—	—
30 months (f30)	A	—	— —	—	—	—	—	—	—	—	—	—	—
	B	—	—	—	—	—	—	—	—	—	—	—	—
36 months (f36)	A	23.83	28.99	22.13	11.12	13.60	99.69	26.91	28.95	11.38	24.06	8.70	100.00
	B	—	—	—	—	—	—	—	—	—	—	—	—
42 months (f42)	A	27.03	27.27	12.44	24.31	8.92	99.97	28.37	26.00	12.88	24.02	8.25	99.52
	B	—	—	—	—	—	—	—	—	—	—	—	—
48 months (f48)	A	—	—	—	—	—	—	—	—	—	—	—	—
	B	—	—	—	—	—	—	—	—	—	—	—	—

[*] A, in wheel tracks.

[†] B, between wheel tracks.

[‡] Interpolated value.

Table 24. Characteristics of asphalt components[70].

Fraction	General description	Specific chemical reactivity	Typical analytical data								Significant function
			Elementary composition					n_D^{25}	d_4^{20}	I No.	
			C	H	N	S	O				
A **Asphaltenes**	Higher molecular weight condensation products	Insoluble in n-pentane	86.5	8.3	2.3	1.5	1.4	–	–	–	Bodying agent
N **Nitrogen bases**	Petroleum resins containing nitrogen bases and other highly reactive compounds	Precipitable with 85% H_2SO_4	86.1	9.3	3.0	0.7	0.9	1.642	1.08	–	Peptizer for asphaltenes
A_1 **First acidaffins**	Resinous hydrocarbons	Precipitable with concentrated H_2SO_4	90.0	7.8	0.3	1.9	–	1.613	1.07	65-100	Solvent for peptized asphaltenes
A_2 **Second acidaffins**	Slightly unsaturated hydrocarbons	Precipitable with fuming H_2SO_4 (30% SO_3)	88.8	9.6	0.0	0.9	0.7	1.558	1.01	5	Solvent for peptized asphaltenes
P **Paraffins**	Saturated hydrocarbons	Nonreactive with fuming H_2SO_4 (30% SO_3)	86.5	13.5	–	–	–	1.486	0.90	–	Gelling agent

determinations). We used it in the study because of its reported ability of differentiating asphalt, of revealing changes in asphalts during ageing, and of characterizing asphalts with respect of durability.

The data have shown, though not very consistently, general increases in A and A_2, decreases in A_1 and P, with ageing in IDT. The N fraction remained relatively constant, and thus appeared to support the previous finding[8] that ageing results from conversion of lighter fractions of components into heavy fractions of larger molecules, especially from resins to asphaltenes.

The composition parameters, $(N + A_1)/(A_2 + P)$, the ratios of more reactive to less reactive components, and N/P, the ratio of the most to the least reactive fractions of maltenes, are calculated and given in Table 25. The ratio $(N + A_1)/(A_2 + P)$ has been correlated with the durability of asphalts as measured by the tendency of asphalts to harden (embrittle) during ageing as determined by the pellet-abrasion test[70,71]. According to durability classification of highway asphalts by this parameter (Table 26), A.C. No. 4 will be in Group I with superior durability (0.54), asphalts No. 1 and 2 will be classified as Group II asphalts with good durability rating and asphalt No. 3 (1.25) will be classified as a Group III asphalt with satisfactory durability. The pattern of change in $(N + A_1)/(A_2 + P)$ with ageing could not be defined. The ratios of N/P varied from 1.25 for asphalt No. 3 to 3.19 for No. 4. This parameter was suggested by Halstead et al.[72] as indicative of the quality of asphalt. The significance of this parameter is yet to be determined.

Table 25. Chemical composition parameters*.

	A.C. No. 1		A.C. No. 2		A.C. No. 3		A.C. No. 4	
	$N + A_1/A_2 + P$	N/P	$N + A_1/A_2 + P$	N/P	$N + A_1/A_2 + P$	N/P	$N + A_1/A_2 + P$	N/P
Original (a)	1.17	1.33	1.04	1.51	1.25	1.25	0.54	3.19
TFOT (d)	0.82	1.11	0.96	1.76	1.22	2.09	1.10	2.80
Lab ageing								
24 hr (d24)	0.93	1.71	0.87	1.50	1.34	3.24	1.36	2.97
48 hr (d48)	0.89	1.76	–	–	–	–	–	–
96 hr (d96)	1.02	1.98	0.90	1.57	–	–	–	–
240 hr (d240)	–	–	–	–	1.17	2.71	1.19	2.83
480 hr (d480)	–	–	0.89	1.22	–	–	–	–
1000 hr (d1000)	0.67	0.92	–	–	1.13	2.30	–	–
Field ageing								
Plant (p)	1.00	1.85	1.02	1.66	1.18	2.58	1.46	2.79
0 months (f0)	0.95	1.55	1.05	1.90	1.20	1.97	1.22	2.68
6 months (f6)	1.08	1.52	1.07	1.27	1.23	3.12	1.14	3.00
12 months (f12)	0.95	1.29	–	–	–	–	–	–
18 months (f18)	1.13	1.71	0.93	1.39	–	–	1.25	3.29

Table 25. Continued.

	A.C. No. 1		A.C. No. 2		A.C. No. 3		A.C. No. 4	
	N + A_1/A_2 + P	N/P	N + A_1/A_2 + P	N/P	N + A_1/A_2 + P	N/P	N + A_1/A_2 + P	N/P
24 months (f24)	0.89	1.29	—	—	—	—	—	—
30 months (f30)	0.93	1.35	—	—	—	—	—	—
36 months (f36)	0.96	2.33	0.89	1.38	2.10	2.20	1.23	3.33
42 months (f42)	0.92	1.64	0.93	1.45	1.20	3.06	1.20	3.15
48 months (f48)	1.17	2.61	—	—	—	—	—	—

*All tests done on A.

Table 26. Durability rating of asphalts from 60 to 100 penetration grade[*].

Group	$N + A_1/P + A_2$[†]	Average abrasion loss[‡] %	Average abrasion loss[‡] mg/revolution	Durability
0[**]	< 0.4	–	–	Decreasing durability with decreasing parameter value
I	0.4-1.0	0-10	0.00-0.40	Superior
II	1.0-1.2	5-15	0.20-0.60	Good
III	1.2-1.5	10-40	0.40-1.60	Satisfactory
IV	1.5-1.7	30-60	1.20-2.40	Fair
V	> 1.7	> 50	> 2.00	Inferior

[*] From Ref. 70.

[†] Based on original composition.

[‡] Average of abrasion @ 77 °F (pellet method) before and after ageing.

[**] Cheesy and putty-like products of consistency not associated with highway asphalt.

Since oxidation is considered as one of the major factors in asphalt hardening, both in mixing and in road service, the oxygen content change and the oxidation susceptibility of asphalts is considered to be an important indicator of the relative potential of asphalt to undergo oxidation. Oxygen content of asphalt and asphaltenes was determined by the combustion method, using a Coleman Model 36 Oxygen Analyzer. Due to inherent weaknesses in the design of the instrument and to intermittent malfunction, the oxygen content results are incomplete and often misleading. However, a gradual increase in oxygen content during ageing (both during the durability test and the road service) is obvious (Table 27). The degree and rate of oxidation is also indicated by weight increase during pressure-oxidation treatment (Table 28 and Fig. 22).

Table 27. Percent weight gain during Iowa Durability Test.

	Hours of pressure-oxidation treatment								
A.C. No.	48	72	96	144	192	240	480	1000	1000A*
1								2.62	
2							1.46		
3								2.98	
4								2.60	0.43
5	0.40							3.14	
6	0.56		0.68	0.95	1.03		1.26	2.00	0.40
7		0.65						2.73	
8	0.63		0.76	0.94	0.98	1.02		2.40	
9	0.52		0.66	0.74	0.81		1.30		

*1000A: 1000 hr at 150 °F and 1 atm air.

Data also indicated that ageing not only increased asphaltene content and oxygen percentage in asphalt, it also caused increases in oxygen percentage in asphaltenes.

Results of spot tests during laboratory ageing are given in Table 29. All original asphalts showed negative spot tests. As asphalts aged, except for asphalt No. 5, all tests became positive at some time during the ageing process. The border line between positive and negative spot testing appeared to be about 20% asphaltenes.

Table 28. Change in oxygen content during Iowa Durability Test.

	Hours of pressure-oxidation treatment								
A.C. No.	a[*]	d[†]	24	48	96	144	192	240	1000
1	1.21 (1.27)[‡]	1.49 (2.16)	1.63 (2.23)	1.79 (2.95)	2.19 (2.99)			2.06 (3.92)	3.17 (–)
2	1.30 (1.43)	1.58 (1.77)	1.69 (3.04)	1.68 (3.26)	1.74 (3.07)			2.49 (3.41)	– (–)
3	0.98 (1.18)	1.08 (2.05)	1.11 (2.33)	1.82 (2.81)	1.74 (3.93)			1.92 (–)	– (–)
4	1.26 (1.81)	1.37 (2.39)		1.33	1.47	2.36	2.77	2.33	
5	1.01 (1.92)	1.19		1.44	1.59	1.70	2.65	2.00	

[*] a = original sample.

[†] d = TFOT residue.

[‡] Figures in parentheses are oxygen content in asphaltenes.

Weathering as characterized by infrared spectroscopy will be discussed in Chapter VI, together with recovered asphalts.

Original, TFOT, and pressure-oxidation test data were kept on marginally punched cards used by Halstead et al.[72] as modified by the author for future reference. A blank card is shown in Fig. 23.

Thin Film Plate Ageing Tests

Also based on the two-stage hardening, functional approach, but using the popular microfilm plate ageing technique[9,46,53,62] is a special series of durability tests that were made on all nine asphalts. In glass plates, using residue from TFO tests, samples were aged in an

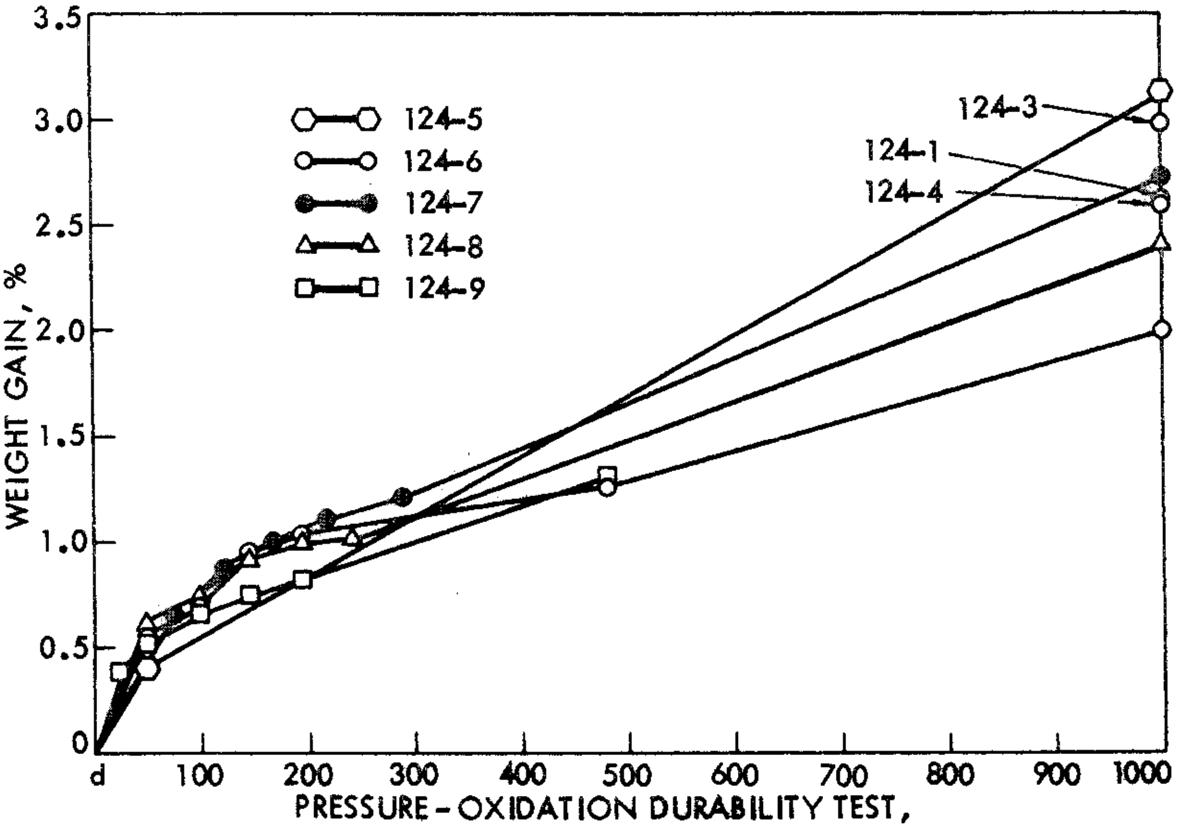

Fig. 22. Oxidation of asphalt during Iowa Durability Test as measured by weight change.

oxygen vessel for 24, 48, and 72 hr under 20 atm of oxygen at 150 °F. Viscosity was determined at the end of each pressure-oxidation period by the sliding-plate microviscometer at 77 °F. Shear susceptibility s, complex flow c, and viscosity at constant load of 1000 g were also calculated in addition to viscosity at 5×10^{-2} $\sec^{-1}$. The results are given in Table 30 and viscosity-time curves are shown in Fig. 24. The increase in viscosity and shear index, and the decrease in complex flow with time, followed the patterns of ageing in standard IDT but at a higher rate, as expected. However, due to difficulties in preparing repeatable constant films of 25 μ, to possible property

Table 29. Spot test.

A.C. No.		1	2	3	4	5	6	7	8	9
Original (a)		n	n	n	n	n	p/n[‡]	p	n	n
TFOT (d)		p	p	n	n	n	n	p/n	n	n
Lab ageing										
24 hr (d24)		p	p	p/n	n	n	—	n	n	n
48 hr (d48)		p	p	p/n	p	n	p	p	n	n
96 hr (d96)		p	p	p	p	n	p	p	n	n
240 hr (d240)		p	p	p	p	n	p	p	n	p
480 hr (d480)		p	p	p	p	n	p	p	p	p
1000 hr (d1000)		p	—	p	p	n	p	p	p	—
Field ageing										
Plant (p)		p	p/n	p/n	p/n	—	n	n	n	n
0 months (f0)	A[*]	p	p	p/n	p	—	n	n	n	n
	B[†]	—	—	—	—	—	—	—	—	—
6 months (f6)	A	p	p	p/n	p	—	p	p	p/n	n
	B	p	p	p/n	p	—	p	p	p/n	n
12 months (f12)	A	p	p	p/n	p	—	p	p	n	n
	B	p	p	p	p	—	p	p	n	n
18 months (f18)	A	p/n	p	p	p	—	p	p	p	n
	B	p/n	p	p	p	—	p	p	n	n
24 months (f24)	A	p	p	p	p	—	p	p	p/n	n
	B	p	p	p	p	—	p	p	p/n	n
30 months (f30)	A	p	p	p	p	—	p	p	p/n	p
	B	p	p	p	p	—	p	p	p/n	p
36 months (f36)	A	p	p	p	p	—	p	p	p/n	p
	B	p	p	p	p	—	p	p	p/n	p

Table 29. Continued.

A.C. No.		1	2	3	4	5	6	7	8	9
42 months (f42)	A	p	p	p	p	—	p	p	p	p
	B	p	p	p	p	—	p	p	p	p
48 months (f48)	A	p	p	p	p	—				
	B	p	p	p	p	—				

[*] A, in wheel tracks.

[†] B, between wheel tracks.

[‡] n = negative spot; p = positive spot.

changes during such film preparations and to the small amount of sample that is available for testing, this process is not considered suitable for routine material testing and control for average highway material laboratories.

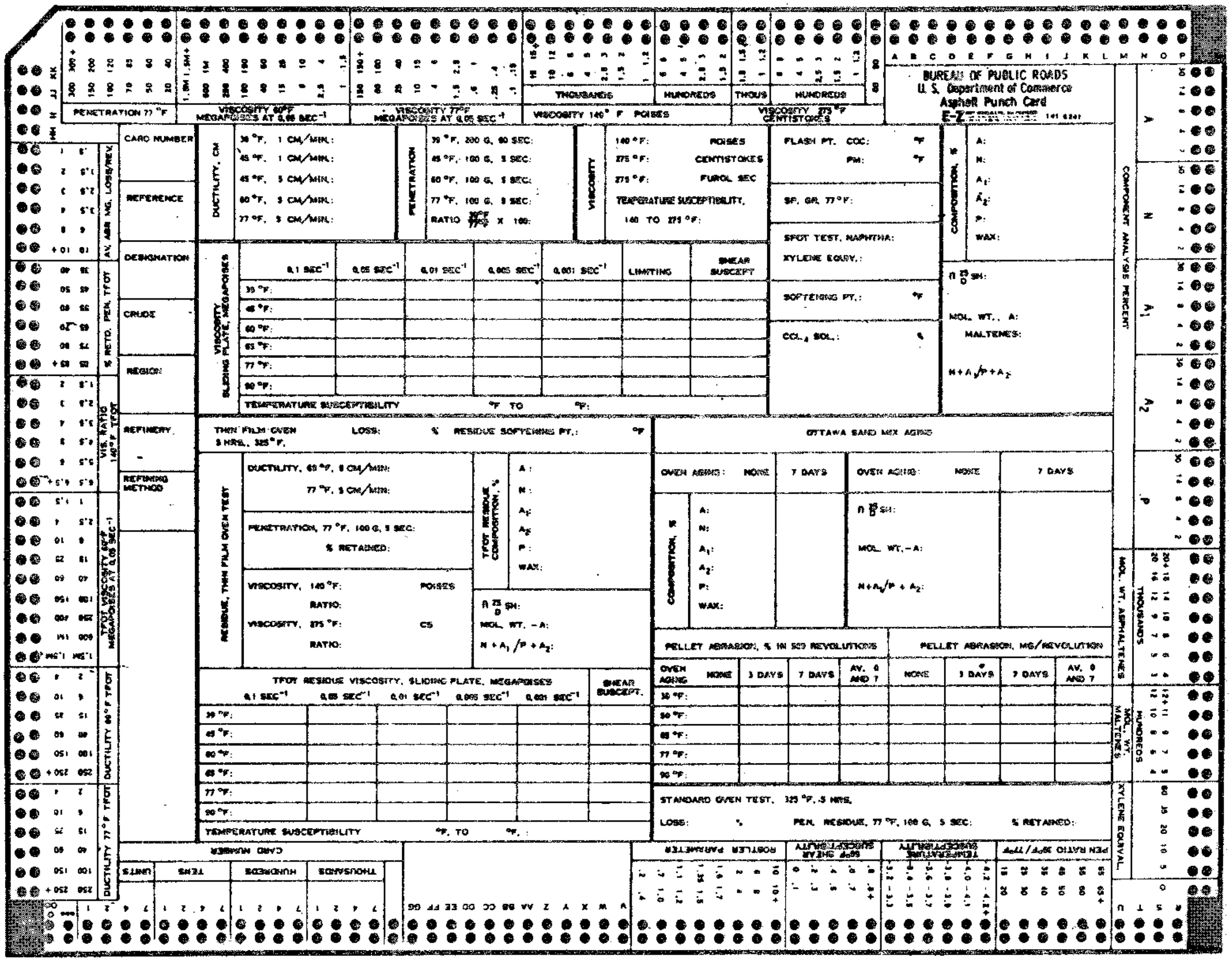

Fig. 23. Marginally punched card.

Table 30. Thin film plate ageing tests.

Film thickness: 20 × 25 μ   Pressure: 20 atm

Film size: 4 × 4 cm   Temp: 150 °F

Sample	Viscosity at 5×10^{-2}	Shear susceptibility index (S)	Complex flow (C)	Viscosity at 1000 g
1dt0	1.01×10^7	0.087	1.015	1.32×10^7
1dt24	2.6×10^7	0.158	0.839	3.8×10^7
1dt48	1.8×10^7	0.344	0.674	–
1dt72	3.0×10^7	0.405	0.578	–
2dt0	1.15×10^7	0.232	0.794	2.05×10^6
2dt24	2.15×10^7	0.268	0.729	4.67×10^7
2dt48	1.9×10^7	0.424	0.577	5.00×10^7
2dt72	2.9×10^7	0.438	0.469	–
3dt0	9.7×10^6	0.087	0.932	1.01×10^7
3dt24	1.8×10^7	0.070	1.192	2.3×10^7
3dt48	2.15×10^7	0.194	0.839	2.43×10^7
3dt72	3.1×10^7	0.140	0.932	4.20×10^7
4dt0	9.5×10^6	0.019	0.985	9.7×10^6
4dt24	1.5×10^7	0.052	0.932	2.19×10^7
4dt48	1.85×10^7	0.424	0.966	2.3×10^7
4dt72	2.5×10^7	0.194	0.903	3.5×10^7
5dt0	3.1×10^6	0.036	1.00	3.25×10^6
5dt24	5.40×10^6	0.070	0.966	5.20×10^7
5dt48	5.7×10^6	0.123	0.966	5.9×10^7
5dt72	8.4×10^6	0.069	0.869	8.7×10^7
6dt0	3.7×10^6	0.231	0.869	8.6×10^6
6dt24	2.0×10^7	0.249	0.726	3.5×10^7
6dt48	1.7×10^7	0.305	0.839	3.4×10^7
6dt72	2.25×10^7	0.424	0.626	5.5×10^7
7dt0	9.0×10^6	0.123	1.15	9.7×10^6
7dt24	1.60×10^7	0.168	0.969	1.73×10^7
7dt48	1.75×10^7	0.158	0.839	2.13×10^6
7dt72	2.35×10^7	0.140	0.809	3.26×10^7

Table 30. Continued.

Film thickness: 20 × 25 μ

Pressure: 20 atm

Film size: 4 × 4 cm

Temp: 150 °F

Sample	Viscosity at 55×10^{-2}	Shear susceptibility index (S)	Complex flow (C)	Viscosity at 1000 g
8dt0	9.0×10^{6}	0.212	0.890	1.19×10^{7}
8dt24	1.26×10^{7}	0.306	0.700	2.34×10^{7}
8dt48	1.40×10^{7}	0.268	0.753	–
8dt72	1.98×10^{7}	0.424	0.577	–
9dt0	5.6×10^{6}	0.222	0.839	6.3×10^{6}
9dt24	1.10×10^{7}	0.176	0.756	1.3×10^{7}
9dt48	9.70×10^{6}	0.287	0.702	1.5×10^{7}
9dt72	1.55×10^{7}	0.370	0.649	3.4×10^{7}

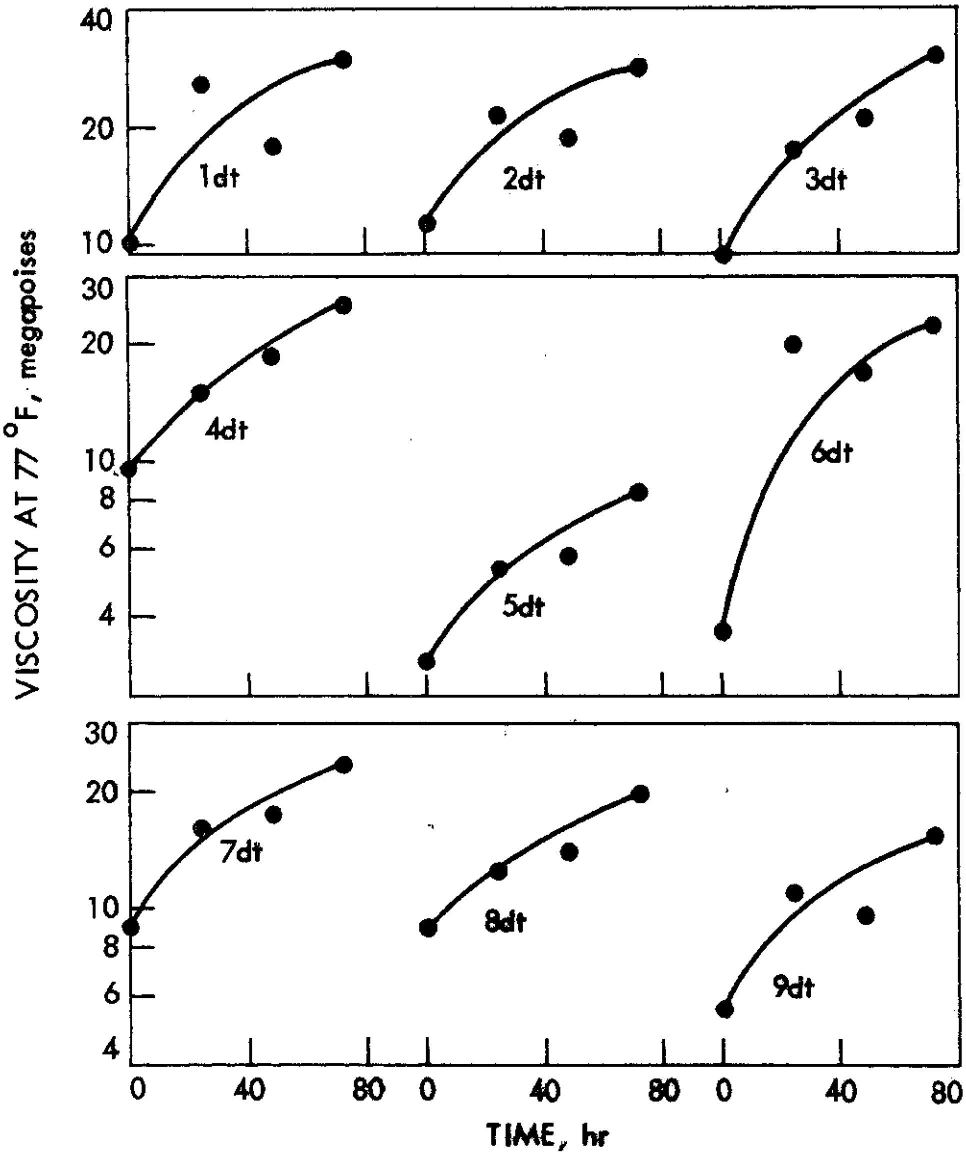

Fig. 24. Log viscosity vs time of thin film plate ageing test.

VI. FIELD AGEING

Density-Voids Change of the Pavements

Changes of density and voids of asphalt pavements were studied because such changes have been found to affect the rate of asphalt hardening, the fatigue resistance, and the water susceptibility of the mixture, and thus they are two relevant factors to be considered in the final analysis of asphalt durability, correlation, and critical asphalt property values.

Bulk specific gravity (d) is determined by the water displacement method at 77 °F (25 °C). Percentage of voids (V) is calculated from bulk specific gravity and maximum theoretical specific gravity (D) data. The latter is determined following Rice's method, which is essentially that described in the ASTM D2041-64T. Values of bulk specific gravity, maximum specific gravity, and percentage of voids for both specimens in wheel tracks (WT) and between wheel tracks (BWT) up to 48 months are tabulated in Table 31. Data of bulk specific gravity represent averages of 4 to 6 specimens and those of maximum specific gravity were results of duplicate determinations. Changes in void contents were plotted in Figs. 25a and 25b, and changes in density were plotted in Figs. 26a and 26b. When the trends are examined and compared with designed mix data supplied by the Iowa State Highway Commission (Table 2), the following observations can be made:

- There were no appreciable initial differences on density-voids values between specimens in wheel tracks and specimens between wheel tracks.

Table 31. Density-voids changes of pavements.

Series		Time, months																	
		0		6		12		18		24		30		36		42		48	
		WT	BWT	WT	BWT	WT	BWT	WT	BWT	WT	BWT	WT	BWT	WT	BWT	WT	BWT	WT	BWT
1	d[*]		2.220	2.240	–	2.294	2.288	2.303	2.313	2.324	2.299	2.310	2.312	2.312	2.306	2.306	2.301	2.315	2.303
	D[†]		2.430	2.363	–	2.350	2.356	2.385	2.392	2.390	2.390	2.358	2.382	2.400	2.389	2.379	2.379	2.384	2.384
	V		8.64	4.94	–	2.38	2.89	3.44	3.30	2.76	3.81	2.04	2.94	3.66	3.47	3.07	3.28	3.89	3.40
2	d		2.144	2.146	2.152	2.170	2.171	2.188	2.178	2.198	2.202	2.162	2.205	2.204	2.169	2.198	2.159	2.206	2.195
	D		2.376	2.383	2.383	2.405	2.405	2.405	2.405	2.429	2.438	2.409	2.409	2.438	2.427	2.414	2.414	2.446	2.431
	V		9.76	9.95	9.69	9.77	9.73	9.03	9.44	9.50	9.68	10.25	9.31	9.60	10.63	8.95	10.56	9.81	9.71
3	d		2.151	2.178	2.154	2.209	2.195	2.184	2.181	2.204	2.197	2.207	2.191	2.211	2.190	2.203	2.194	2.207	2.190
	D		2.433	2.417	2.417	2.406	2.397	2.402	2.402	2.417	2.395	2.377	2.386	2.393	2.411	2.400	2.400	2.405	2.409
	V		11.59	9.89	10.88	8.19	8.45	9.08	9.20	8.82	8.28	7.15	8.17	7.60	9.17	8.21	8.58	8.23	9.09
4	d		2.108	2.110	2.098	2.132	2.156	2.176	2.176	2.197	2.182	2.154	2.175	2.168	2.184	2.161	2.148	2.176	2.168
	D		2.404	2.377	2.377	2.397	2.362	2.384	2.384	2.408	2.403	2.379	2.386	2.403	2.396	2.392	2.392	2.391	2.391
	V		12.30	11.23	11.76	11.06	8.72	8.72	8.72	8.76	9.20	9.46	8.84	9.77	8.84	9.66	10.20	8.99	9.33
6	d		2.309	2.373	2.325	2.377	2.333	2.381	2.331	2.397	2.340	2.376	2.333	2.376	2.326	2.385	2.356	–	–
	D		2.443	2.487	2.464	2.461	2.461	2.474	2.479	2.463	2.468	2.489	2.477	2.480	2.480	2.481	2.481	–	–
	V		5.49	4.58	5.46	3.41	5.20	4.16	5.92	5.11	5.18	4.53	5.81	4.19	6.21	3.87	5.04	–	–
7	d		2.114	2.241	2.238	2.260	2.249	2.263	2.222	2.251	2.253	2.259	2.251	2.250	2.258	2.249	2.251	–	–
	D		2.274	2.382	2.381	2.406	2.406	2.381	2.369	2.388	2.381	2.413	2.393	2.416	2.416	2.416	2.416	–	–
	V		7.04	5.92	6.00	6.07	6.50	4.96	6.31	5.73	5.38	6.38	5.93	6.87	6.54	6.91	6.81	–	–
8	d		2.214	2.231	2.294	2.292	2.260	2.272	2.282	2.306	2.289	2.287	2.320	2.303	2.290	2.295	2.296	–	–
	D		2.373	2.394	2.394	2.426	2.426	2.439	2.408	2.399	2,430	2.441	2.439	2.447	2.447	2.443	2.443	–	–
	V		6.70	6.77	4.18	5.52	6.84	6.85	5.23	3.88	5.80	6.31	4.88	5.88	6.42	6.06	6.02	–	–
9	d		2.303	2.356	2.337	2.350	2.363	2.326	2.318	2.360	2.326	2.326	2.316	2.335	2.319	2.374	2.336	–	–
	D		2.425	2.448	2.433	2.436	2.436	2.425	2.434	2.438	2.427	2.436	2.440	2.441	2.441	2.427	2.434	–	–
	V		5.03	3.76	3.95	3.53	3.00	4.53	4.77	4.07	4.20	4.52	5.08	4.34	5.00	2.18	3.24	–	–

[*] d = bulk specific gravity 77/77 °F.

[†] D = maximum theoretical specific gravity.

[‡] V = percent of air voids, $V = \frac{D - d}{D} \times 100$.

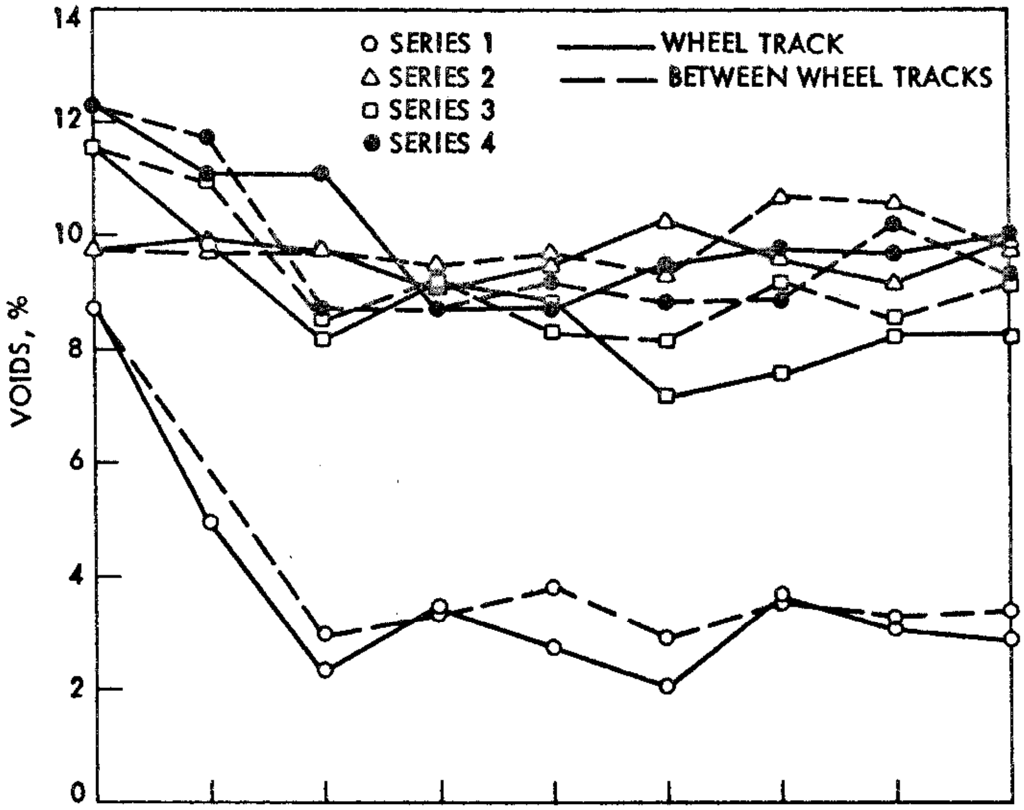

Fig. 25a. Pavement voids vs time, series No. 1 through 4.

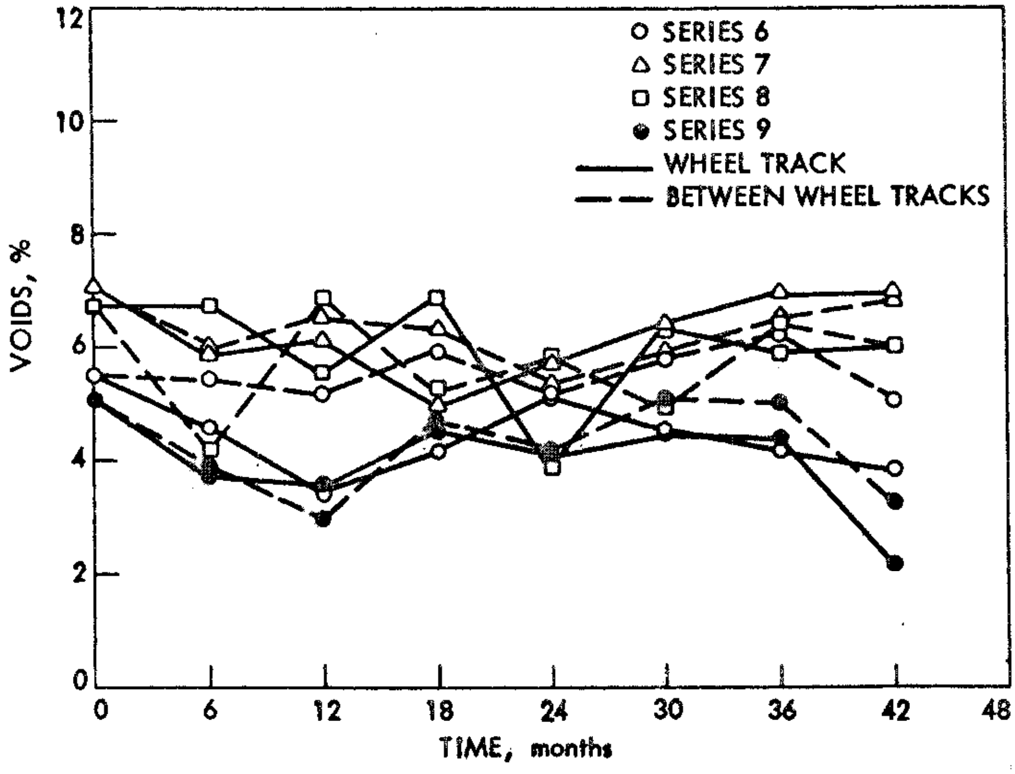

Fig. 25b. Pavement voids vs time, series No. 6 through 9.

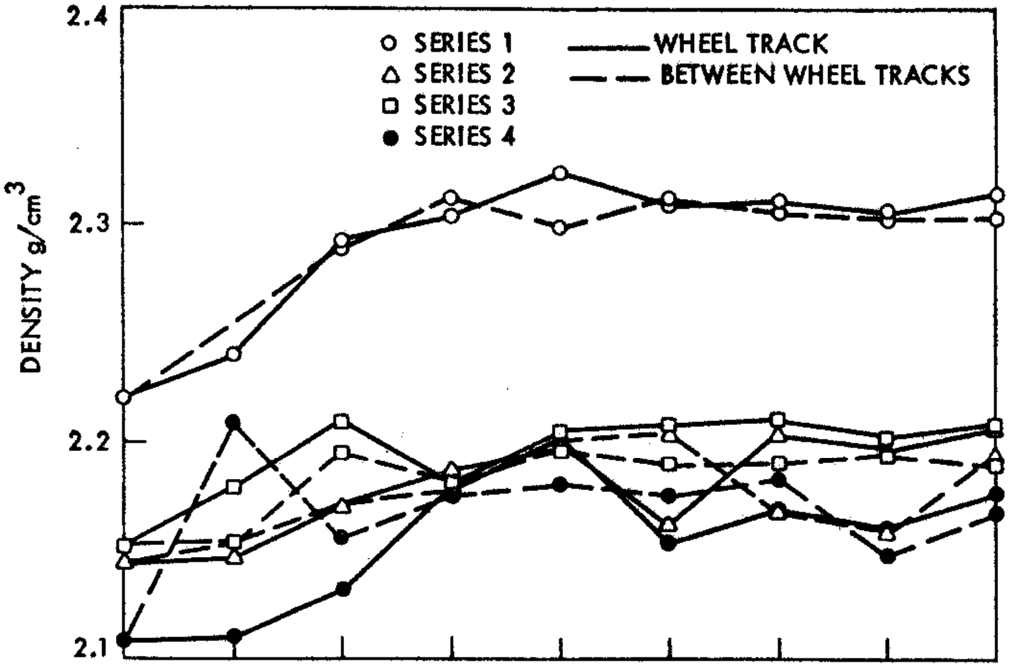

Fig. 26a. Pavement density vs time, series No. 1 through 4.

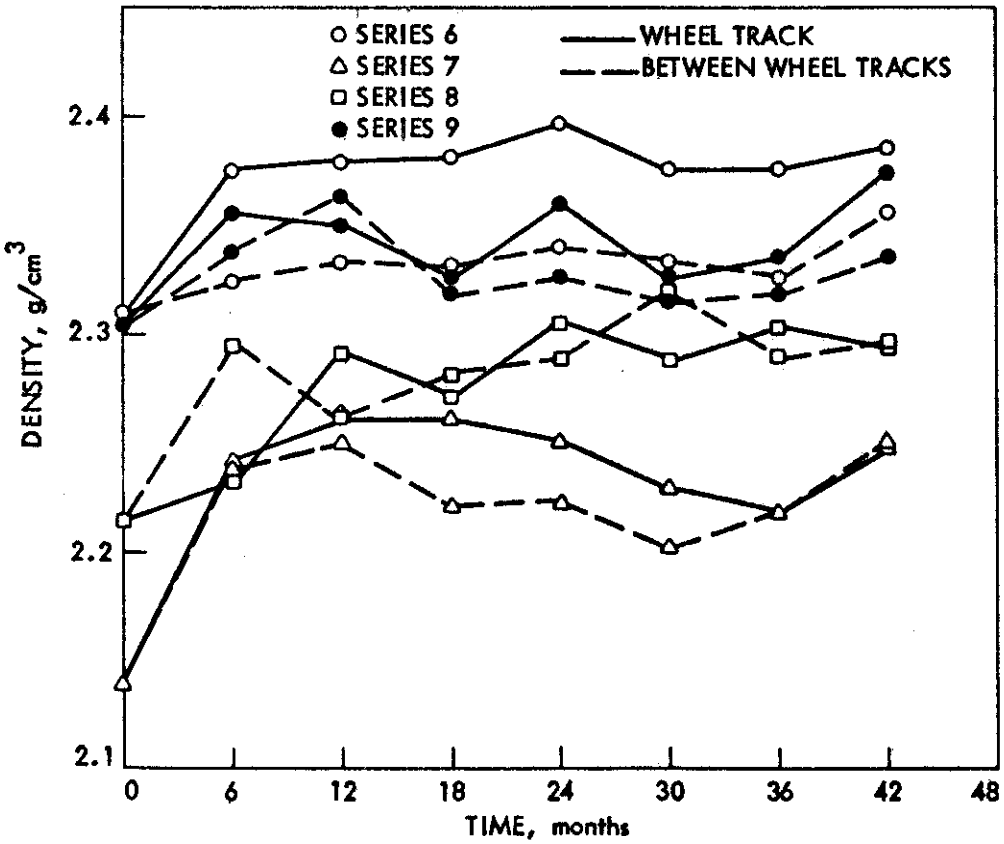

Fig. 26b. Pavement density vs time, series No. 6 through 9.

- None of the eight pavements reached, as built, densities of the designed Marshall densities. After 42 to 48 months of traffic compaction, only two of these pavements have reached design densities. Pavement No. 1 (Chickasaw) reached design density and voids after one year of road service; pavement No. 6 (Monona) reached design density and voids after 6 months of pavement service. Based on voids criteria only, pavement No. 7 (Keokuk) reached designed voids content after 6 months of traffic compaction and pavement No. 9 (Jackson) reached designed voids content during pavement construction.
- Pavements constructed during the second period (Projects 6-9) of warmer weather approached higher density and lower voids relative to design density and voids than those built during the first period (Projects 1-4).
- Half of the projects reached design density and voids at the end of one year or after one summer of traffic densification.
- Changes of density and voids appeared to have leveled off after one year of traffic compaction.
- Due to the inherent problems in sampling, the inexactness of density determinations and the sensitive dependence of voids on density, trends of density and voids with respect to time lack desired consistency; however, it can be stated that, after traffic, the areas in wheel tracks displayed greater densification than areas between wheel tracks.

Behavior of Asphalts in the Pavements

Eight asphalt cements and paving projects using these asphalts were selected by the Iowa Highway Commission engineers. The project location and mix type were carefully selected to represent different weathering conditions throughout Iowa and different types of mixes used in Iowa. Times of pavement construction were also well distributed from October 1967 to July 1968.

Physical and chemical changes in asphalts in pavements were determined for 42 months on 4 projects and for 48 months on the other 4 projects. The general changes of physical and chemical properties of recovered asphalts with field ageing time were found to follow the time-rate-of-change curves established in laboratory ageing during IDT.

Physical Properties

All physical properties (especially rheological) that appeared to be suited to evaluate asphalt durability and that have been conducted on original and laboratory aged asphalt were also determined on recovered asphalts from plant (p) to just compacted (f0) and up to 48 months at 6-month intervals.

Changes in Properties during Mixing Within the range of mixing temperatures of 290 to 310 °F that were recorded at the plants for the eight paving projects, no appreciable differences were detected in the hardening of asphalt as determined by increase in penetration ratio (Table 14). The comparison between results of the TFOT (d) and the hardening during mixing (p and f0) in terms of penetration, penetration ratio, viscosity at 77 °F and 140 °F, ageing index (viscosity ratio) at these two temperatures, and softening point showed slightly higher overall hardening in TFOT than in plant mixing for various asphalts used in this project. However, the close parallel between results of these two processes has reconfirmed the ability of the TFOT in simulating hardening of asphalt in an average hot mixing plant.

Changes in Properties during Pavement Service Life The change in penetration, softening point, viscosity at 77 °F and at 140 °F, microductility at 77 °F, Fraass brittle point, and dynamic modulus by sonic method for 42 to 48 months of service life are given in Tables 5, 6, 7, 9, 10, 19 and 20. The curves showing drop in penetration, Figs. 7a through 7i, have the normally expected shapes of hyperbolic function of time, with a rather rapid rate of hardening in the first 20 months and a tendency for the rate of hardening to decrease thereafter. Hyperbolic curve fittings were made on all recovered asphalts (both in and between wheel tracks) for all properties between property change (ΔY) and time (T) by linear least square regression analysis between $T/\Delta Y$ and T. The resulting time-property change curves were all indicated by dotted line curves with equations shown in terms of $\Delta Y = T/a + bT$. Also shown with the fitted curves is the correlation coefficient (R). Tabulations of constant a, b, and R values for all properties and all asphalts are given in Table 11. Calculated and given in Table 11 are limiting maximum or change values 1/b, which may be used as one of the basic criteria for asphalt durability, since the asphalt having higher limiting change 1/b would be a potentially harder asphalt and vice versa. This is illustrated in Figs. 12a and 12b. Of two asphalts with identical initial properties, the one with the larger ($b_2 > b_1$) would be expected to have smaller ultimate change ($1/b_2 < 1/b_1$) and thus would be a more hardening resistant and durable asphalt.

The increase in softening point with field service time of the eight asphalts are shown in Figs. 10a through 10i. The viscosity at 77 °F and the 5×10^{-2} $\sec^{-1}$ increase with time also followed a hyperbolic function, as shown in Figs. 8a through 8i. The effects of field ageing on complex flow c and on shear susceptibility s are given in Table 8. Typical plots of log viscosity vs log rate of shear and log shearing stress vs log rate of shear with corresponding c and s values are shown in Fig. 14a for field aged asphalt No. 1. The general trends of decreasing c and increasing s with field service life can be observed. A hyperbolic increase of viscosity at 140 °F with field ageing time are shown in Figs. 9a through 9i (Table 7).

The microductility change with field ageing time was less consistent, possibly due to the complex properties which the ductility test measures and to the existence of an optimum consistency for ductility. For four of the eight asphalts (1, 3, 4, and 7), the ductility at 77 °F remained high or increased up to 30 months, and could not be fitted with hyperbolic curves. Other asphalts (2 and 9) showed a definite decrease in ductility after 20 months. Only two asphalts (7 and 8) showed a marked decrease in ductility from the beginning of field ageing and could be fitted with hyperbolic curves.

Results of the Fraass brittle point testing of recovered field aged asphalts are given in Table 19 and are shown in Figs. 18a through 18d. There is a general parallel between field and laboratory ageing, with increased brittle point (becoming brittle at increasingly higher temperatures) with ageing time. Within a limited field service time of 42 to 48 months, no drop in brittle point was indicated as in laboratory ageing of asphalts 4, 6, and 8.

Changes of the sonic modulus (E_s) with field ageing time are given in Table 20. A general increase in E_s with time was observed for asphalts 2, 3, 4, 6, 8, and 9. No trends could be noted for asphalts 1 and 7 due to difficulties in determining the sonic modulus at a constant transducer penetration depth. Effects of field ageing on softening points as determined by TMA and DSC on asphalt 1 are shown in Fig. 20b and 20d. No conclusions are drawn from these data at the present time. However, the potentials of these two tests in evaluating brittle and elastic properties of asphalts cannot be overlooked.

Chemical Properties

Changes in the percentage of asphaltenes, as determined by the Skelly F precipitation test, with time of field service of recovered asphalts are given in Table 22, and are shown in Figs. 21a through 21i. An increase in asphaltene content with ageing or hardening is apparent. Although curve fittings were not as good as were those for rheological data, hyperbolic relations between an increase in asphaltenes and the time of field ageing can be established.

Chemical analysis by the Rostler and White method was made on recovered field aged asphalts 1 to 4 (Table 23). The ratios of reactive to nonreactive components, $(N + A_1)/(A_2 + P)$, were calculated and reported in Table 25. The changes of the five fractions with ageing followed the general patterns found for laboratory aged asphalts. However, no consistent trends could be found for the two so-called quality parameters: $(N + A_1)/(A_2 + P)$ and N/P.

Results of spot tests of recovered field samples are presented in Table 29. Except for asphalts 8 and 9, all the other asphalts showed positive after 12 months service.

Effects of field ageing as characterized by IR spectroscopy are discussed, together with laboratory aged asphalts, in the next section.

Weathering of Asphalts as Characterized by Infrared Multiple Internal Reflection Technique Theory

Theory

Unlike the conventional transmission IR technique where application is limited due to sample handling and other complexity, the IR multiple internal reflection technique has recently established itself as a useful analytical tool. Its applications include not only in the usual spectropical properties, but also the precision measurement and construction of optical structures.

Because of the previously stated difficulties and limitations in transmission IR techniques (either asphalt in solution or in thin films), the IR multiple internal reflection technique was adopted in this investigation. In this technique the absorption is controlled by the number of total reflections, and variations due to sample preparation can be eliminated.

According to definition, internal reflection spectroscopy is a technique of recording the optical spectrum of a sample material that is in contact with an optically denser-but-transparent medium and of then measuring the wavelength dependence of the reflectivity of this interface by introducing light into the denser medium. Radiation from within the sample at angles exceeding the critical angle at the surface will be totally reflected within this material, provided that the frequency of the radiation does not correspond to an absorption frequency of the material. When it does, radiation will be absorbed and a spectrum closely resembling a normal transmission spectrum of the sample material will be obtained (Fig. 27).

For the detailed study of the principles of internal reflection spectroscopy the reader should consult the extensive literature on this subject[97,98].

Sample Preparation

The Thalium-Bromine-Iodine Internal Reflectance crystal (KRS-5) was first cleaned and rinsed thoroughly with benzene, and then placed in a vacuum oven at 95 °C and at a vacuum of 27.5 in. of Hg for 15 min to remove all traces of benzene. The clean crystal was then placed under an infrared heat lamp. The sample was heated under this heat lamp to about 100 °C and was then brushed on one side of the crystal carefully so that none of the sample got over the edges. The crystal was then cooled to room temperature and a piece of wax paper and a rubber the size of the plate were placed over the asphalt to prevent sticking to the MIR attachment. The wax paper must not come in contact with the surface of the crystal, as it will cause a paraffin spectrum. The hot sample was then brushed on the opposite side

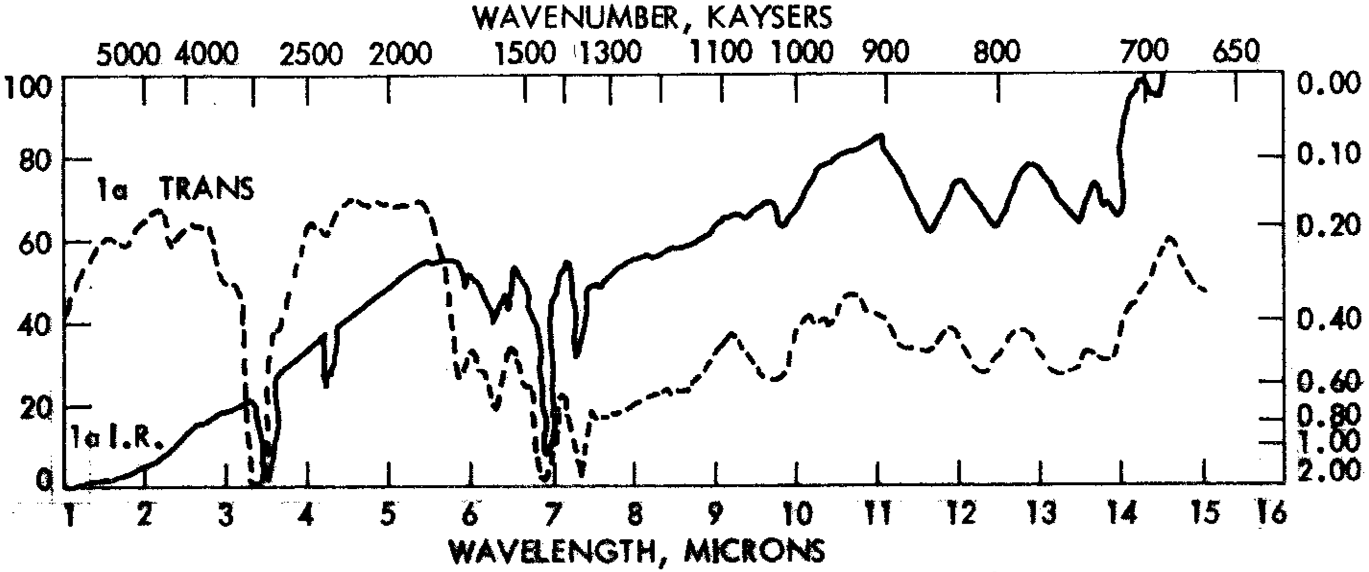

Sample No. 1a
Treatment TRANS + IR
Run No. 1
Spectrum No. 1028 (IR) 1a (TRANS)
Project HR-124
Date 6/8/71, 5/21/70
Operator P.M., K.O.

Transmission X

Crystal NaCl
Path 45 μ mm
Reference
Solvent

Reflectance FMIR X
ATR

Crystal NaCl
Face Angle
Sample Preparation

SPEED 0.5, 1 μ/min SCALE in./μ
GAIN 46.0, 31.3
PERIOD 2 SLIT SCHED 2, 1-1/2
ORDINATE SCALE SB DB X

Fig. 27. IR transmission vs reflection scans, A.C. No. 1.

of the plate, cooled, and the wax paper was affixed. For identification purposes the sample number was scratched onto the wax paper. The sample was then placed in the MIR attachment and aligned to obtain the highest intensity possible. A double beam spectrum from 15 to 1 μ was therefore obtained, coupled with an attenuator for adjusting the reference beam radiation.

The base-line method was employed in spectra analysis. In all cases the base line drawn was chosen on the basis of the relative reproducibility of the point or points, from which the base line is constructed, from among the spectra being compared (Fig. 28a). This method is illustrated in Fig. 28b. It is the reflectivity of the base line while I_p is the reflectivity of the band peak. The absorbance of this band will be $\Delta A = \log 1/I_p - \log 1/I_o$.

Results and Discussions

The IR scans were run on both laboratory and field aged samples for A.C. No. 1 to 4. Although analyses were made on double beam spectra, single beam scans were also made. Figure 27 shows the comparison of transmission and MIR spectra in the 15 to 1 μ region for sample 1a. Figure 29a shows the effects of laboratory IDT ageing on MIR spectra. Figure 29b shows the effects of field ageing of up to 48 months on the same asphalt. Differences in MIR spectra between original asphalts 1 to 4 are shown in Fig. 29c, and similar IR spectra comparison is shown in Fig. 29d for 48-month, field aged asphalts.

The infrared spectra were obtained on linear reflectance-linear wavelength chart paper. The corrected values for the carbonyl band

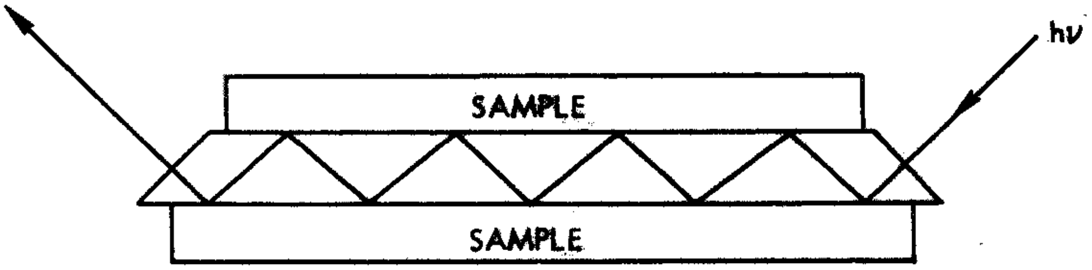

Fig. 28a. MIR diagram.

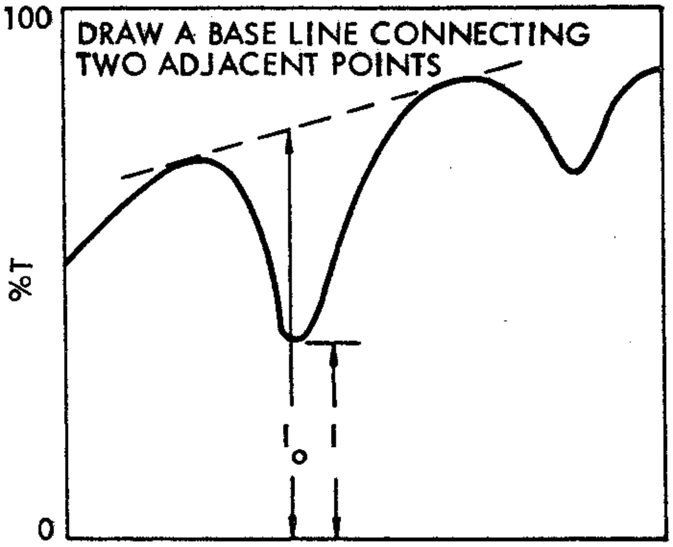

Fig. 28b. Base line method.

(5.88 μ), as well as for the other structural groups, were determined by using the base-line method. The carbonyl index is defined as the difference in the absorbance of the carbonyl band of the weathered and unweathered film of asphalt.

The absorbance changes of all peaks obtained on A.C. No. 1 to 4 are presented in Table 32. Only one value for each asphalt treatment (96-hr lab and 48-month field) was chosen for comparison purposes.

The infrared spectra of asphalts obtained from multiple internal reflection techniques for four different sources showed a marked similarity in their absorption characteristics. All the asphalts had absorption bands at the same or very nearly the same wavelengths

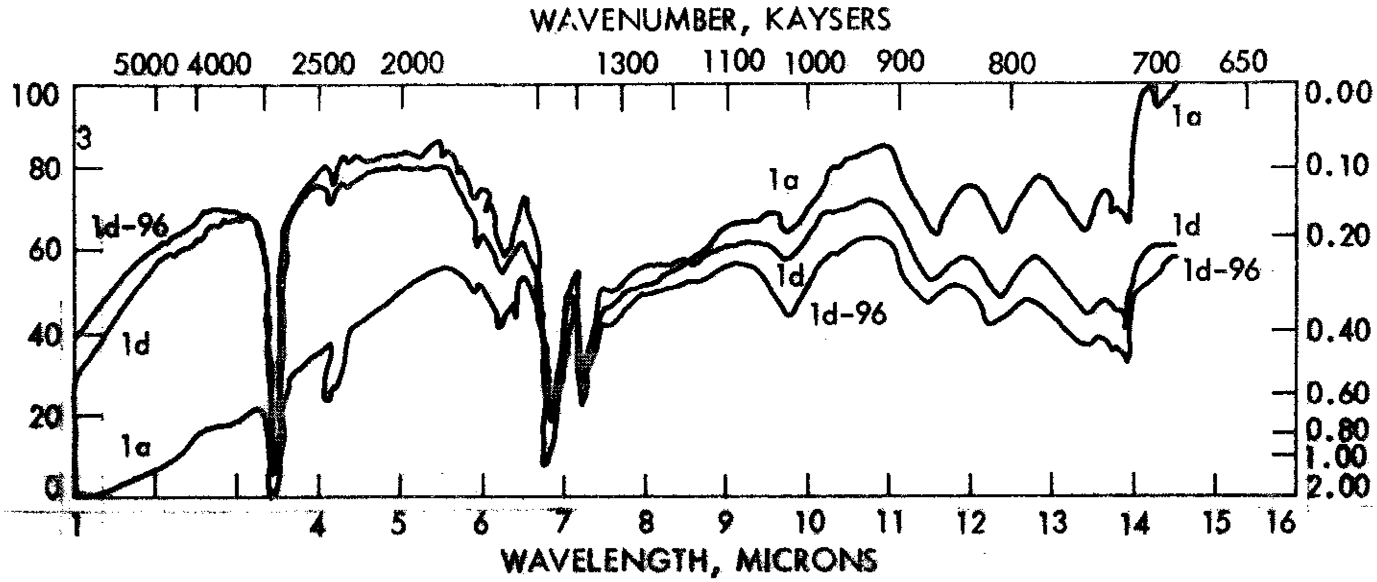

Sample No. 1a, 1d, 1d96
Treatment
Run No.
Spectrum No. 1028, 1051, 1048
Project HR-124
Date 6/8/71, 6/16/71, 6/15/71
Operator P.M., P.M., P.M.

Transmission
Crystal
Path mm
Reference
Solvent

Reflectance FMIR X
ATR
Crystal NaCl
Face Angle
Sample Preparation

SPEED 0.5 in./sec SCALE 2 in./μ
GAIN 46.0, 27.5, 25.0
PERIOD 2 SLIT SCHED 2/1
ORDINATE SCALE SB DB X

Fig. 29a. IR spectra of laboratory aged asphalt, A.C. No. 1.

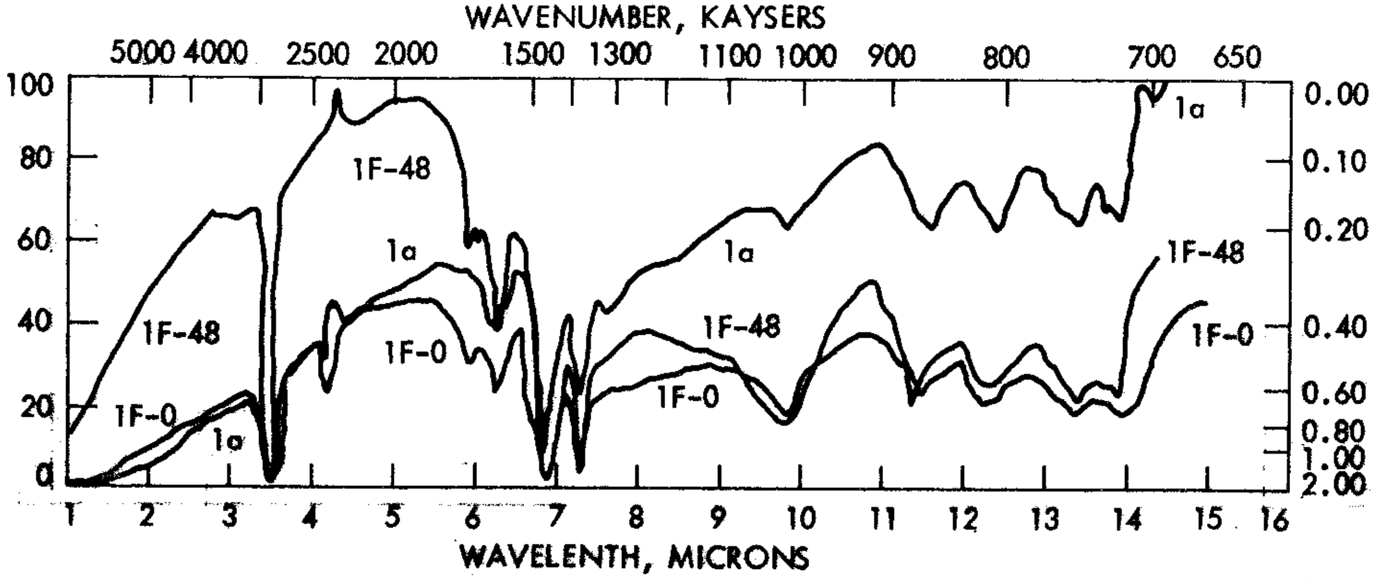

Sample No. 1a, 1F, 1F 48

Treatment

Run No.

Spectrum No. 1028, 1007, 1190

Project HR-124

Date 6/8/71, 5/12/71, 12/12/71

Operator

P.M., P.M., L.V.

Transmission

Crystal

Path mm

Reference

Solvent

Reflectance FMIR X

ATR

Crystal NaCl

Face Angle

Sample Preparation

SPEED 0.5, 0.5, 1.0 in./sec SCALE 2 in./μ

GAIN 46.0, 54.5, 33.0

PERIOD 2 SLIT SCHED 2/1

ORDINATE SCALE SB DB X

Fig. 29b. IR spectra of field aged asphalt, A.C. No. 1.

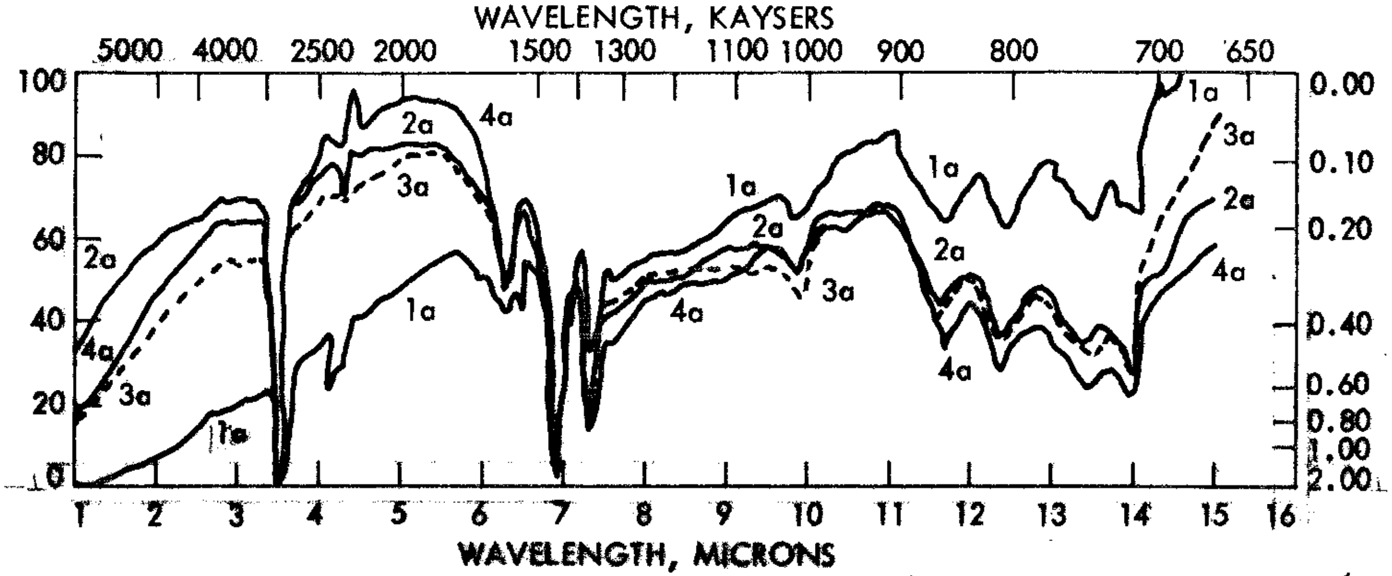

Sample No. 1a, 2a, 3a, 4a

Treatment ______

Run No. ______

Spectrum No. 1028, 1052, 1090, 1177

Project HR-124

Date 6/8/71, 6/16/71, 6/30/71, 11/17/71

Operator P.M., P.M., P.M., L.V. & R.P.

Transmission ______

Crystal ______

Path ______ mm

Reference ______

Solvent ______

Reflectance FMIR X ATR ______

Crystal NaCl

Face Angle ______

Sample Preparation ______

SPEED (0.5, 0.5, 0.5, 1.0) in./sec SCALE 2 in./μ

GAIN 46.0, 25.0, 32.0, 30.0

PERIOD 2 SLIT SCHED 2/1

ORDINATE SCALE ______ SB ______ DB X

Fig. 29c. IR spectra of original asphalts, A.C. No. 1 to 4.

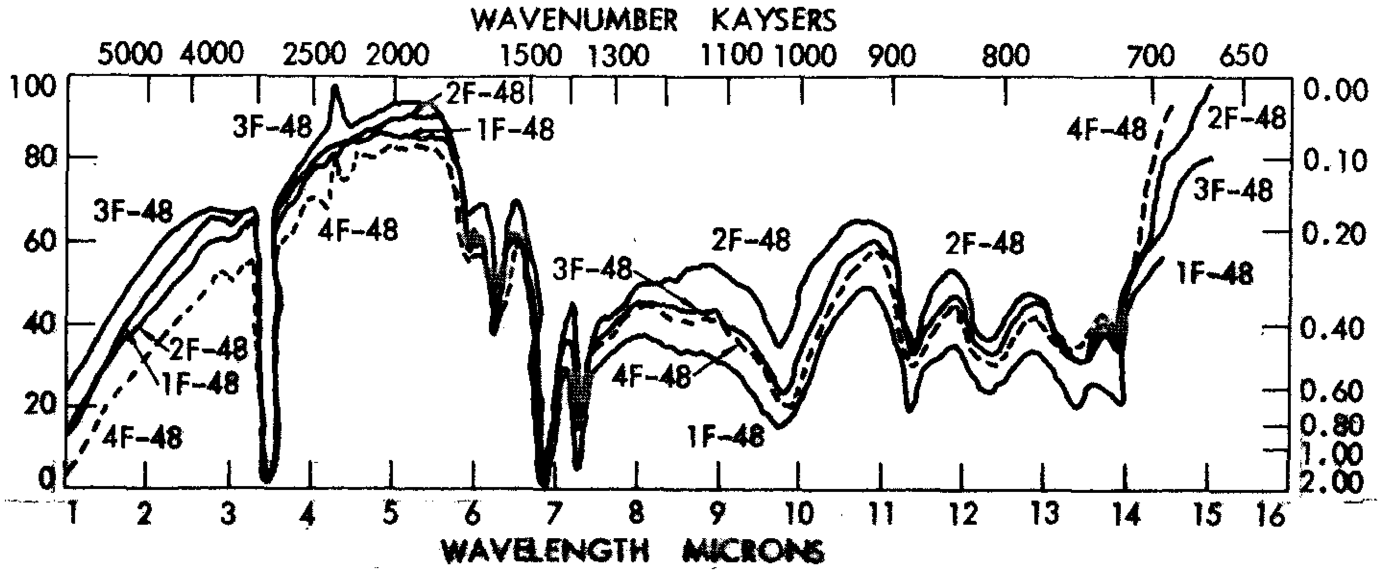

Sample No. 1f48, 2f48,

Treatment 3f48, 4f48

Run No.

Spectrum No. 1190, 1192,

Project HR-124 1194, 1198

Date 12/12/71, 12/11/71,

Operator 12/11/71, 12/12/71

L.V., L.V., L.V., L.V.

Transmission

Crystal

Path mm

Reference

Solvent

Reflectance FMIR X

ATR

Crystal NaCl

Face Angle

Sample Preparation

SPEED 1 in./sec SCALE 2 in./μ

GAIN 33.0, 33.0, 33.0, 35.0

PERIOD 2 SLIT SCHED 2/1

ORDINATE SCALE SB DB X

Fig. 29d. IR spectra of field aged asphalts, A.C. No. 1 to 4.

Table 32. Comparison among the asphalts through changes in IR absorbance due to weathering.

$\bar{\nu}$, cm^{-1}	2924	2370	1700	1600	1466	1380	1030	866	811	750	720
λ, μ	3.42	4.22	5.88	6.25	6.82	7.25	9.71	11.55	12.33	13.33	13.89
Assigned structure groups	Aliphatic carbonate -hydrogen	NC=O	C=O	Aromatic	-C-H$_2$- C-CH$_3$	C-CH$_3$	C-O S=O, or S$_i$O	Aromatic substitution			-(CH$_2$)$_4$-
A.C. No.	Absorbance change										
1 a	–	0.213	0.060	0.119	0.979	0.340	0.048	0.117	0.115	0.139	0.165
d96	1.357	0.036	0.092	0.143	0.605	0.313	0.123	0.105	0.111	0.143	0.192
f48	1.855	0.149	0.149	1.664	0.793	0.466	0.338	0.189	0.309	0.301	–
2 a	–	0.048	0.036	0.144	1.355	0.437	0.060	0.144	0.147	0.206	0.272
d96	–	0.033	0.136	0.211	1.222	0.448	0.157	0.146	0.144	0.199	0.270
f48	–	0.000	0.120	0.122	1.768	0.574	0.224	0.233	0.134	0.105	0.145
3 a	–	0.027	–	0.174	1.273	0.401	0.106	0.151	0.156	0.211	0.269
d96	1.789	0.045	0.093	0.192	1.228	0.419	0.199	0.138	0.156	0.144	0.228
f48	1.875	0.033	0.110	0.194	1.349	0.550	0.366	0.284	0.173	0.178	0.238
4 a	–	–	–	0.343	1.444	0.490	0.075	0.208	0.201	0.301	0.329
d96	1.820	–	0.110	0.343	1.550	0.825	0.466	0.291	0.296	0.403	0.519
f48	–	–	0.116	0.209	1.668	0.418	0.407	0.215	0.183	0.252	0.274

and their spectra differed primarily in the reflectance values of some of these bands.

The structural groups which appeared to be present in all the asphalts are hydroxyl, $-CH_2-$, $C-CH_3$, carbonyl, $-(CH_2)_6-$ and aromatic rings. There were also absorption bands which indicated aromatic substituents or fused rings.

The two band intensities at 5.88 and 9.71 μ seem to show distinct relationships to weatherability. Absorbances in the region of 5.88 μ (1700 cm^{-1}) due to the carbonyl functional group is attributed primarily to the presence of aldehydes, ketones, and acids, with no contribution from anhydrides and little or no contribution from esters, based on infrared and colorimetric analyses. Changes in carbonyl absorbance of all samples studies are given in Table 33. Figure 30 shows that a hypobolic relationship may exist between carbonyl inolex and weathering time. When carbonyl indices were plotted against the asphaltene content (Fig. 31) linear relationships were indicated. Therefore carbonyl indices may be used as a chemical indicator of asphalt weatherability.

An increase of the 9.71 μ (1030 cm^{-1}) absorbance peak was also observed in all weathered asphalts. Stewart[74] observed this absorbance peak in aged and unaged asphalt specimens and considered -C-O, S=O, or SiO as the most likely groups to be responsible for this absorbance. Smith et al.[99] attributed the absorbance increase in this region to an increase in asphaltene content. However, this was not true in our case. The increase in the 9.71 μ absorbance peak was not consistent. When a peak ratio of ΔA 9.71 μ/ΔA 6.25 vs time was plotted (Fig. 32),

Table 33. Changes in carbonyl index of asphalts due to weathering.

A.C. No.	1	2	3	4
Original	0.060	0.036	0.042	–
TFOT	0.045	0.068	0.045	0.030
Lab ageing				
24 hr	0.076[†]	0.090	0.060	0.051
48 hr	0.079	0.122	0.069	0.096[†]
96 hr	0.092	0.136	0.093	0.110[†]
240 hr	0.117	0.163	0.127	0.140[†]
480 hr	–	0.192	–	–
1000 hr	0.197	–	0.178[†]	0.232
Field ageing[*]				
Plant	0.118	0.089	0.067	0.081
0 month	0.145	0.099	0.101	0.060
6 months	0.087	0.084	0.063	0.107
12 months	0.103	0.098	0.088	0.129
18 months	0.074	0.107	0.064	0.081
24 months	0.098	0.88	0.095	0.110
30 months	0.129	0.119	0.089	0.153
36 months	0.109	0.107	0.093	0.067
42 months	–	0.096	0.130	0.084
48 months	0.149	0.120	0.110	0.116

[*] All samples are in the wheel track.

[†] Ratio adjusted to other peak bases.

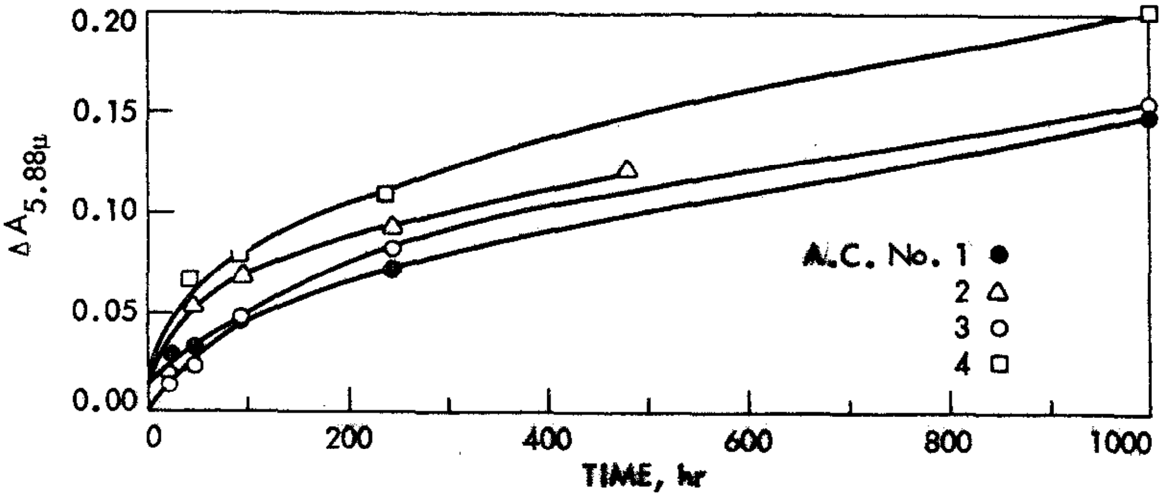

Fig. 30. Carbonyl index vs time of lab ageing.

an inverse relationship was clearly indicated. It seems that C-O and C=O linkages in the asphalt structure may have changed due to weathering.

Linear relations were found between the ageing index at 77 °F and the carbonyl index at 5.88 μ, and between the viscosity at 77 °F and the carbonyl index at 5.88 μ. Figures 33a and 33b show plots of $\Delta A_{5.88}$ vs ageing index at 77 °F for both laboratory and field aged samples. Figures 34a and 34b show similar relations for $\Delta A_{5.88}$ and viscosity at 77 °F. In both cases, the laboratory samples showed better correlations.

Conclusions

Shifts among the characteristic peaks showed some correlation with weatherability. In general, the more weatherable asphalt exhibited stronger hydroxyl absorption than the less weatherable asphalts. The same held for carbonyl index. The weatherability of the asphalts showed inverse relationship with changes in absorption at 9.71 μ. The correlation of weatherability with changes in carbonyl and hydroxyl absorption and also with changes in values of absorbance at 9.71 μ suggest that the changes at these wavelengths may have been caused by changes in concentration of C-O and C=O linkages. There is a strong possibility that the IR spectra of asphalt, and especially changes in these characteristic peaks, can be used to characterize and evaluate the weathering or durability of paving asphalts.

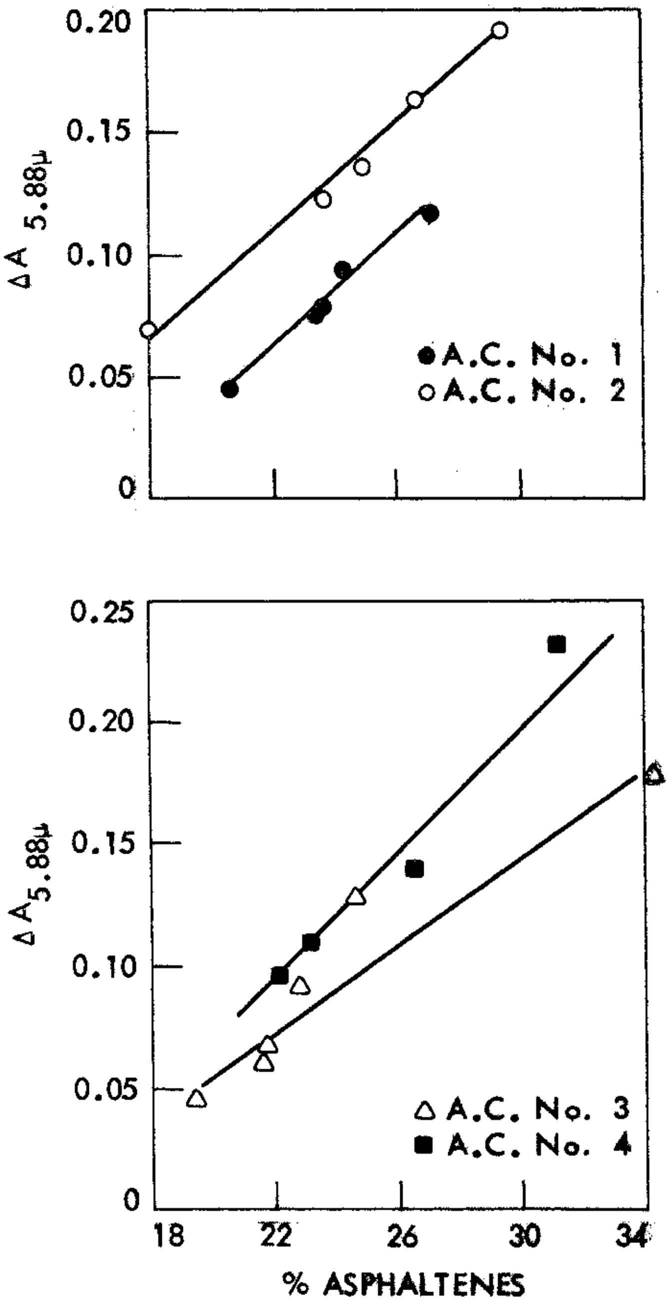

Fig. 31. Carbonyl index vs asphaltene content.

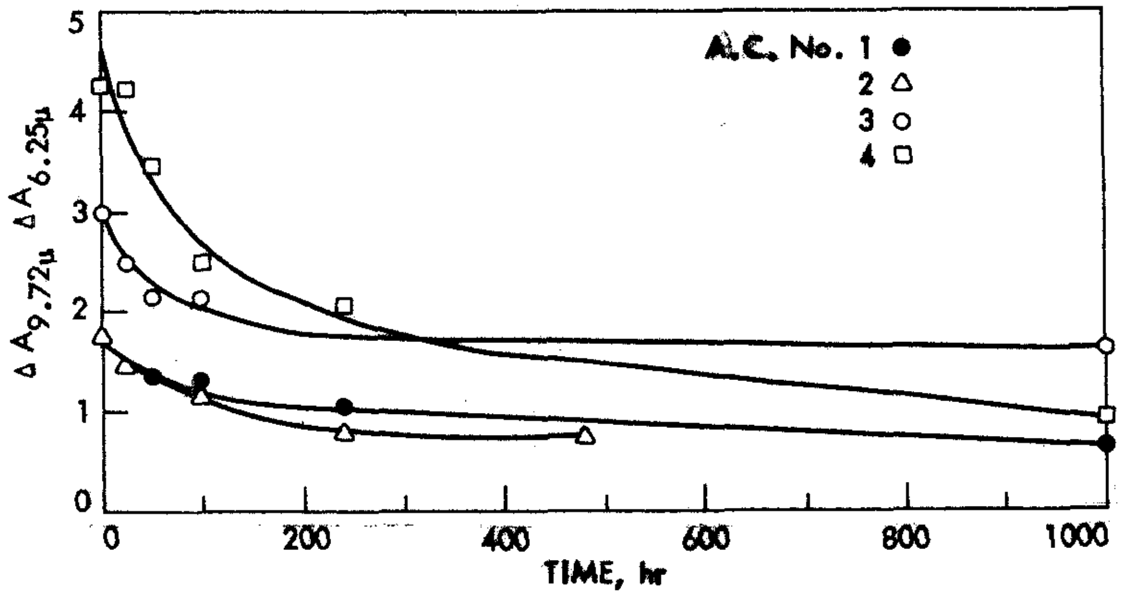

Fig. 32. Peak ratio ΔA9-72 μ/ΔA6.25 μ vs lab ageing time.

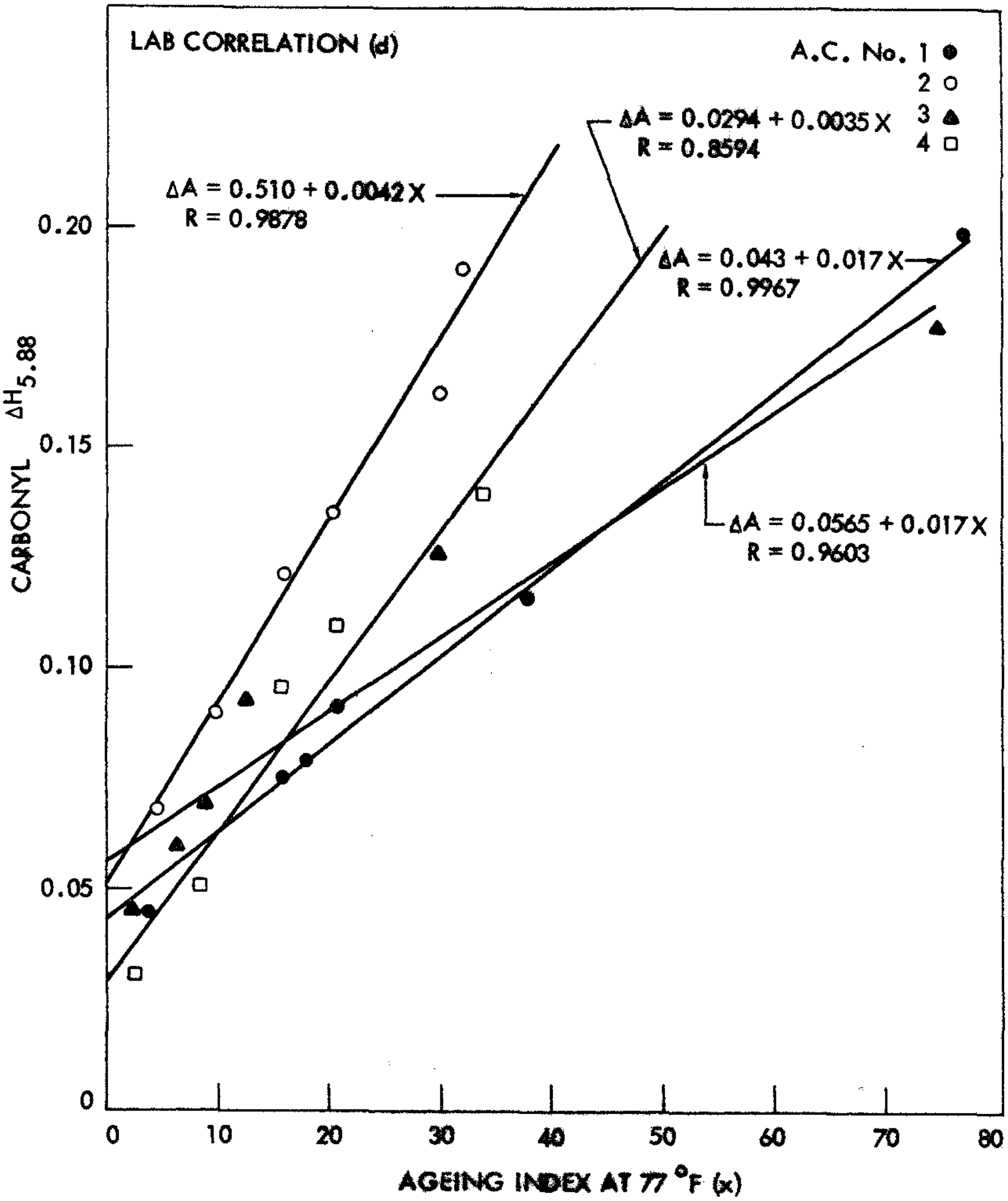

Fig. 33a. Carbonyl index vs ageing index.

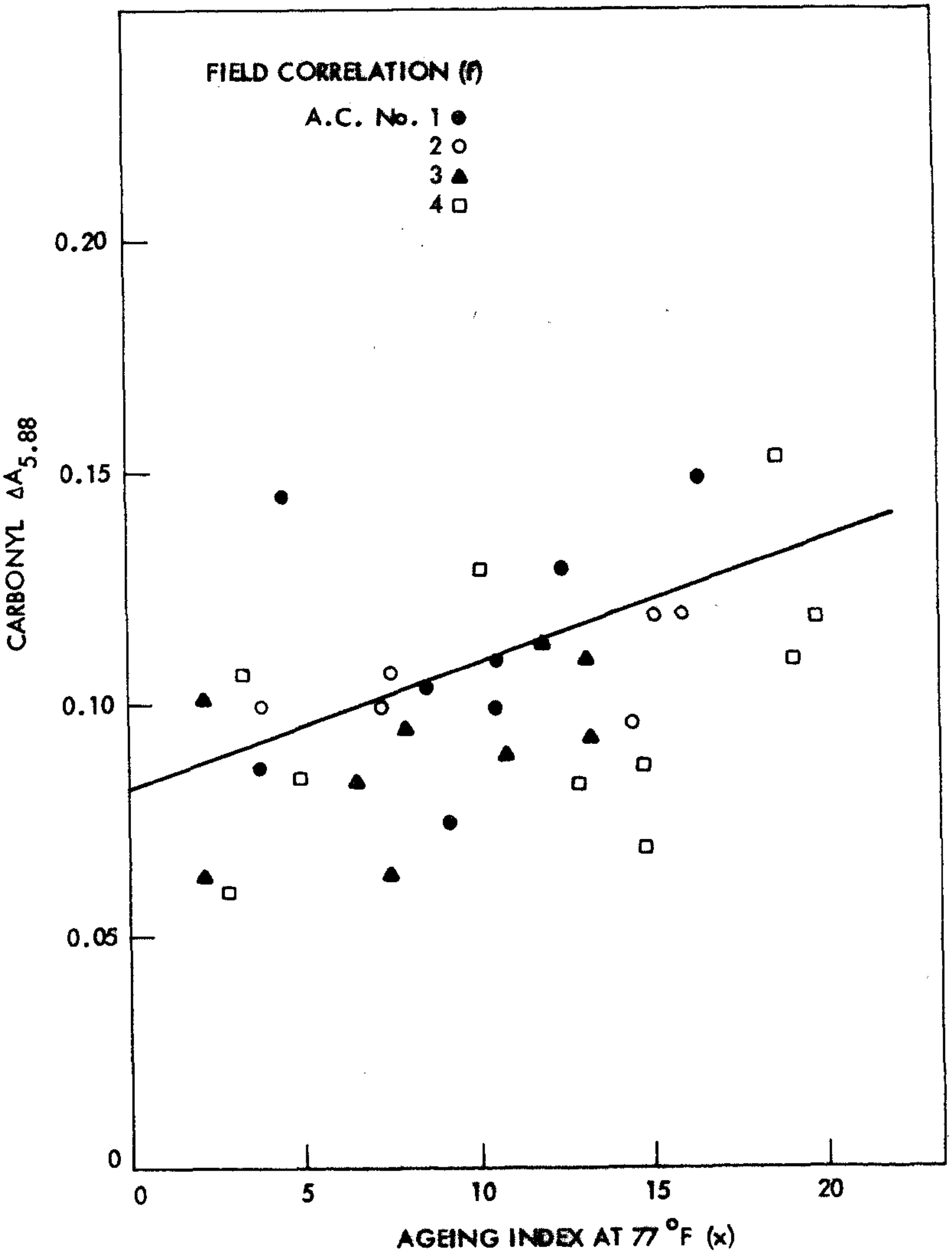

Fig. 33b. Carbonyl index vs ageing index.

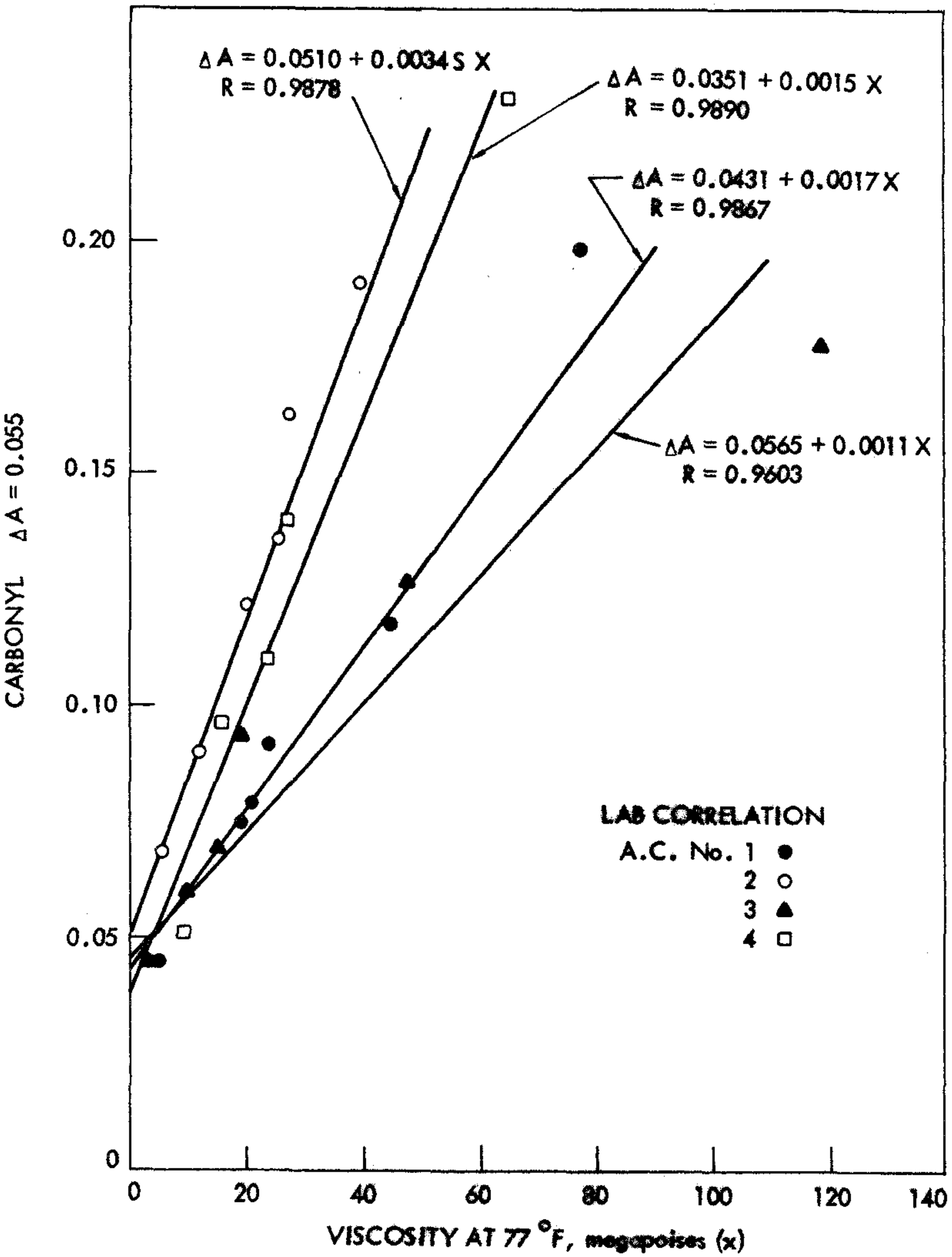

Fig. 34a. Changes in viscosity at 77 °F.

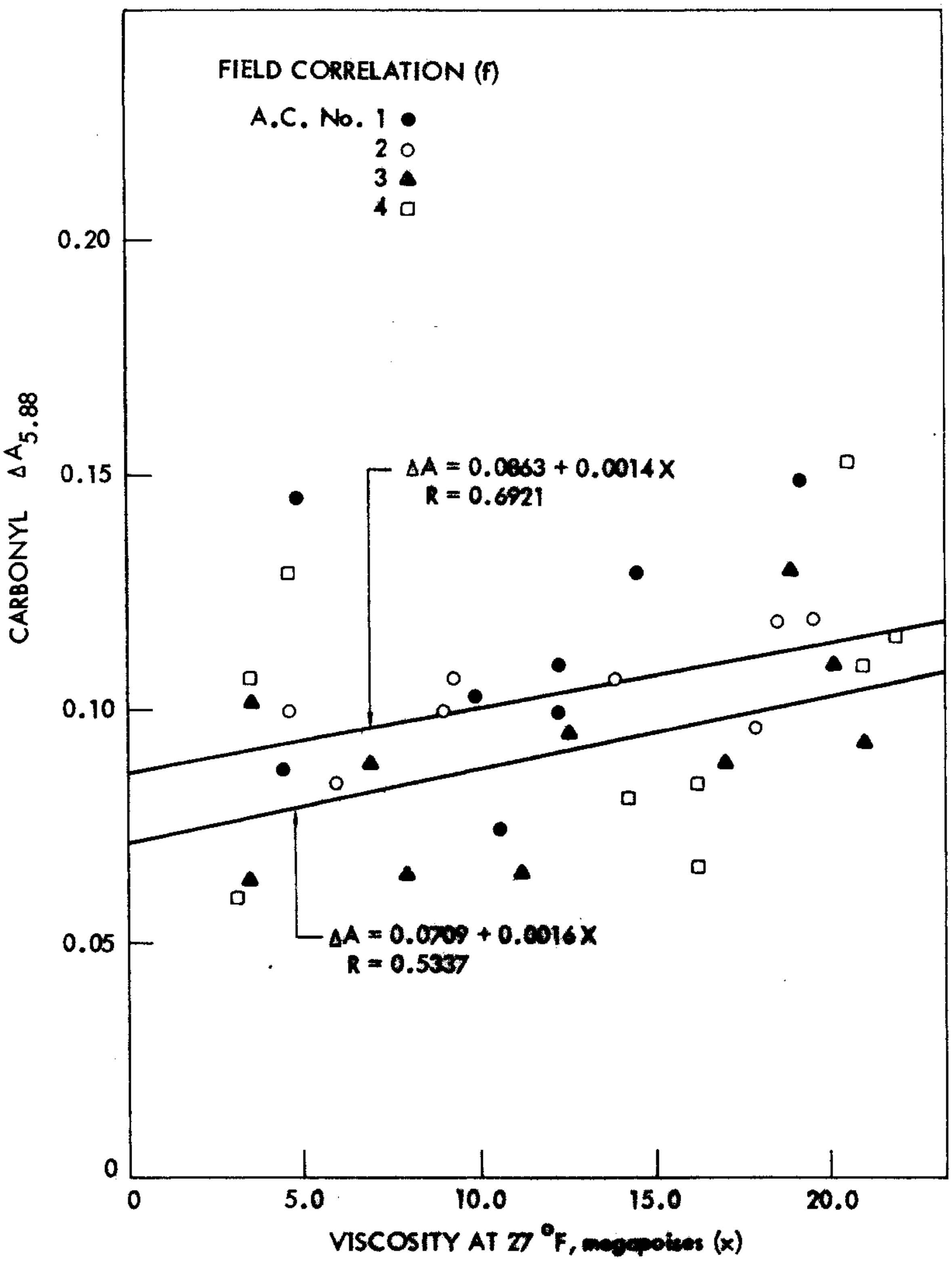

Fig. 34b. Changes in viscosity at 77 °F.

VII. CORRELATIONS

It has been pointed out that the value and usefulness of any laboratory durability test depends not only upon how logical or realistic acceleration process is in the laboratory as compared with what actually occurs in the field but also upon how good the correlation is between laboratory and field data. One of the major efforts in this investigation was, as stated in the original proposals, to establish correlation of hardening and other relevant property changes in asphalts in the developed Iowa Durability Test (IDT) and changes in the same asphalts in the pavements in Iowa in terms of time-equivalency curves or acceleration factors between ageing in IDT in hours and ageing in the pavement in months. With the correlation or calibration curves and the selected durability criteria, functional approach specifications of paving asphalt can then be established and the durability of asphalts in Iowa pavement can be predicted in more reasonably exact terms (Ch. VIII).

Time-equivalency correlation curves were established for each asphalt and for all relevant properties. Correlation curves were drawn from the property-time curves for each asphalt for a certain property. The time in hours in IDT and the equivalent time in months in the pavement required for each asphalt to reach a certain value were determined from the property curves. Seven to fifteen points were taken from each set of property-time curves for each asphalt and each property. They were plotted on a semilog scale with log laboratory time (T_ℓ, hours) as ordinate and field service time (T_f, months) as abscissa.

Time-equivalency correlation curves for penetration are shown in Figs. 35a to 35h for asphalts 1 to 4 and 6 to 9 respectively. Correlation curves for viscosity at 77 °F are shown in Figs. 36a to 36c. Correlation curves for softening point are given in Figs. 37a to 37c. Similar curves for viscosity at 140 °F and asphaltene content are given in Figs. 38a to 38c and Figs. 39a to 39c.

Since the majority of these curves were of hyperbolic nature, curve fittings for all time-equivalency data for penetration, softening point, viscosity at 77 °F, viscosity at 140 °F, percent of asphaltenes, and microductility were attempted for all asphalts with the following model:

$$\log T_\ell = \frac{T_f}{a + bT_f}$$

where T_ℓ = laboratory IDT time (hours) to reach certain property value,

T_f = equivalent field time (month) to reach same value of same property for the same asphalt, and

a and b = constants.

Constants a and b were determined through linear least square regression analysis by using

$$\frac{T_f}{\log T_\ell} = a + bT_f$$

Table 34 gives coefficients a, b, and R^2, and observation number n for 46 of the single-property, single-asphalt curves. It can be readily observed, except for microductility for A.C. No. 2 for reasons already given, that all other fittings were excellent.

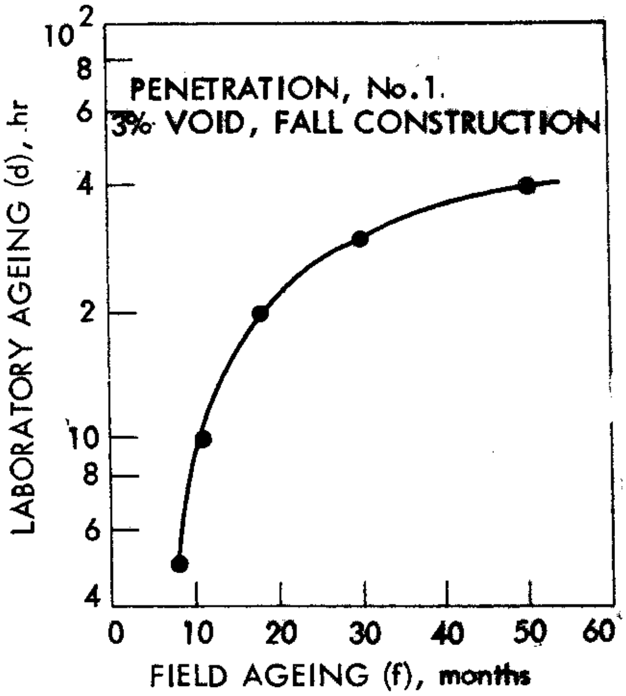

Fig. 35a. Penetration correlation curves.

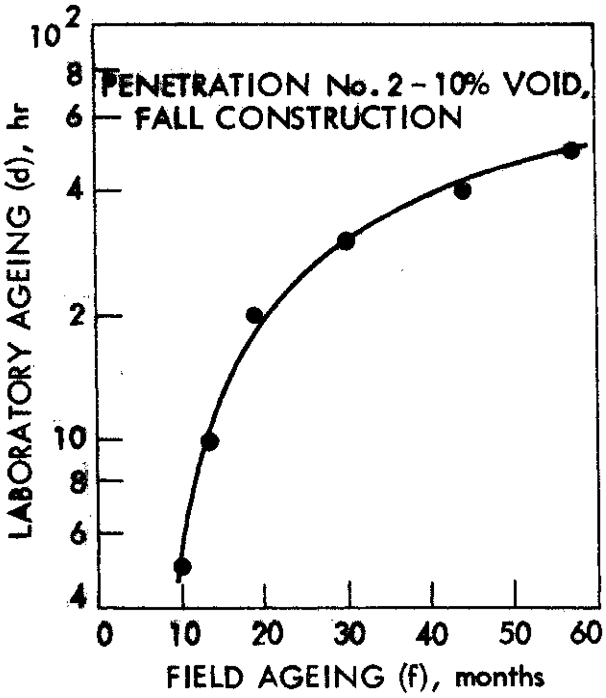

Fig. 35b. Penetration correlation curves.

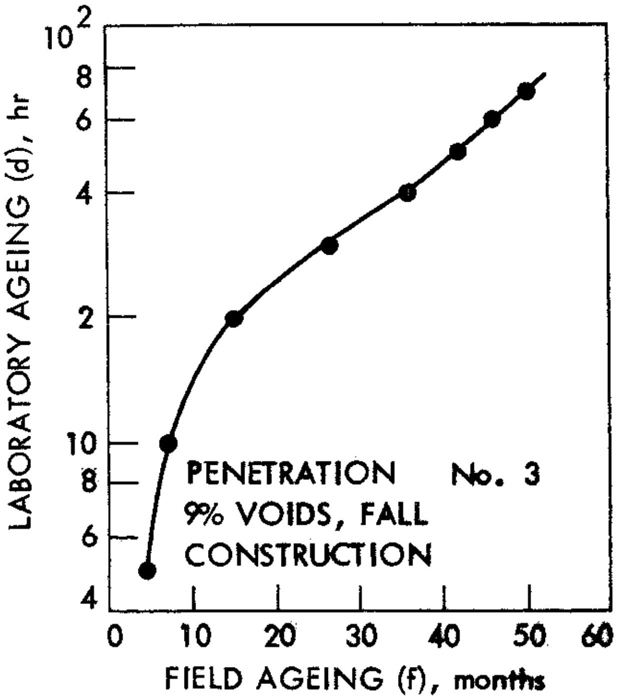

Fig. 35c. Penetration correlation curves.

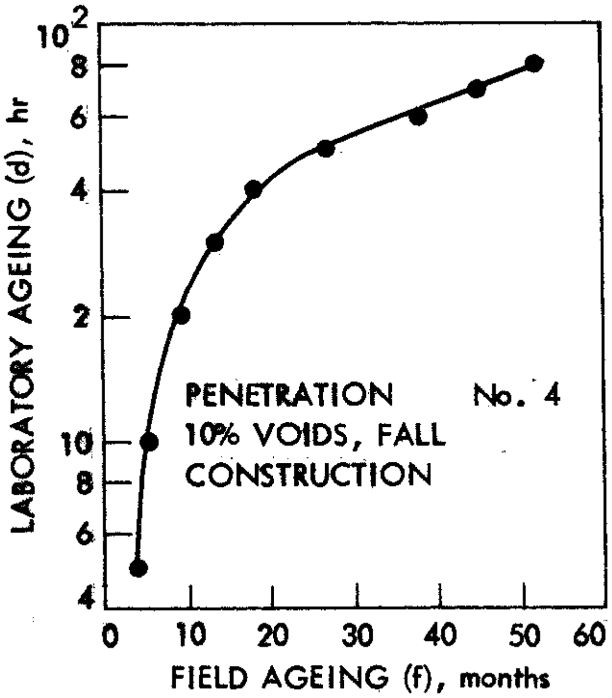

Fig. 35d. Penetration correlation curves.

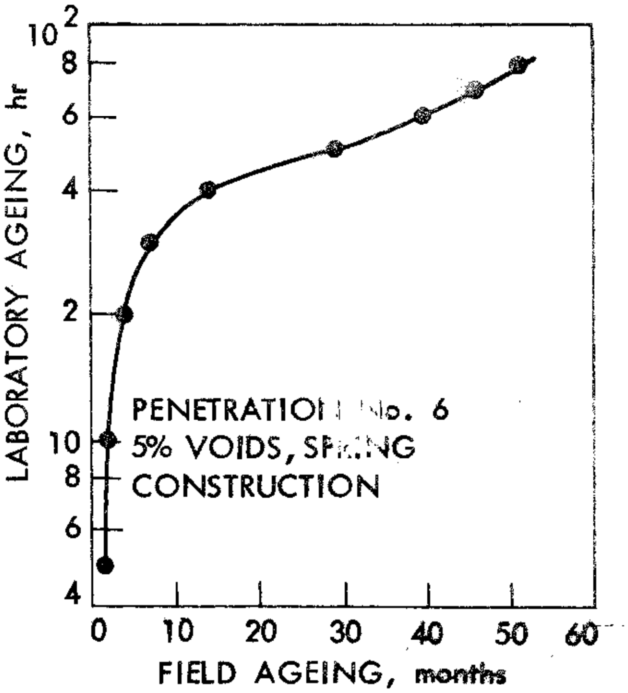

Fig. 35e. Penetration correlation curves.

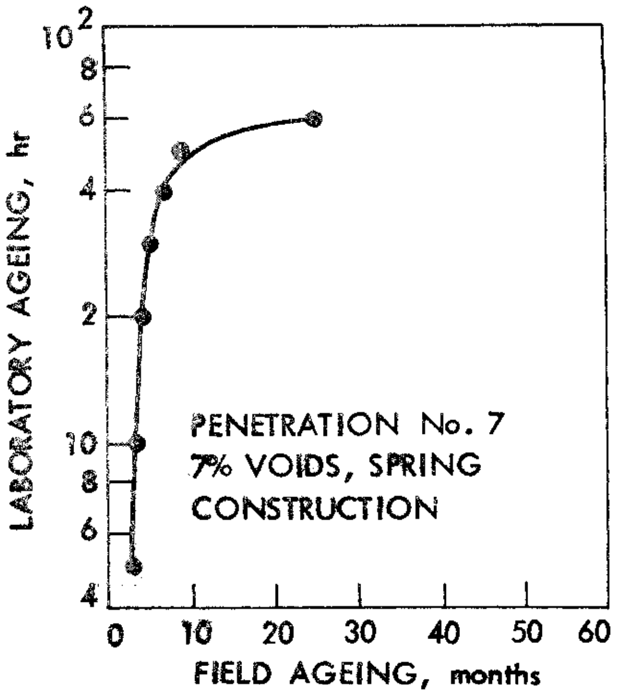

Fig. 35f. Penetration correlation curves.

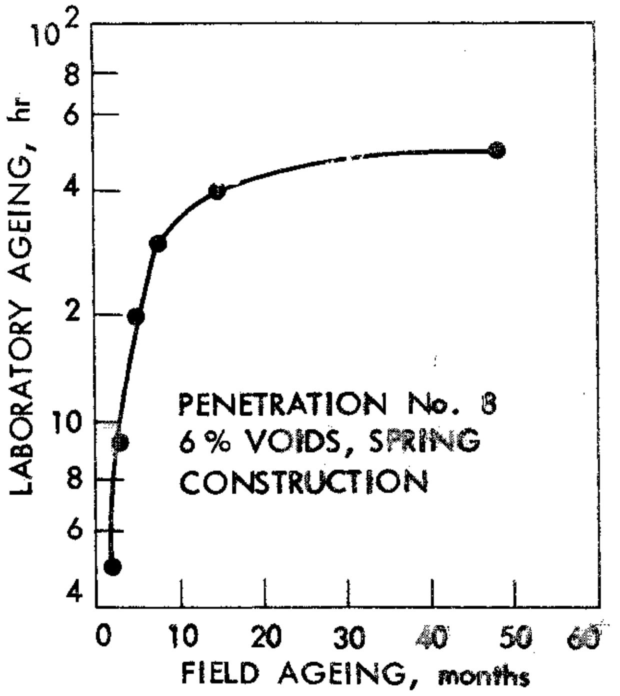

Fig. 35g. Penetration correlation curves.

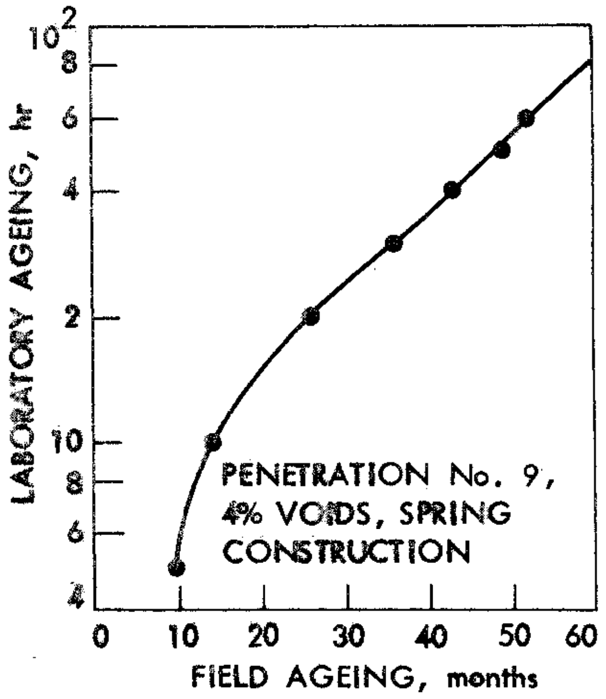

Fig. 35h. Penetration correlation curves.

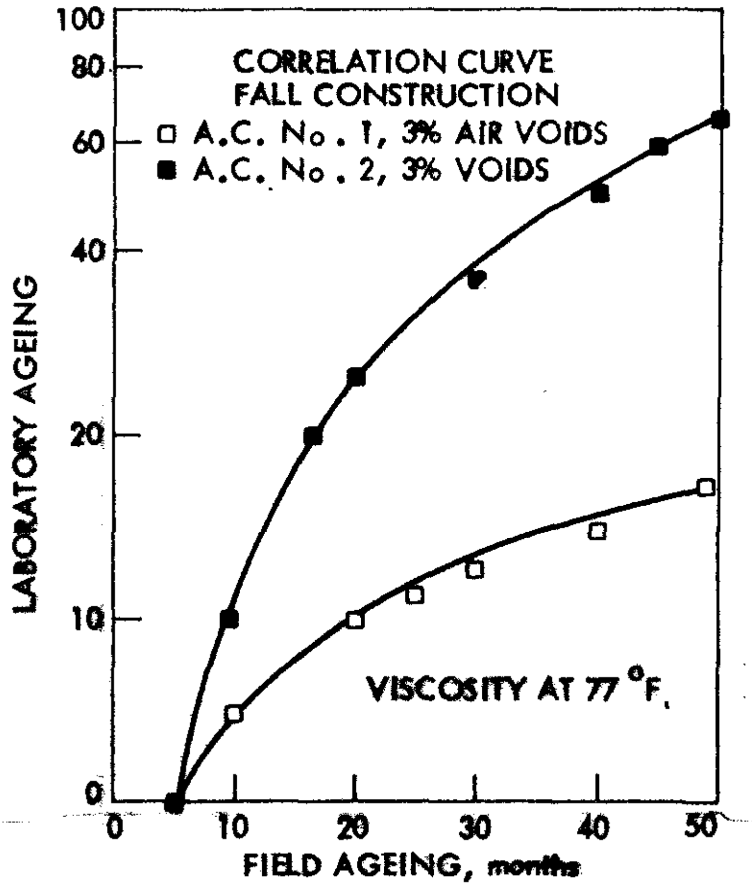

Fig. 36a. Correlation curves for viscosity at 77°F.

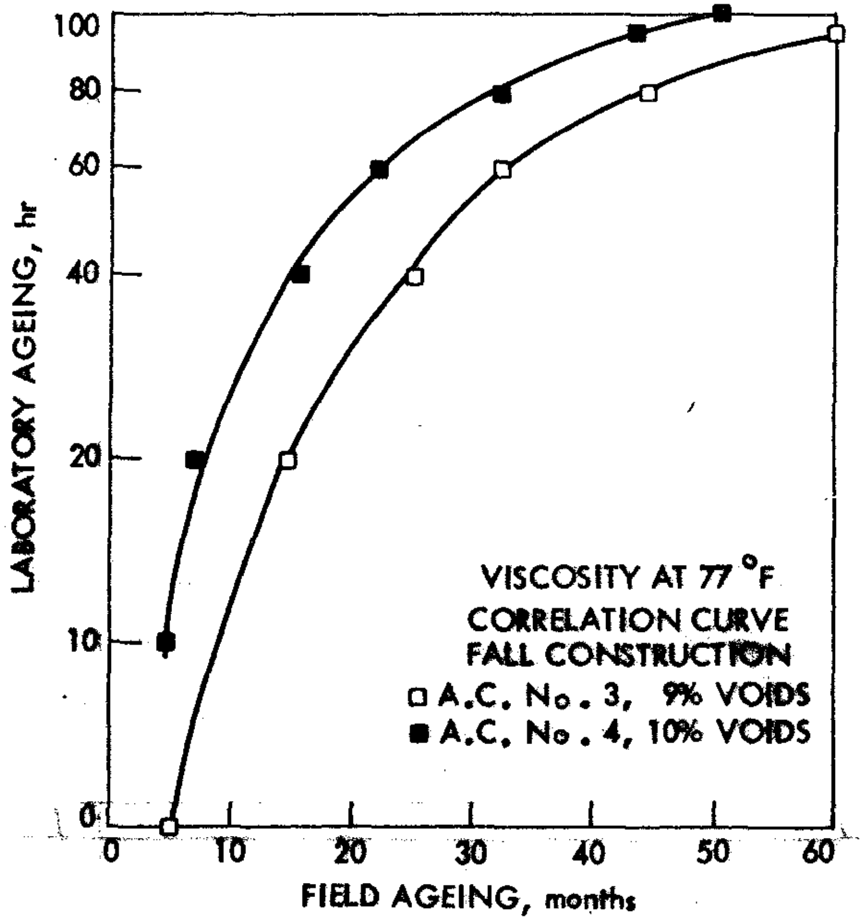

Fig. 36b. Correlation curves for viscosity at 77°F.

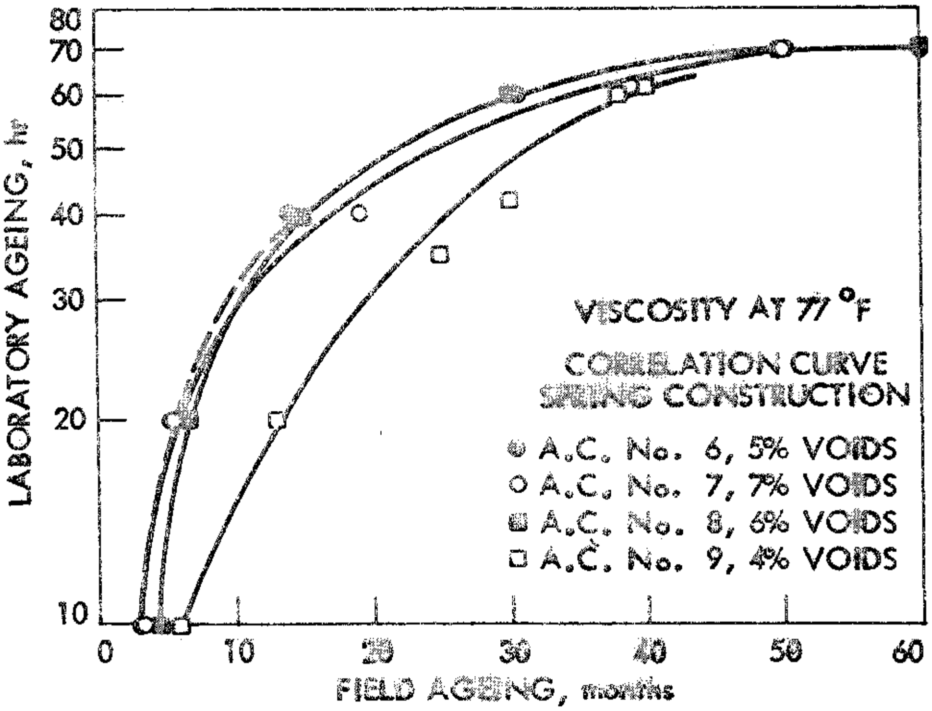

Fig. 36c. Correlation curves for viscosity at 77 °F.

In order for the time-equivalency curves to be useful, general correlation curves were established for each property by combining eight individual curves for that property. General time-equivalency curves for penetration, softening point, viscosity at 77 °F, viscosity at 140 °F, asphaltene content, and microductility are indicated in Table 34 as Regression No. 50, 54, 58, 62, 66, and 70, and were plotted in Fig. 40. Since each test determines a different asphalt property or behavior the variation of these curves were to be expected. Of great importance is that all six general curves excellently fit data from individual asphalts. (Linear correlation coefficients were significant at 1% level.) The significance of these general correlation curves will be discussed in the next chapter.

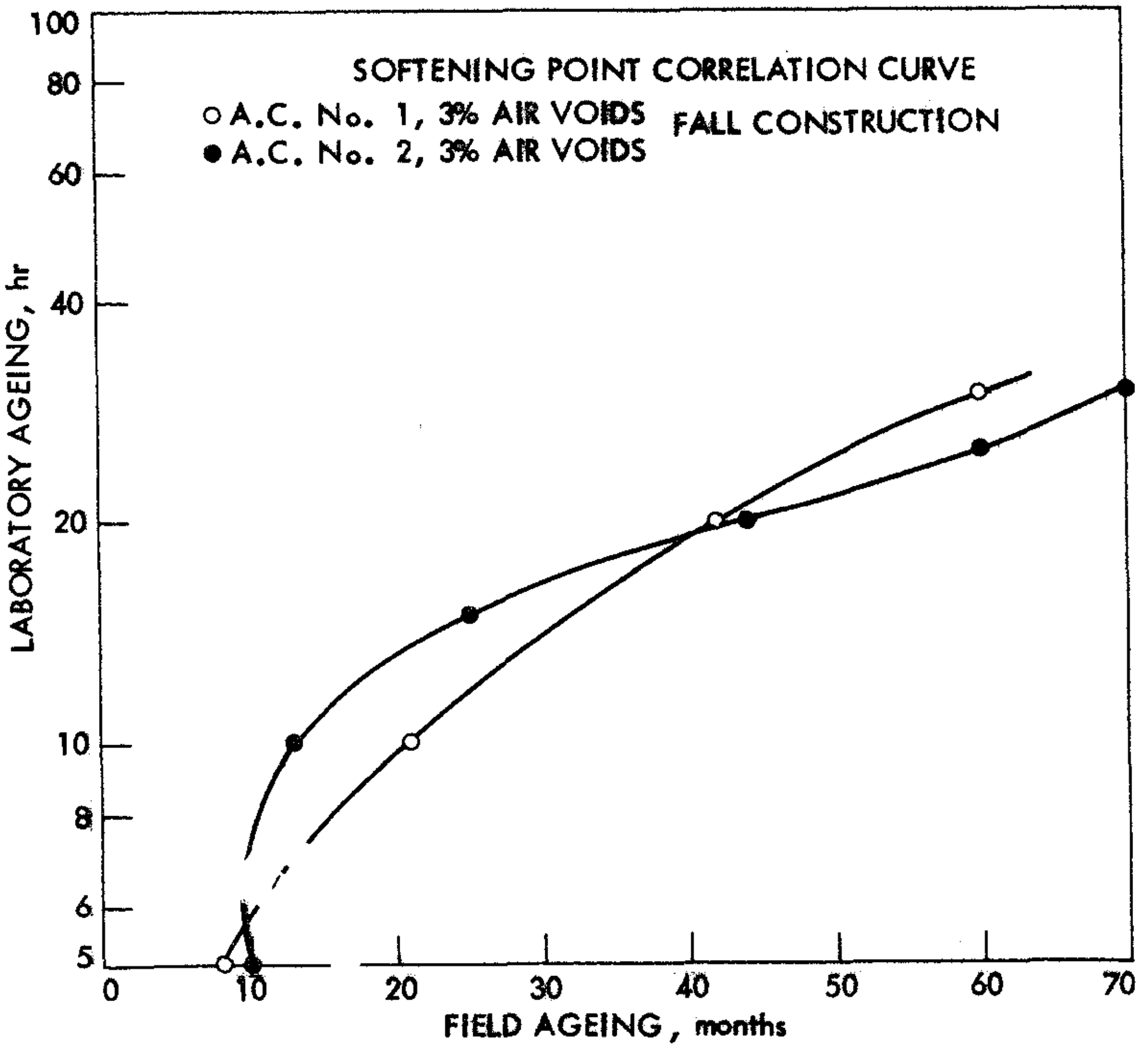

Fig. 37a. Softening point correlation curves.

If we realize that many other variables — aggregate type and gradation, asphalt content, mixing temperature, compaction, traffic, and voids — also influence the rate of change of asphalts in pavements, the minor variations among curves of different asphalts for the same property criterion are to be expected.

Since all pavements studied in this project were regular paving projects of the Iowa State Highway Commission, materials and construction

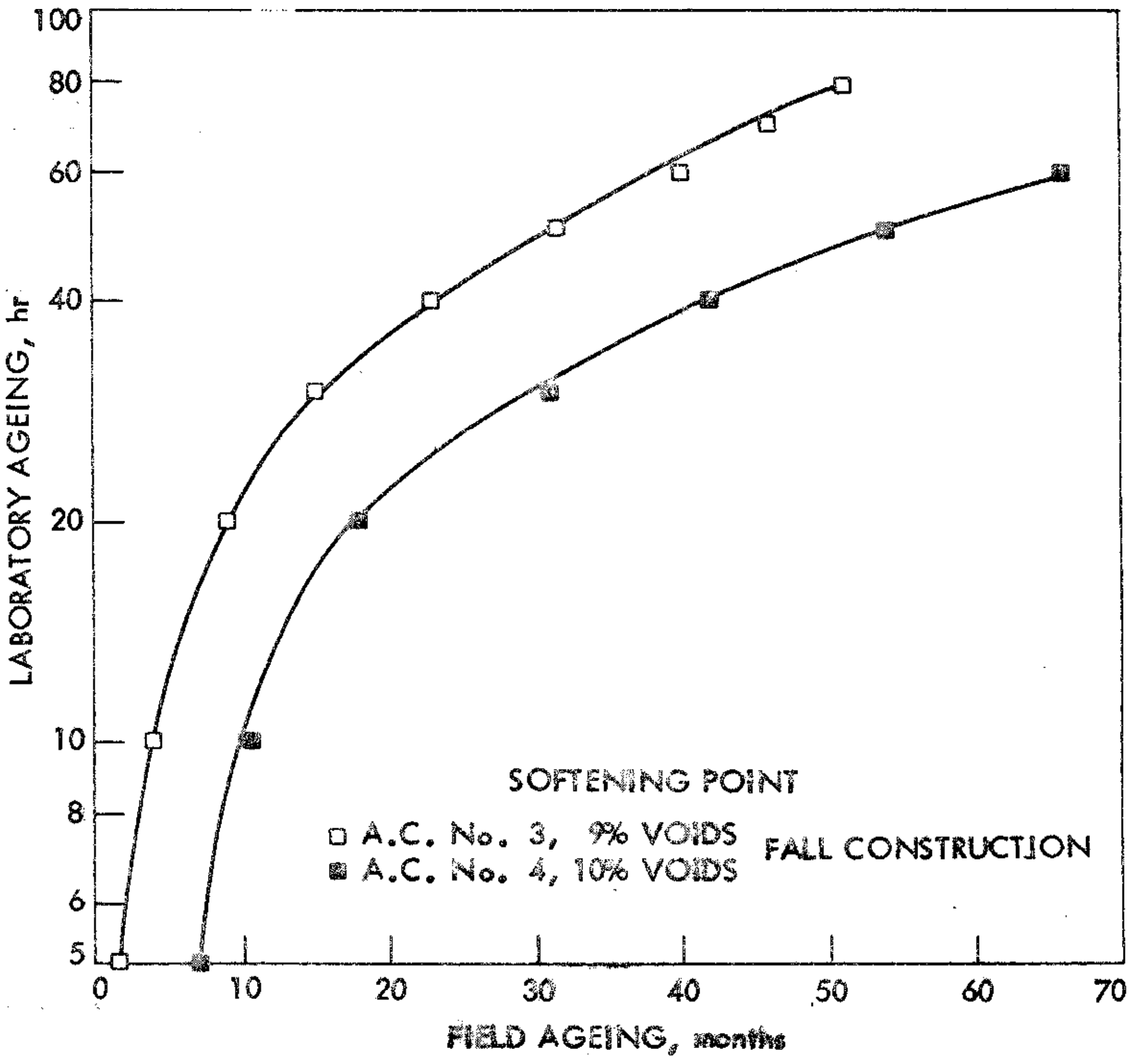

Fig. 37b. Softening point correlation curves.

practices could be safely assumed to have met minimum and acceptable standards. Effects due to variations in mixing temperatures were not obvious, as discussed previously. Effects on hardening due to variation in asphalt content and film thickness were examined by correlating film thickness (6.2 to 9.7 μ) and viscosity and penetration of 42-month recovered asphalts. No relationship was found. Thus the only variable, in addition to differences among asphalts, that could

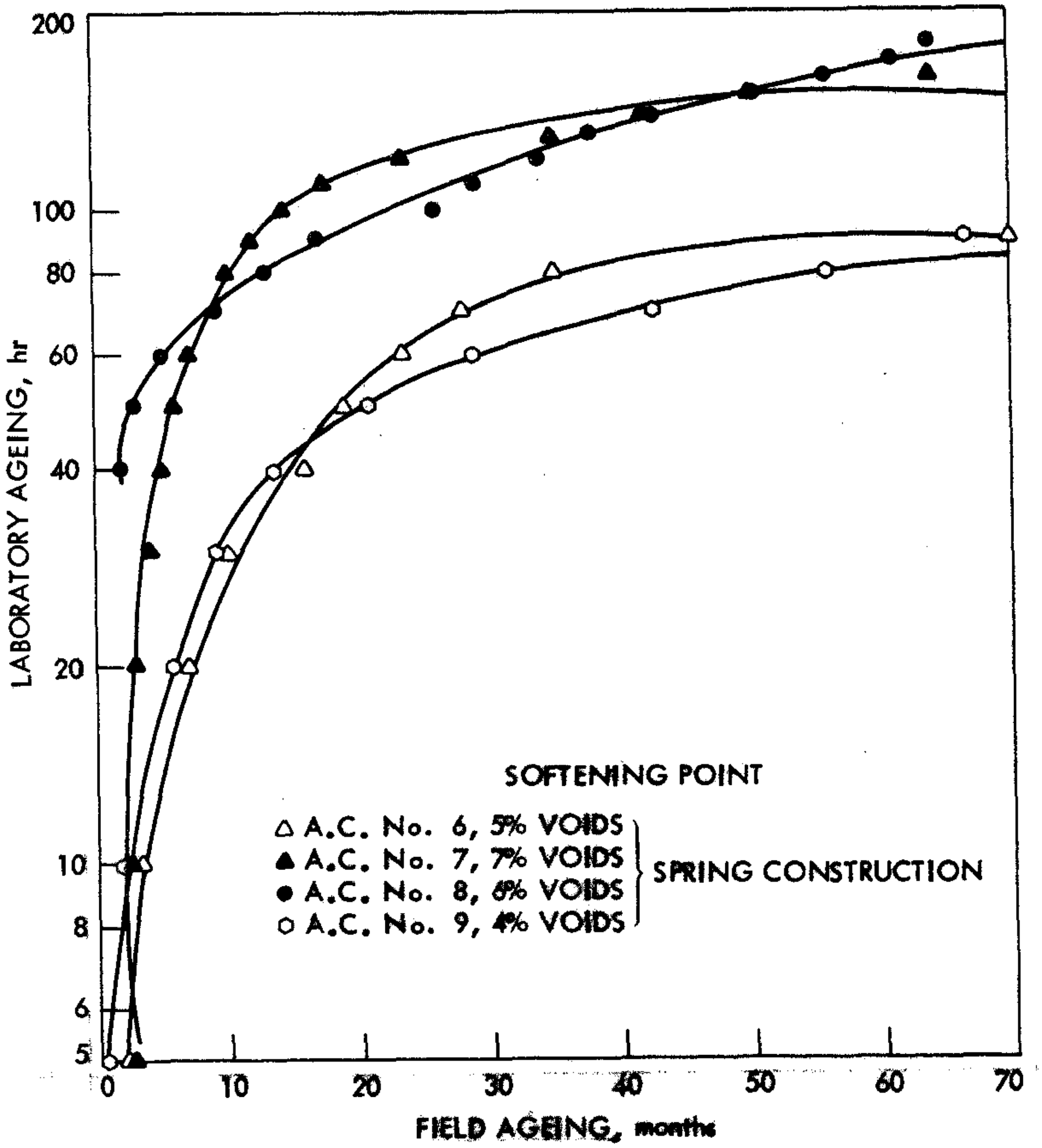

Fig. 37c. Softening point correlation curves.

asphalt hardening rate was voids content. Relationships between initial and final voids content and 42-month penetration and viscosity at 77 °F are plotted in Fig. 41. Linear least square regression analyses were also run on: (a) log penetration vs log initial voids, (b) log penetration

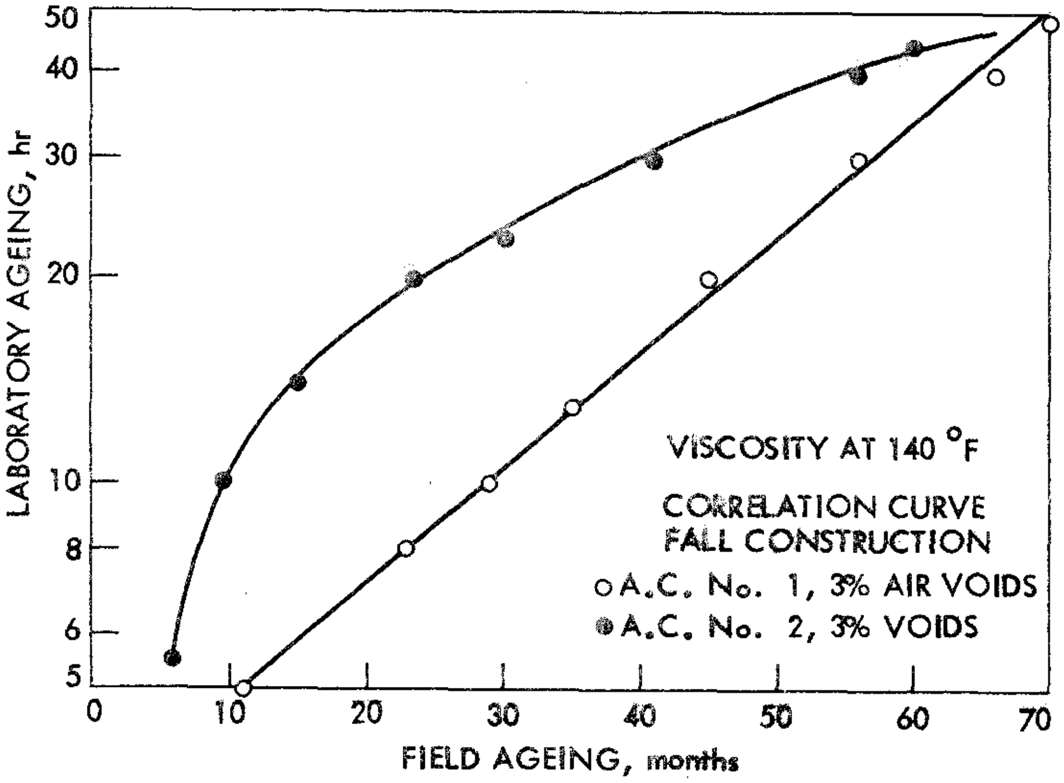

Fig. 38a. Correlation curves for viscosity at 140 °F.

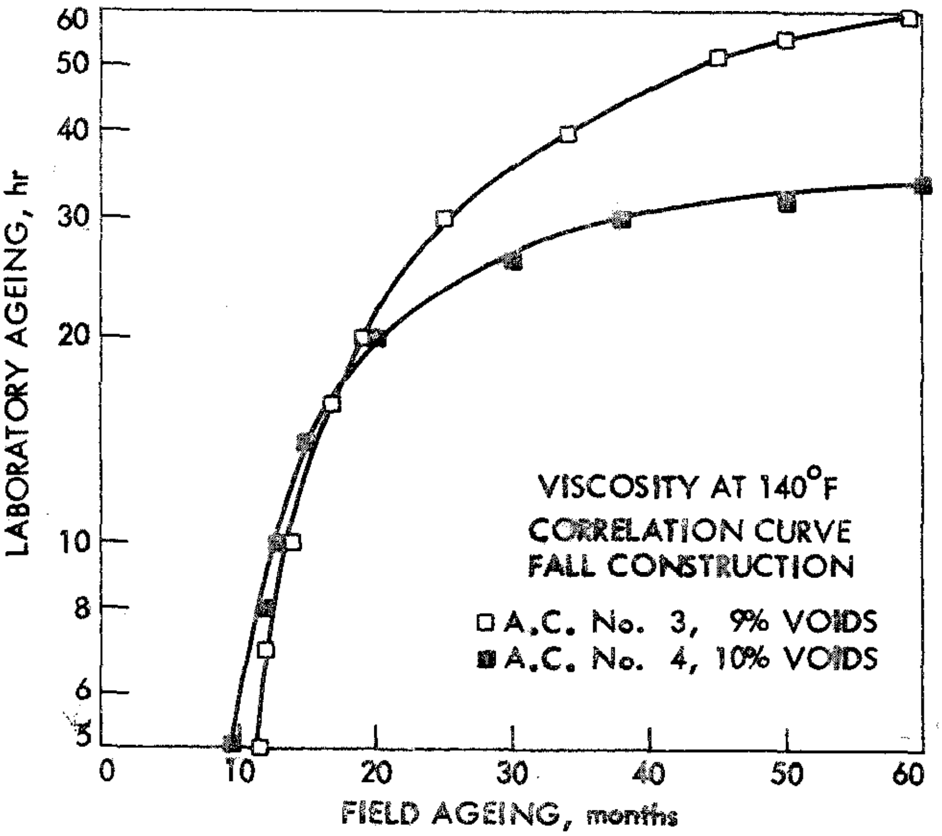

Fig. 38b. Correlation curves for viscosity at 140 °F.

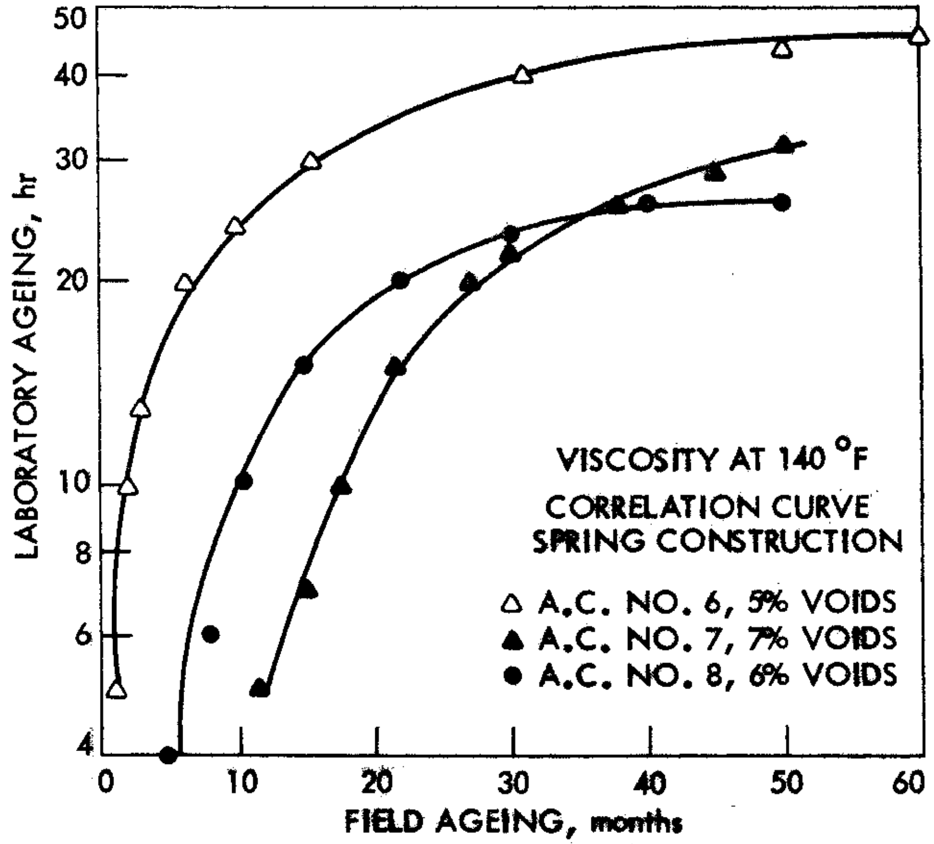

Fig. 38c. Correlation curves for viscosity at 77 °F.

vs log final voids, (c) log viscosity vs log initial voids, and (d) log viscosity vs log final voids. No relation was found between penetration and initial voids; some general trend could be detected between penetration and final voids (correlation not significant). Though correlations were not good, there was a linear relationship between log viscosity and log void content (significant at 5% level for both initial and final voids), i.e., there is a general indication of higher viscosity for asphalts recovered from higher voids pavements. Even though this relationship between pavement voids and asphalt hardening seems to support earlier findings[8,11], its implications in this study

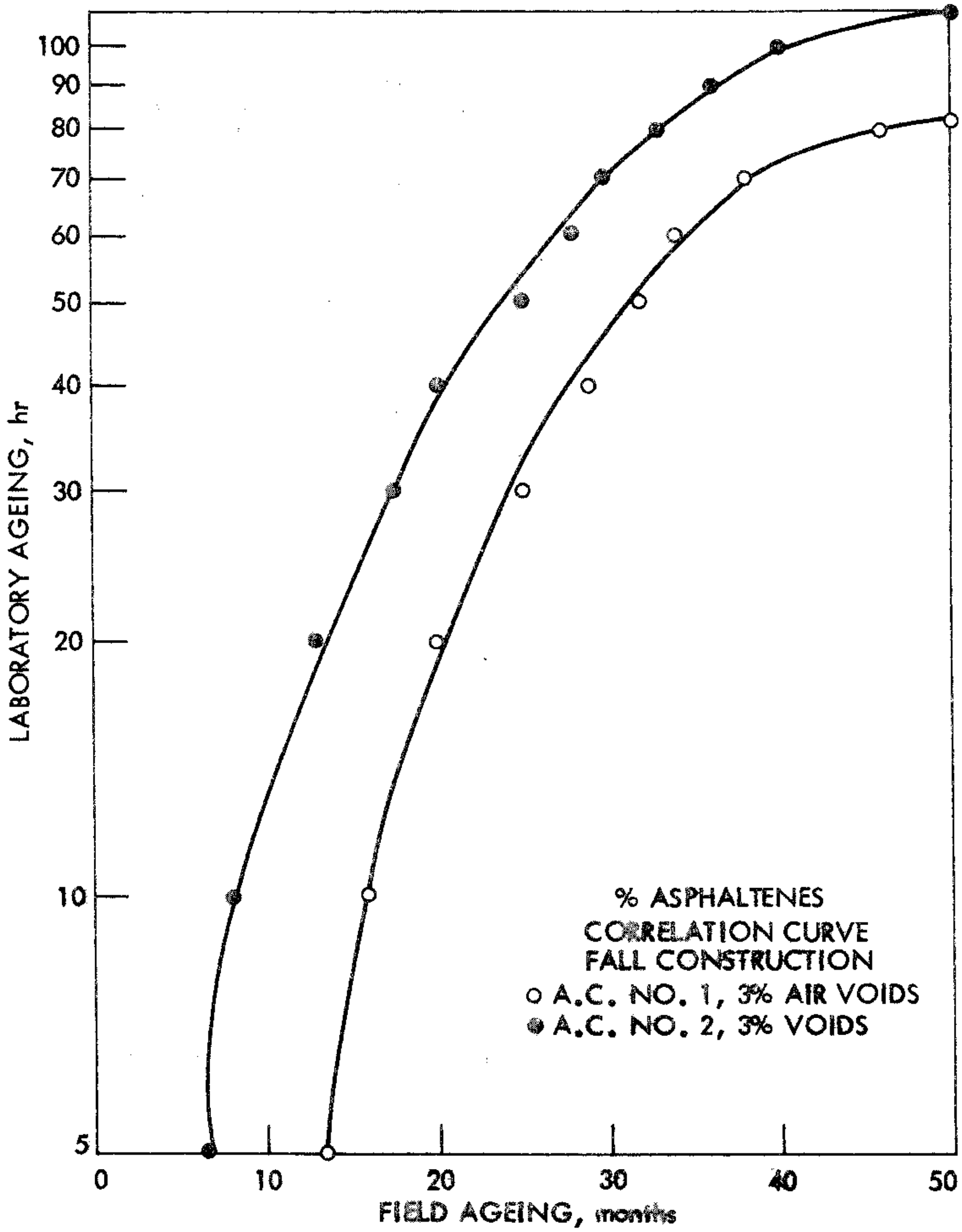

Fig. 39a. Asphaltene content correlation curves.

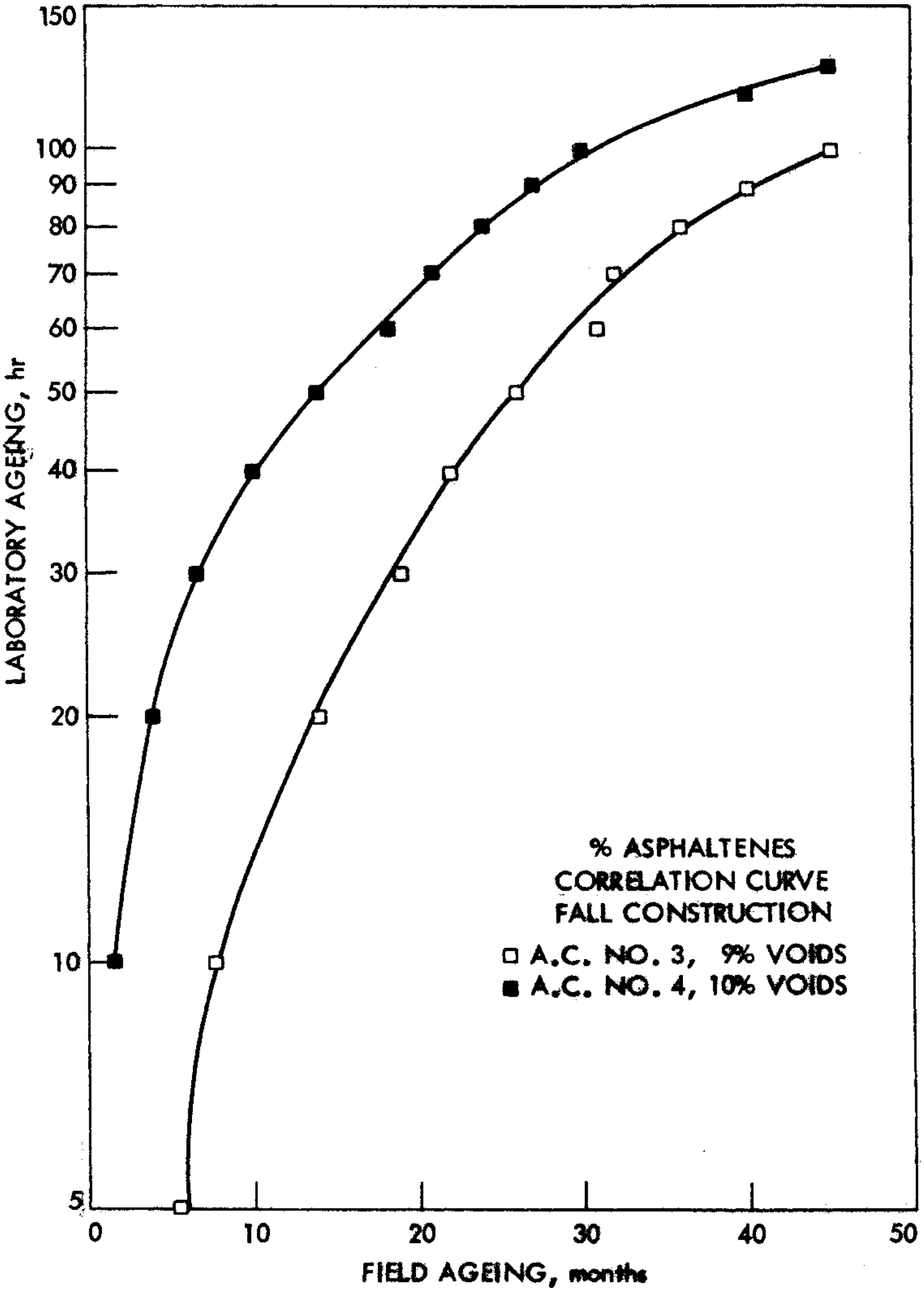

Fig. 39b. Asphaltene content correlation curves.

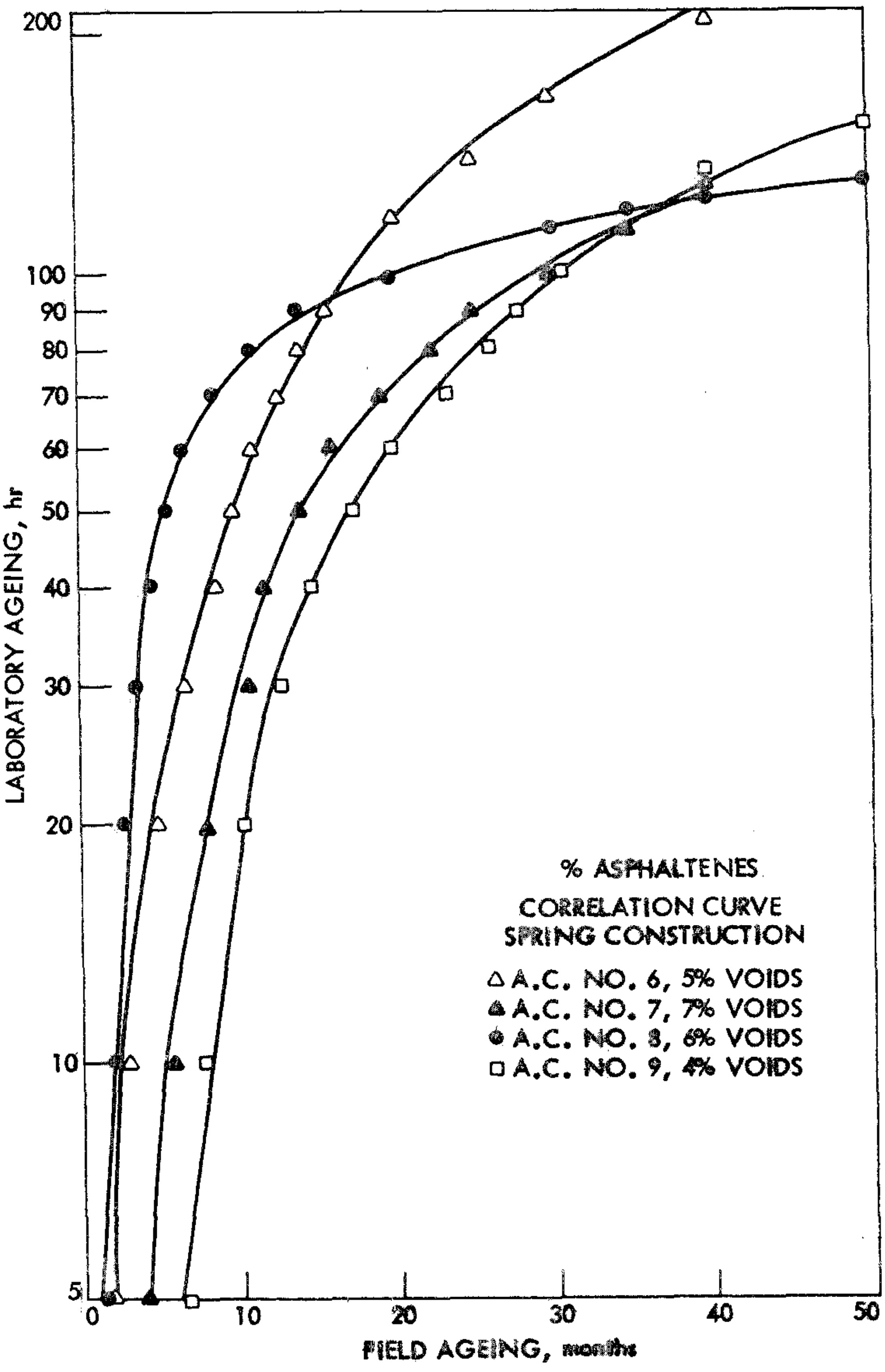

Fig. 39c. Asphaltene content correlation curves.

Table 34. Hyperbolic curve fittings for model: $\log T_\ell = \frac{T_f}{a + bT_f}$, time-equivalency correlation curves.

Regression No.	Property	A.C. No.	a	b	R^2	n
1	Penetration	1	5.739	0.497	0.986	7
2		2	7.631	0.446	0.979	8
3		3	4.408	0.474	0.993	8
4		4	3.120	0.470	0.998	9
5		6	1.291	0.516	0.998	9
6		7	1.521	0.485	0.970	8
7		8	1.116	0.562	1.000	8
8		9	9.345	0.397	0.993	8
9	Softening point	1	8.161	0.561	0.994	8
10		2	8.584	0.551	0.922	8
11		3	2.268	0.497	0.996	9
12		4	5.735	0.480	0.998	8
13		6	1.891	0.482	1.000	10
14		7	1.116	0.436	0.998	17
15		8	0.958	0.439	0.998	15
16		9	1.307	0.509	0.998	9
17	Viscosity at 77 °F	1	4.560	0.747	0.996	10
18		2	5.399	0.448	0.998	10
19		3	5.231	0.406	1.000	9
20		4	2.013	0.462	0.996	9
21		6	1.540	0.515	1.000	10
22		7	1.672	0.513	0.999	10
23		8	1.976	0.500	1.000	10
24		9	3.707	0.475	0.997	10
25	Viscosity at 140 °F	1	15.227	0.403	0.943	8
26		2	5.120	0.535	0.998	8
27		3	8.597	0.397	0.955	10
28		4	6.144	0.535	0.984	9
29		6	1.074	0.587	1.000	9
30		7	9.871	0.450	0.972	9
31		8	4.551	0.598	0.994	8
32	Asphaltenes	1	12.149	0.241	0.733	10
33		2	5.638	0.363	0.988	11
34		3	5.361	0.380	0.996	9
35		4	1.521	0.453	0.996	11
36		6	1.964	0.384	1.000	10
37		7	3.424	0.385	0.996	9
38		8	0.964	0.453	1.000	10
39		9	5.210	0.341	0.974	8
40	Microductility	1	17.174	0.342	0.562	8
41		2	68.601	- 0.878	-0.546	7
42		3	6.808	0.353	0.992	8
43		4	5.891	0.310	0.982	8

Table 34. Continued.

Regression No.	Property	A.C. No.	a	b	R^2	n
44		6	9.998	0.554	0.957	10
45		8	2.540	0.595	0.998	11
46		9	21.506	0.575	0.845	9
47	Penetration	1 & 2	6.799	0.467	0.978	15
48		3 & 4	3.584	0.478	0.989	17
49		6-9	1.906	0.544	0.953	33
50		1-9	3.162	0.518	0.943	65
51	Softening point	1 & 2	8.359	0.557	0.964	16
52		3 & 4	3.582	0.500	0.974	17
53		6-9	1.379	0.452	0.986	51
54		1-9	2.806	0.499	0.852	84
55	Viscosity at 77 °F	1 & 2	4.979	0.598	0.799	20
56		3 & 4	3.452	0.445	0.958	18
57		6-9	2.013	0.501	0.992	40
58		1-9	2.177	0.569	0.856	78
59	Viscosity at 140 °F	1 & 2	8.469	0.506	0.912	16
60		3 & 4	7.346	0.464	0.945	19
61		6-9	3.934	0.587	0.943	26
62		1-9	5.081	0.536	0.925	61
63	Asphaltenes	1 & 2	7.724	0.337	0.808	21
64		3 & 4	2.851	0.435	0.958	20
65		6-9	2.410	0.409	0.964	20
66		1-9	3.213	0.424	0.898	78
67	Microductility	1 & 2	35.913	- 0.094	0.010	15
68		3 & 4	6.350	0.331	0.916	16
69		6-9	8.789	0.642	0.588	30
70		1-9	10.854	0.493	0.297	61
71	All	1 & 2	8.395	0.494	0.579	103
72	All	3 & 4	3.762	0.473	0.910	107
73	All	6-9	2.599	0.541	0.747	217
74	All	1-9	3.664	0.536	0.720	427

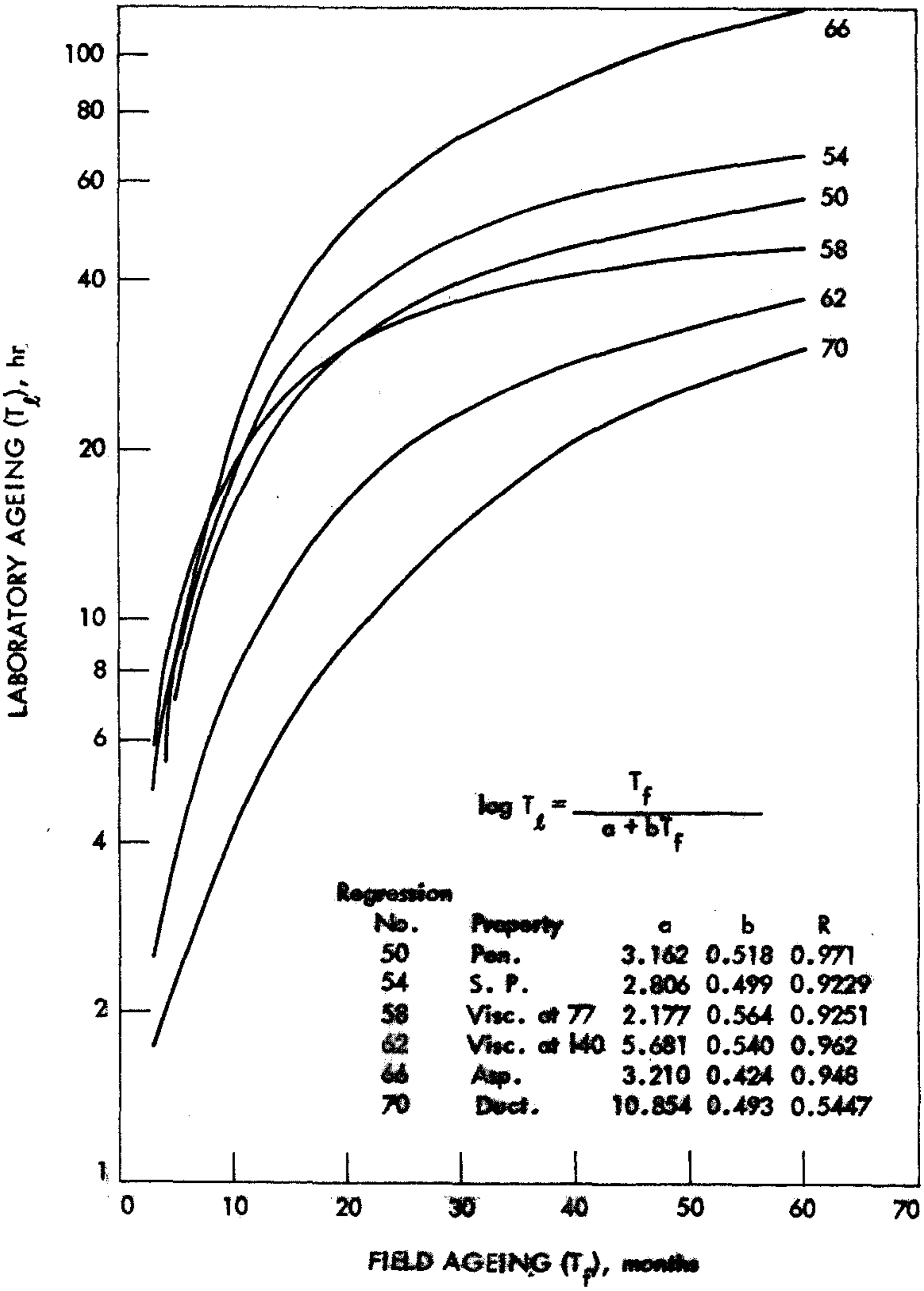

$$\log T_\ell = \frac{T_f}{a + bT_f}$$

Regression No.	Property	a	b	R
50	Pen.	3.162	0.518	0.971
54	S. P.	2.806	0.499	0.9229
58	Visc. at 77	2.177	0.564	0.9251
62	Visc. at 140	5.681	0.540	0.962
66	Asp.	3.210	0.424	0.948
70	Duct.	10.854	0.493	0.5447

Fig. 40. Time-equivalency correlation curves for various properties.

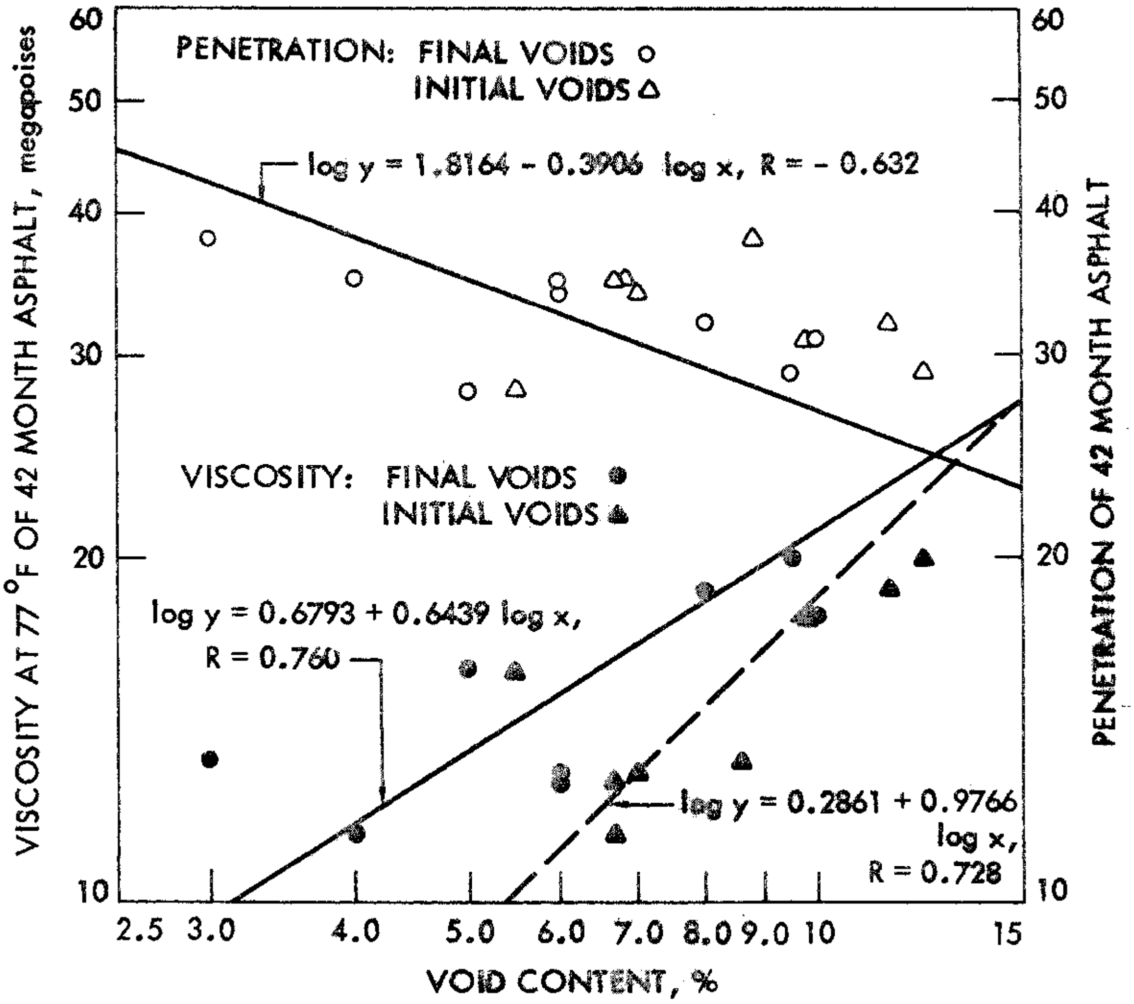

Fig. 41. Log viscosity (log penetration) vs log void content of 42-month field asphalts.

should be viewed with caution because, while all eight asphalts were of 85 to 100 penetration, their initial viscosity were not identical.

Nevertheless, to account for possible differences due to voids content among pavements, equations for time-equivalency correlation curves were also established by combining asphalts of different voids level. In Table 34, Regression No. 47, 51, 55, 59, 63, and 67 were equations obtained by combining pavement of 3% void (A.C. No. 1 and 2), Regression No. 49, 53, 57, 61, 65, and 69 were equations obtained by combining asphalts from pavements with void contents between 4 to 7% (A.C. 6 to 9); and Regression No. 48, 52, 56, 60, 64, and 68 were equations obtained by combining asphalts from pavements with void contents larger than 9% (A.C. No. 3 and 4). It is worth noting that, except for viscosity at 77 °F, and while all curve fittings by void level were good, they did not improve the fit.

Regression No. 74, which was obtained by combining all properties and all asphalts and which is a surprisingly good fit (linear correlation significant at 1% level), will be called the master time-equivalency curve, and is plotted in Fig. 42, and, as will be indicated later, is of great importance in this investigation.

Regression No. 71, 72, and 73 were obtained by combining all properties of only asphalts from pavements of the same void levels. Note again that except for extremely high void contents (A.C. No. 3 and 4) fit did not improve. However, the relative positions of the three curves as shown in Fig. 42 are of significance: as percent voids in the pavements increased, longer laboratory IDT time is required to reach equivalent field service hardening. For all practical purposes, the use of the master curve (Regression No. 74) for all asphalts used in all acceptable construction procedures should provide reasonable correlation and prediction for Iowa conditions. It is therefore recommended that, at least for a trial period, this curve be used for specification purposes by IDT method.

On the basis of the master curve, 46 hr of ageing in IDT will result in hardening in asphalts equivalent to that attained after 60 months of service life in Iowa conditions.

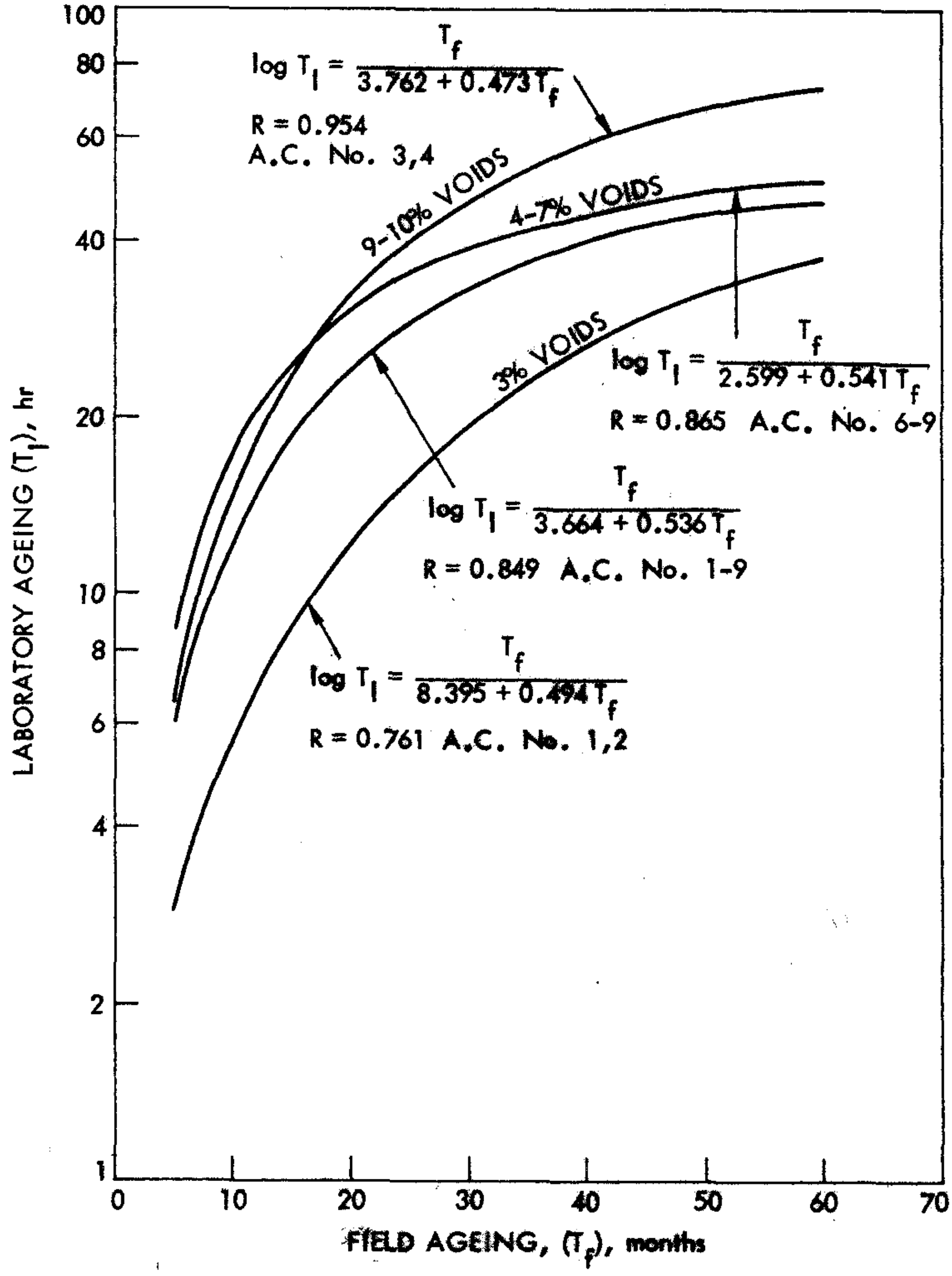

Fig. 42. Time-equivalency correlation curves by voids level.

VIII. APPLICATION AND ENGINEERING IMPLICATIONS OF RESULTS

It has been shown repeatedly that asphalts meeting the same present-day specifications can and do exhibit a considerable range and variety of behavior, as measured by a number of different parameters, in the field. It appears justifiable to state that at the present time, standard test procedures and specifications provide no satisfactory means of determining whether or not asphalt will be durable – whether it will retain the desirable properties of consistency and adhesiveness and resist hardening and embrittlement for a long period of time. The need for new specifications for paving asphalts has also been recognized by a number of other investigations.

As has been stated, the ultimate goal of HR-124 is the establishment of a functional approach asphalt specifications with emphasis on meaningful durability quality control by means of IDT.

Based on results discussed in previous chapters in comparison with research reported by other investigators, the Iowa Durability Test procedure result can be considered logical, realistic, and simple; the facilities are inexpensive and the procedure is reproducible and effective. With the established time-equivalency correlation curves, the IDT can be used to reasonably predict the changes and useful life of asphalt in Iowa pavements. If parameters, tests and critical values of asphalts are properly selected, the results of this investigation can be applied to asphalt specification for assurance of durable paving asphalts.

The work by the State of California[46] has demonstrated the value and the validity of our hypothesis. While their procedures are time-consuming, their equipment expensive, some tests have poor reproducibility, and some accelerated weathering processes (such as 210 °F on 20-μ films) are debatable, the State of California has developed tests and specifications geared to California weathering conditions after 25 years of study and correlation, based on the functional approach which describes asphalt during each phase of use as has been done in HR-124.

For application of our results to functional specifications, durability criteria and/or critical values of selected significant properties must be established based on observations of pavement performance and information from other studies.

Selection and/or establishment of durability criteria and critical values of critical properties are complex problems. To evaluate relative durability of asphalts studied in HR-124, the following approaches were investigated:

1. Limiting Values of Selected Properties

Limiting values is based on the hypothesis, which was verified in this study, that changes in asphalt, both in the laboratory IDT and in field service ageing, is a hyperbolic function of time in the form

$$\Delta Y = \frac{T}{a + bT} .$$

When a and b are determined and initial property value Y_o is known, the ultimate value Y_u can be calculated from the ultimate change

$$\Delta Y_{t \to \infty} = 1/b.$$

The ultimate changes 1/b and ultimate values Y_u in terms of penetration, softening point, and viscosity at 77 °F were calculated for asphalts studied in this work and are given in Table 12 for laboratory IDT ageing and in Table 13 for field ageing. Based on this approach, larger ultimate change (or lower ultimate penetration and higher ultimate viscosity and softening point) would be considered properties of less durable asphalts. Rankings of the eight asphalts are tabulated in Table 35a for laboratory aged and in Table 35b for field aged asphalts. Numbers in parenthesis are rankings, with lowest number being the most durable asphalt.

2. Predicted Time to Harden to Certain Critical Values of Critical Properties

This is also based on the hyperbolic time-property change curve model as in approach 1 above. But, instead of ultimate change or limiting value, the time it takes for a certain asphalt to harden to a critical value of a selected property is calculated from the predictive equation or from the time-property curve. Times for asphalts to harden to a critical penetration of 20, a critical softening point of 160 °F, and a critical viscosity at 77 °F, and 0.05 $\sec^{-1}$ of 20 to 30 megapoises were calculated and, together with rankings (longer time to reach a critical value means more durable asphalt), are given in Tables 35a and 35b for HR-124 asphalts.

Table 35a. Durability rankings based on different criteria — lab ageing.

Criterion	A.C. No.							
	1	2	3	4	6	7	8	9
Penetration ratio[*]	0.28	0.24	0.39	0.35	0.29	0.38	0.25	0.16
	(4)	(2)	(8)	(6)	(5)	(7)	(3)	(1)
Ageing index[†] at 77 °F	0.44	0.32	0.70	0.48	0.49	0.74	0.59	0.37
	(3)	(1)	(7)	(4)	(5)	(8)	(6)	(2)
Ageing index[‡] at 140 °F	0.81	0.93	0.84	1.04	0.69	0.63	0.63	0.54
	(3)	(1)	(6)	(8)	(4)	(2)	(2)	(1)
Limiting penetration	10	16	4	8	20	6	15	22
	(5)	(3)	(8)	(6)	(2)	(7)	(4)	(1)
Limiting viscosity at 77 °F, megapoises	56	56	91	56	23	45	81	36
	(4)	(4)	(8)	(4)	(1)	(3)	(7)	(2)
Limiting softening point, °F	183	181	179	185	194	206	182	160
	(5)	(3)	(2)	(6)	(7)	(8)	(4)	(1)
Time to 30 megapoises (hr)	110	160	130	70	180	130	180	310
	(7)	(4)	(5)	(8)	(2)	(5)	(2)	(1)
Time to 20 penetration (hr)	144	134	129	190	340	235	550	900
	(6)	(7)	(8)	(5)	(3)	(4)	(2)	(1)
Time to 160 °F S.P., hr	240	310	530	510	410	500	360	∞
	(8)	(7)	(2)	(3)	(5)	(4)	(6)	(1)
$(N + A_1)/(A_2 + P)$	1.17	1.04	1.25	0.54	—	—	—	—
	(3)	(2)	(4)	(1)				

---

[*] Slope of log penetration ratio vs log time of ageing.

[†] Slope of log viscosity at 77 °F vs log time of ageing.

[‡] Slope of log viscosity at 140 °F vs log time of ageing.

Table 35b. Durability ranking based on different criteria – field ageing.

	A.C. No.							
Criterion	1	2	3	4	6	7	8	9
Penetration ratio[*]	0.21 (4)	0.29 (7)	0.27 (6)	0.38 (8)	0.15 (3)	0.09 (1)	0.13 (2)	0.25 (5)
Ageing index[†] at 77 °F	0.49 (5)	0.60 (6)	0.74 (7)	0.77 (8)	0.30 (2)	0.27 (1)	0.30 (2)	0.45 (4)
Ageing index[‡] at 140 °F	0.40 (4)	0.55 (8)	0.46 (5)	0.53 (7)	0.25 (3)	0.15 (1)	0.19 (2)	0.48 (6)
Limiting penetration	24 (5)	19 (7)	14 (8)	28 (3)	26 (4)	36 (1)	33 (2)	21 (6)
Limiting viscosity at 77 °F, megapoises	17 (3)	126 (8)	37 (7)	24 (6)	21 (4)	16 (2)	23 (5)	15 (1)
Limiting softening point, °F	163 (5)	144 (3)	163 (5)	286 (7)	144 (3)	142 (2)	322 (8)	140 (1)
Time to 20 °, megapoises (months)	∞ (1)	48[**] (6)	88[**] (5)	45[**] (7)	277[††] (4)	∞ (1)	39[**] (8)	∞ (1)
Time to 20 penetration (months)	147[**] (5)	287[**] (4)	109[**] (6)	57[††] (8)	∞ (1)	∞ (1)	∞ (1)	81[‡‡] (7)
Time to 160 °F S.P. (months)	1986[††] (5)	∞ (1)	408[††] (6)	112[**] (8)	∞ (1)	∞ (1)	118 (7)	∞ (1)
$(N + A_1)/(A_2 + P)$	1.17 (3)	1.04 (2)	1.25 (4)	0.54 (1)	–	–	–	–

[*] Slope of log penetration ratio vs log time of ageing.

[†] Slope of log viscosity at 77 °F vs log time of ageing.

[‡] Slope of log viscosity at 140 °F vs time of ageing.

[**] Average of A and B.

[††] A, in wheel tracks.

[‡‡] B, between wheel tracks.

3. Penetration Ratio vs Time Curves

It has been established in earlier discussion that log penetration ratio and log time of ageing is linear. Then the slope of such plots would be indicative of the relative rate of hardening of various asphalts with time. Slopes of HR-124 asphalts for these plots (Figs. 15a to 15i) were determined and are given in Tables 35a and 35b. A small slope will indicate a more durable asphalt. Such an approach can also be applied to retained penetration data.

4. Ageing Index vs Time Curve

Ageing index as defined by the ratio of viscosity of aged and original asphalt can be used as an index of the relative degree of hardening of asphalt. It has also been established that the log ageing index and the log time of ageing is linear. The slope of such a plot can then be used to indicate the relative rate of hardening with time, or the durability of asphalt. A small slope will imply a more durable asphalt. Slopes of HR-124 asphalts of such plots for viscosity at 77 °F (Figs. 16a to 16i) and viscosity at 140 °F (Figs. 17a to 17c) were determined and are given in Tables 35a and 35b.

5. Chemical Parameters

Changes in chemical parameters such as $(N + A_1)/(A_2 + P)$[70,72], carbonyl index[75,76,78], and perhaps the asphaltenes content, can also be used to rate the relative durability of asphalt. Rankings by

$(N + A_1)/(A_2 + P)$ for A.C. No. 1 to 4 are given in Tables 35a and 35b. A lower ratio is suggested to indicate higher durability.

It can be readily noted by examining Tables 35a and 35b that ratings of asphalt durability by different criteria are not consistent, except for A.C. No. 9, which ranked high by all criteria. The ultimate test in determining which of the criteria is most accurate and suited for Iowa conditions is a continued careful observation of the performance of the eight pavements since at this time they are essentially all in good condition after 42 to 48 months of field service.

The selection of critical values of various asphalt properties for Iowa conditions presents another problem. This can be solved by either another research study examining failure pavements in Iowa (see Recommendations) or by using critical values of selected significant properties reported by other studies. Tables 36 and 37 summarize such reported data and can be used for immediate application of results of this study to asphalt specifications.

Based on available information is is proposed that a penetration at 77 ^{o}F of 20 and a viscosity of 20 megapoises at 77 ^{o}F, and a rate of shear at 0.05 sec^{-1} are to be used to control durability of asphalt for pavement service of 60 months (46 hr IDT ageing obtained from master curve). Since various studies have consistently shown that the most drastic changes in asphalt properties in pavement occur during the first 30 to 36 months of service life, it is believed that an equivalent of 60 months service life in the field (46 hr in IDT) is sufficient to evaluate an asphalt in terms of durability.

Table 36. Correlation of pavement condition with physical properties of recovered bitumen[*].

Data source	Pavement locations	Pavement condition	Tests of recovered bitumen: Penetration, 77 °F	Ductility at 77 °F, cm	Softening point, °F
Shattuck	Detroit, Mich.	Very good	20+	50+	—
		Good	20+	25+	—
		Badly cracked	20-	25-	—
Thomas	Minn.	Good[†]	41	—	—
		Fair[†]	26	—	—
		Poor[†]	20	—	—
Hubbard and Gollomb	Ohio, Mich., N.Y., Ind., D. Col.	Sound	30+	—	—
		Prone to crack	30-	—	—
		Cracking type	20-	—	—
				—	—
Vokac	Ohio, Pa., Md., Va., Mo., Ill., Ind., Mich., N.Y., N.J., D. Col.	Sound	25+	24+	—
		Prone to crack	18-25	4-24	160-
		Cracking type	18-	4-	160+
Powers	Arizona	Good	10+	10+	160-
		Cracked	10-	10-	160+
Pub. Rds. Admin.	Cuba	Good[†]	9	1.5	199
		Cracked[†]	5	0.5	217

[*] After Lewis and Welborn, Proc. Assoc. Asph. Pav. Tech. 17: 228 (1948).

[†] Average values.

Table 37. Summary of critical recovered asphalt properties for acceptable performance of asphaltic surfacing[*].

Reference	Penetration, 0.1 mm	Ductility 77 °F, 5 cm	45 °F, 1 cm	Softening point, °F	Viscosity at 77 °F, poises
Dow	38-90				
Lewis and Welborn	< 20	< 10		> 150	
Hubbard and Gollomb	< 20				
Shattuck	< 20	< 25			
Thomas	< 20				
Hubbard	< 20				
Vokac	< 25	< 24		> 160	
Powers	< 10	< 10		> 160	
Halstead[†]	50	100			
	25	10			
Clark		< 15			
Doyle			< 8		
Hveem et al.[‡]		16		151	20×10^6
Simpson et al.[**]					$10^7 - 10^8$

[*] After Finn, F. N., NCHRP Report 39: "Factors Involved in the Design of Asphaltic Pavement Surfaces" (1967) (modified by the author).

[†] Critical penetration (arithmetic)-ductility (logarithms) relationship as established by line connecting these values[100].

[‡] Based on results of Zaca-Wigmore test project[46].

[**] Ref. 15.

To include control of durability in terms of IDT, it is recommended that in Iowa Standard Specifications 1972 (or AASHO M20), a maximum of 20 megapoises in viscosity at 77 °F, and/or a minimum penetration of 20 be specified for residue from 46 hr IDT, in lieu of requirements regarding TFOT.

As alternatives, ductility at 77 °F of 10 to 25 cm and softening point (R & B) of 160 °F can be also considered. A service life of 10 years can be used instead of 60 months. It is believed that this proposed approach to durability test application has advantages over all current specifications, including those research specifications of the Asphalt Institute and California. It not only specifies durability, but it also considers design life (balanced design) and can predict behavior of asphalt throughout pavement life by use of IDT and time-equivalency curves.

IX. CONCLUSIONS AND RECOMMENDATIONS

1. A laboratory durability method (Iowa Durability Test) for predicting the durability of paving asphalts during mixing and pavement service life has been developed and correlated with field performance under Iowa conditions.

2. The ageing process of paving asphalts follows a hyperbolic function of time both in the field and in the developed IDT laboratory conditions, but at different rates.

3. Good correlations between field service ageing in Iowa and laboratory ageing during Iowa Durability Test have been obtained. The master time-equivalency curve between IDT in hours and pavement service life in months, established by combining all asphalts (void levels) and all properties, indicates that 46 hours in IDT will age asphalts to the equivalent of 60 months in Iowa pavements. Correlation curves for different properties and different levels of pavement voids were also obtained.

4. Laboratory and field performance tests have shown that asphalts meeting current specifications can have various degrees of durability under similar conditions of construction practices, traffic, and climate in the field and identical ageing treatments in the laboratory. These observations imply that the current asphalt specification requirements are not sufficiently restrictive to guarantee a durable material.

5. A tentative specification for paving asphalts, including durability requirements based on IDT, is recommended in lieu of current TFOT.

6. To improve the tentative specifications (weaknesses due to lack of sufficient data on critical values of critical properties under Iowa weathering and traffic conditions), continued observations and tests of the eight pavements are recommended. Also recommended is a research project to determine critical property values for Iowa conditions. Such a project can be easily and inexpensively conducted by examining selected 20 to 30 failure asphalt pavements across the State, making certain that failures are not caused by improper design and construction of bases and subbases or other reasons not associated with asphalt quality.

ACKNOWLEDGMENTS

This report is the end result of a comprehensive four-year study under Project HR-124, sponsored by the Iowa Highway Research Board and the Iowa State Highway Commission. This study under the same title was designated as Projects 717S and 828S of the Engineering Research Institute Iowa State University. I am indebted to the Board for its support of this study and to the engineers of the Iowa State Highway Commission, Messrs.Steve E. Roberts and Bernard Ortgies in particular, for their interest and cooperation.

I wish to thank Dr. Rodney J. Huang, Soils Research Laboratory, for his help in infrared spectroscopic work of this investigation, Drs. L. C. Semanski and J. P. Creedon, both of the E. I. DuPont Instruments Division, Wilmington, Delaware, for their help in running selected asphalts by DSC and TMA analyses, and Drs. Herbert T. David and Richard W. Mensing, Statistical Laboratory, for their consultation on regression analyses.

The following individuals contributed, in various capacities at various times, to this investigation: Pam Long, Tish Davis, Karen Ogburne, Rose Potts, Larry Volkening, Jeff Wisted, Jack Shoemaker, and Duane Jansen.

I would like to dedicate this report to the late Professor Ladis H. Csanyi, who generated my interests and taught much of what I know on asphalt technology. He was largely responsible for the existence of the Bituminous Research Laboratory in which this research was conducted.

REFERENCES

1. Lee, D. Y., Research Report No. 067-036, "Development of a Laboratory Durability Test in Asphalt," Engineering Research Institute, Iowa State University, Ames (1967) (HR-124).

2. Lee, D. Y., HRR, 231, 34 (1968).

3. Lee, D. Y., "Durability and Durability Test for Paving Asphalt," Special Report, Engineering Research Institute, Iowa State University (1969).

4. Vallerga, B. A., C. L. Monismith, and K. Granthem, Proc. Assoc. Asphalt Paving Tech., 26, 126 (1957).

5. Traxler, R. N., Proc. AAPT, 32, 44 (1963).

6. Moavenzadeh, F., and W. H. Goetz, HRR, 24, 106 (1963).

7. Goode, J. F., and L. A. Lufsey, Proc. AAPT, 34, 430 (1965).

8. Lee, D. Y., and L. H. Csanyi, J. Materials, 3, 538 (1968).

9. Griffin, R. L., T. K. Miles, and C. J. Penter, Proc. AAPT, 24, 31 (1955).

10. Pfeiffer, J. P., The Properties of Asphaltic Ritumen, Elsevier Publishing Co., N.Y. (1950).

11. Welborn, J. Y., "Asphalt Hardening — Fact and Fallacy," Public Roads, 35, 12, 279 (1970).

12. Vallerga, B. A., and W. J. Halstead, "Effects of Field Ageing on Fundamental Properties of Paving Asphalts," HRR, 361, 71 (1971).

13. Heithaus, J. J., and R. W. Johnson, Proc. AAPT, 27, 17 (1958).

14. Bright, R., and E. T. Reynolds, "Effect of Mixing Temperature on Hardening of Asphaltic Binder in Hot Bituminous Concrete," Highway Res. Rd. Bull., 333, 20 (1962).

15. Simpson, W. C., R. L. Griffin, and T. K. Miles, ASTM Special Tech. Publ., 277, 52 (1959).

16. Finn, F. N., "Factors Involved in the Design of Asphaltic Pavement Surfaces," NCHRP Report 39 (1967).

17. Dell, P. S., Proc. Second International Conference on Structural Design of Asphalt Pavements, U. of Michigan, p. 459 (1967).

18. Heukelom, W., and A. J. G. Klomp, Proc. AAPT, 33, 92 (1964).

19. Vallerga, B. A., F. N. Finn, and R. G. Hicks, Proc. Second International Conference on Structural Design of Asphalt Pavements, U. of Michigan, Ann Arbor, p. 484 (1967).

20. British Road Research Laboratory," Bituminous Materials in Road Construction," HMSO, p. 74 (1962).

21. Richardson, C., The Modern Asphalt Pavement, John Wiley and Sons, New York (1905).

22. Hubbard, P., and C. S. Reeve, Office of Public Roads Bull., No. 38 (1911).

23. Hubbard, P. and C. S. Reeve, Jour. Ind. Eng. Chem., 5: 15 (1913).

24. Reeve, C. S., and R. H. Lewis, Jour. Ind. Eng. Chem., 9: 743 (1917).

25. Lewis, R. H., Proc. AAPT, 5, 63 (1933).

26. Lewis, R. H., and W. O'B. Hillman, Public Roads, 15: 4 (1934).

27. Lewis, R. H., and W. O'B. Hillman, Public Roads, 16: 6 (1935).

28. Lewis, R. H., and W. O'B. Hillman, Public Roads, 18: 5 (1937).

29. Lewis, R. H., and J. Y. Wilborn, Proc. AAPT, 11, 86 (1940); 12: 14 (1940).

30. Skidmore, H. W., and G. Abson, Proc. AAPT, 9, 195 (1937).

31. Shattuck, C. O., Proc. AAPT, 11, 186 (1940).

32. Clark, R. G., Proc. AAPT, 27, 196 (1958).

33. Thurston, R. R., and E. C. Knowles, Jour. Ind. Eng. Chem., 33, 320 (1941).

34. Anderson, A. P., F. H. Stross, and A. Ellings, Ind. Eng. Chem. An. Ed., 14, 45 (1942).

35. Ebberts, A. R., Jour. Ind. Eng. Chem., 34, 1048 (1942).

36. Van Oort, W. P., Jour. Ind. Eng. Chem., 48, 1196 (1956).

37. Blokker, P. C., and H. Van Hoorn, Proc. Fifth World Petroleum Congress, Section VI, p. 417 (1959).

38. Griffin, R. L., T. K. Miles, and C. J. Penter, Proc. AAPT, 24, 31 (1955).

39. Heithaus, J. J., and R. W. Johnson, Proc. AAPT, 27, 17 (1958).

40. Traxler, R. N., Proc. AAPT, 30, 359 (1961).

41. Hveem, F. N., Proc. AAPT, 15, 111 (1943).

42. Stanton, T. E., and F. N. Hveem, ASTM STP No. 94, p. 84 (1949).

43. Pauls, J. T., and J. Y. Welborn, Public Roads, 27(a), 187 (1953).

44. Martin, K. G., Jour. Appl. Chem., 16, 197 (1966).

45. British Road Research Laboratory, Bituminous Materials in Road Construction, Her Majesty's Stationery Office, London (1962).

46. Hveem, F. N., E. Zube, and J. Skog, Proc. AAPT, 32, 271 (1963).

47. Pauls, J. T., and J. Y. Welborn, Proc. AAPT, 21, 48 (1952).

48. Hveem, F. N., E. Zube, and J. Skog, ASTM STP No. 277, p. 3 (1960).

49. Bright, R., and E. T. Reynolds, HRB Bull., 333, 20 (1962).

50. Way, P. J. et al., Proc. Fifth World Petroleum Congress, Section VI, p. 433 (1959).

51. Lammiman, K. A., T. Les, and P. J. Way, Jour. Appl. Chem., 12, 510 (1962).

52. Simpson, W. C., R. L. Griffin, and T. K. Miles, ASTM STP No. 277, 52 (1959).

53. Traxler, R. N., Proc. AAPT, 32, 229 (1963).

54. Gallaway, B. M., Proc. AAPT, 28, 280 (1959).

55. Halstead, W. J., and J. Z. Zenewitz, Public Roads, 31, 211 (1961).

56. Kari, W. J., "Paving Asphalts for Future Highways," Proc. Canadian Tech. Asphalt Assoc., 14, 146 (1969).

57. Halstead, W. J., and J. Y. Welborn, "Development of Specifications for Viscosity-Graded Asphalts," Highway Res. Rec., 350, 1 (1971).

58. Skog, J., and G. Sherman, "Viscosity Grading for Asphalt Cements," Hwy. Res. Rec., 350, 26 (1971).

59. Skog, J., Proc. AAPT, 36, 387 (1967).

60. Schmidt, R. J. et al., Proc. AAPT, 37, 476 (1968).

61. Traxler, R. N., Asphalt: Its Composition, Properties, and Uses, Reinhold Publ. Corp., New York, p. 53 (1961).

62. Santucci, L. E., and R. J. Schmidt, "The Effect of Asphalt Properties on the Fatigue Resistance of Asphalt Paving Mixtures," Proc. AAPT, 38, 65 (1969).

63. Sisko, A. W., Highway Research Record, 67, 27 (1964).

64. Gotolski, W. H. et al., Proc. AAPT, 33, 285 (1964).

65. Lee, A. R., and E. J. Dickinson, Road Research Laboratory Tech. Paper No. 31 (1954).

66. Jones, P. M., Proc. CTAA, 7, 15 (1962).

67. Jones, P. M., Ind. Eng. Chem., 4: 1, 57 (1965).

68. ASTM Standards, Method F89-68, "Standard Method of Test for Modulus of a Flexible Barrier Material by Sonic Method" (1968).

69. Schmidt, R. J., Proc. AAPT, 35, 263 (1966).

70. Rostler, F. S., and R. M. White, Proc. AAPT, 31, 35 (1962).

71. Halstead, W. et al., Proc. AAPT, 35, 91 (1966).

72. Halstead, W. J. et al., "Fingerprinting of Highway Asphalt," paper presented at the Annual Meeting of the AAPT, Feb. 14-16 (1972).

73. Csanyi, L. H., and H. P. Fung, Proc. AAPT, 23, 64 (1954).

74. Stewart, J. E., "Infrared Spectra of Chromatographically Fractionated Asphalts," J. Res. NBS, 58, 265 (1957).

75. Beitchman, B. D., "Infrared Spectra of Asphalts," J. Res. NBS, 63A, 189 (1959).

76. Wright, J. R., and P. G. Campbell, "Determination of Oxidation Rates of Air-Blown Asphalts by Infrared Spectroscopy," J. Appl. Chem., 12, 256 (1962).

77. Greenfeld, S. H., and J. R. Wright, "Four Methods for Predicting the Durability of Roofing Asphalts," Materials Res and Std., 2, 738 (1962).

78. Campbell, P. G., and J. R. Wright, "Oxidation Products in an Oxygen-Blown Kuwait Asphalt," Ind. and Eng. Chem. Prod. Res. and Dev., 5, 319 (1966).

79. Januszke, R. M., "Paving Asphalt — Additives in Durability Determination," Ind. and Eng. Chem. Prod. Res. Dev., 10, 209 (1971).

80. Mertens, E. W., "Predicting Weatherability of Coating-Grade Asphalts from Asphaltene Characteristics," ASTM Bull No. 250, p. 40 (1960).

81. Wright, P. H., and P. J. Paquette, "Hardening of Asphalt in Hot Bituminum Mixing during the Hauling Process," HRR, 132, 10 (1966).

82. Winniford, R. S., ASTM SPT No. 212, p. 51 (1957).

83. Brown, A. B., J. W. Sparks, and O. Larsen, Proc. AAPT, 26, 66 (1957).

84. Gallaway, B. M., Proc. AAPT, 26, 151 (1957).

85. Pauls, J. T., and W. J. Halstead, Proc. AAPT, 27, 123 (1958).

86. Heithaus, J. J., and R. W. Johnson, Proc. AAPT, 27, 17 (1958).

87. Heukelom, W., Proc. AAPT, 35, 358 (1966).

88. Pfeiffer, J. P., and P. J. Van Doormall, J. Inst. Petrol., 22, 414 (1936).

89. Van der Poel, C., J. Appl. Chem., 4, 221 (1954).

90. McLeod, N. W., "A 4-Year Survey of Low Temperature Transverse Pavement Cracking on Three Ontario Test Roads," paper presented at the Annual Meeting of AAPT (1972).

91. Rigden, P. J., and A. R. Lee, J. Appl. Chem., 9, 219 (1959).

92. Breen, J. J., and J. E. Stephens, Proc. Canadian Tech. Asphalt Assoc., 12, 137 (1967).

93. Schmidt, R. J., and L. E. Santucci, Proc. AAPT, 35, 61 (1966).

94. Schmidt, R. J., Proc. AAPT, 35, 263 (1966).

95. duPont Instruments, Technical Report 900TRI (June 1969).

96. Gotolski, W. H. et al., "Rates of Asphalt Hardening at In-Service Temperatures," Engr. Res. Bull. B-100, Penn. State Univ., University Park, Penn. (1969).

97. Harrick, J., Internal Reflection Spectroscopy, InterScience Pub., New York (1967).

98. Fahrenfort, J., *Attenuated Total Reflection – A New Principal for Production of Useful Infrared Reflection Spectra of Organic Compounds, Molecular Spectroscopy*, Vol. 2, A Mangini, Ed., Pergamon, London, p. 701 (1962).

99. Smith, C. D., D. Schuetz, and R. S. Hodgson, Ind. Eng. Chem. Prod. Res. Deve., *5*, 153 (1966).

100. Halstead, W. J., Proc. AAPT, *32*, 247 (1963).

orm 124-100 Date 11-1-68

APPENDIX A

IDENTIFICATION OF MATERIALS SUBMITTED TO ISU BITUMINOUS LAB FROM IOWA STATE HIGHWAY COMMISSION FOR RESEARCH PROJECT HR-124 EXTENSION

Construction Project Chickasaw FN-63-8(1)20-19

Contractor Highway Surfacers, Inc. Project Location U.S. 63 N. of New Hampton

I. Asphalt Cement

(a) Penetration Grade 85-100 (b) Supplier Bituminous Mat'l & Supply, Algona, Iowa

(c) Source of crude or other ident. to trace crude See Note Attached Earlier

(d) Temperature of A.C. just prior to mixing 295 °F.

II. Aggregate

(a) Water absorption 1.0 %

(b) Temperature of aggregate just prior to mixing 300 °F.

(c) Sp. gr. (combined aggregate) 2.726 (HRB).

III. Job Mix

(a) Recommended Asphalt content(s) 7.5 %

(b) Trial mix, Marshall Densitie(s) 2.275 psf

(c) Hveem side press, at 400 psi vertical load 60

(d) Voids 68 %

(e) Trial mix gradation (below) (f) Temp of Mix 290°F

Percent Passing

	1½"	1"	3/4"	1/2"	3/8"	#4	#8	#16	#30	#50	#100	#200
Cold Feed,					100	82	63		32			8.7
Field Grading					100	81	61.5	44	29.5	16	11.5	9.3

IV. Field Cores

(a) Date taken 10-14-68

(b) Sample Location (Longitudinal & Transverse) Sta 259+60

Box A	Box B
Left lane wheel track	Left lane between wheel tracks
1f-12-A	1f-12-B

(c) Sta. to Sta. of truck load to be sampled 258+10 to 260+25 S. Bound Lane

APPENDIX B

HR-124 Testing Program

I. Asphalts:

A. Heat asphalt in 1-gal can in oven at 325 °F for 60 to 90 min. Stir the asphalt thoroughly and transfer into clean 1,000-ml beakers. Store one beaker of asphalt in a cooker in vacuum as control sample (identified as c). Melt asphalt in beaker No. 2, transfer in 3-oz penetration cans (identified as a sample), run penetration test immediately following ASTM D5-65, and seal the other cans for testings in IB.

B. Tests on original asphalts:

1. Penetration (ASTM D-5-65),
2. Softening point (ASTM D36-66T),
3. Flash and fire points (ASTM D92-66),
4. Specific gravity (ASTM D70-52),
5. Spot test (AASHO T102-57),
6. Viscosity at 77 °F (sliding-plate viscometer and cone-plate viscometer),
7. Viscosity at 140 °F (Cannon-Manning Vacuum Capillary) (ASTM D2171-66),
8. Percentage of oxygen,
9. Percentage of asphaltene,
10. Percentage of oxygen in asphaltene,
11. Microductility at 77 °F (ASTM D113-44),
12. Brittle point,
13. Chemical analysis by Rostler and White method, and

14. Special tests (thermal analysis, dynamic modulus, IR analysis, etc.).

To avoid overheating and unnecessary re-melt, use one can for tests 1, 6, 8, 9 and 13; one can for tests 2, 4, 5 and 11; one can for test 3, one can for tests 7 and 12; and one can for special tests.

C. Thin Film Oven Test (TFOT) (ASTM D1754-67T):

1. Pour 12 TFOT (50 g ± 0.5 g) samples from beaker No. 3 in IA.
2. Weigh samples to 0.0001 g on an analytical balance.
3. Expose all samples in a TFOT oven at 325 °F for 5 hr.
4. Determine the weight change.
5. Pour the contents (TFOT residues) of two TFOT dishes into 3-oz penetration cans, stir well, and seal (identified as d).
6. Run penetration tests on one and tests in IB on the other (except flash and fire).

D. Pressure-oxygen treatment on TFOT residues:

1. Place 10 TFOT residues from IC in a pressure vessel.
2. Assemble the vessel and check for leakage.
3. Evacuate the vessel twice and fill slowly with oxygen to a pressure of 20 atm at 150 °F.
4. Put vessel and contents in an oven at 150 °F.
5. Take two samples out at the end of 24 hr, 48 hr, 96 hr, 240 hr, and 480 hr; determine the weight changes.
6. Transfer treated samples into 3-oz cans (identified as d24, d48, ...) and run tests as in IB, except for flash and fire points.

E. Tests on control samples:

  1. Run tests as in IB on control samples at 6-month intervals.

II. Mixes from plant:

A. Determine the maximum theoretical specific gravity by Rice method when mix is received.

B. Directions for hot extraction and recovery of asphalt by Abson method (ASTM D1856-65):

  1. Use 4,000 g of loose mix,
  2. Use analytical grade trichloroethylene,
  3. Complete the recovery in 8 hr, and
  4. Pour the recovered asphalt into 3-oz cans (identified as p) and run tests as in IB, except for flash and fire points.

III. Field core samples:

A. Determine the average bulk specific gravity of the cores.

B. Determine the maximum theoretical specific gravity of the mix for the same cores.

C. Heat about 4,000 g of the cores slightly in oven to break up the sample.

D. Recover the asphalt as in IIB (identified as f-x-A and f-x-B).

E. Run tests on recovered asphalts as in IB, except for flash and fire points.

APPENDIX C

Field Sample Treatment Procedures

1. Samples:

Date received	County	No.	Month	Wheel track (wt)	Between wt	Thickness, inches
5-10-71	Chickasaw	1	42	Box A	Box B	1
6-10-72	Dickinson	2	42	Box A	Box B	1
5-13-71	Harrison	3	42	Box A	Box B	1
4-19-71	Polk-Story	4	42	Box A	Box B	3/4
5-10-71	Monona	6	36	Box A	Box B	1-1/2 1-3/4
5-13-71	Bremer	7	36	Box A	Box B	1/2
5-13-71	Keokuk	8	36	Slab A	Slab B	1/2
8-26-71	Jackson	9	36	Box A (cores 1 to 10)	Box B (cores 11 to 20)	2

2. Preparation of cores and slabs:

   A. Separate the top layer of samples from the rest by cutting with the diamond saw or by warming the sample in an oven at 200 to 210 °F for 20 to 30 minutes and by using a spatula.

   B. Put all of the top layer sample into a pan and designate. For example:

   Chickasaw: 1-42-A-1,2,3,...;1-42-B-1,2,3,...

   Chickasaw Co. No. = 1
   42 = months
   A = in wheel track; B = between wheel track
   1,2,3..., = sample number

   Discard bottom layer.

3. Tests:

   A. Determine bulk sp. gr. (d) on at least 4 samples per box – AASHO-T166.

   B. Loosen enough of the samples used above for duplicate determination of Rice max. sp. gr. (Dm.). Calculate V. (air voids) – MS-2, Appendix C.

   C. Loosen the rest of the top layer samples (about 3000 g) for asphalt recovery. (Obtain about 100 g asphalt) – AASHO; T-164, Method B; AASHO; T-170.

   D. Recovered asphalt should also be designated as in 2-B and dated.

   E. Run sp. gr., spot, softening point, ductility, brittle point, viscosity at 77 °F., 140 °F, etc. on recovered asphalts.

APPENDIX D

Iowa Durability Test Procedure (TFOT - Pressure-Oxidation)

To stimulate or reproduce the two-stage ageing and hardening of the asphalts in the field, the laboratory durability test procedure finally adopted was:

1. Run the thin film oven test (TFOT) as prescribed in ASTM D-1754.
2. Load TFOT residue (in TFOT pans) on pressure-oxidation (P-O) sample holder and place sample and holder in pressure vessel.
3. Position lid and tighten bolts and nuts.
4. Evacuate the vessel to about 29 in. Hg.
5. Apply oxygen at 20 to 30 psig.
6. Evacuate the vessel again to 29 in. Hg.
7. Apply oxygen slowly to desired gauge pressure (P') depending on room temperature to give an oxygen pressure of 279 psig (294 psi or 20 atms) at 150 °F (338.6 °K).

Room temp (T')			Filling pressure (P')	
F°	C°	K°	psi	psig
65	18.3	291.4	252.9	238.2
70	21.1	294.2	255.4	240.7
75	23.9	297.0	257.8	243.1
80	26.7	299.8	260.3	245.6
85	29.4	302.5	262.7	248.0

8. Set oven at 150 °F.
9. Put pressure vessel with sample in oven and record time.
10. Check pressure after 30 to 60 min to make sure the gauge pressure is 279 psig.

11. Remove the vessel at the end of 24 or 48 hr.

12. Release the pressure slowly and remove the sample from the vessel for tests: penetration, viscosity, etc.

APPENDIX E

Procedure of Brittle Point Tests

Brittleness is the tendency of a material to fracture with little or no plastic deformation. Brittleness of asphalt at low temperatures has caused much concern among highway engineers. It is believed that cracking of asphalt films in the pavements may be closely associated with the increase in brittleness of an asphalt at low temperatures and the loss in ability to deform plastically.

The measurement of asphalt brittleness in this study is desirable because:

- The initial brittleness of an asphalt may provide insight to the potential service of an asphalt, and
- The change of brittleness of an asphalt at various stages, both in the field and under laboratory durability treatments, may be used as one of the indices to predict the durability and quality of an asphalt.

The Fraass brittle point test has been used in Europe for a number of years to study the low temperature behavior of asphalts. The test is described in the Institute of Petroleum Specification IP 80/53. In this test a spring steel plaque is coated with a specific amount of asphalt, placed in a flexing apparatus, and cooled. Flexing is carried out manually in conjunction with cooling, at a rate of 1 °C/min, until a crack appears in the asphalt film. The temperature at which this occurs is the brittle point.

In this study two improved brittle point testers obtained from Polytronics Co. of Toronto, Canada are used. In this modified tester the flexing mechanism is accomplished by a synchron motor with a spindle speed of 1 rpm and a circular eccentric cam. The sample preparation and cooling controls were developed at the Bituminous Research Laboratory. Testing is done in a specially designed and fabricated Plexiglass chamber.

Sample Preparation

Standard-size stainless steel of 41 ± 0.05 mm long, 20 ± 2 mm wide and 0.15 ± 0.02 mm thick are used for coating of asphalt films. In preparation of the test plate, about 0.3 g of asphalt is placed on a cleaned, tared plate and covered with a lightly greased aluminum cover plate. The assembly is placed upon the lower portion of a film former and pressure (and sometimes warm air) is applied to cause the asphalt to flow to a desired thickness of 550 μ. The film formers are preset with spacers to produce this thickness. After the samples have been cooled and trimmed they are stored in a covered petri dish in a refrigerator until testing. Preliminary studies show that time of sample storage up to one week has no appreciable effect on brittle point.

Cooling

Cooling is accomplished by using a methanol-water mixture in proportion of 7:3 in a closed circulation system. The coolant is cooled by both a refrigerated bath and a dry-ice heat exchanger. The diagram shows the circuit connection of the system.

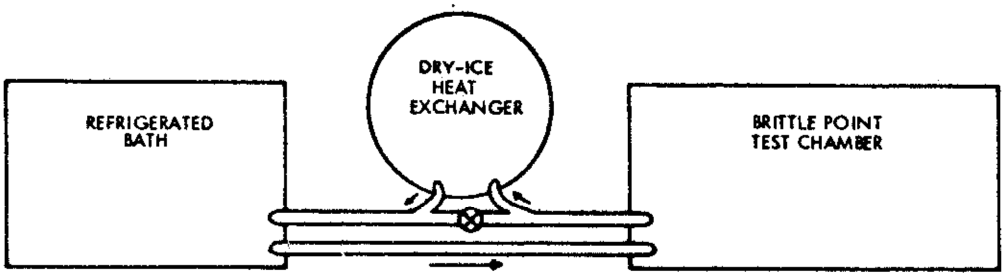

Fig. E.1. Cooling circuit connection.

To insure uniform cooling of the test specimen, the coolant is stirred by air bubbling in the flexing chamber.

The temperature of the specimen is indicated and recorded by a copper-constant thermocouple placed near the rear center of the plate. The output of the thermocouple is recorded on a Leeds and Northrup strip chart recorder. This facilitates determination of the rate of temperature drop by drawing a predetermined line on the recorder chart (1 °C/min) and manually controlling the rate of cooling to follow this line by adjusting the rate of flow of coolant into the test chamber.

Procedure

Following assembly of the apparatus, flexing and cooling is started, the former at a rate of 1 flex/min traversing a distance of 3.5 ± 0.2 mm, and the latter at a rate of 1 °C/min. Flexing and cooling begin at 0 °C and are continued until the brittle point is reached – the temperature when a crack appears halfway across the plate.

Accuracy

A series of six specimens were prepared using A.C. No. 5. An average value of - 15.3 °C was obtained with a standard deviation of 0.8 °C. The accuracy of the test is limited by the accuracy and readability of the recorder used.